Controls on upper Viséan (Carboniferous) depositional environments in Ireland

Volume II (of II)

Figures & Appendices

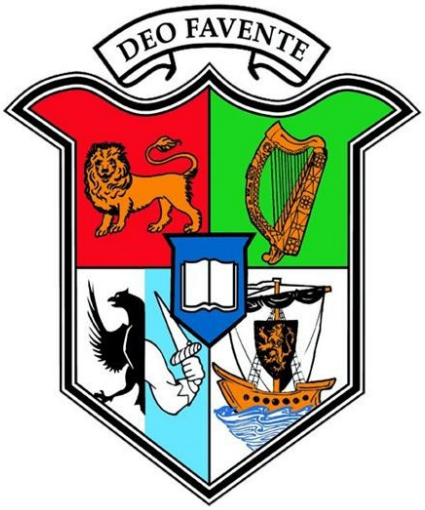

Milo Barham

Supervisors: Dr. John Murray and Prof. D. Michael Williams

A thesis submitted for the degree of Doctor of Philosophy

Earth and Ocean Sciences
School of Natural Sciences
National University of Ireland, Galway

November 2010

CONTENTS

CHAPTER 1

CHAPTER 2

CHAPTER 3

CHAPTER 4

CHAPTER 5

CHAPTER 6

APPENDICES

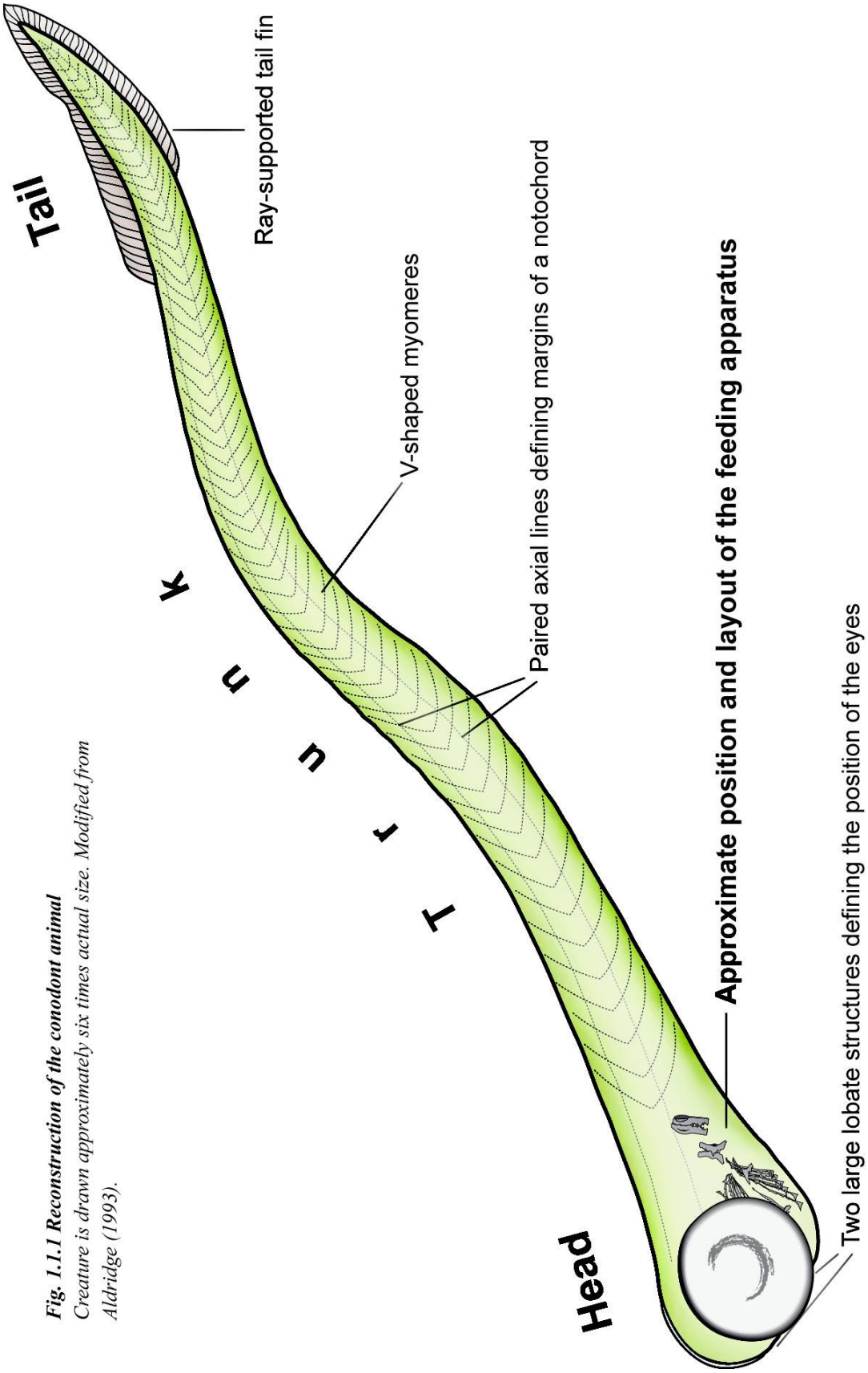

Fig. 1.1.1 Reconstruction of the conodont animal
Creature is drawn approximately six times actual size. Modified from Aldridge (1993).

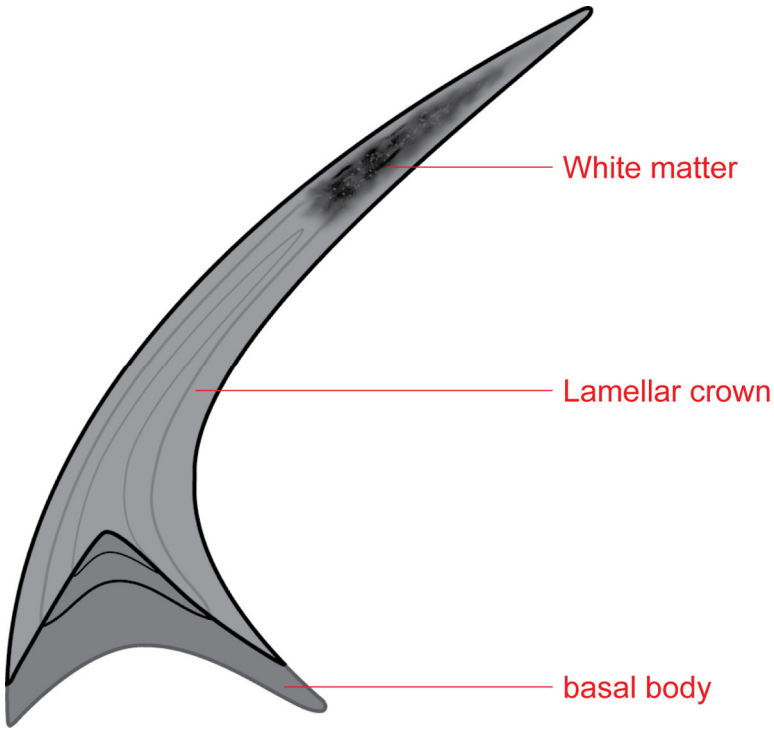

Fig. 1.1.2a Schematic composition and growth patterns in a conodont coniform element.

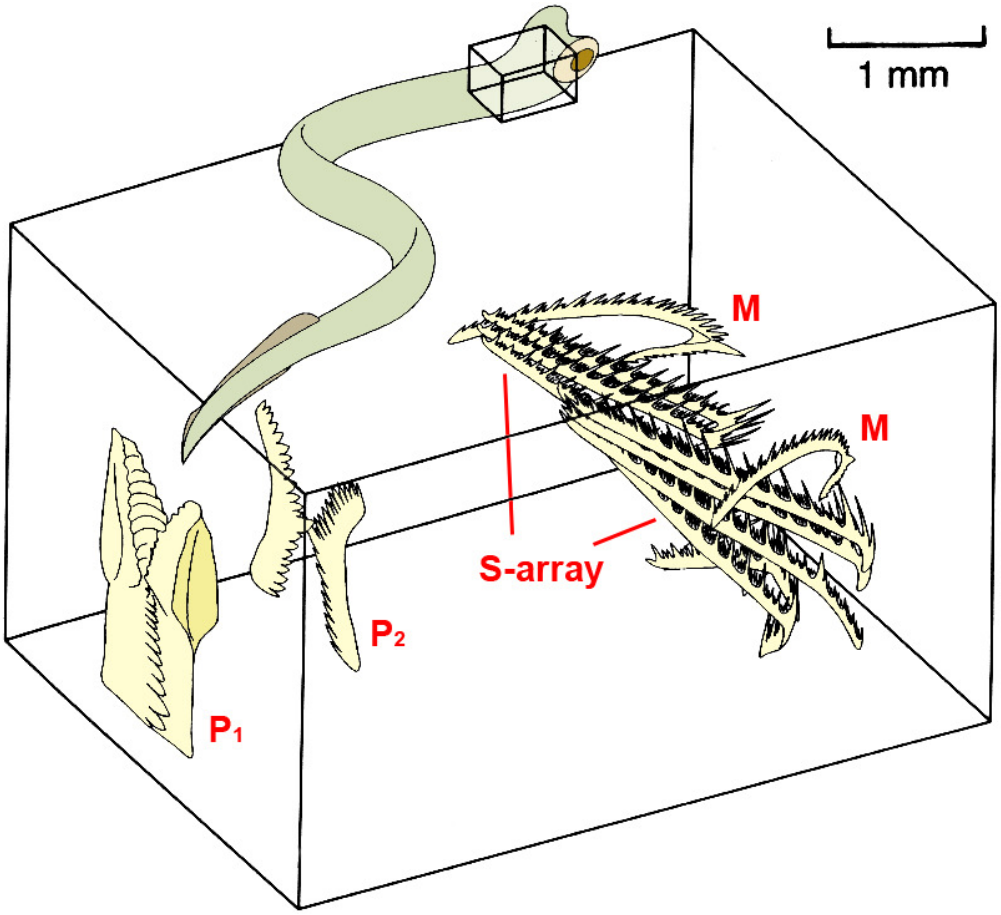

Fig. 1.1.2b The Ozarkodinid conodont element layout.

The smaller box represents the position of the larger box (showing the expanded element array) relative to the overall creature. Modified from Aldridge & Purnell (1996).

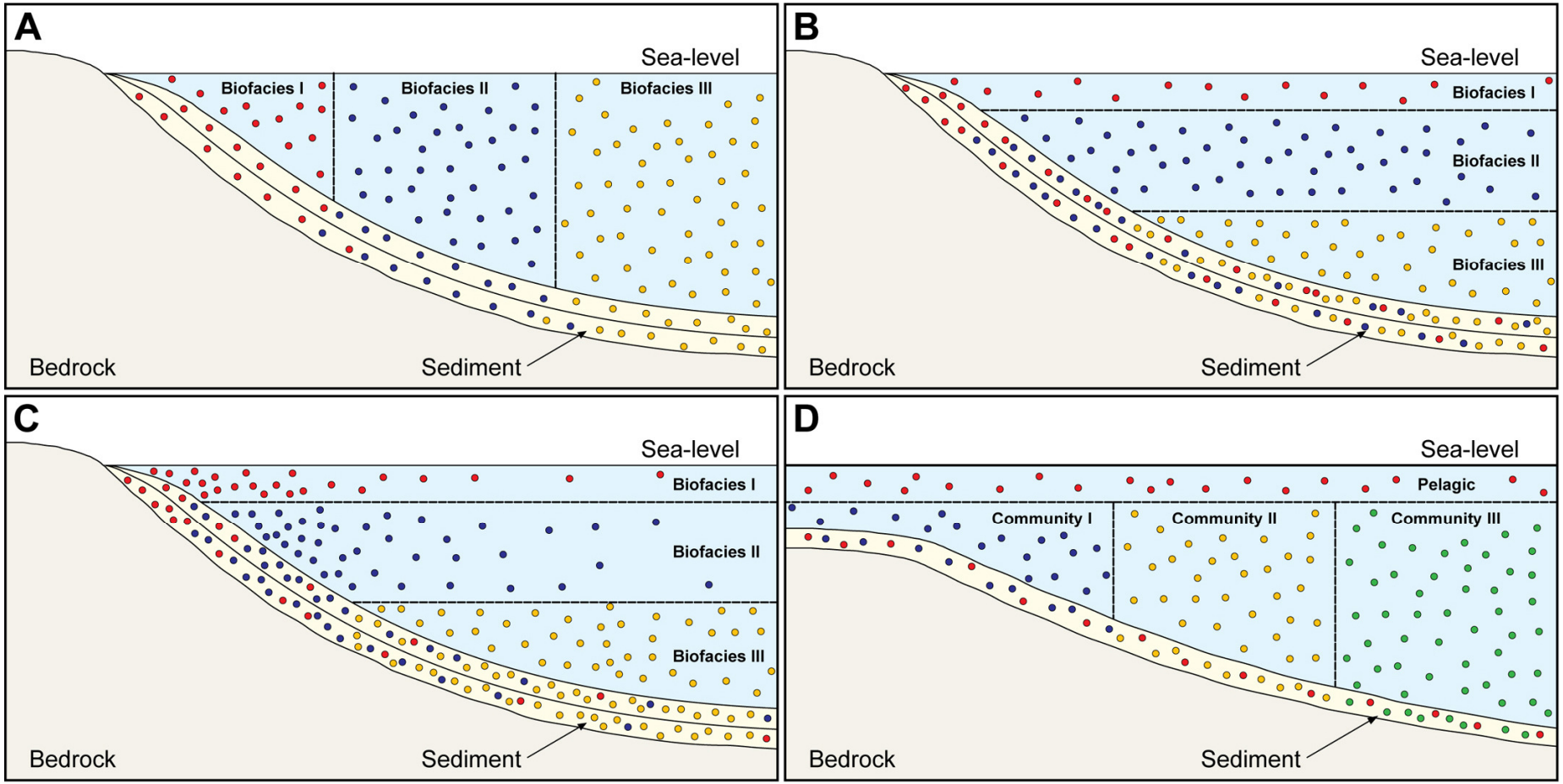

Fig. 1.1.3a Early conodont Biofacies models.

Coloured dots represent different conodont communities whose distribution, as shown, was thought to explain the patterns of fossils in the sediments. A – Lateral segregation model of Druce (1973), B – Depth stratification model of Seddon (1970, in Druce, 1973), C – Pelagic model of Druce (1973), D – Necto-benthic model of Barnes & Fahraeus (1975).

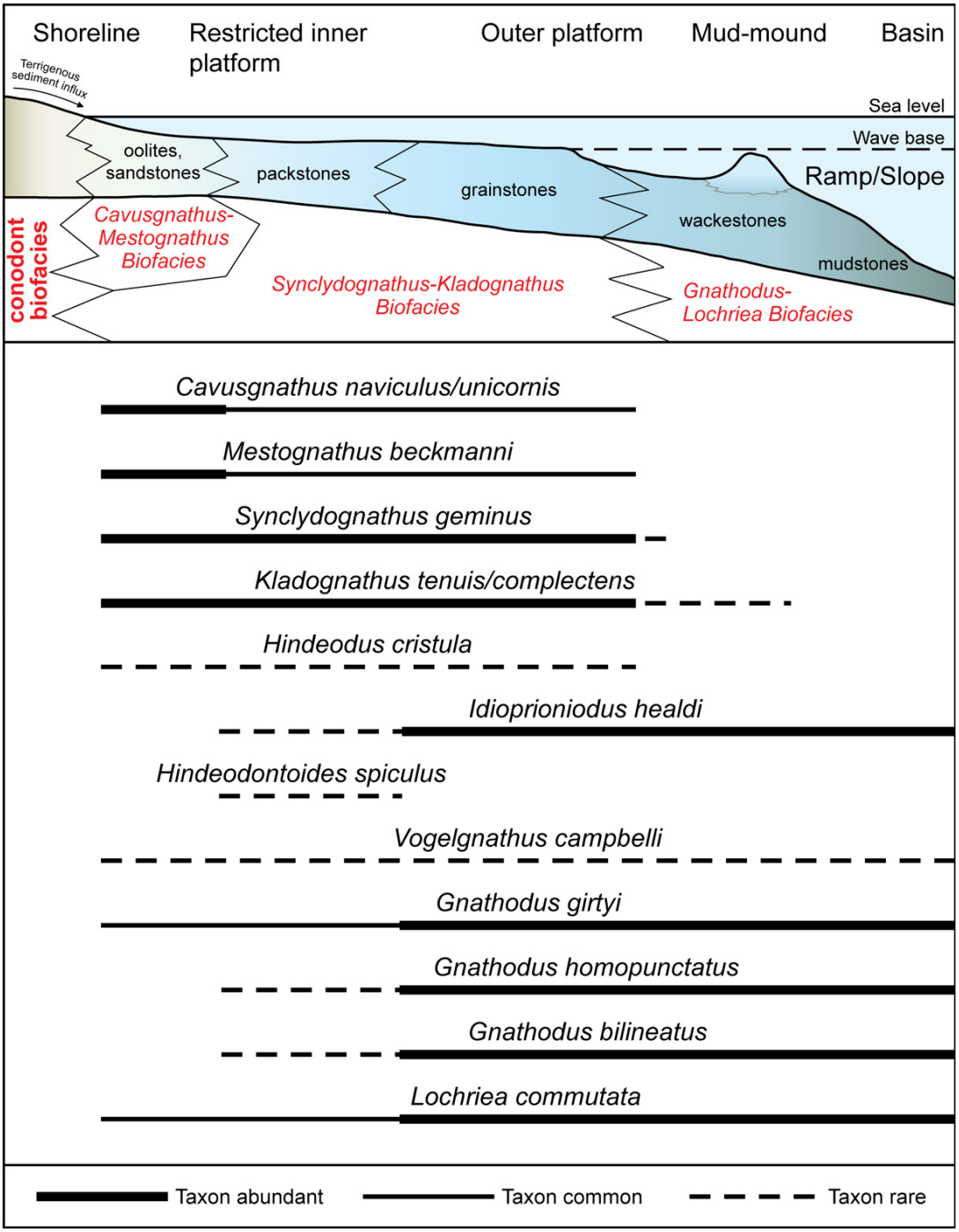

Fig. 1.1.3b Biofacies of an upper Viséan (Asbian) carbonate platform and basin.
Modified from Somerville (1999).

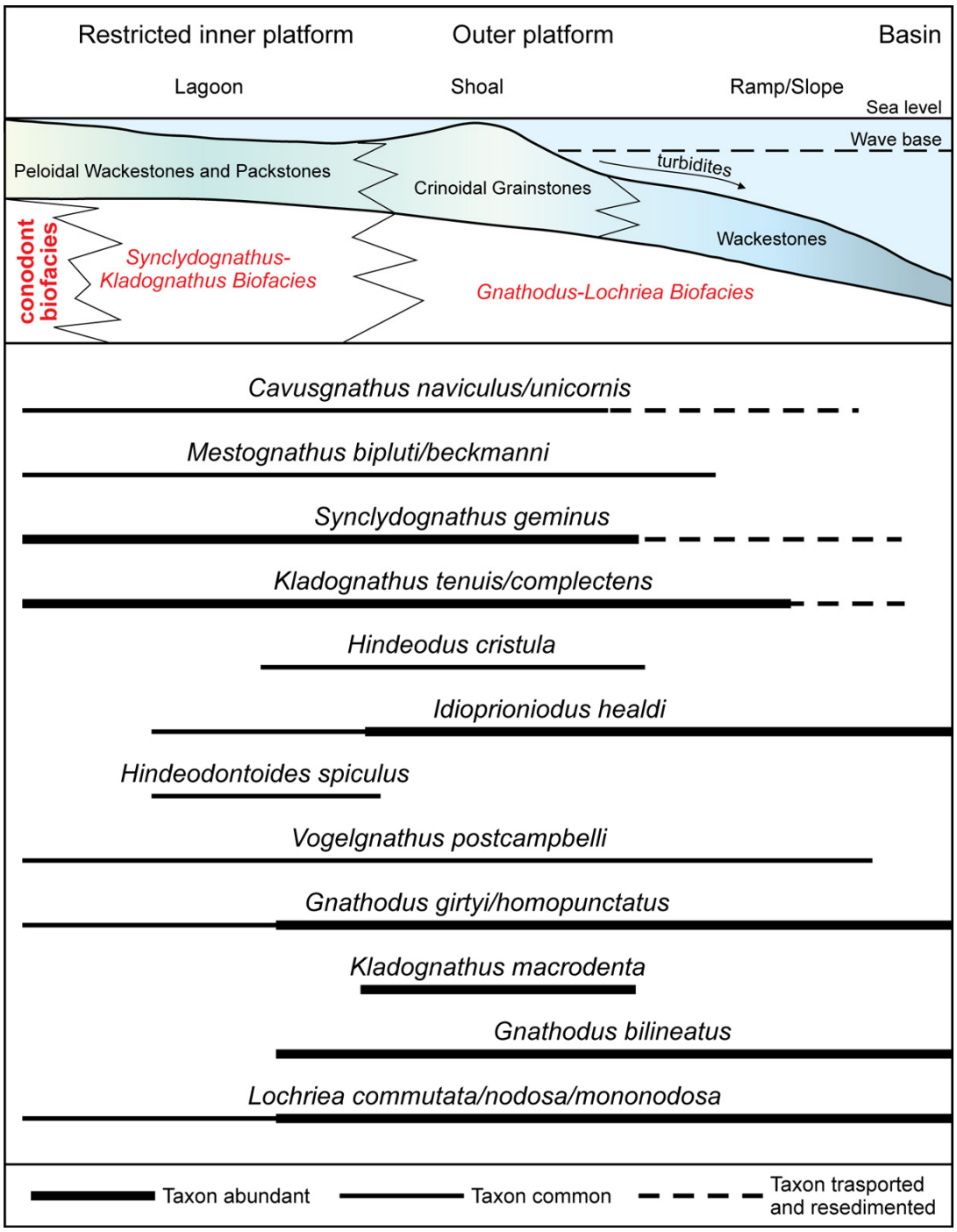

Fig. 1.1.3c Biofacies of an upper Viséan (Brigantian) carbonate ramp and basin. *Modified from Somerville (1999).*

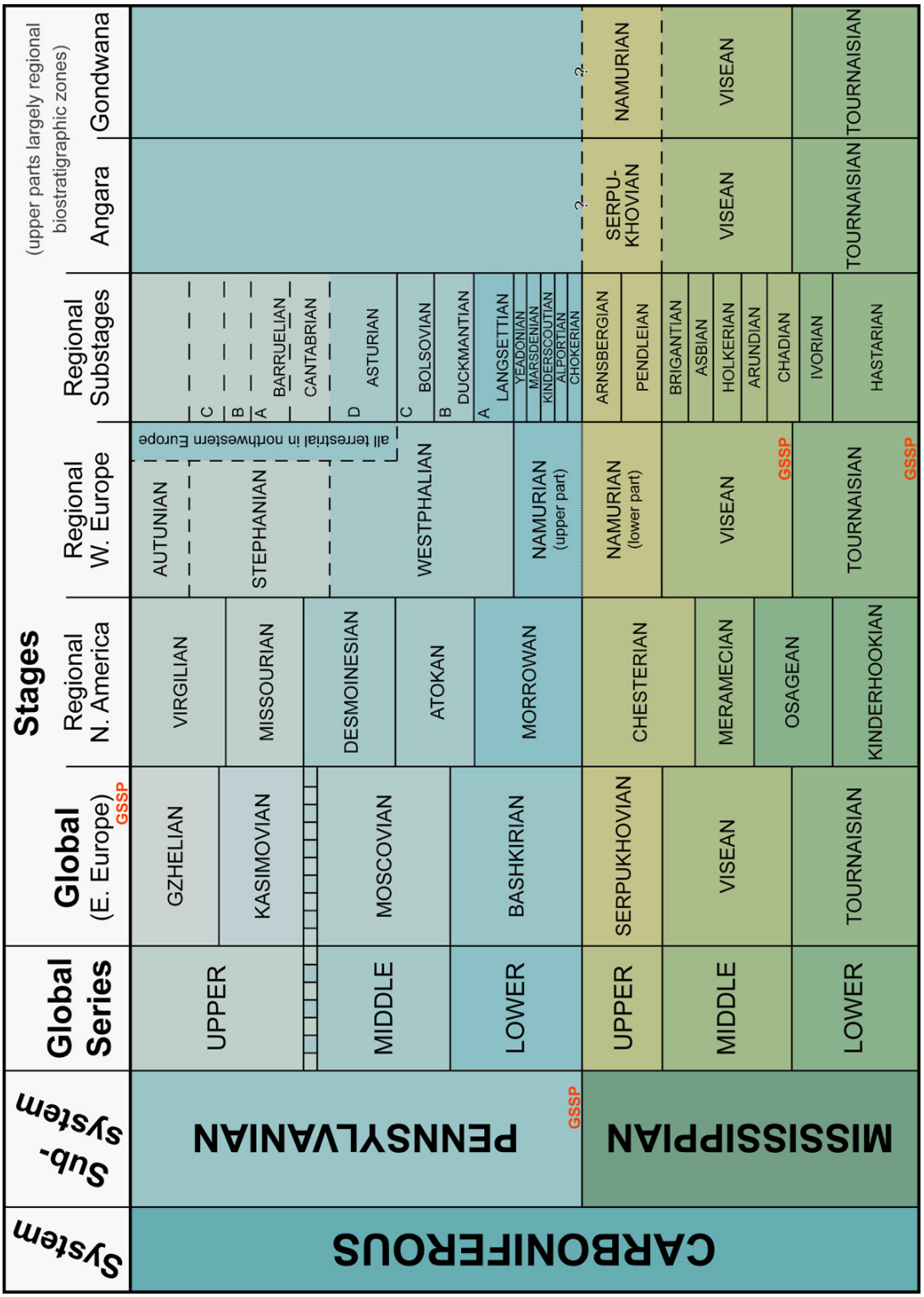

Fig. 1.2 Ratified subdivisions of the Carboniferous.

System, Sub-system, Series as well as global Stage and western European Substage terms are variously used in the text. The alternating horizon separating the Middle and Upper Pennsylvanian Series (Moscovian and Kasimovian Stages) reflects the range of uncertainty for the definition of the boundary at present. Modified from Heckel (2004) with colours according to the commission for the Geological Map of the World [CGMW].

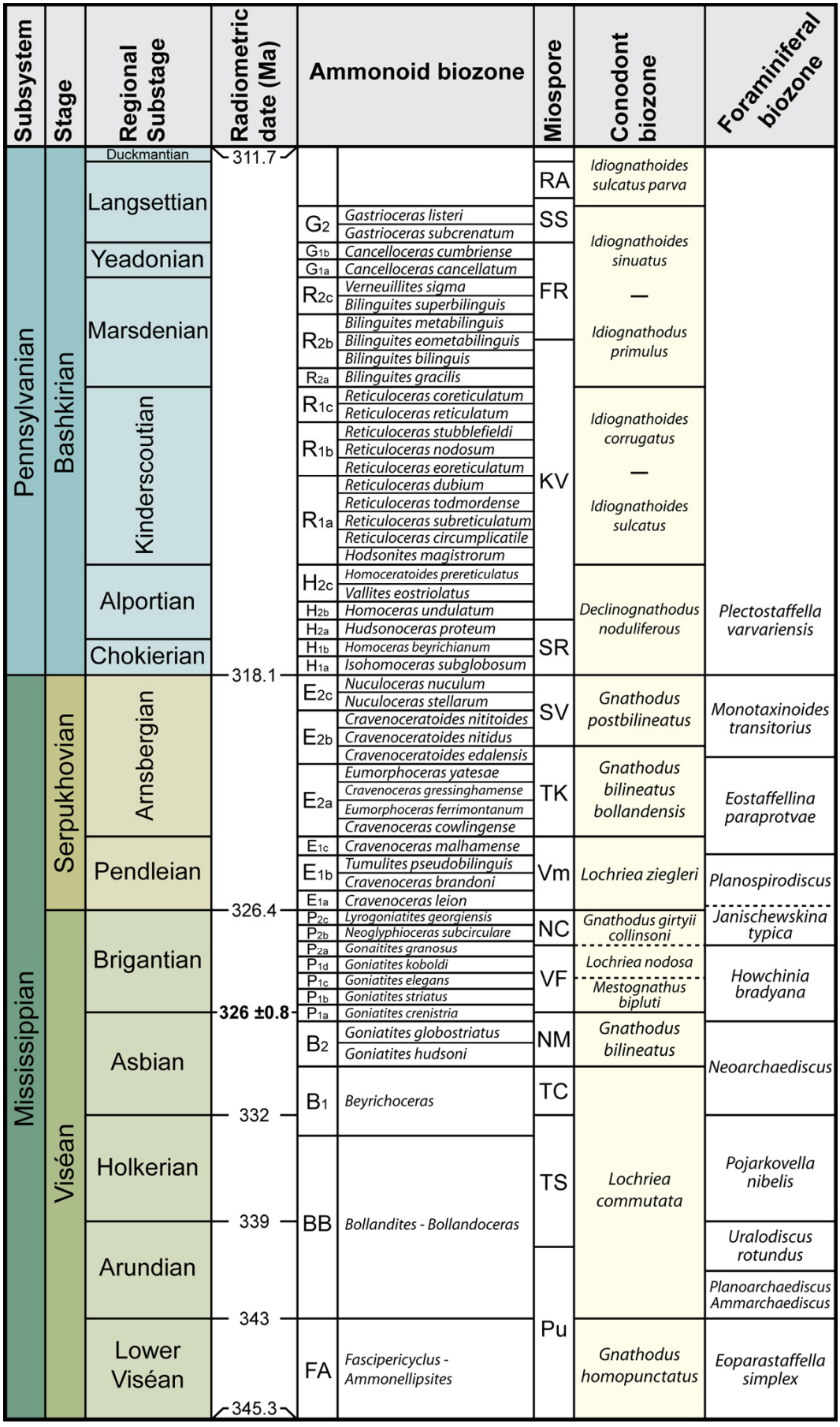

Fig. 1.2.1a Comparison of biozonation schemes for part of the Carboniferous.

From previous Fig. 1.2.1a. Modified from Sevastopulo (2009) and Sevastopulo & Wyse Jackson (2009) with contributions taken from Alekseev et al. (1996), Brandon & Hodson (1984), Jones & Somerville (1996), Korn & Kaufmann (2009), Riley (1993) and Varker & Sevastopulo (1985) with colours according to CGMW.

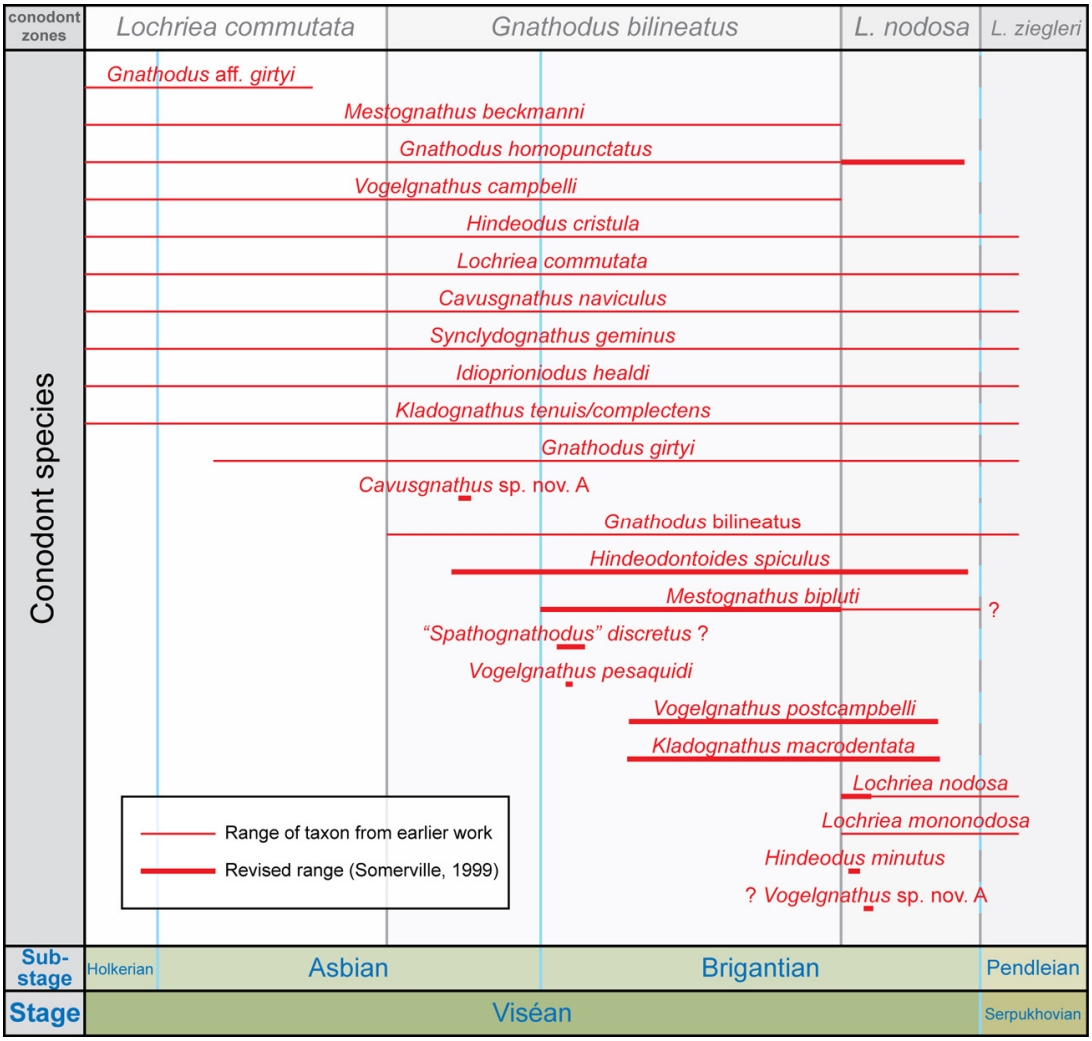

Fig. 1.2.1b Biostratigraphic ranges of some upper Viséan conodont species.

Modified from Somerville (1999) with Stage and Sub-stage colours according to the CGMW.

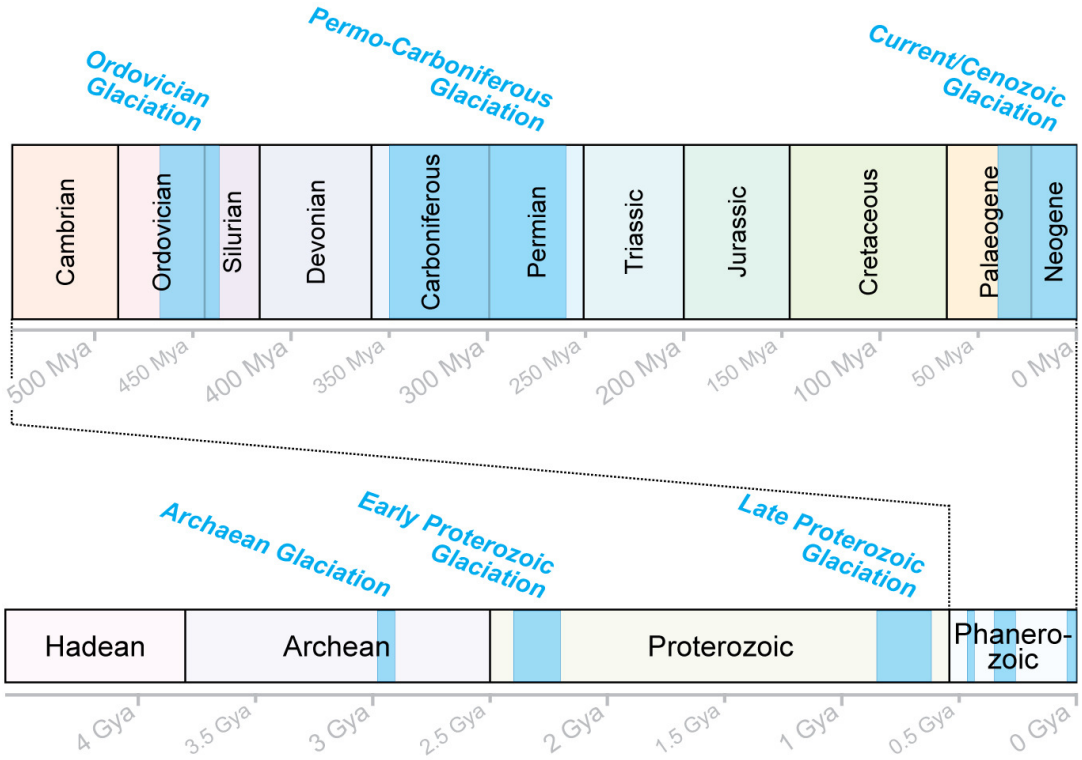

Fig. 1.3 Significant Ice-Ages in Earth's history.

Schematic diagram illustrating the temporal distribution of geological evidence for the largest glacial periods which are shown in transparent blue (largely sourced from Crowell, 1999).

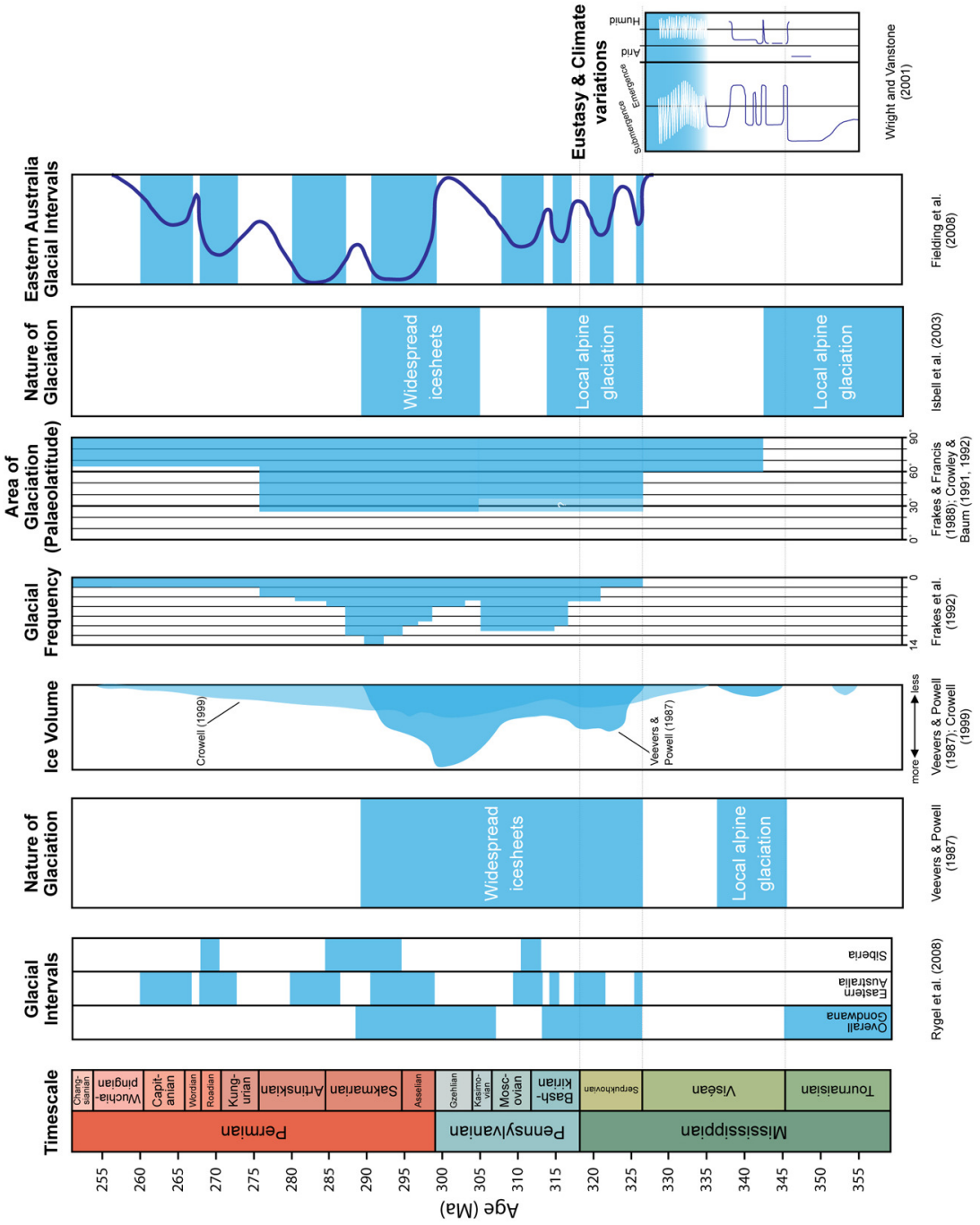

Fig. 1.3.1a Comparison of the timing of onset of the Carboniferous glaciation.

Blue portions represent an interval identified as being significantly cool with resulting ice advance. Note that, despite the confusion between the models, the Viséan-Serpukhovian boundary is widely recognised as a time of either ice-sheet initiation or significant growth. Figure modified from Fielding et al.(2008), data from multiple sources (Crowell, 1999; Crowley & Baum, 1991, 1992; Fielding et al., 2008; Frakes & Francis, 1988; Frakes et al., 1992; Isbell et al., 2003; Rygel et al., 2008; Veevers & Powell, 1987; Wright & Vanstone, 2001) and colours according to the CGMW.

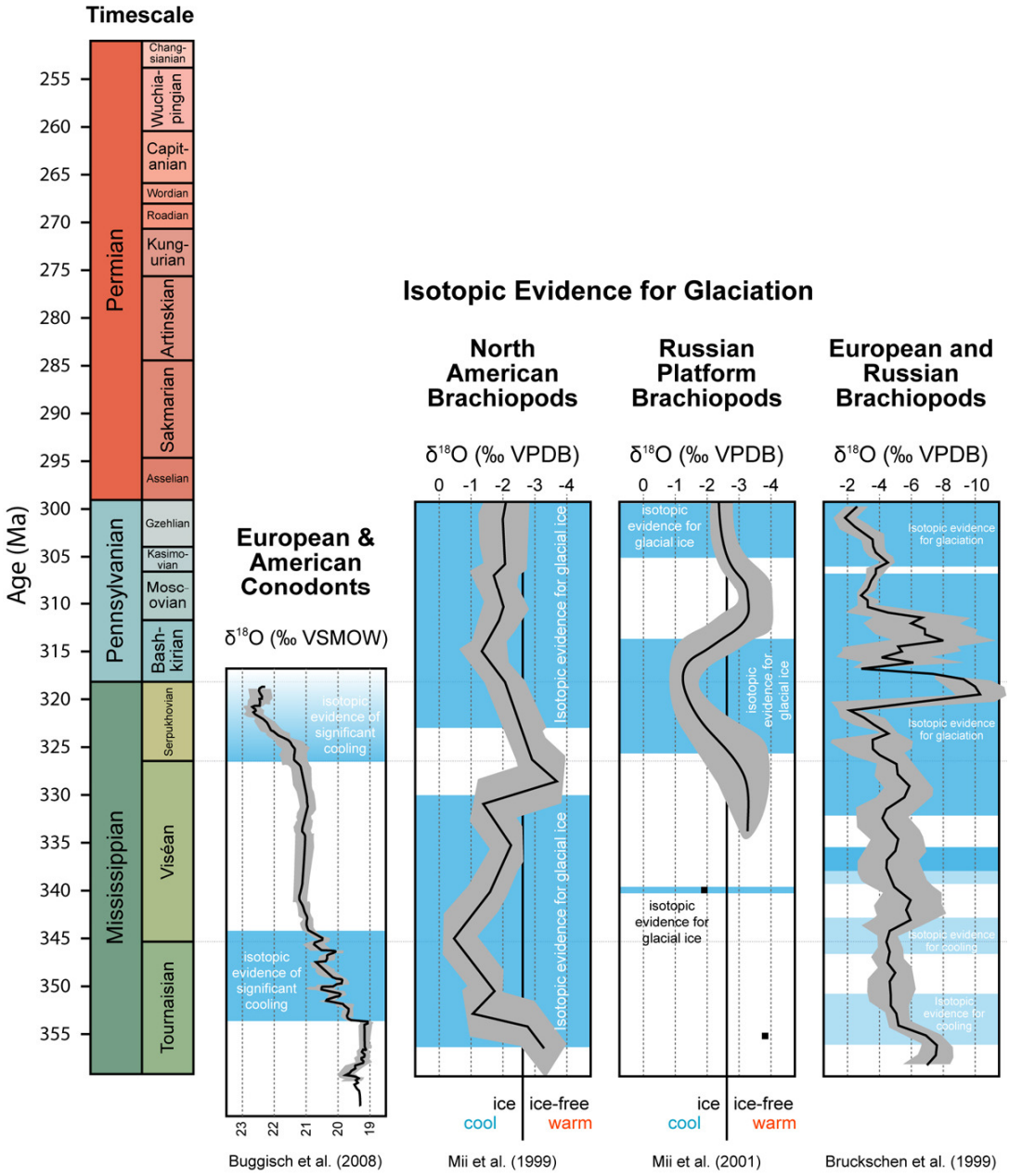

Fig. 1.3.1b Comparison of isotopic models for the timing of the Carboniferous glaciation.
Some of the more significant isotopic studies of the Carboniferous are shown. Of note is that despite their conflicting patterns, all studies recognise cooling in the Serpukhovian with a peak in the mid to late Serpukhovian. Data from multiple sources (Bruckschen et al., 1999; Buggisch et al., 2008; Mii et al., 1999; 2001), geological timescale from Rygel et al. (2008) and colours according to the CGMW.

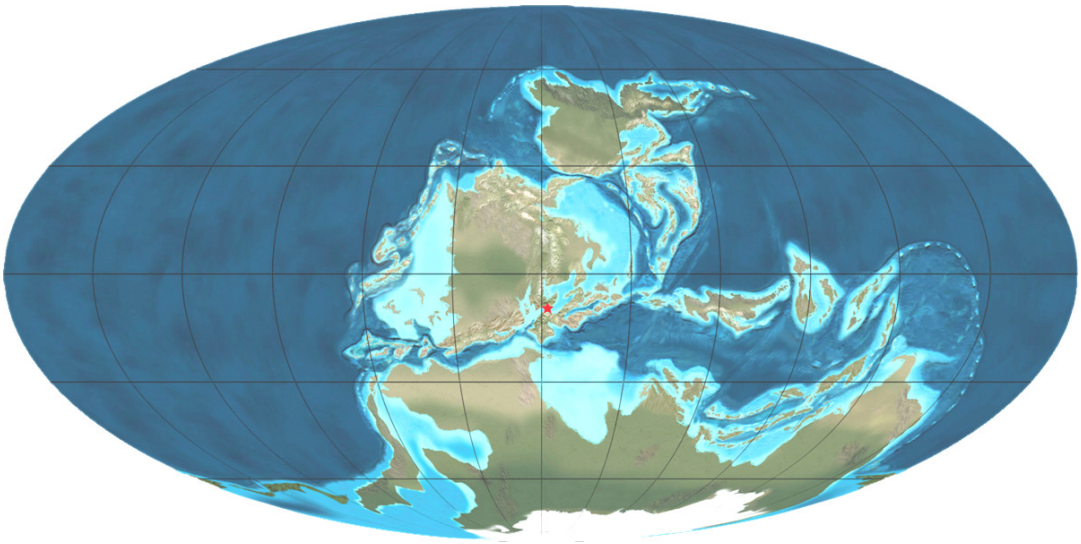

Fig. 1.4a Palaeogeographic map of the world during the Mississippian, c.340Mya.
Red star equates to the position of Ireland during this time. Modified from Blakey (2009).

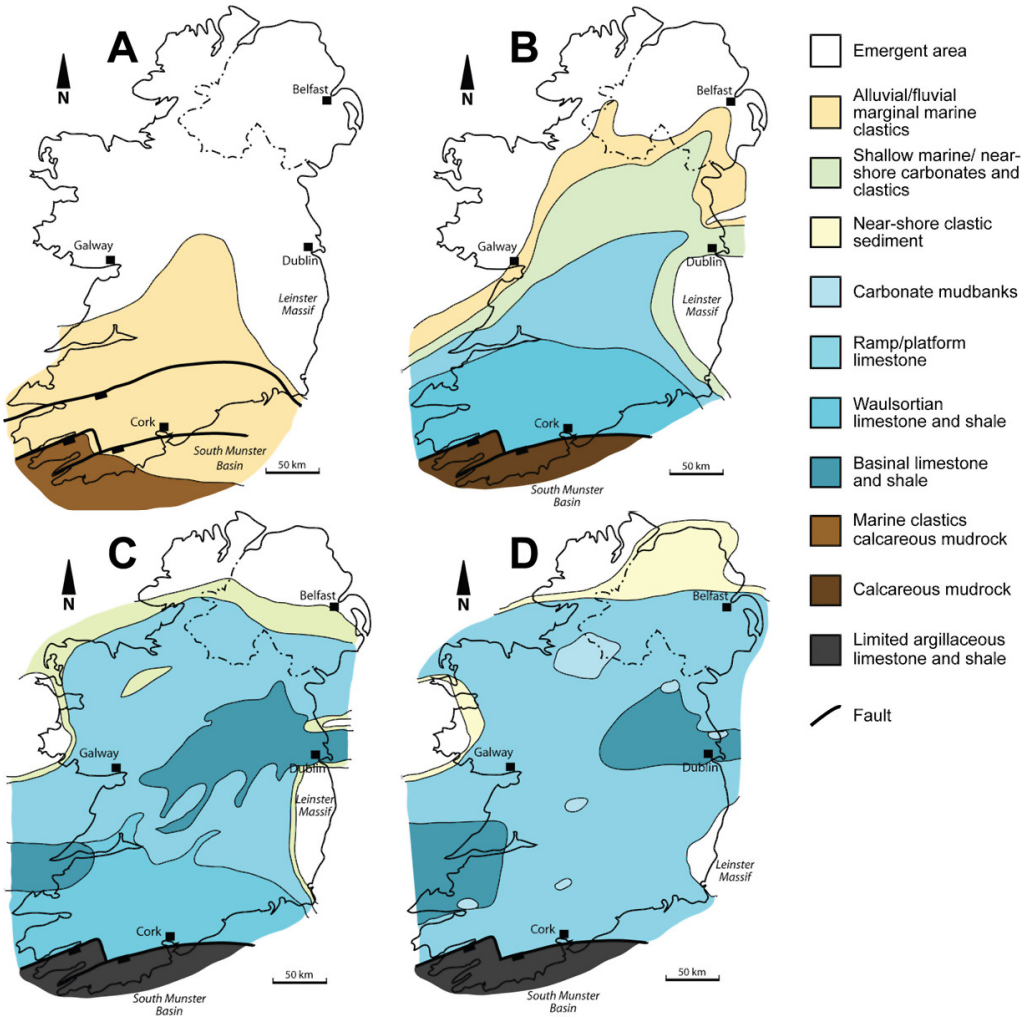

Fig. 1.4b Time series of the Carboniferous marine transgression in Ireland.
A – late Devonian, B – mid Tournaisian, C – mid Viséan and D – mid-late Viséan. Compiled from Anderson et al. (1995) and Sevastopulo & Wyse-Jackson (2009).

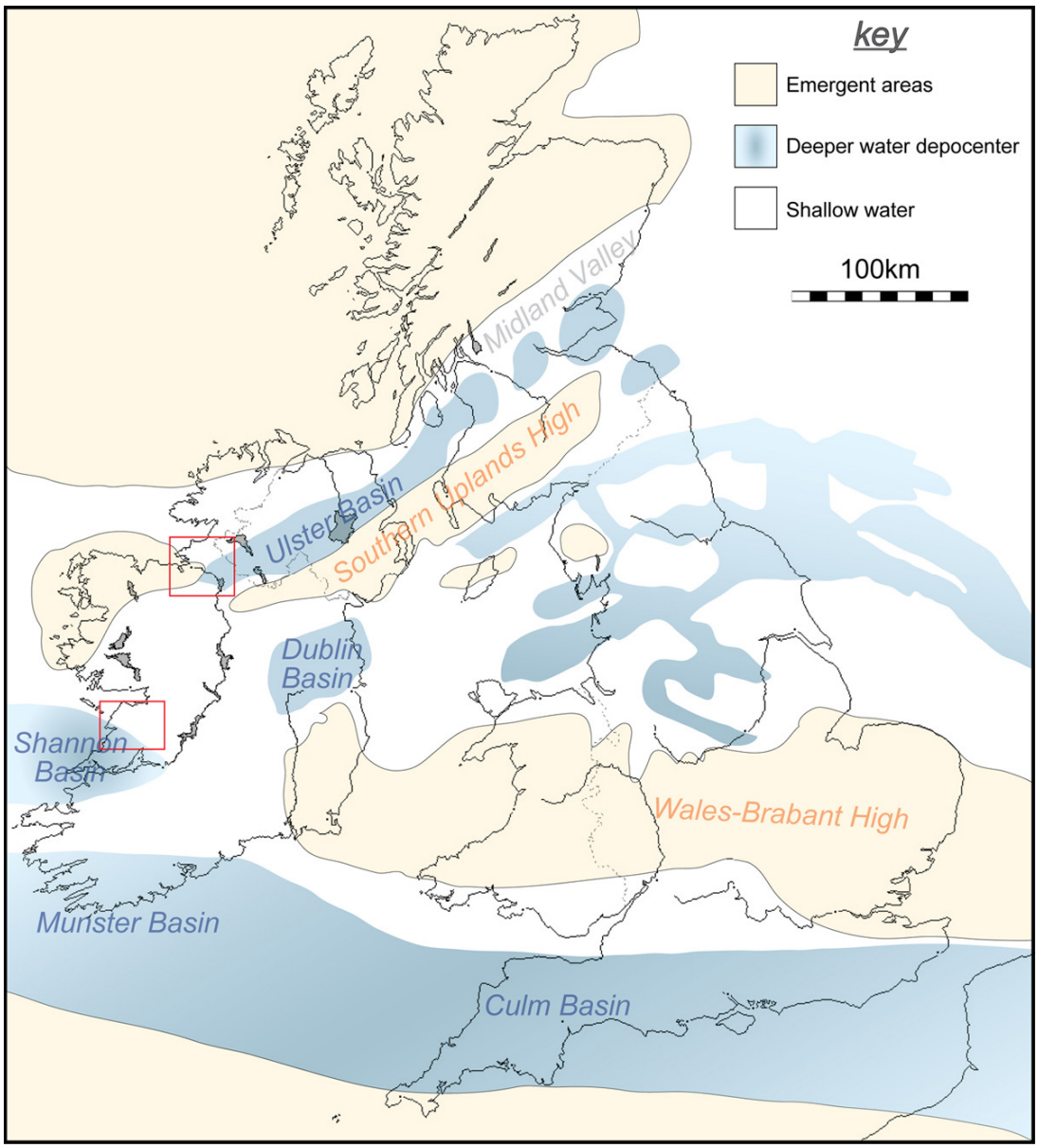

Fig. 1.4c Late Mississippian palaeo-configuration of Britain and Ireland.

The map broadly demonstrates the areas of emergence, shallow water deposition and basin development during the late Viséan. The red boxes correspond to Figs. 1.5a and 1.5b which show the geology of the study areas. Modified from Davies (2008) and Timmerman (2004).

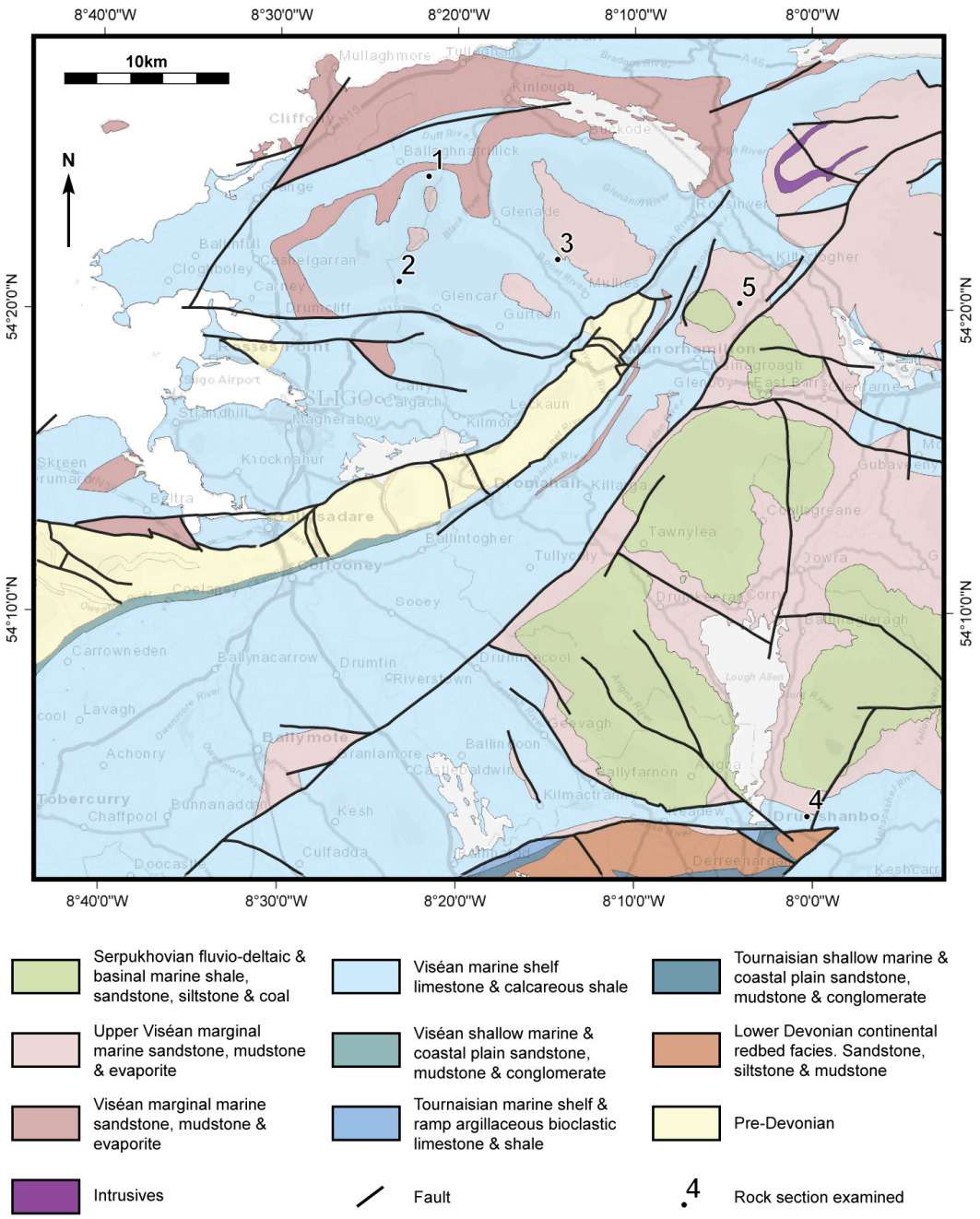

Fig. 1.5.1a Sections examined in northwest Ireland.

See Fig. 1.4c for the broader geographical context of the area covered here. Numbers refer to Sections described in Chapter 2. ***1*** *– Tievebaun (GL03),* ***2*** *– Glencar (DAGL),* ***3*** *– Glenade (DAGN),* ***4*** *– Aghagrania (AGHA),* ***5*** *– Carraun/Lugasnaghta (CNLG). Geology shown as mapped by the Geological Survey of Ireland 1:500,000.*

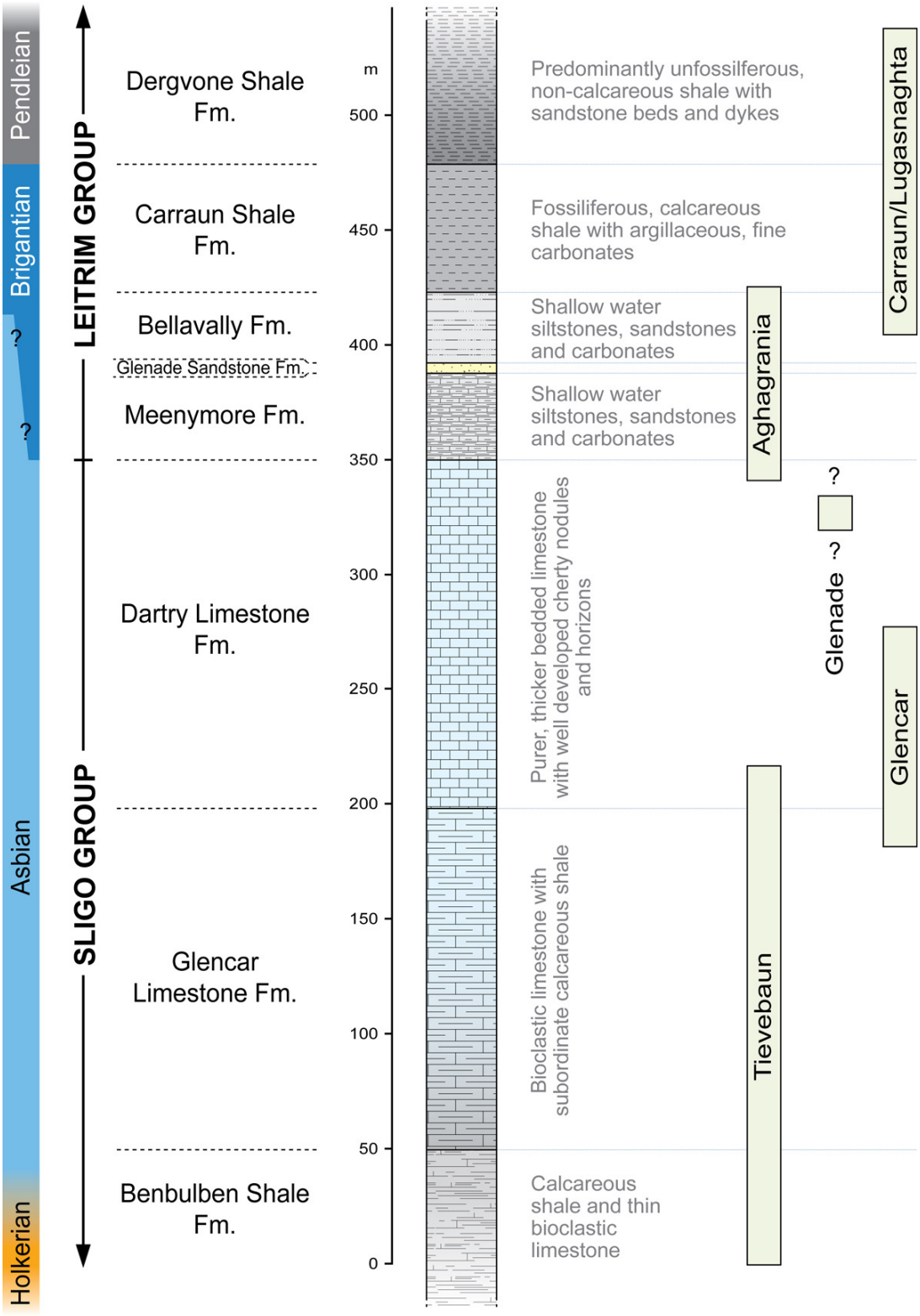

Fig. 1.5.1b Stratigraphy of the NW field area, Counties Sligo and Leitrim.

Thicknesses of the formations listed on the left are illustrated as seen in the sections examined. Pale green boxes on the right demonstrate the relative stratigraphy exposed in the named section. Two definitions for the Asbian-Brigantian boundary are shown, with question marks illustrating the uncertainty between the two (see Section 1.5.1).

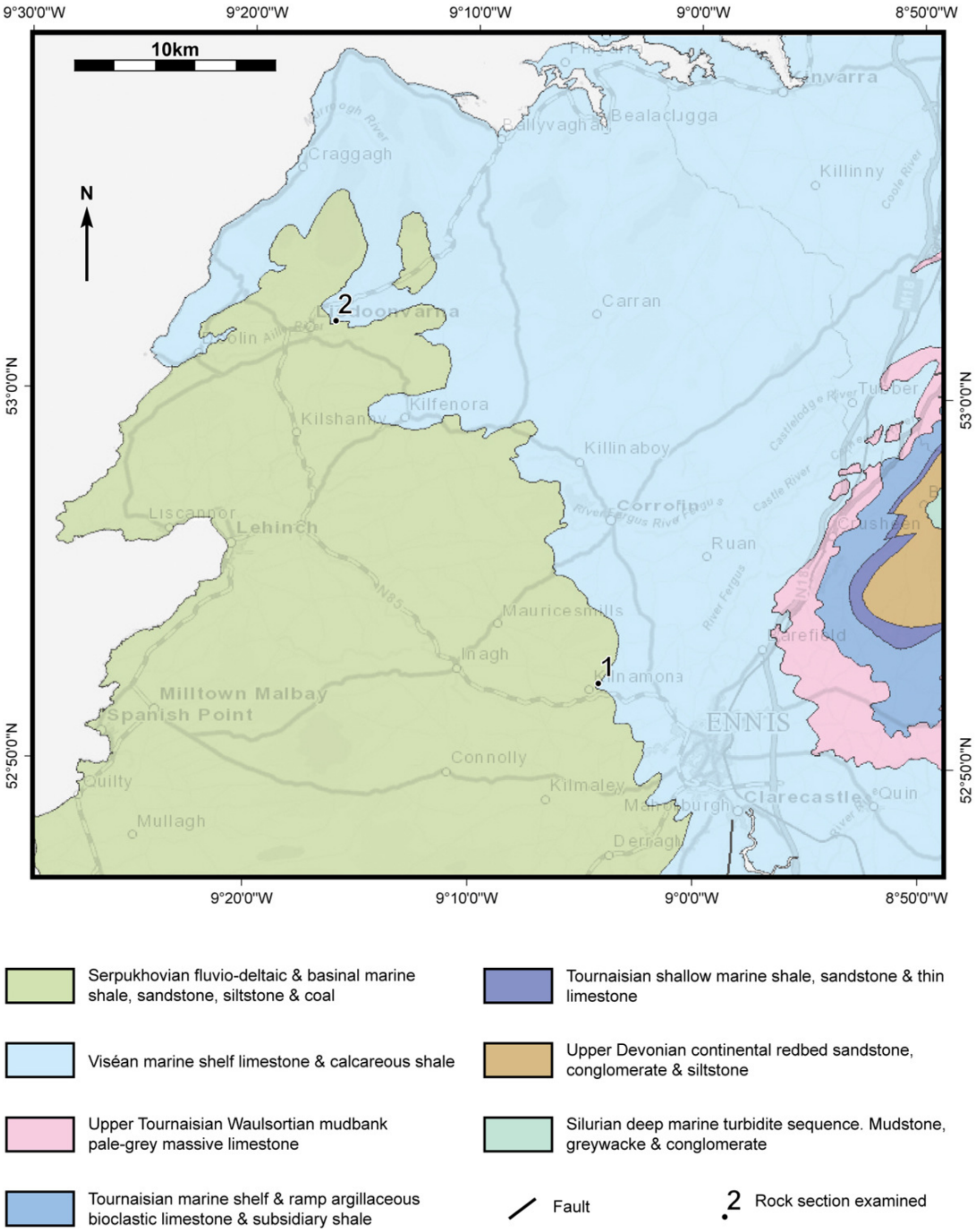

Fig. 1.5.1c Sections examined in the west of Ireland.

See Fig. 1.4c for an indication of the area (relative to the whole of Ireland) covered by this map. Numbers refer to Sections described in Chapter 3. ***1*** *– Kilnamona (KMONA),* ***2*** *– St. Brendan's Well (BW). Geology shown as mapped by the Geological Survey of Ireland 1:500,000.*

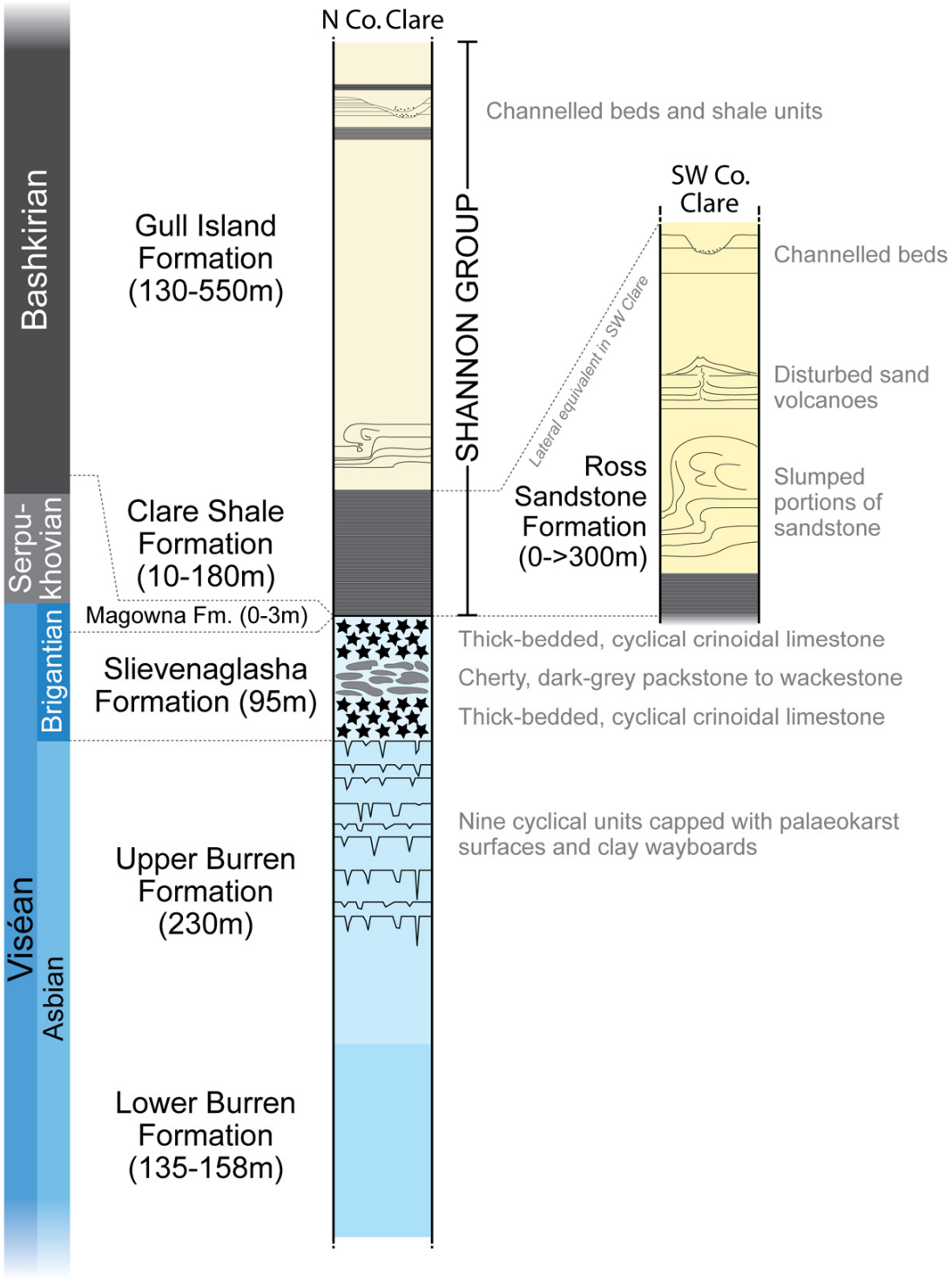

Fig. 1.5.1d Stratigraphy of the Clare region in western Ireland.

Significant lateral variation is apparent in the Clare region. The two sections examined span the immediate interval of the uppermost Slievenaglasha Formation through to the base of the Clare Shale Formation. Viséan stratigraphy modified from Gallagher et al. (2006).

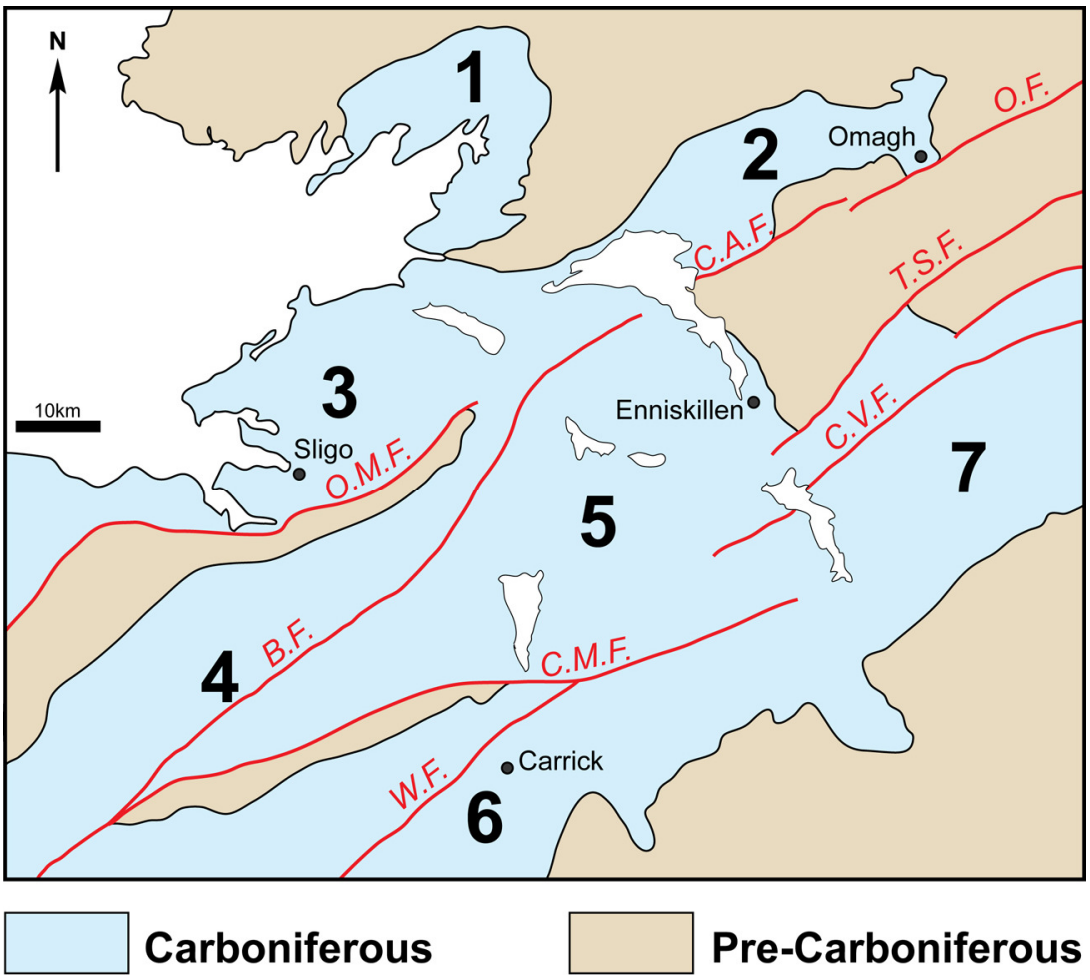

Fig. 2.1a Carboniferous basins in northwest Ireland.

1 *– The Donegal Syncline (George & Oswald, 1957),* ***2*** *– The Omagh Syncline (Simpson, 1953),* ***3*** *– The Sligo Syncline (Oswald, 1955),* ***4*** *– The Ballymote Syncline (Dixon, 1972),* ***5*** *– The Lough Allen Syncline (Brandon, 1968),* ***6*** *– The Carrick Syncline (Caldwell, 1959),* ***7*** *– The Slieve Beagh Syncline (Padget, 1952). Faults;* ***O.M.F.*** *– Ox Mountains Fault,* ***C.A.F.*** *– Castle Archdale Fault,* ***O.F.*** *– Omagh Fault,* ***T.S.F.*** *– Tempo Sixmilecross Fault,* ***C.V.F.*** *– Clogher Valley Fault,* ***B.F.*** *– Belhavel Fault,* ***C.M.F.*** *– Curlew Mountain Fault,* ***W.F.*** *– Woodbrook Fault. Modified from Kelly (1989).*

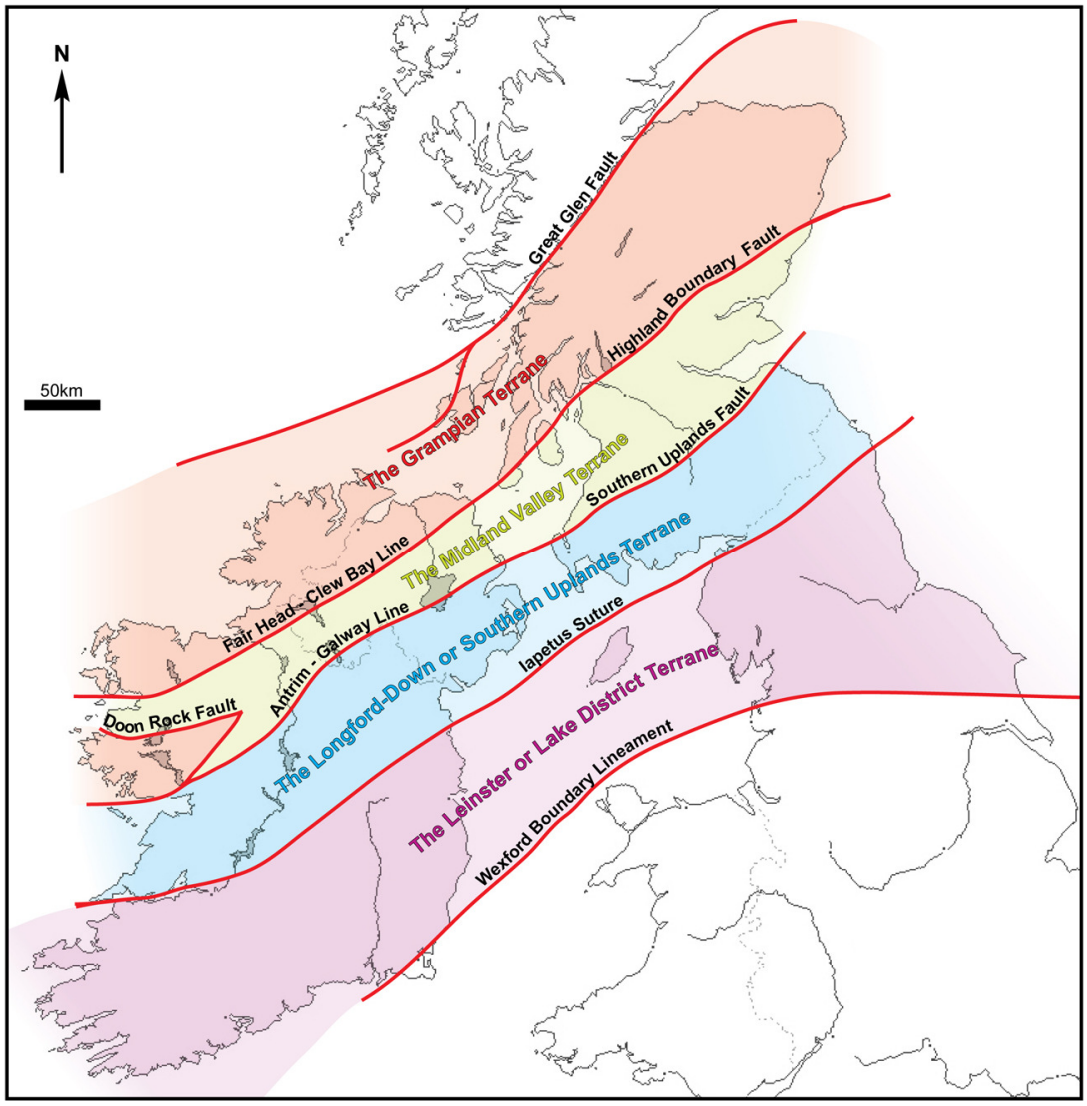

Fig. 2.1b Correlation of major terrane boundaries between Ireland and the UK.

The position and equivalence of significant pre-Carboniferous structures which define the boundaries of important terranes is depicted. Many of the structures continued to play a role in the development of basins during the Carboniferous. Constructed using information sourced from Chew & Stillman (2009) and Woodcock & Strachan (2000).

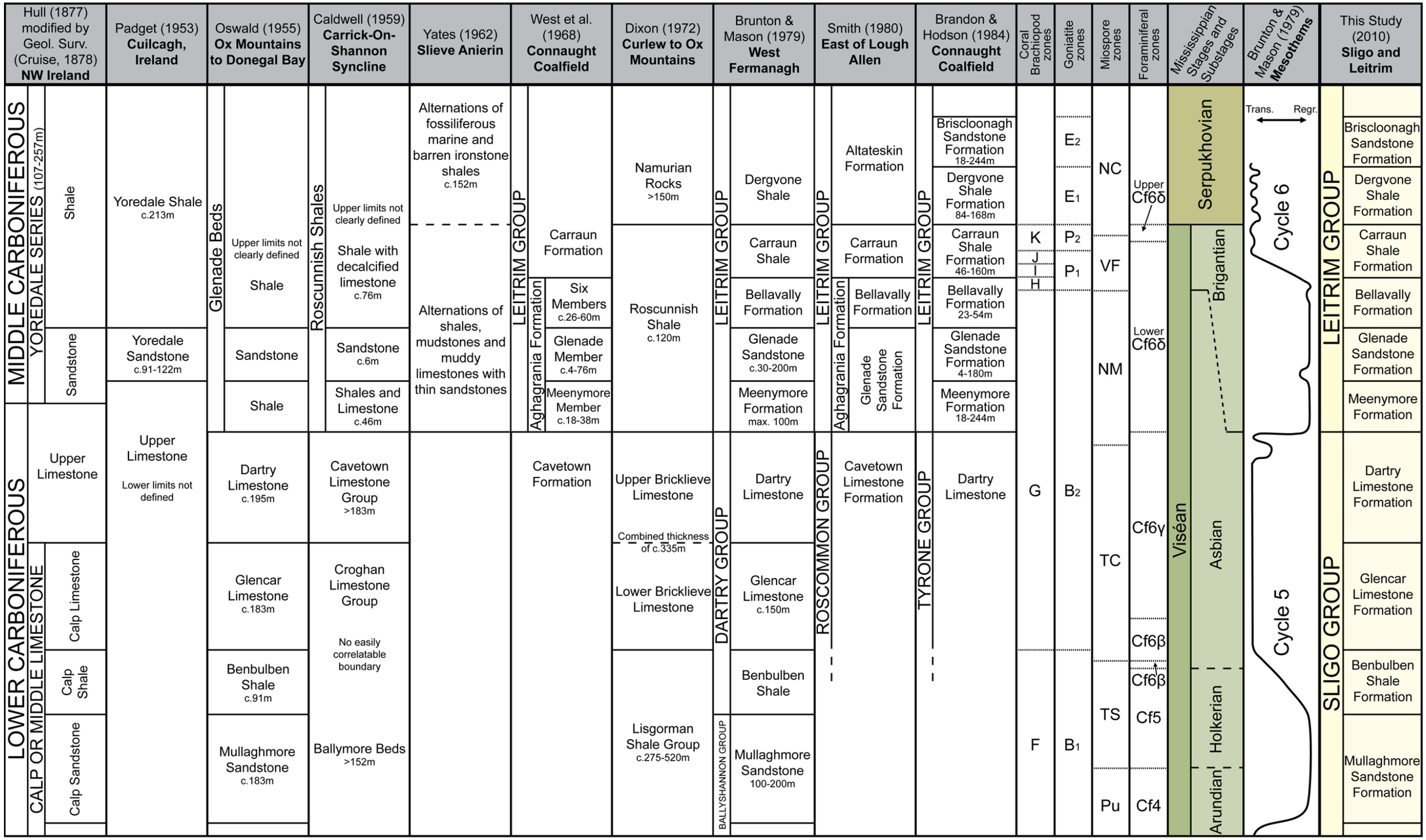

Fig. 2.1c Comparison of terminology used during geological studies in the northwest region of Ireland.

Modified from Brandon & Hodson (1984) with extracts from Brunton & Mason (1979), Caldwell (1959), Cózar et al. (2006), Higgs (1984), Jones & Somerville (1996) and Smith (1980).

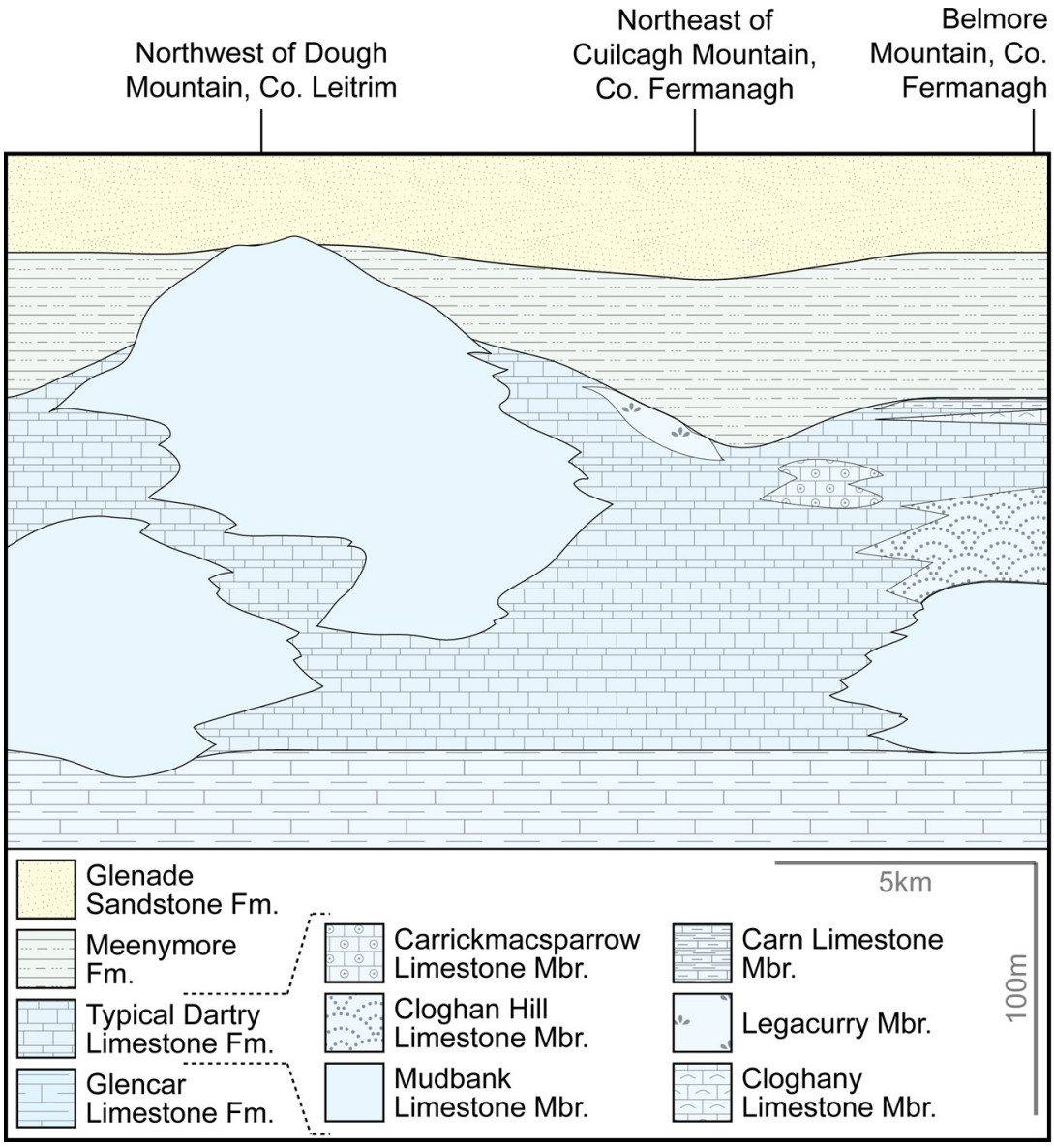

Fig. 2.1.4 Members of the Dartry Limestone Formation.

A schematic interpretation of the relative stratigraphical order of the members of the Dartry Limestone Formation as well as the formations relationship to the bounding Glencar Limestone, Meenymore and Glenade Sandstone Formations is shown. Several points are of note:

(1) The Dartry Limestone Fm. thickens considerably where mudmounds are developed.

(2) The Meenymore Fm. is strongly influenced by the palaeotopography created by the Dartry Limestone Fm.

(3) The Glenade Sandstone Fm. rests directly on top of Dartry Limestone mudmounds where they attained such a palaeotopography that Meenymore Formation sedimentation failed to fill depressions and cover the mounds.

(4) Small-scale, local erosion has been described for all the formational contacts shown.

(5) Members of the Dartry Limestone Formation (bar the mudmounds) are usually only identifiable locally with many of the ones shown described principally from Cuilcagh Mountain and the surrounding highlands in Co. Fermanagh.

The figure is drawn from information predominantly in Brunton & Mason (1979) and Kelly (1996).

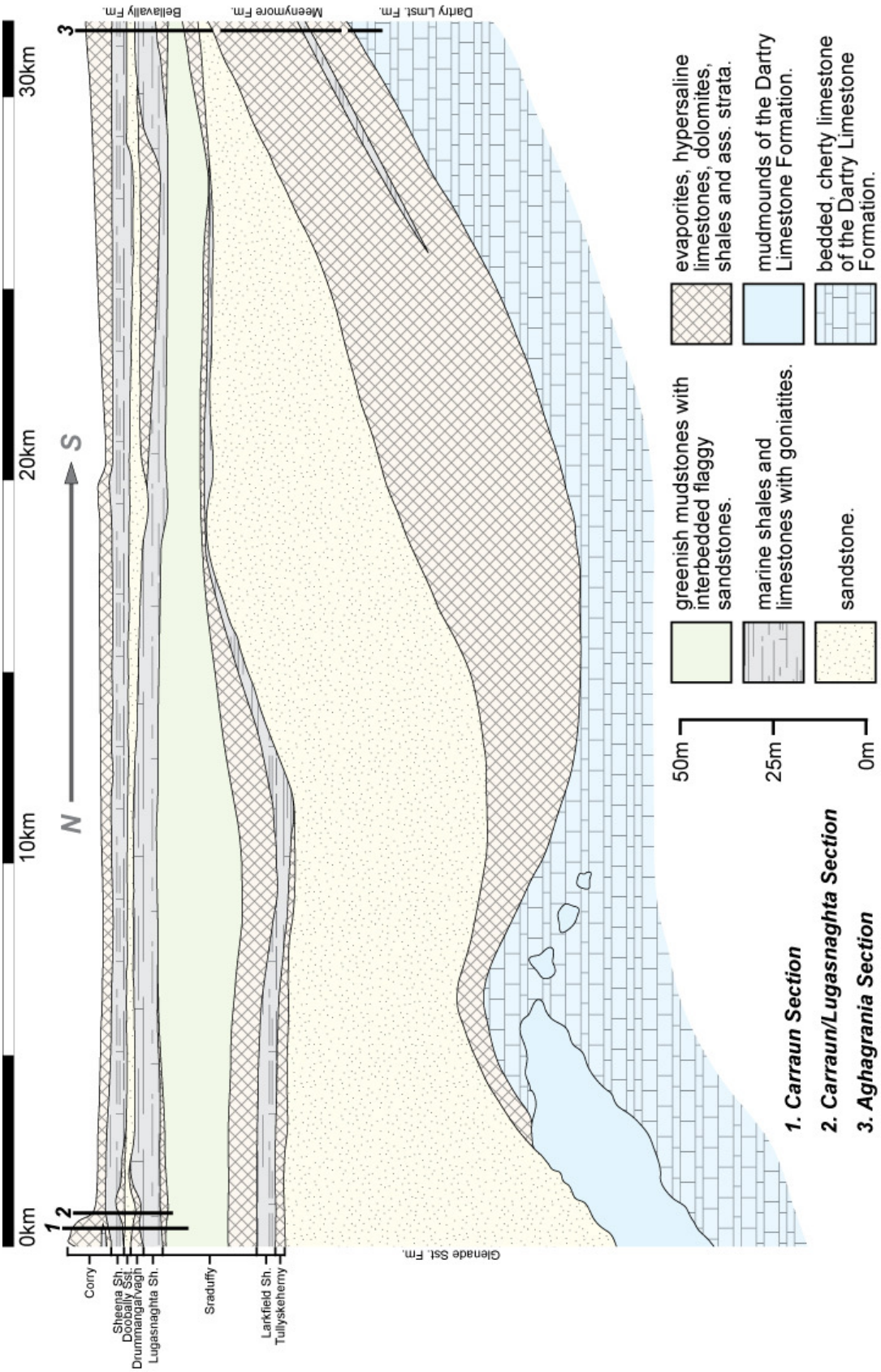

Fig. 2.1.5a Geographical variations in the development of the lower Leitrim Group.

This figure artistically demonstrates how the Dartry Limestone, Meenymore, Glenade Sandstone and Bellavally Formations (and their members) may vary in their development from Dough Mountain (N) to Aghagrania (S). Modified from Brandon & Hodson (1984).

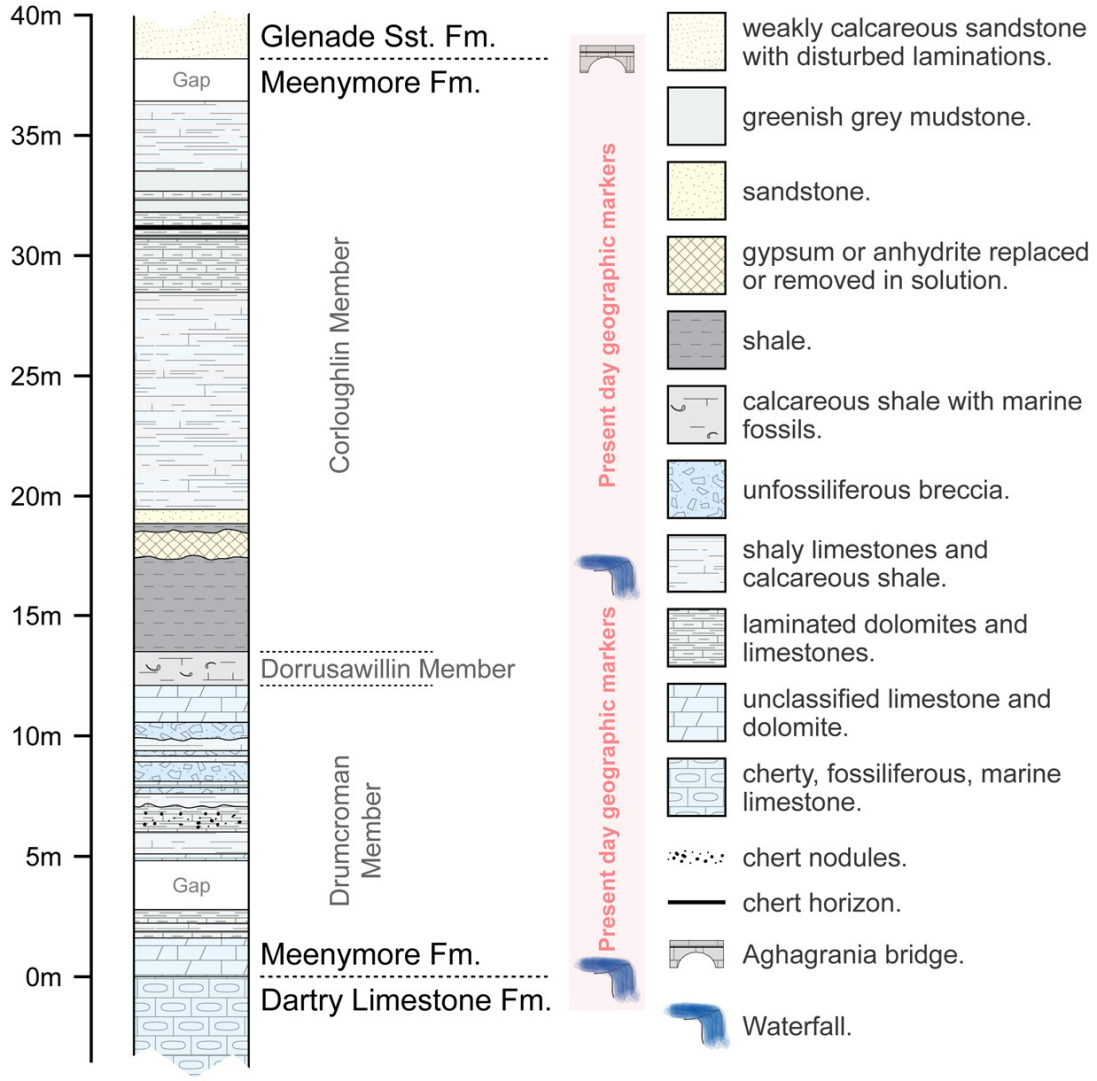

Fig. 2.1.5b Members of the Meenymore Formation in its type section.

The lithological development and stratigraphic relationships of the three members erected in the Meenymore Formation in its type section at Aghagrania, Co. Leitrim is presented. Modified from Smith (1980).

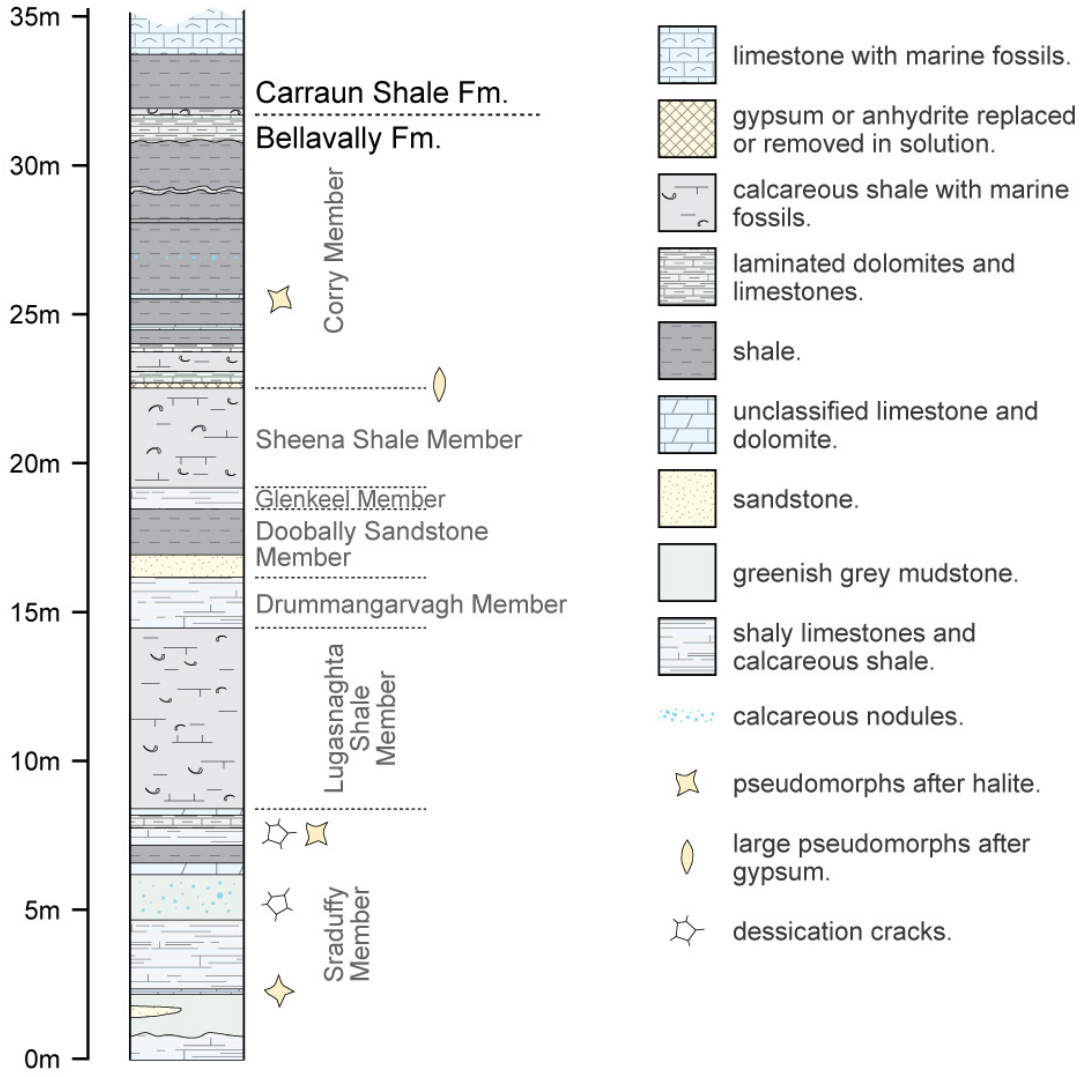

Fig. 2.1.7 Members of the Bellavally Formation at Carraun, Co. Leitrim.

The lithological character and relative thicknesses of the majority of the members of the Bellavally Formation is illustrated, as they are developed in the Carraun Section of Brandon (1968) on the north face of Dough Mountain, Co. Leitrim. Modified from West et al. (1968).

Fig. 2.1.8 Members of the Carraun Shale Formation in its type section.

The relative stratigraphic order, thickness and lithological character of the members of the Carraun Shale Formation is shown, as developed in its type section in the stream between the townlands of Carraun and Lugasnaghta on the north face of Dough Mountain, Co. Leitrim. Modified from MacDermot et al. (1983) and Brandon (1968).

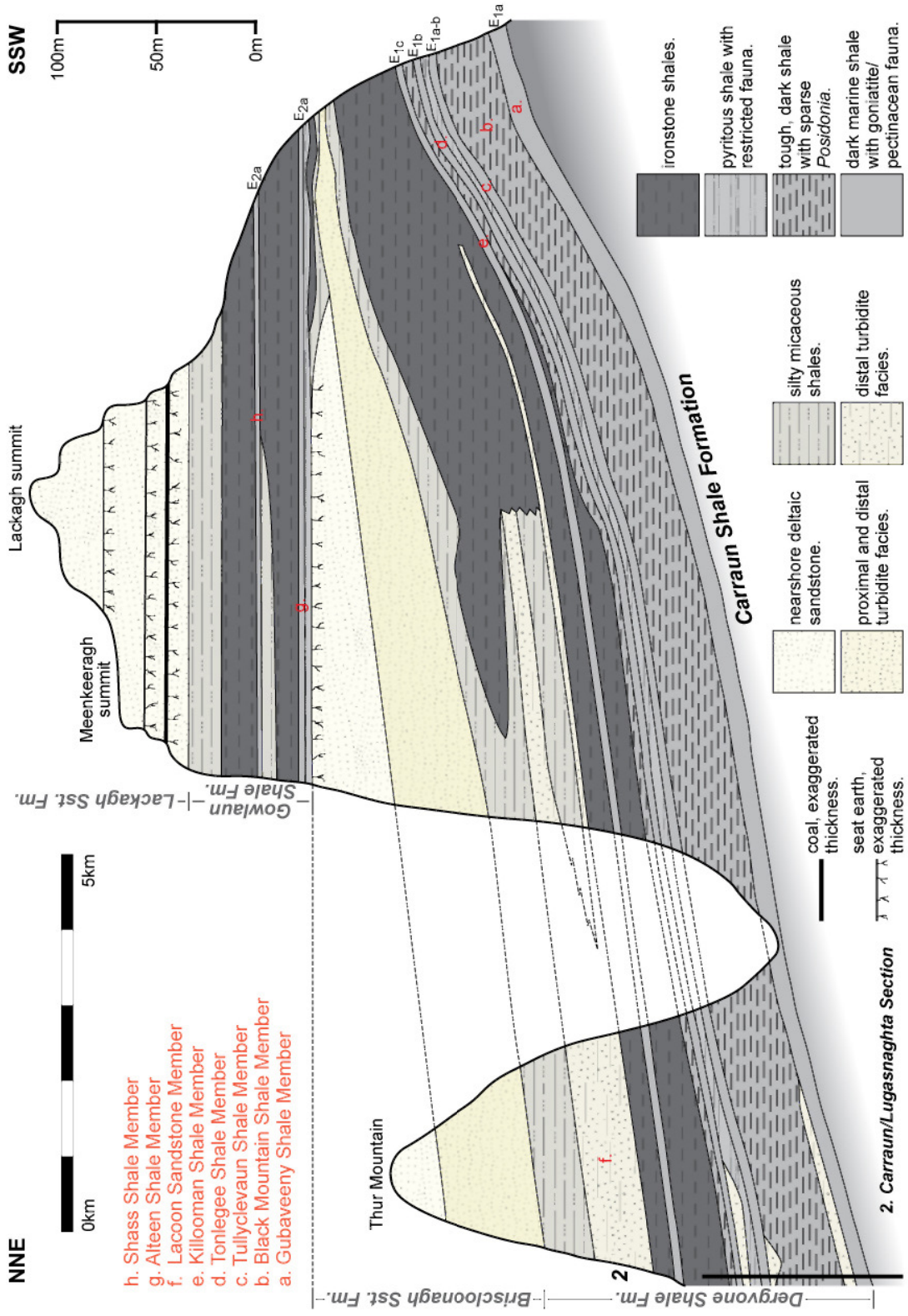

Fig. 2.1.9a Geographical variation in some Serpukhovian strata of the Leitrim Group.

The lateral variability within the Dergvone Shale, Briscloonagh Sandstone, Gowlaun Shale and Lackagh Sandstone Formations from Thur Mountain (NNE) to the summit of Lackagh (SSW) in Co. Leitrim is artistically demonstrated. Modified from Brandon & Hodson (1984).

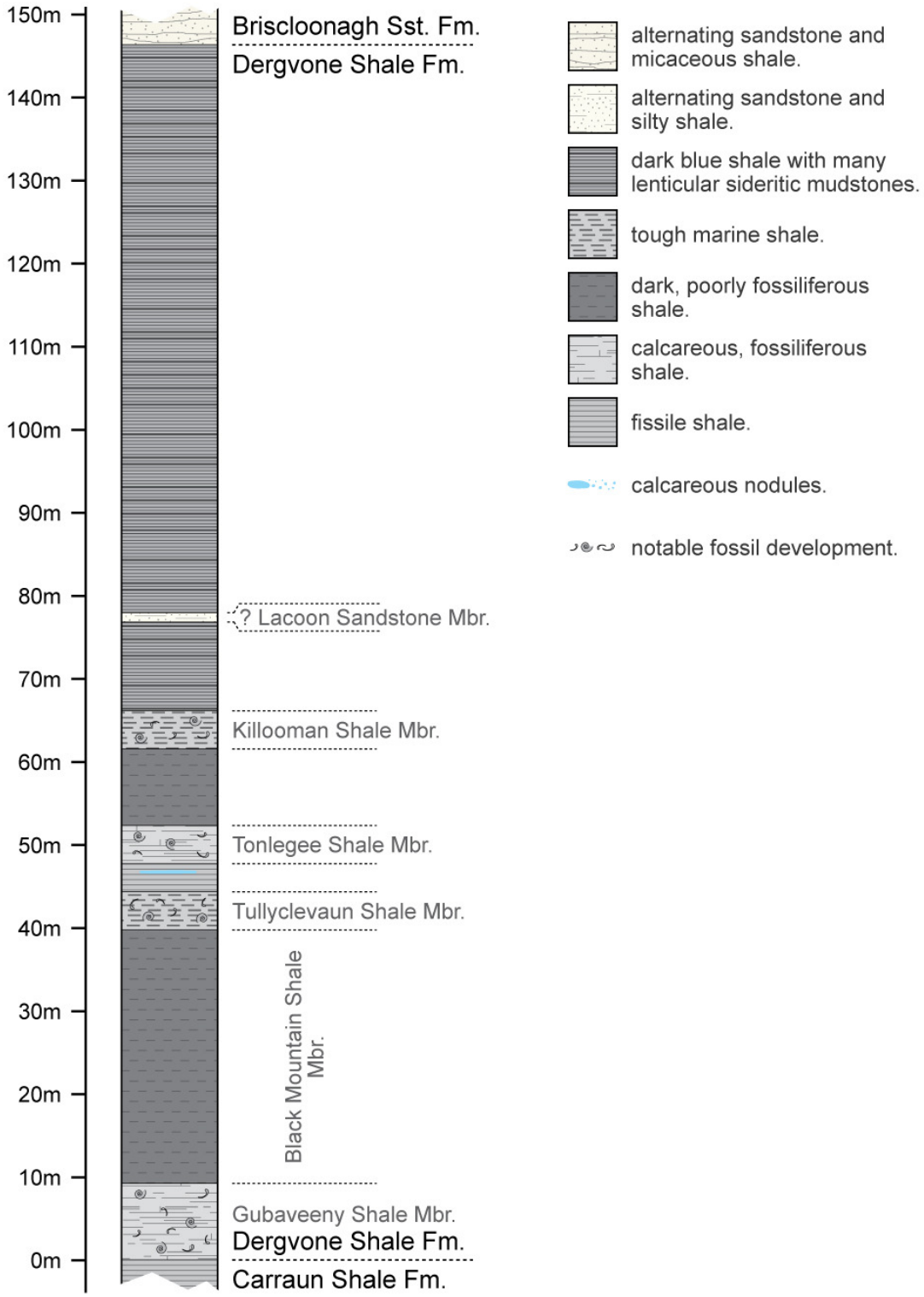

Fig. 2.1.9b Members of the Dergvone Shale Formation in its type section.

The stratigraphic order, lithology and thicknesses of the members of the Dergvone Shale Formation is displayed, as exposed in the formations type section in a stream in the townland of Dergvone, on the east flank of Boleybrack Mountain, County Leitrim. Compiled from Brandon (1968).

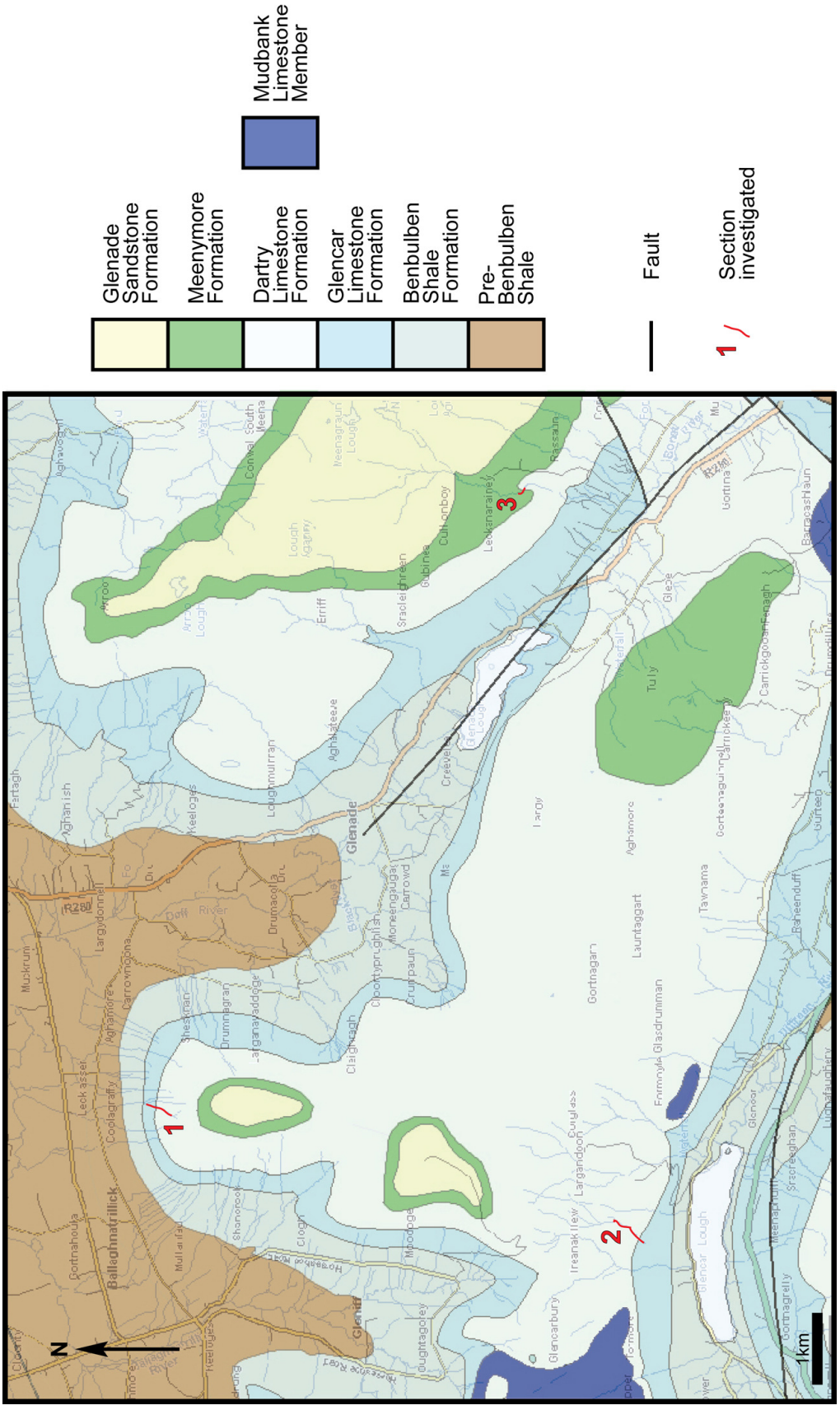

Fig. 2.2 Sligo Group sections studied in northwest Ireland.

Red lines represent the extent of rock sections examined. The simplified geology of the area (GSI 1:100,000) is overlain upon an OSI map. Note that geological boundaries are locally inaccurate. ***1*** *– Tievebaun Section,* ***2*** *– Glencar Section and* ***3*** *– Glenade Section.*

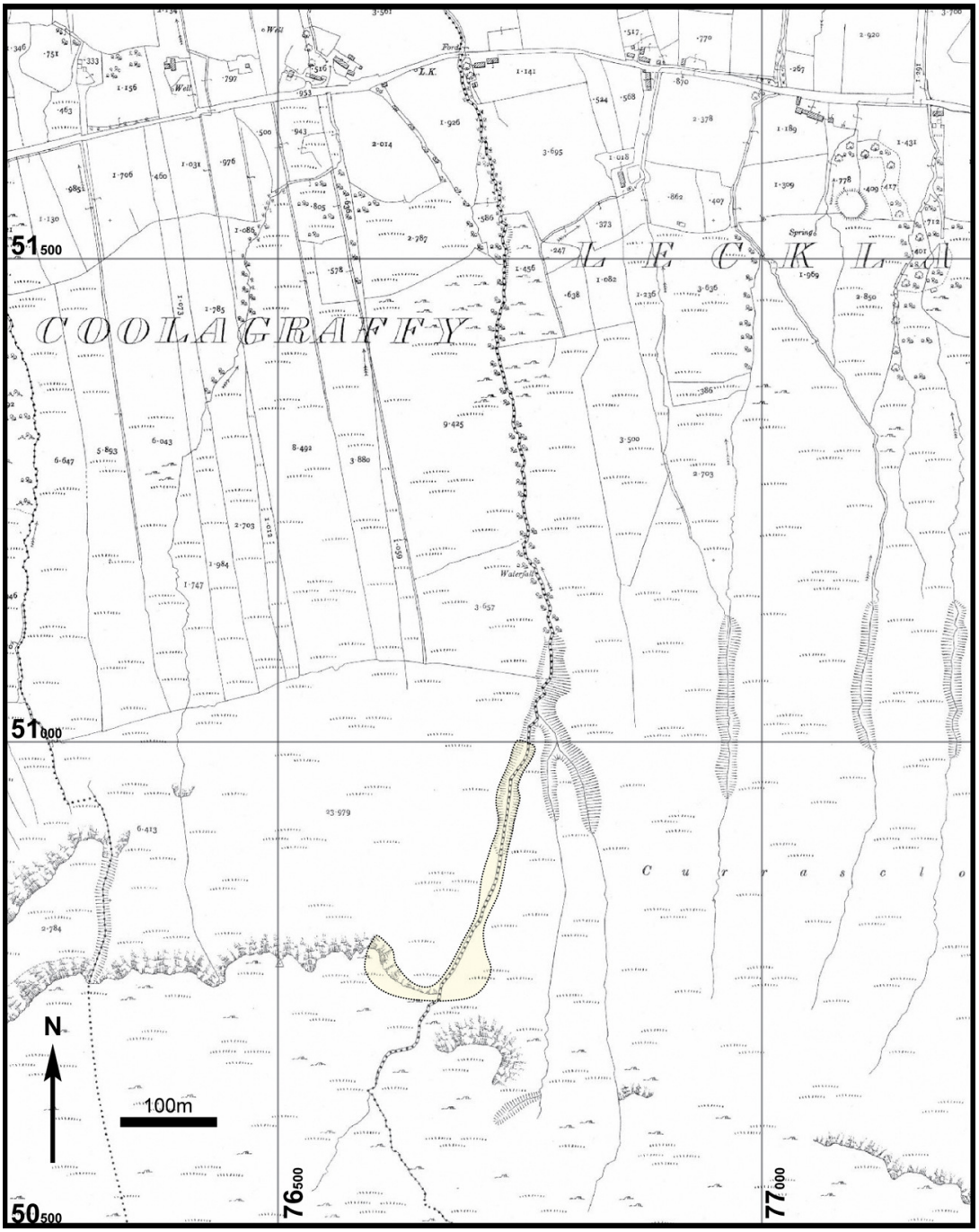

Fig. 2.2.1a Map of the Tievebaun Stream Section.

Gridlines taken from an Ordnance Survey of Ireland 1:50,000 map have been overlain on a 25" to a mile map of the area. The main river in the centre of the figure represents the stream examined, with the section highlighted in yellow.

Fig. 2.2.1b View south towards the prominent tributary exposing the Tievebaun Section.
The section (highlighted by a pale yellow area bound by dotted white lines) follows the stream on the right upwards, eventually finishing at the top of the prominent knoll.

Fig. 2.2.1c Start of the Tievebaun Section.
View upstream to where the section begins at the lowest, small, stepped waterfall in the bottom of the picture.

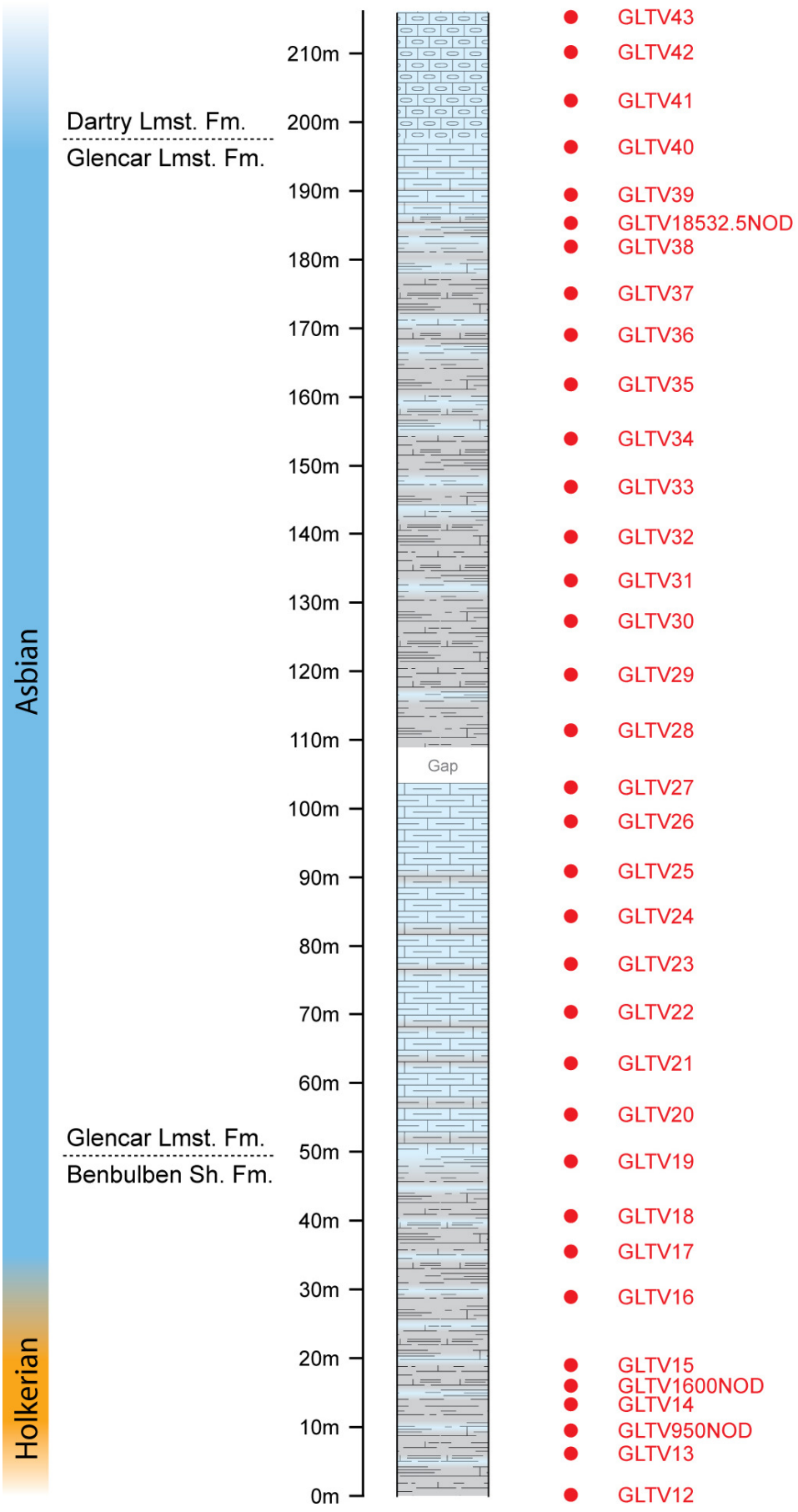

Fig. 2.2.1d Composite log of the Tievebaun Section with sampled horizons marked.

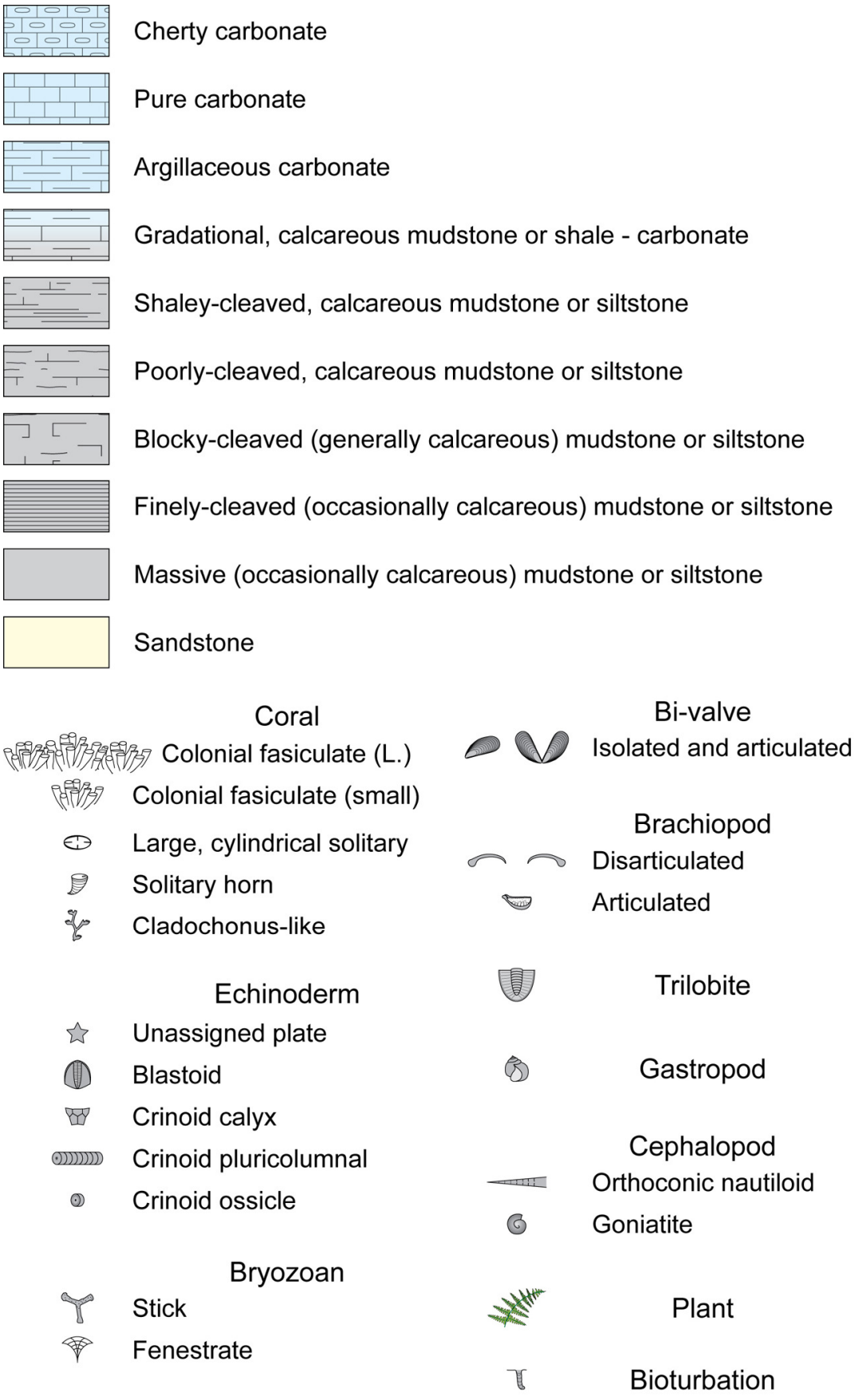

Fig. 2.2.1e Key to logs.

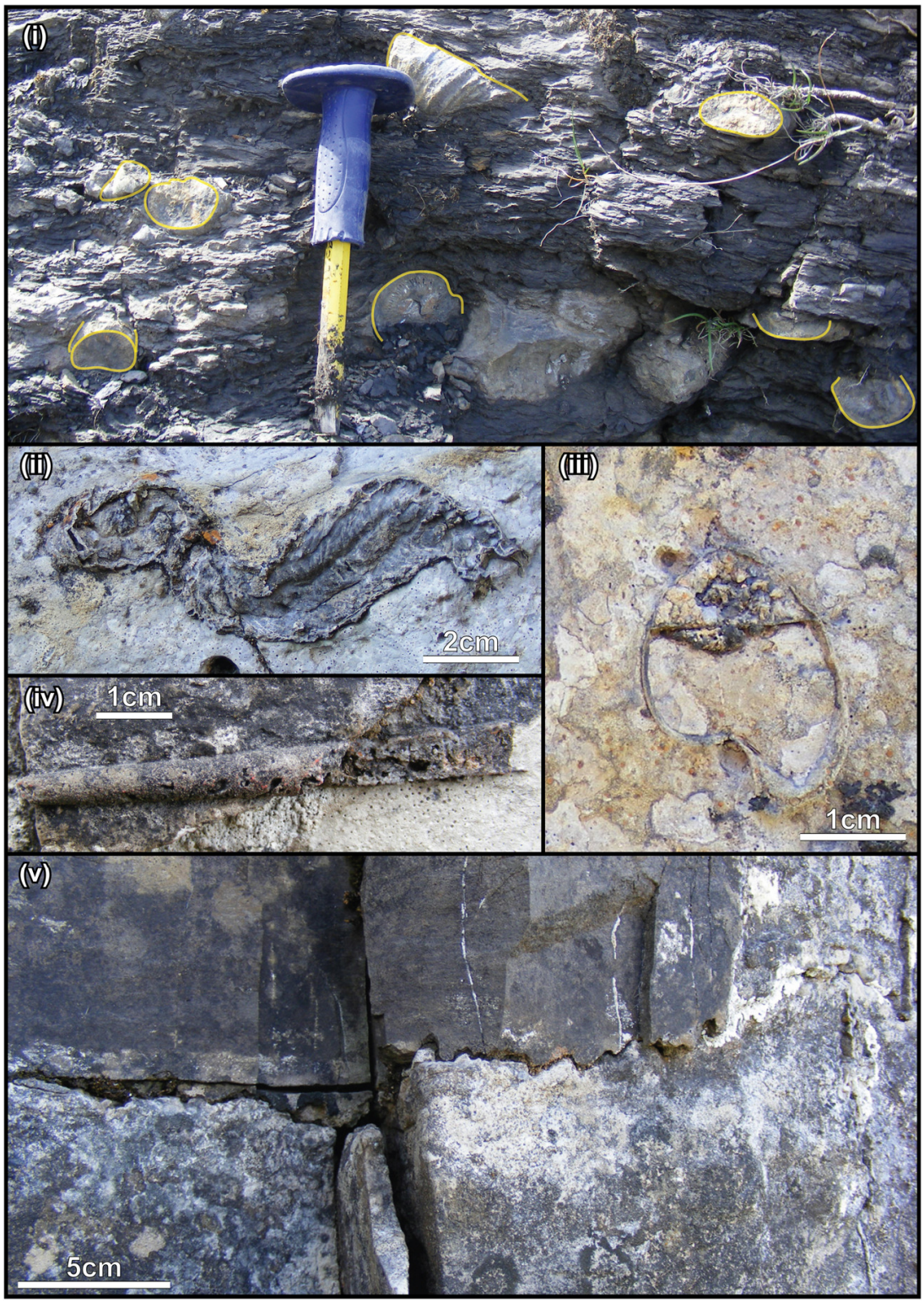

Fig. 2.2.1f Notable structures and fossils in the Tievebaun Section.

(i) *Concentration of large solitary corals (highlighted in yellow) in the Benbulben Shale Formation 3-4m ASB.* ***(ii)*** *Contorted solitary coral, Glencar Limestone Formation ~186m ASB.* ***(iii)*** *Articulated brachiopod geopetal indicating the right way up in the Glencar Limestone Formation, ~185m ASB.* ***(iv)*** *Poorly silicified ?orthocone in the Dartry Limestone Formation, ~212m ASB.* ***(v)*** *Stylolite horizon in the Dartry Limestone Formation, ~203m ASB. Note the smoother weathering of the chert above the stylolite horizon.*

Fig. 2.2.1g Macrofossils from the Tievebaun Section (I).

Scale bars represent 1cm. ***(1)*** *Solitary coral, Benbulben Sh., 3.45m ASB.* ***(2a-b)*** *Ventral and dorsal views of an articulated Orthid brachiopod. Glencar Lmst., ~74m ASB.* ***(3)*** *Ventral view of an articulated Spiriferid brachiopod. Loose.* ***(4a-b)*** *Zaphrentid coral, Benbulben Sh., 20m ASB.* ***(5a-b)*** *Coral colony encrusting a crinoid pluricolumnal, Glencar Lmst., 111m ASB.* ***(6)*** *Ramose bryozoan with remnant of an epibiont. Benbulben Sh., ~1m ASB.* ***(7a-c)*** *Various views of a crinoid pluricolumnal displaying different encrusting organisms. Glencar Lmst., 110m ASB* ***(8)*** *Possible incomplete crinoid holdfast. Glencar Lmst., ~189m ASB.* ***(9-14)*** *Variety of crinoid pluricolumnals, most with significant amounts of cirri. Benbulben Sh. and Glencar Lmst. (11) Note also epibionts.*

Fig. 2.2.1h Macrofossils from the Tievebaun Section (II).

Scale bars represent 1cm. ***(1a-b)*** *Sample with a dense accumulation of trilobite material, some specimens appear complete and partially coiled. Glencar Lmst., 61.5m ASB.* ***(2)*** *Sample with a radiating array of relatively undisturbed fine echinoid spines. Loose.* ***(3)*** *Sample with a variety of fossil material but most significantly, a number of incomplete, thick archaeocidarid (echinoid) spines (see top left of sample). Benbulben Sh., 20m ASB.* ***(4a-b)*** *Ventral and dorsal view of a cladid crinoid crown. Loose.* ***(5)*** *Ventral view of a cladid crinoid crown. Loose.* ***(6)*** *Sample with an accumulation of tuberculate echinoid plates. Glencar Lmst., 118m ASB.*

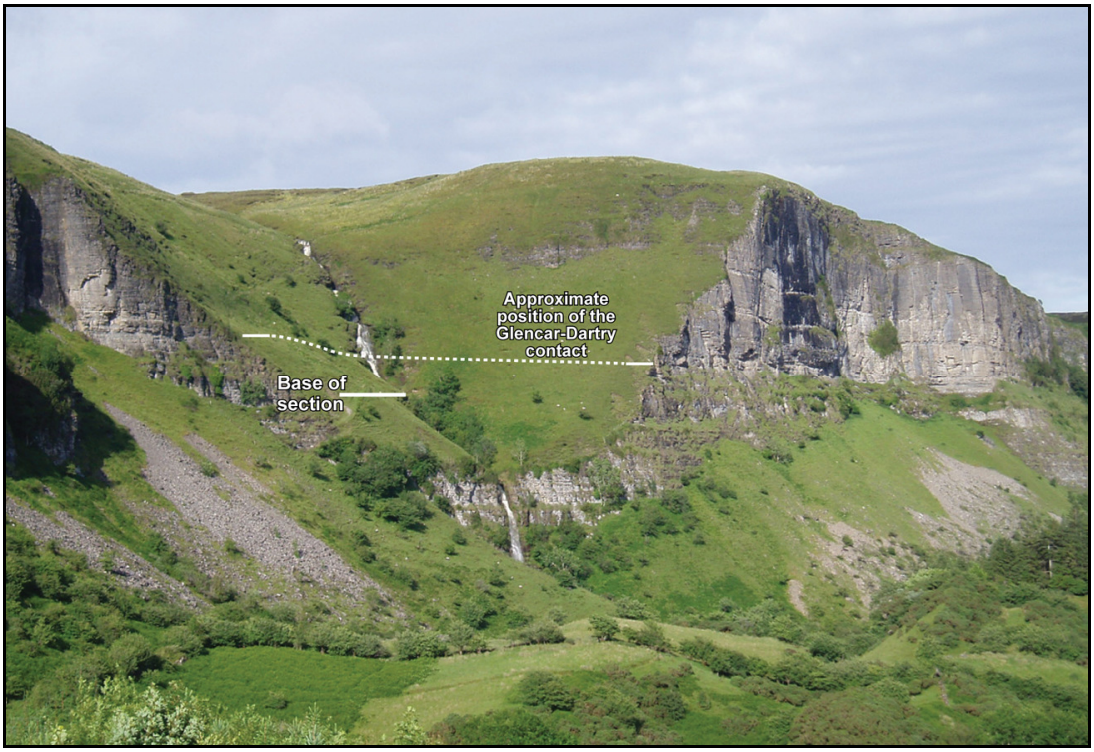

Fig. 2.2.2a Glencar Section, north of the Swiss Valley.

View from the SW towards the stream which cuts the classic cliffs of the Dartry Mountains. The section was examined from where the stream emerges from the lower wooded portion of the hanging valley.

Fig. 2.2.2b Base of the Glencar section.

View from the east bank, towards where the hammer (circled in white) rests on the bed surface of DAGL01 (marked in faded yellow).

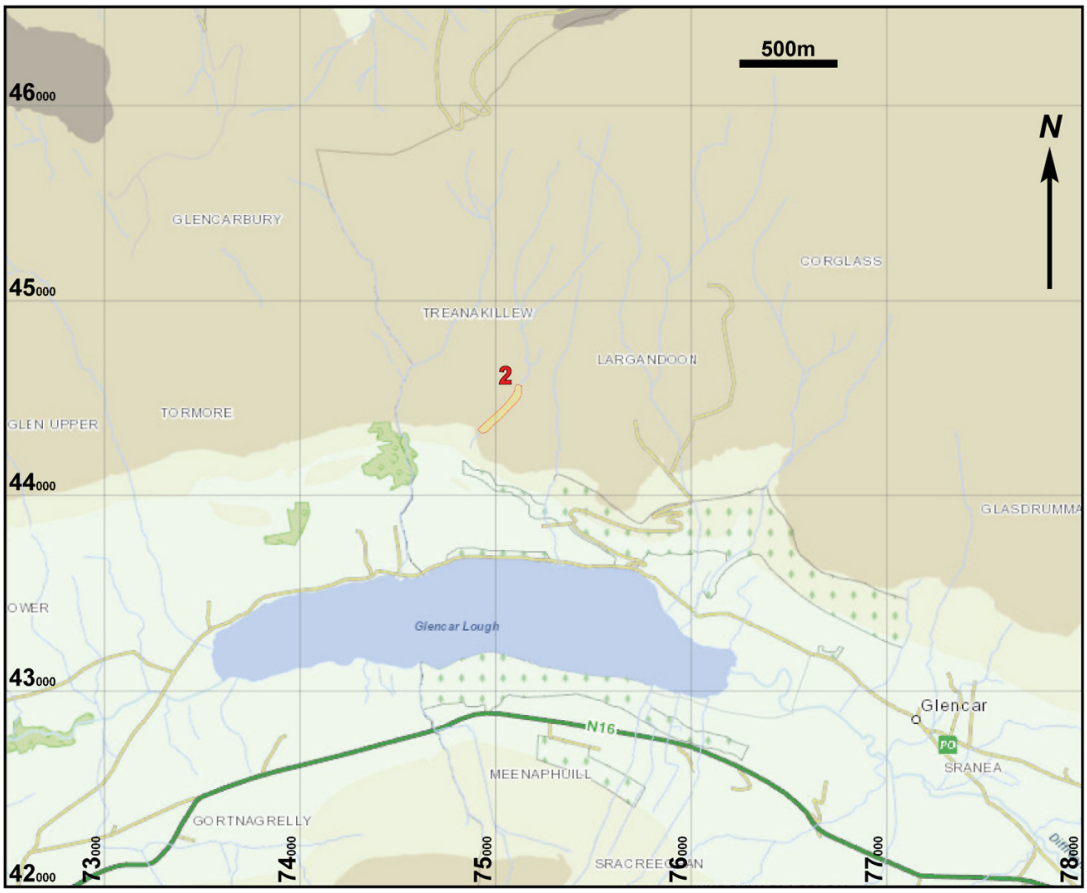

Fig. 2.2.2c Map of the Glencar Stream Section and surrounding area.

Gridlines taken from an Ordnance Survey of Ireland 1:50,000 map have been overlain on a basic geographic map of the area. The portion of the stream representing the Glencar Section is numbered and highlighted.

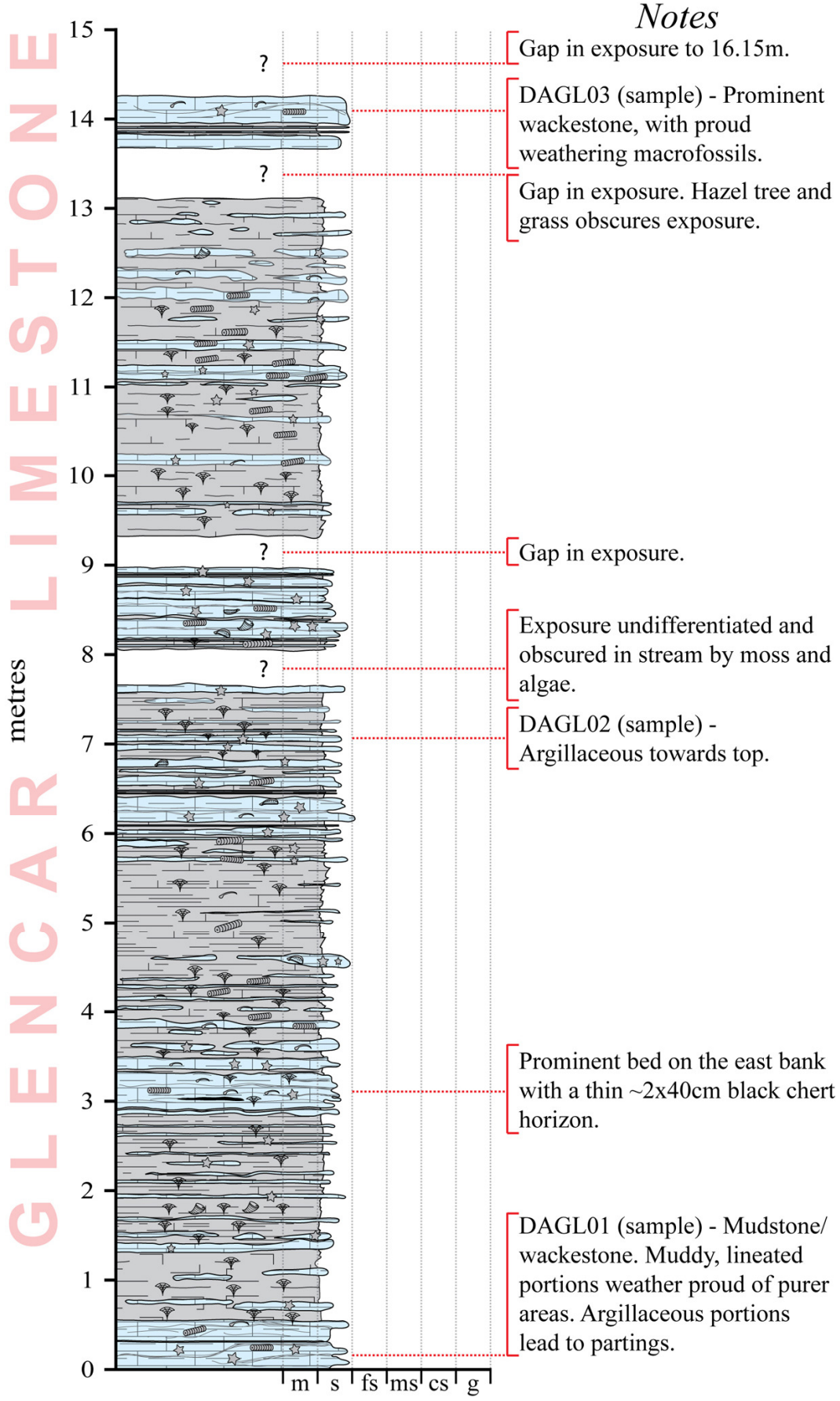

Fig. 2.2.2d Log of the basal ~14m of the Glencar Section.
Key as in Fig. 2.2.1e.

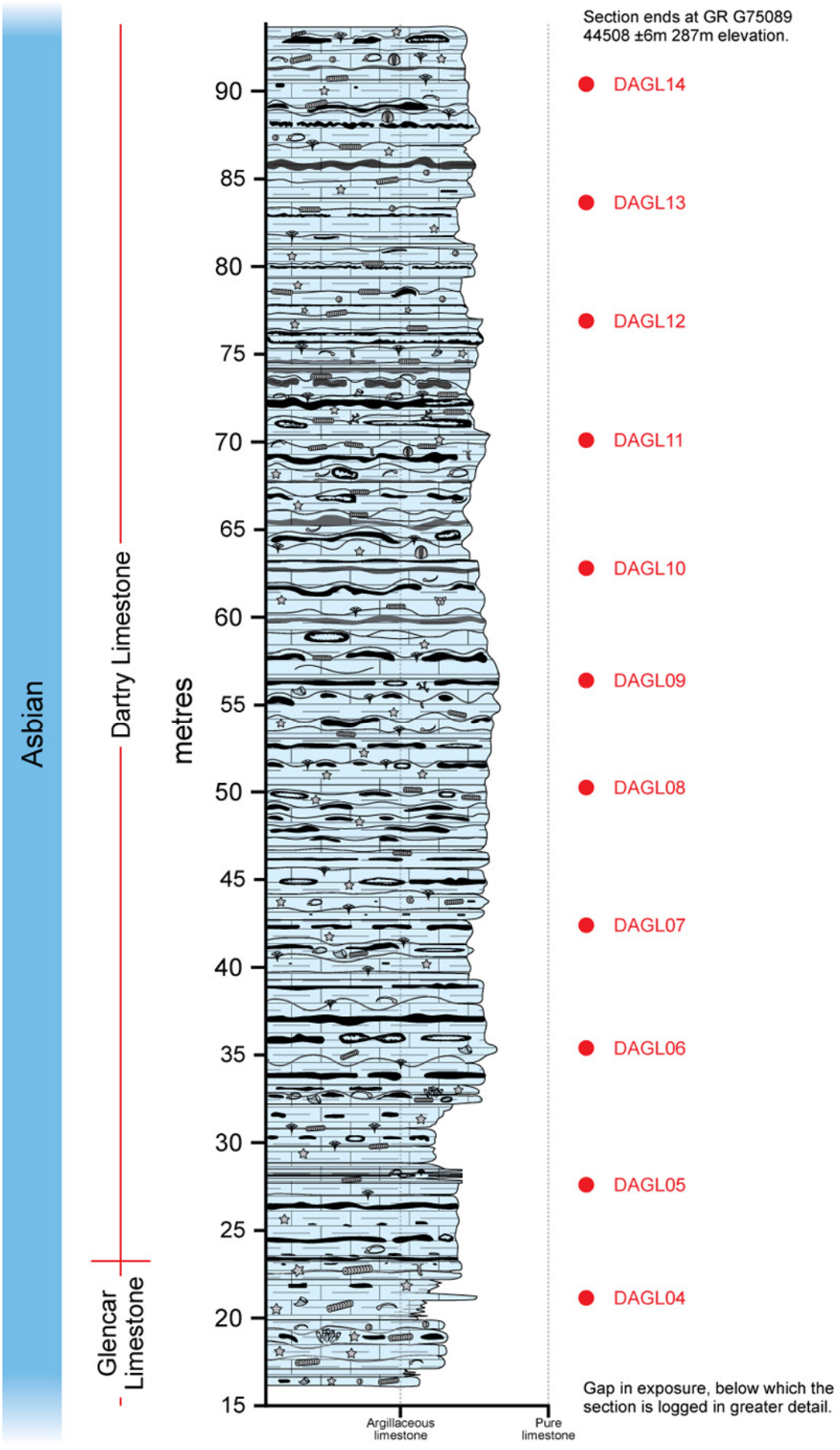

Fig. 2.2.2e Schematic lithological variation and sample locations in the Glencar Section.

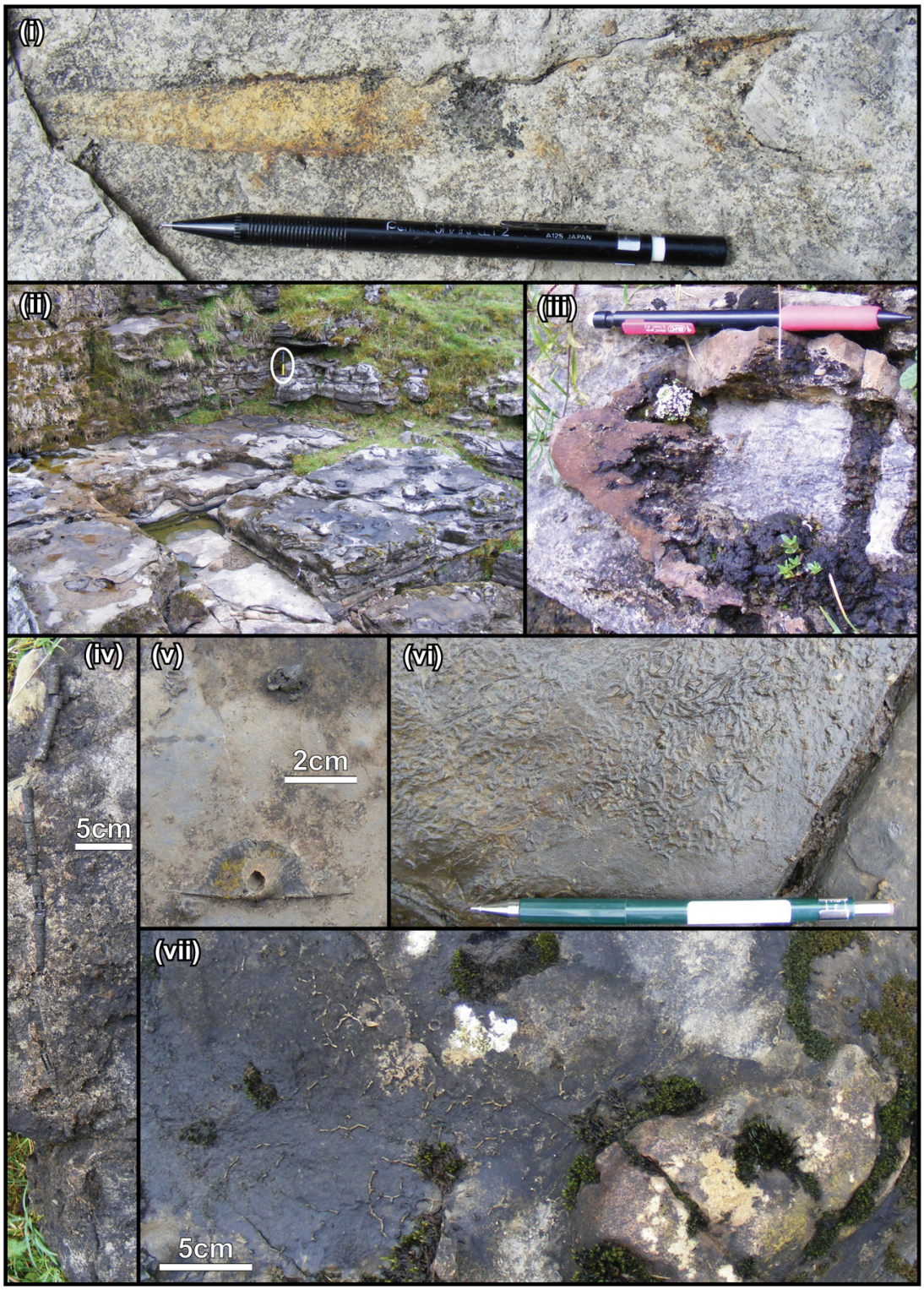

Fig. 2.2.2f Notable features of the Glencar Section.

(i) *Flattened orthocone impression on shale surface in the Glencar Lmst., 1.5m ASB.* ***(ii)*** *Typical irregular bedding surfaces of the Dartry Lmst. Hammer circled for scale.* ***(iii)*** *Chert "halo", Dartry Lmst.* ***(iv)*** *Slightly disturbed length of crinoid stem, Dartry Lmst., ~55m ASB..* ***(v)*** *Delicate silicified brachiopods, Dartry Lmst., ~69m ASB.* ***(vi)*** *Intense bioturbation in shale interval in the Dartry Lmst., ~69m ASB* ***(vii)*** *Large delicate colony of Cladochonus preserved in shale between chert (bottom right), Dartry Lmst., ~71m ASB.*

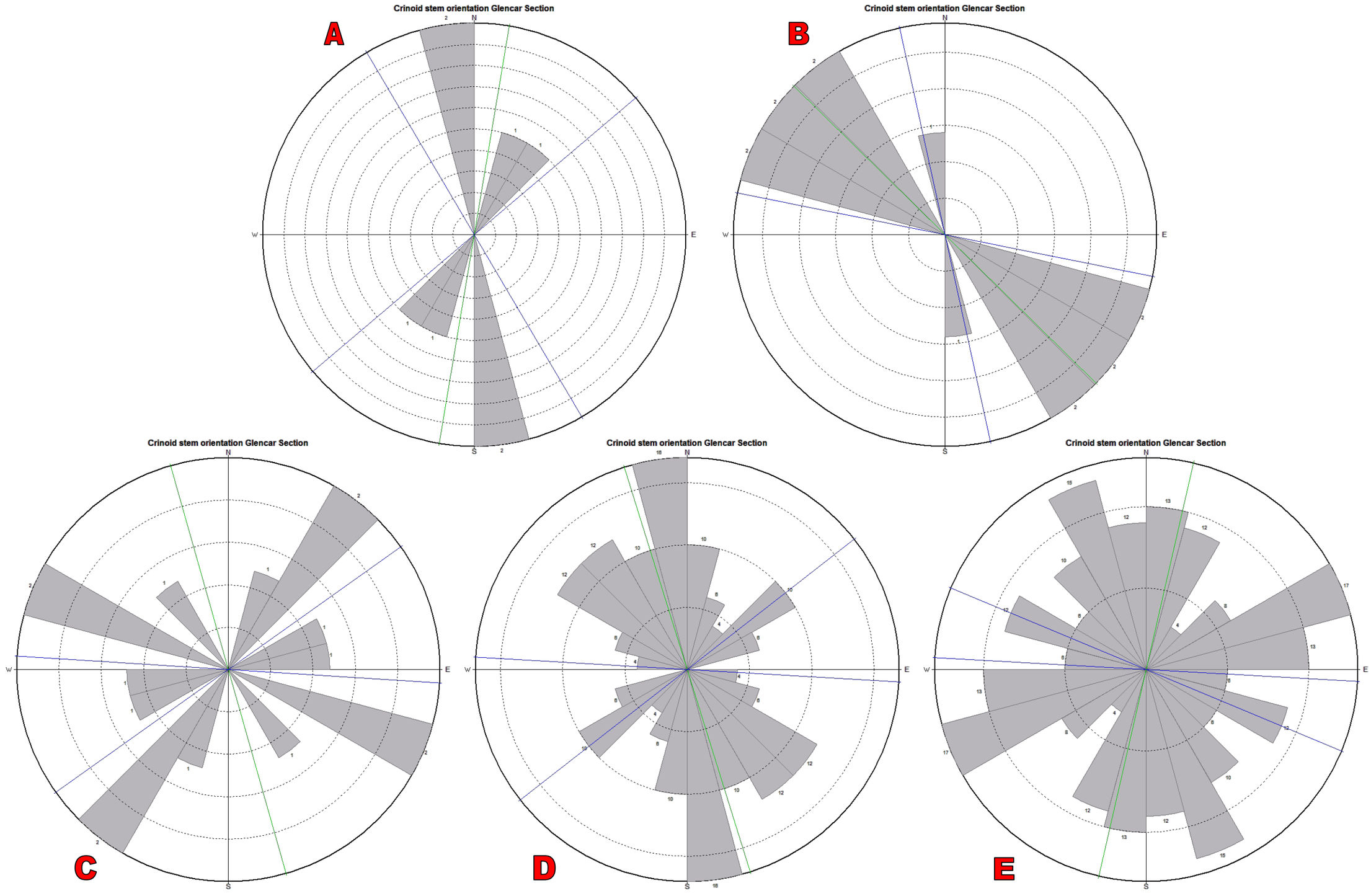

Fig. 2.2.2g Crinoid stem orientation in the Glencar Section.

Green lines represent the mean value while the blue lines demonstrate the standard deviation of the readings. ***A*** *was produced from just four stem readings at ~28m ASB.* ***B*** *was constructed from seven readings from a bedding plane ~31m ASB.* ***C*** *was produced from eight orientation readings at 55.9m ASB.* ***D*** *was plotted from 48 orientation readings taken from 55.98m ASB.* ***E*** *was graphed from 128 readings taken from 69.2m ASB.*

Fig. 2.2.2h Highest sampled exposure in the Glencar Section.

View upstream towards the final exposure on the outside side of the river bend. The hammer (circled in white) rests on the sampled horizon DAGL15.

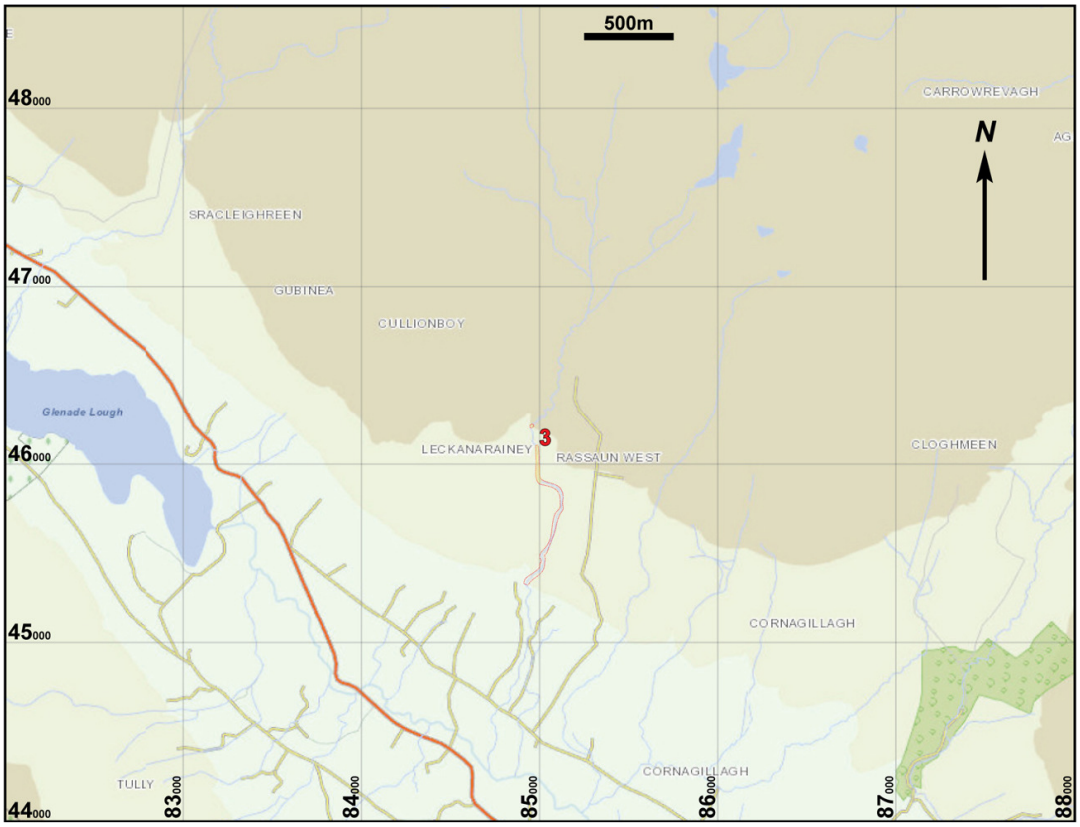

Fig. 2.2.3a Map of the Glenade Section and surrounding area.

Modified from OSI maps and data. The Glenade Section is highlighted (in yellow) in the stream east of the townland of Leckanarainey, continuous exposure is marked in red.

Fig. 2.2.3b Microfossil sample DAGN2 in the Leckanarainey Stream, Glenade Section.

Head of hammer (circled in white) rests on the top of DAGN2. Stream flows left to right.

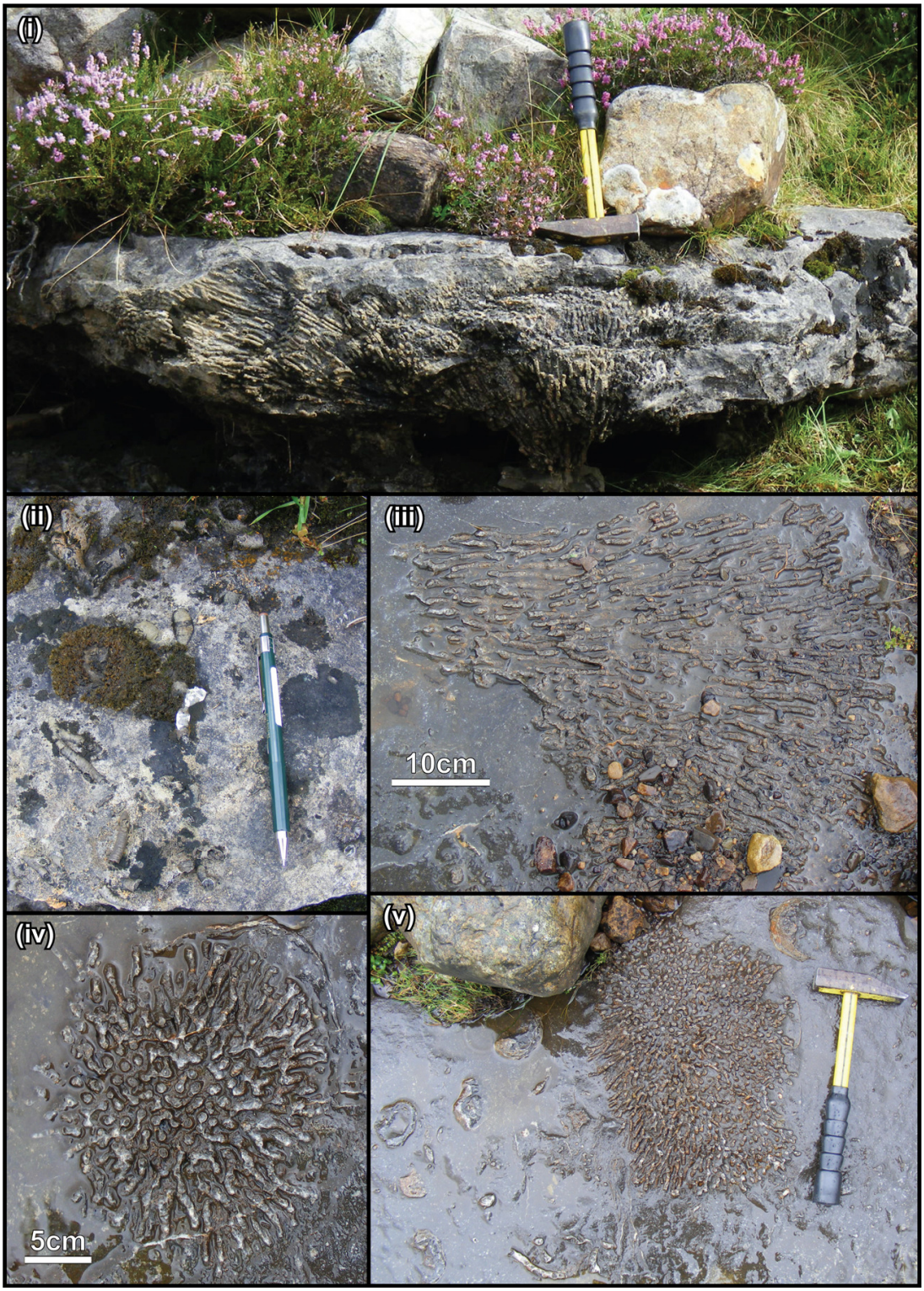

Fig. 2.2.3c Notable coral fossils in the Glenade Section, Leckanarainey Stream.

(i) *Autochthonous Siphonodendron colony, DAGN1 horizon.* ***(ii)*** *Small solitary and branching corals typical of the Dartry Limestone between DAGN1 and DAGN2.* ***(iii)*** *Siphonodendron colony on its side. Corallites converge to the left and slightly upwards, DAGN1 horizon.* ***(iv)*** *Apparently overturned Siphonodendron colony, with corallites appearing to converge upwards towards the viewer, DAGN1 horizon.* ***(v)*** *Apparently overturned Siphonodendron colony, with corallites appearing to converge upwards towards the viewer. Large brachiopods and other coral material are also visible on the DAGN1 horizon.*

Fig. 2.2.3d Microfossil sample DAGN1 in the Leckanarainey Stream, Glenade Section.
View upstream towards the bedding surface of the sampled unit. Position of hammer (circled in white) denotes exact point of DAGN1 sampling.

Fig. 2.2.3e Meenymore exposure in the Leckanarainey Stream, Glenade Section.
Picture taken facing upstream. Orange competent bands (highlighted in fine dashed white lines) represent weathered carbonate beds attributed to the Meenymore Formation.

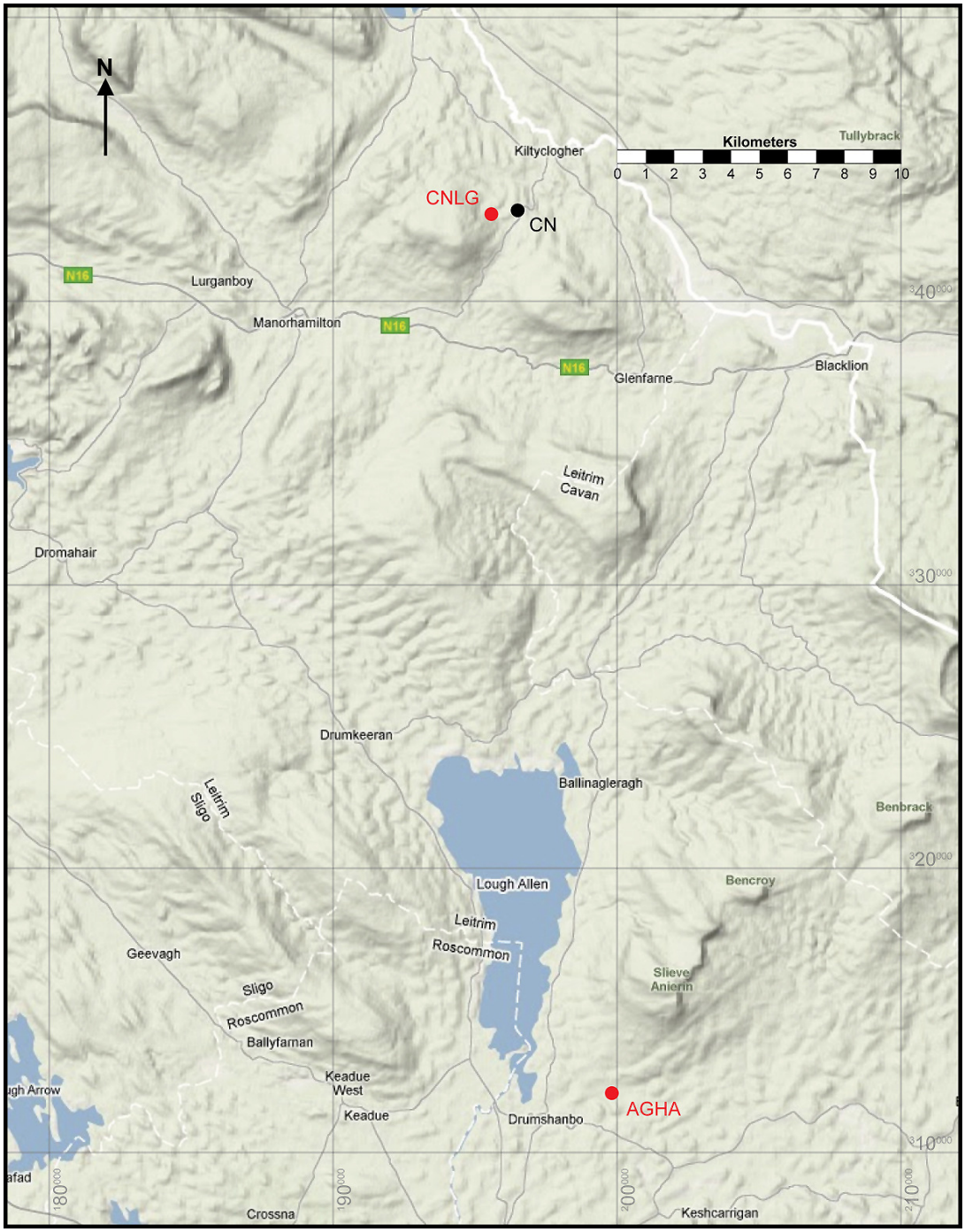

Fig. 2.3 Geographic location map of sections exposing the lower Leitrim Group.

The black dot refers to a section visited but ultimately deemed unsuitable, red dots are sections that were examined and sampled, see Section 2.3. Image produced using Google Maps data.

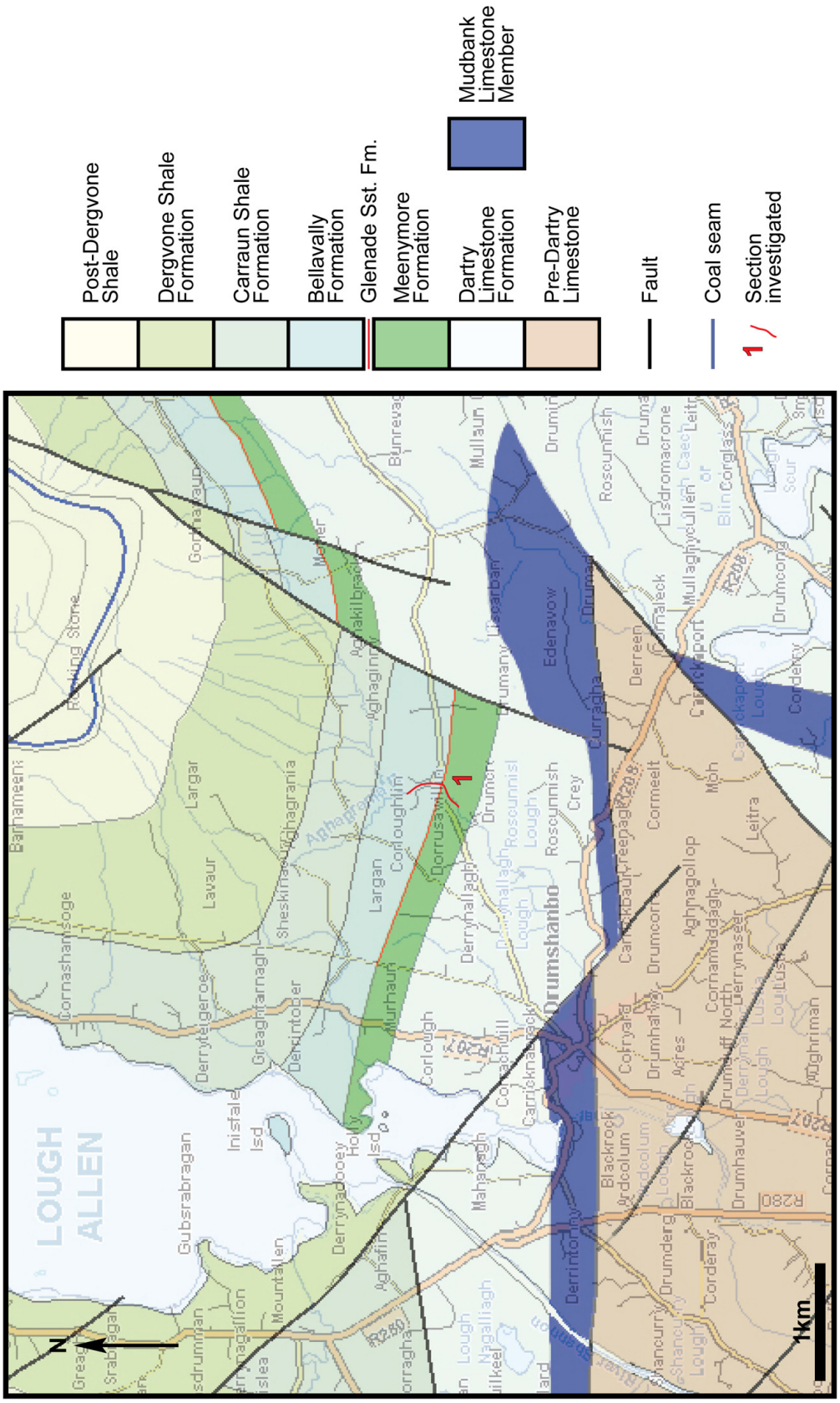

Fig. 2.3.1a Location map for the Aghagrania Section, NW Ireland.

The red line indicates the portion of the Aghagrania River that was investigated herein. Overlain on the Ordnance Survey of Ireland map is a simplified version of the 1:100,000 scale geology as mapped by the Geological Survey of Ireland. Note that the boundaries mapped by the GSI are locally inaccurate.

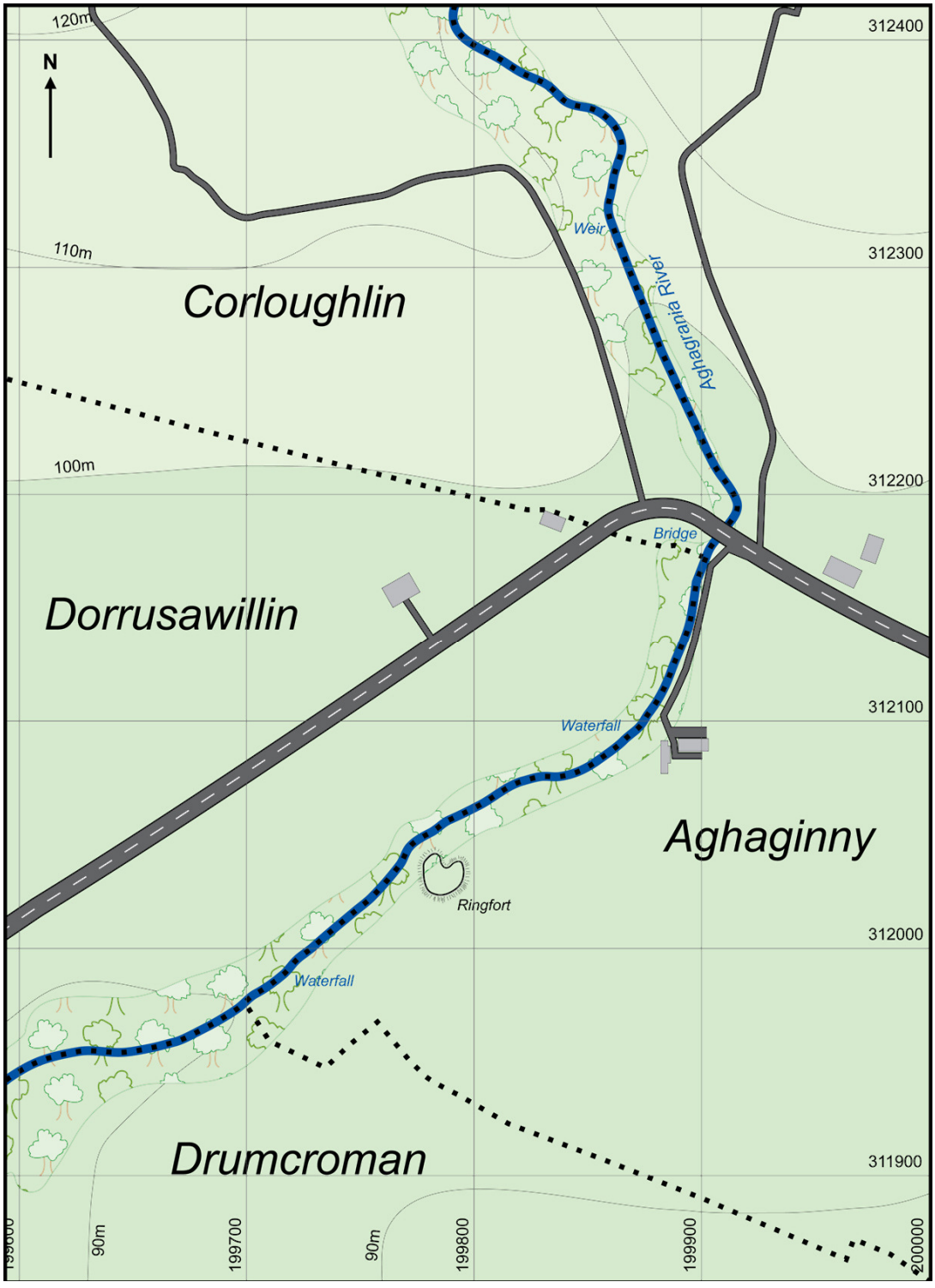

Fig. 2.3.1b Digitised geography of the Aghagrania Section.

Dotted lines represent the boundaries between townlands (large italics) roads and tracks are shown in dark grey while buildings are represented by pale grey blocks.

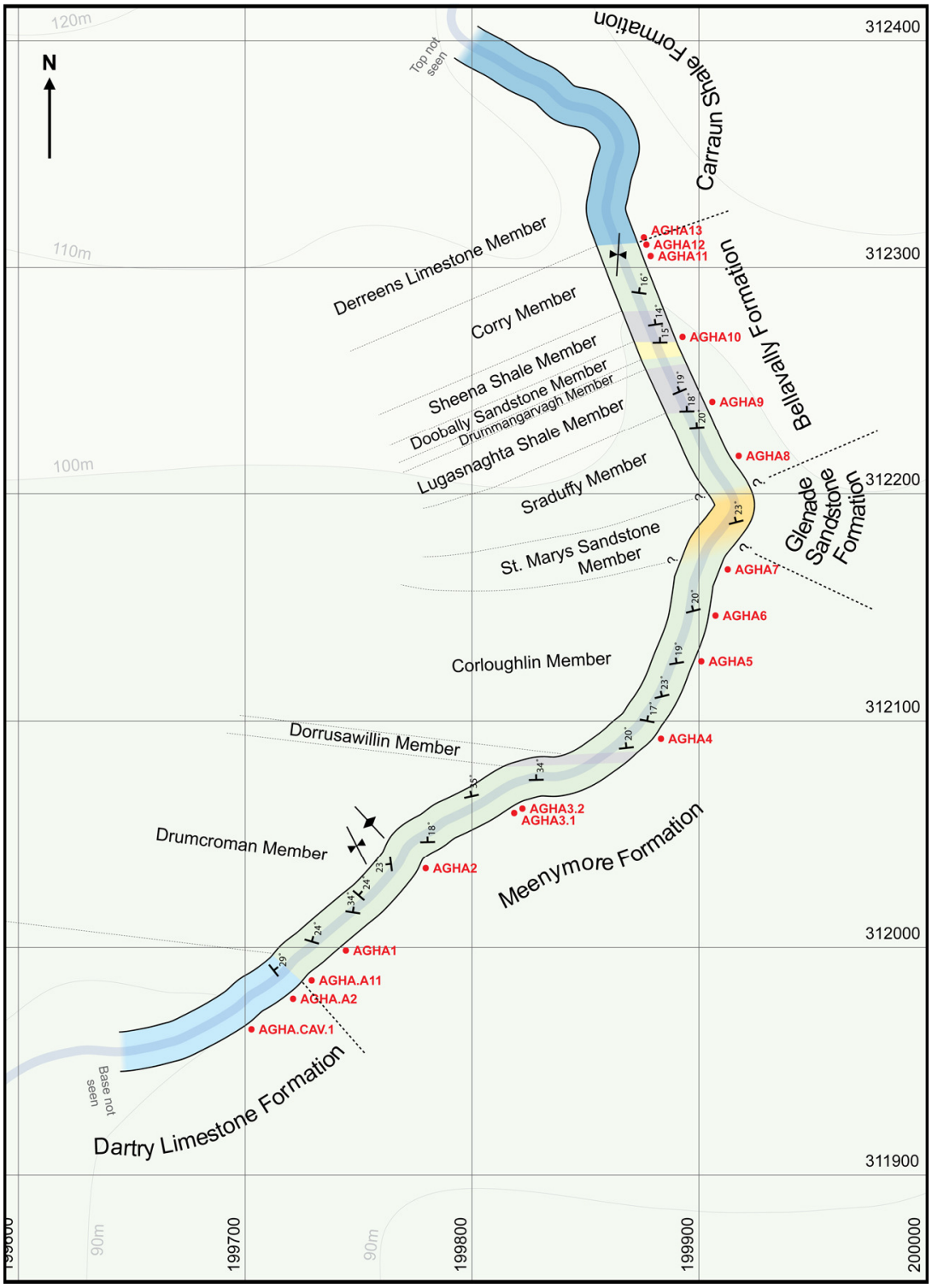

Fig. 2.3.1c Digitised geology of the Aghagrania Section.

Dark lines bounding the coloured geological units represent the expanded margins of exposure within the stream. Map is displayed at the same scale as Fig. 2.3.1b. Red dots represent the location where rock samples were taken for microfossil analysis.

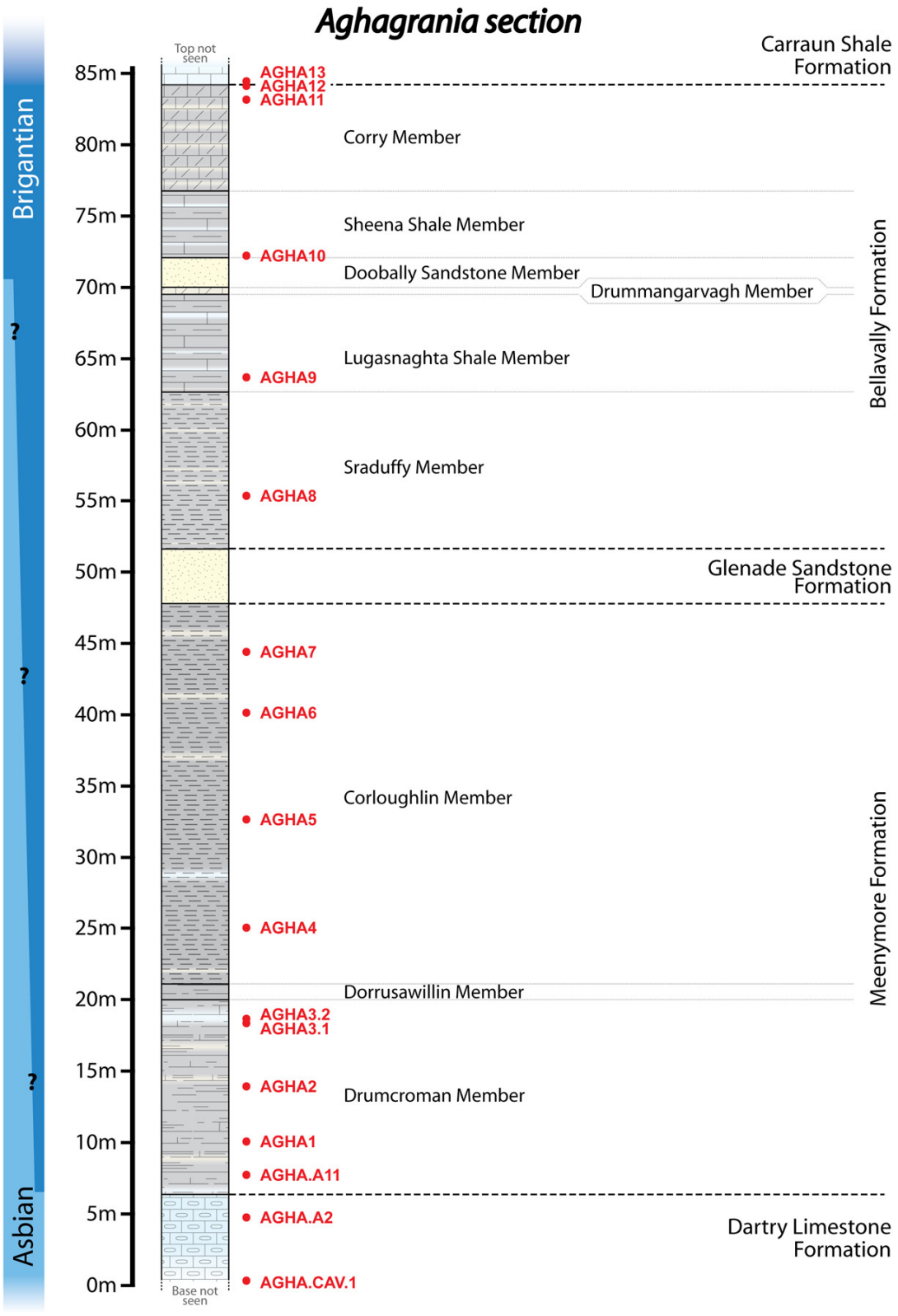

Fig. 2.3.1d Stratigraphy of the Aghagrania Section.

Question marks on the substage scale (left) highlight disagreement between different biostratigraphical markers. Red dots represent microfossil samples. Modified from West et al. (1968). Key as in Fig. 2.2.1e.

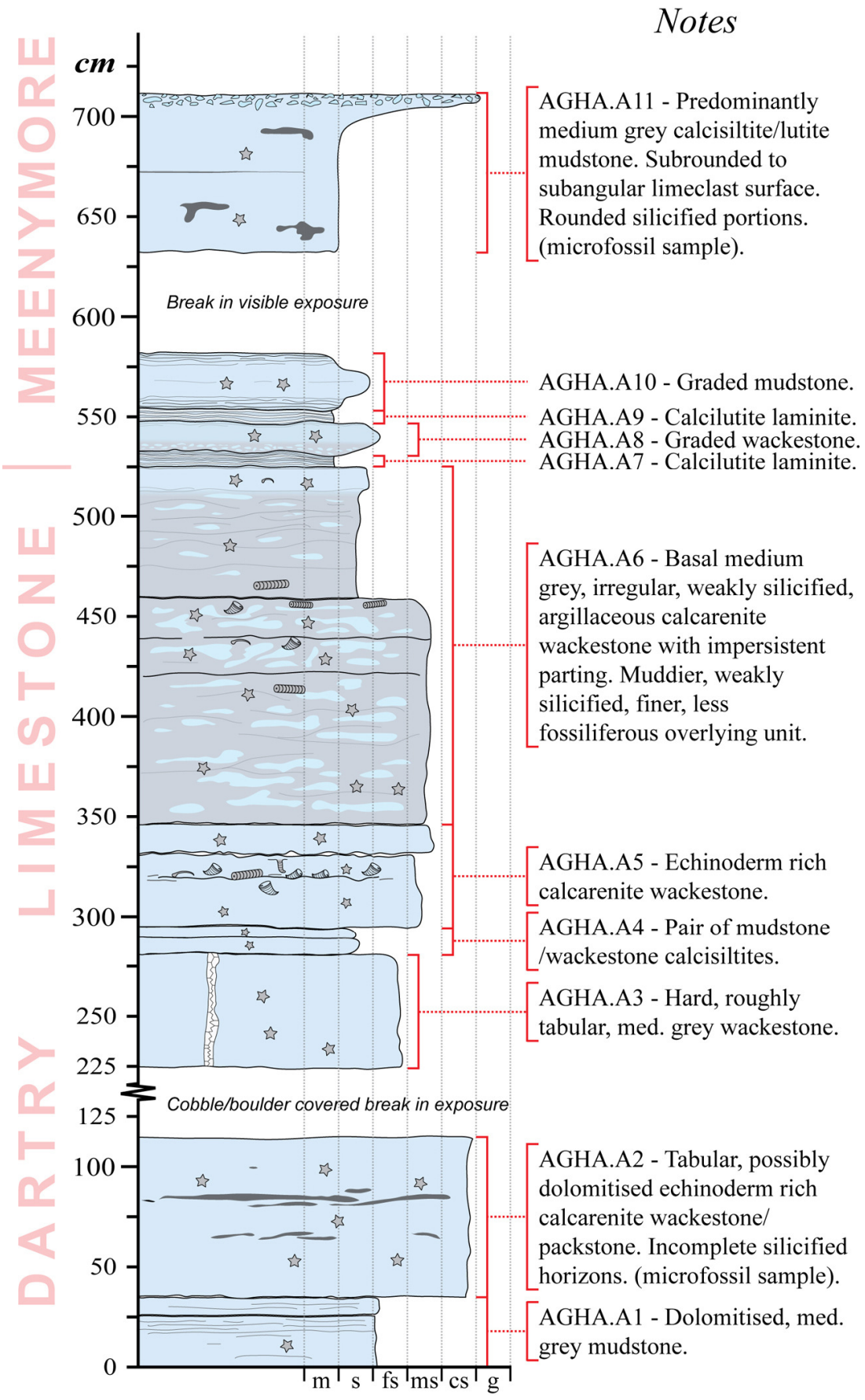

Fig. 2.3.1e Log of the Dartry Limestone-Meenymore contact in the Aghagrania Section.
Unless stated, key follows Fig. 2.2.1e. The contact is at the first laminite (525cm ASB).

Fig. 2.3.1f Dartry Limestone–Meenymore contact in the Aghagrania Section.

View upstream towards ~2m high waterfall exposing the contact (highlighted by a white dashed line) of the Dartry Limestone Formation and the Meenymore Formation. Faint white lines mark the boundaries of the logged units shown in Fig. 2.3.1e.

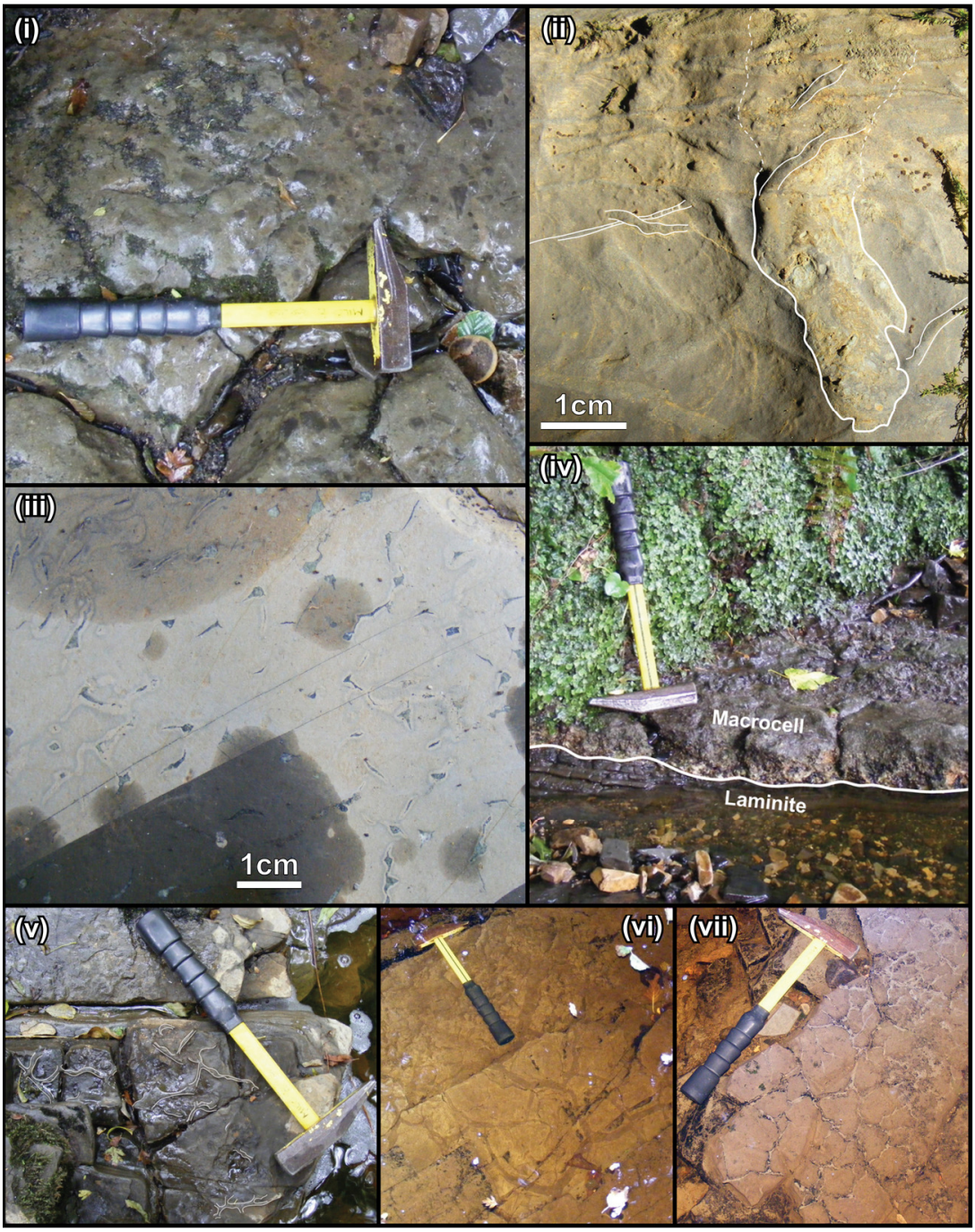

Fig. 2.3.1g Notable features of the Aghagrania Section.

(i) *Limeclast breccia surface of AGHA.A11 horizon, Drumcroman Mbr., Meenymore Fm.* ***(ii)*** *Bioturbation (highlighted in white) in sampled horizon AGHA1, Drumcroman Mbr., Meenymore Fm. Largest burrow in the centre is filled by overlying coarse fossiliferous sediment.* ***(iii)*** *Possible syneresis diamond, trilete and irregular cracks in the Drumcroman Mbr., Meenymore Fm.* ***(iv)*** *Laminite and macrocell horizons in the Corloughlin Mbr., Meenymore Fm.* ***(v)*** *Possible desiccation cracks in the Corloughlin Mbr., Meenymore Fm.* ***(vi & vii)*** *Desiccation structures in the Sraduffy Mbr., Bellavally Fm.*

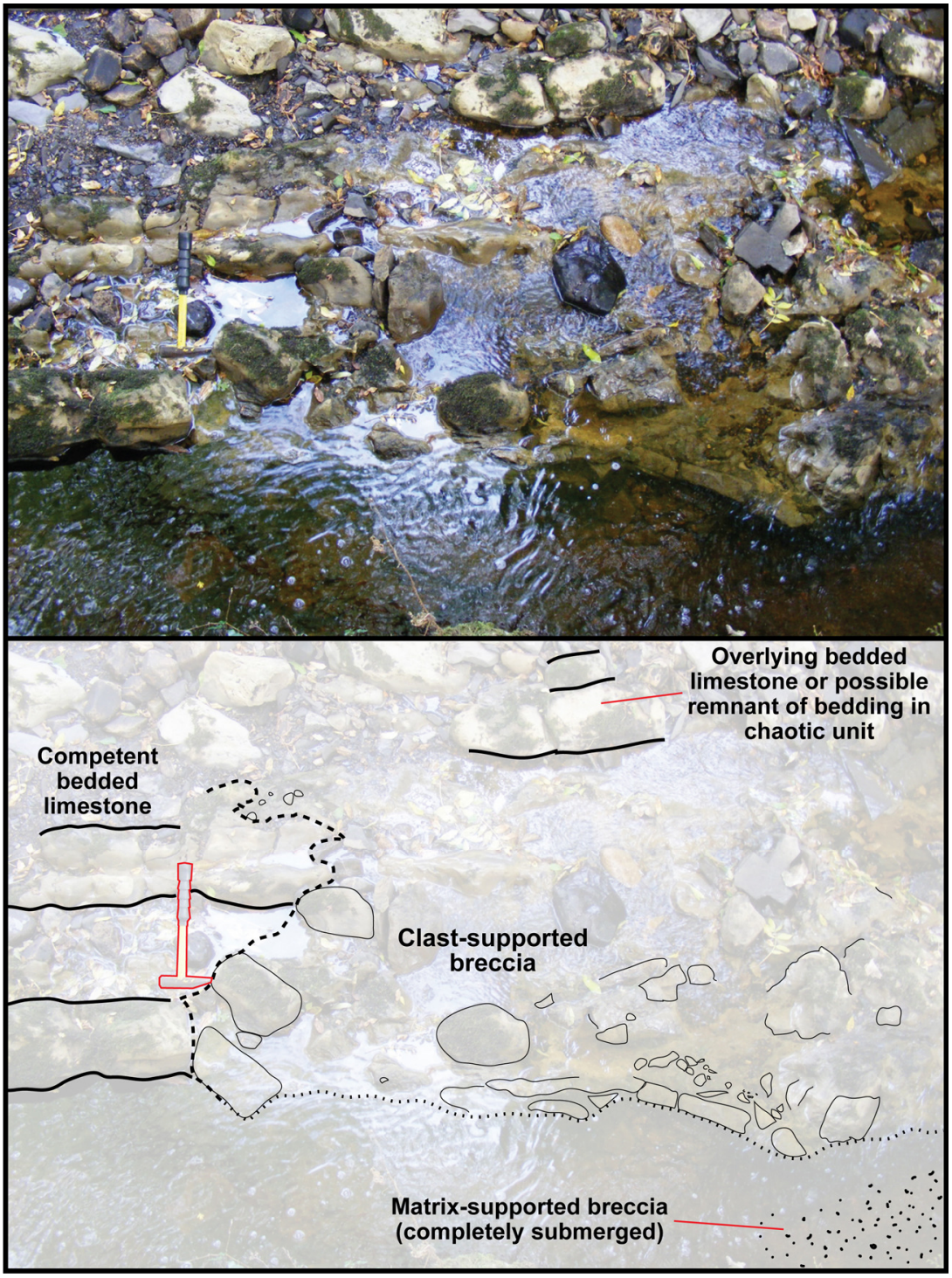

Fig. 2.3.1h Possible collapse breccia in the Aghagrania Stream Section.

The upper image represents the actual view of the outcrop from the southeast bank. The lower image is the same photograph but faded and with a basic interpretation overlain. Competent, bedded units can be discerned on the left (thick black lines). To the right of the hammer, the breccia is near wholly developed and the rock appears more irregular (boundary marked by a dashed line, individual clasts by thin black lines).

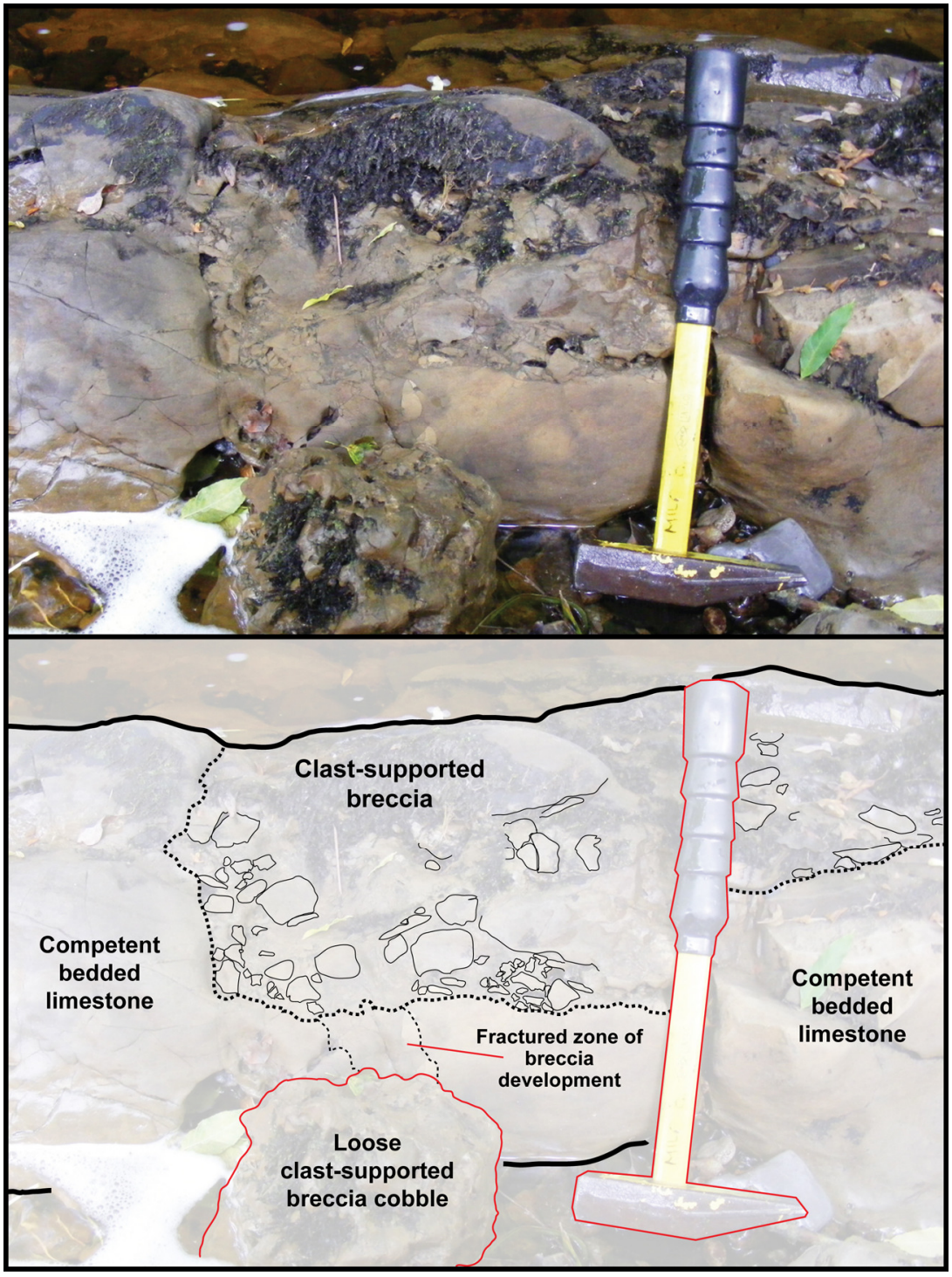

Fig. 2.3.1i Isolated pocket of epidiagenetic(?) breccia in the Aghagrania Stream Section.
The upper image represents the actual view of the discrete breccia, whilst the lower image is the same photograph but faded with a basic interpretation overlain. The bed is competent to the left of the picture but a defined "channel" (dashed line) filled with clasts (outlined by thin black lines) is visible in the centre of the photograph.

Fig. 2.3.1j Synsedimentary deformation in the Bellavally Fm., Aghagrania Section.

*Oblique view facing NE. Note that beds at **A** and **F** are completely undisturbed while points B to E exhibit deformation (marked with a white dashed line). Point B marks a small recumbent fold, **C** marks a fold with internal truncation of lamination along a low angled synsedimentary fault plane, **D** marks small parasitic chevron folds that should connect approximately with units at point **E** following the fold marked by C.*

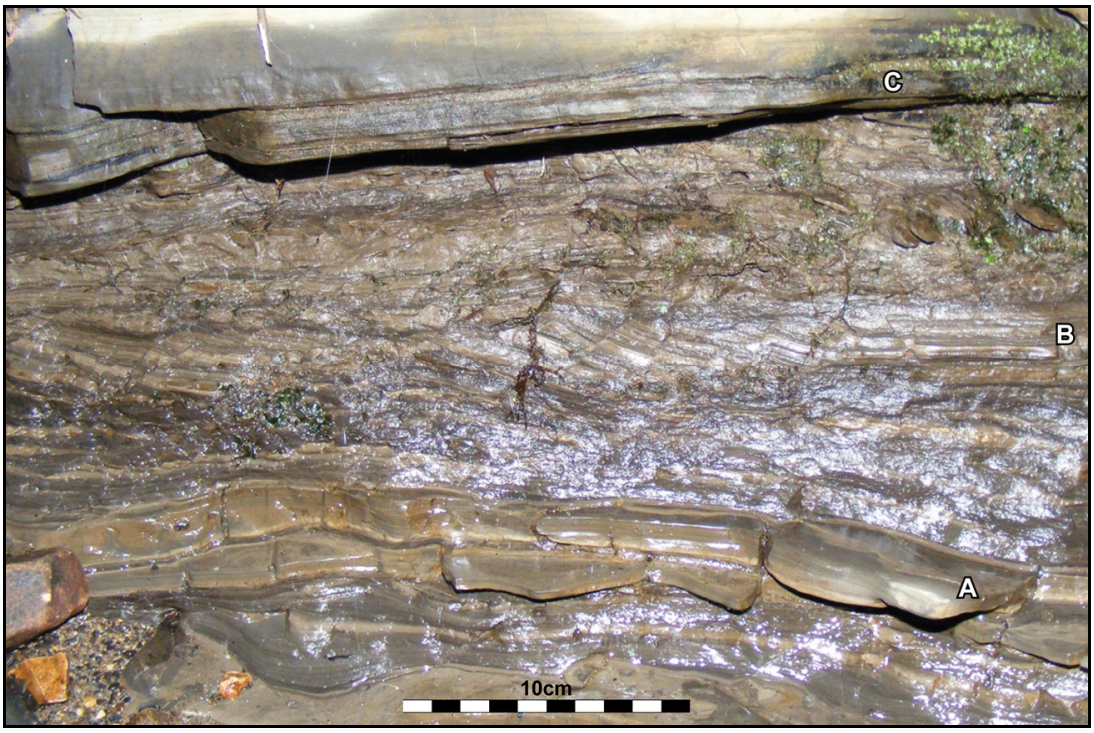

Fig. 2.3.1k Synsedimentary brittle deformation in the Bellavally Fm., AGHA Section.

Sectional view of exposure in the NE bank. Beds at A and C are completely undisturbed whilst those in between (B) display small scale faulting and rotation.

Fig. 2.3.1l Bellavally-Carraun Shale contact in the Aghagrania Stream Section.
View facing towards the NE bank with the hammer head resting on top of the basal bed of the Carraun Shale Formation (AGHA13).

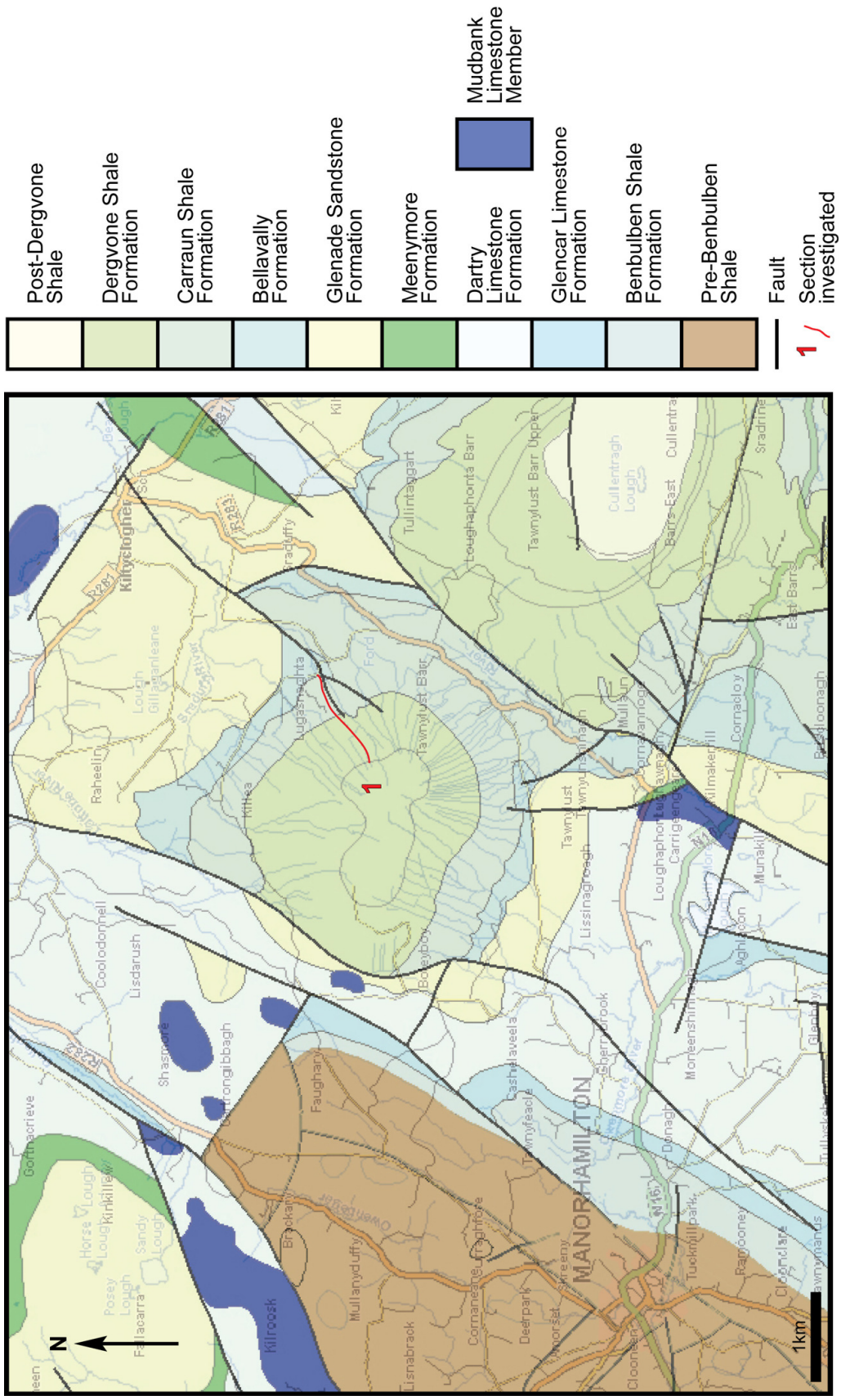

Fig. 2.3.2a Location map for the Carraun/Lugasnaghta Section, NW Ireland.

The red line indicates the portion of the river that was investigated herein. A simplified version of the 1:100,000-scale geology (according to the GSI) is overlain on an OSI map. Note that the boundaries as shown by the GSI are inaccurate locally.

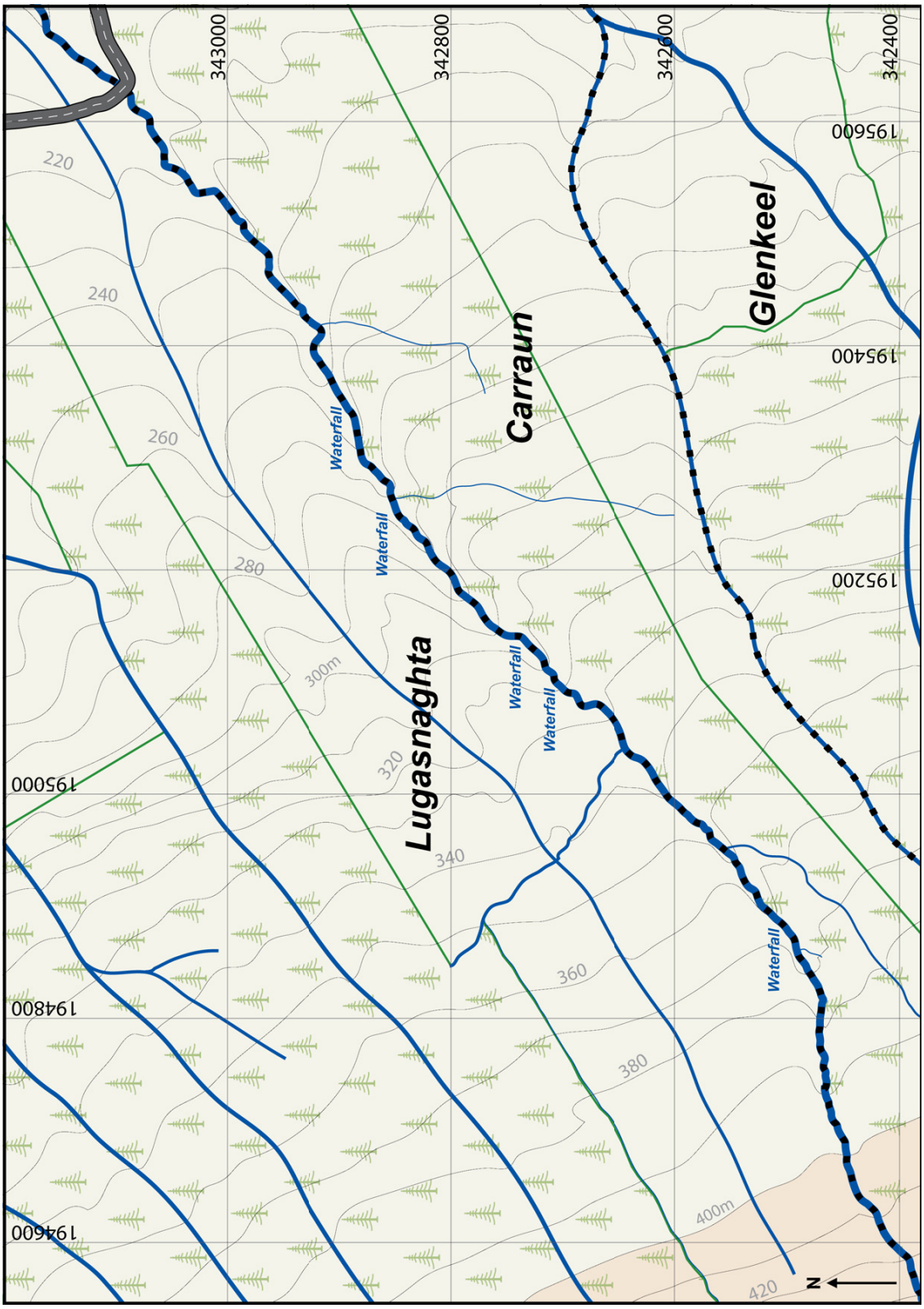

Fig. 2.3.2b Digitised geography of the Carraun/Lugasnaghta Section.

Note that north is to the left of the image. The main stream that exposes the section is shown the thickest. The townland to the right of the stream is Carraun while that on the left is Lugasnaghta. Green lines represent the borders of forestry plantations.

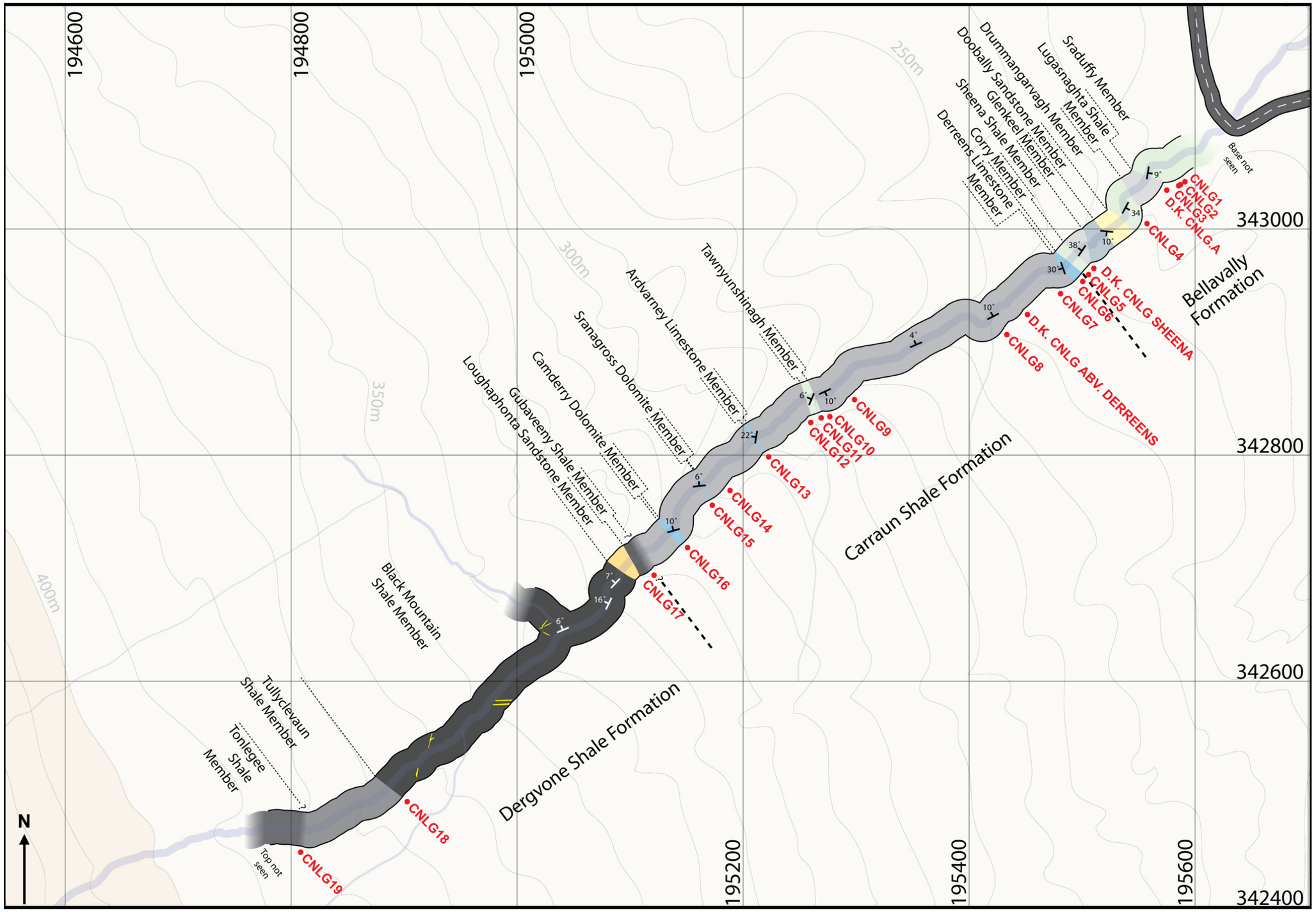

Fig. 2.3.2c Digitised geology of the Carraun/Lugasnaghta Section.

Red dots represent microfossil samples. Yellow lines in the Dergvone Shale Formation schematically represent sandstone dykes. Question marks and gradational intervals represent uncertainties in the placing of a contact. Note that the geology depicted has been expanded to a significant degree from its limited exposure in the stream and the contacts drawn do not demonstrate the overall direction of the boundaries exactly.

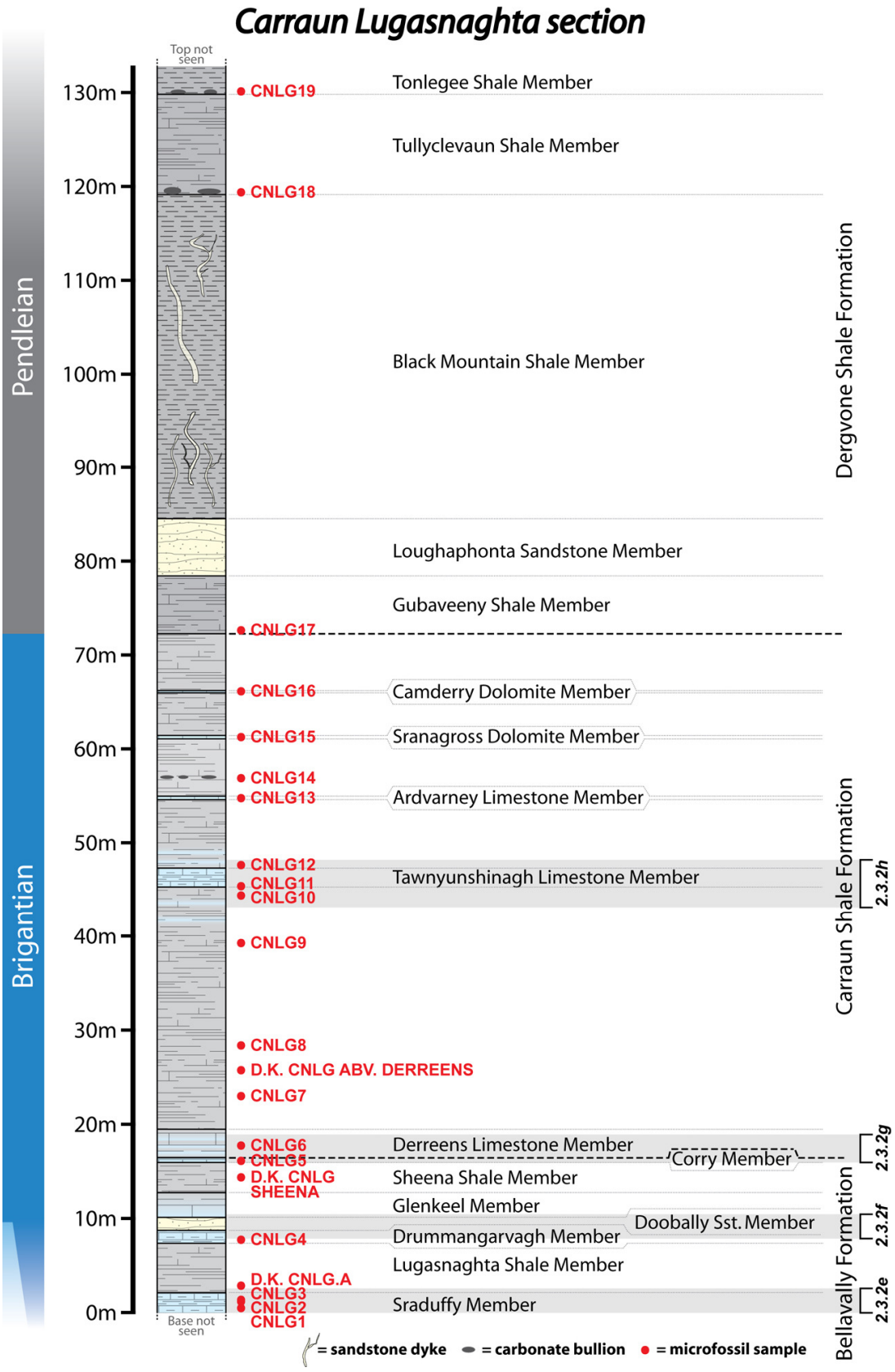

Fig. 2.3.2d Stratigraphy of the Carraun/Lugasnaghta Section.

Note that the sandstone dykes are drawn artistically and their occurrences are greatly simplified in the figure. Numbers on the right correlate to the figures which detail the lithostratigraphy of the grey areas indicated. Modified from Smith (1995). Key as in Fig. 2.2.1e.

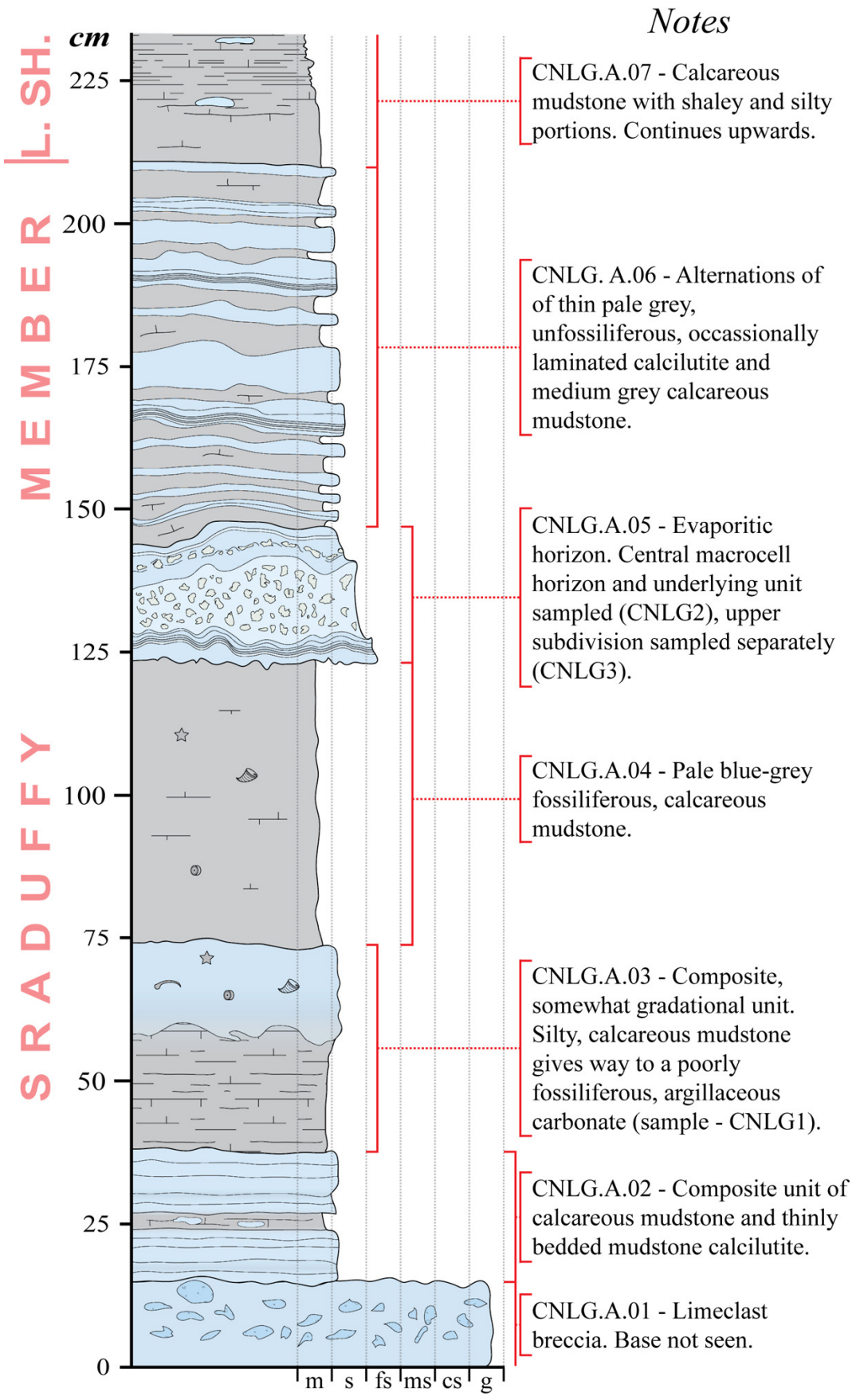

Fig. 2.3.2e Sraduffy-Lugasnaghta Shale contact, Bellavally Fm., CNLG Section.

Key as in Fig. 2.2.1e. The contact between the Sraduffy and Lugasnaghta Members of the Bellavally Fm. lies at 211cm ASB. CNLGX, in brackets, represents microfossil samples.

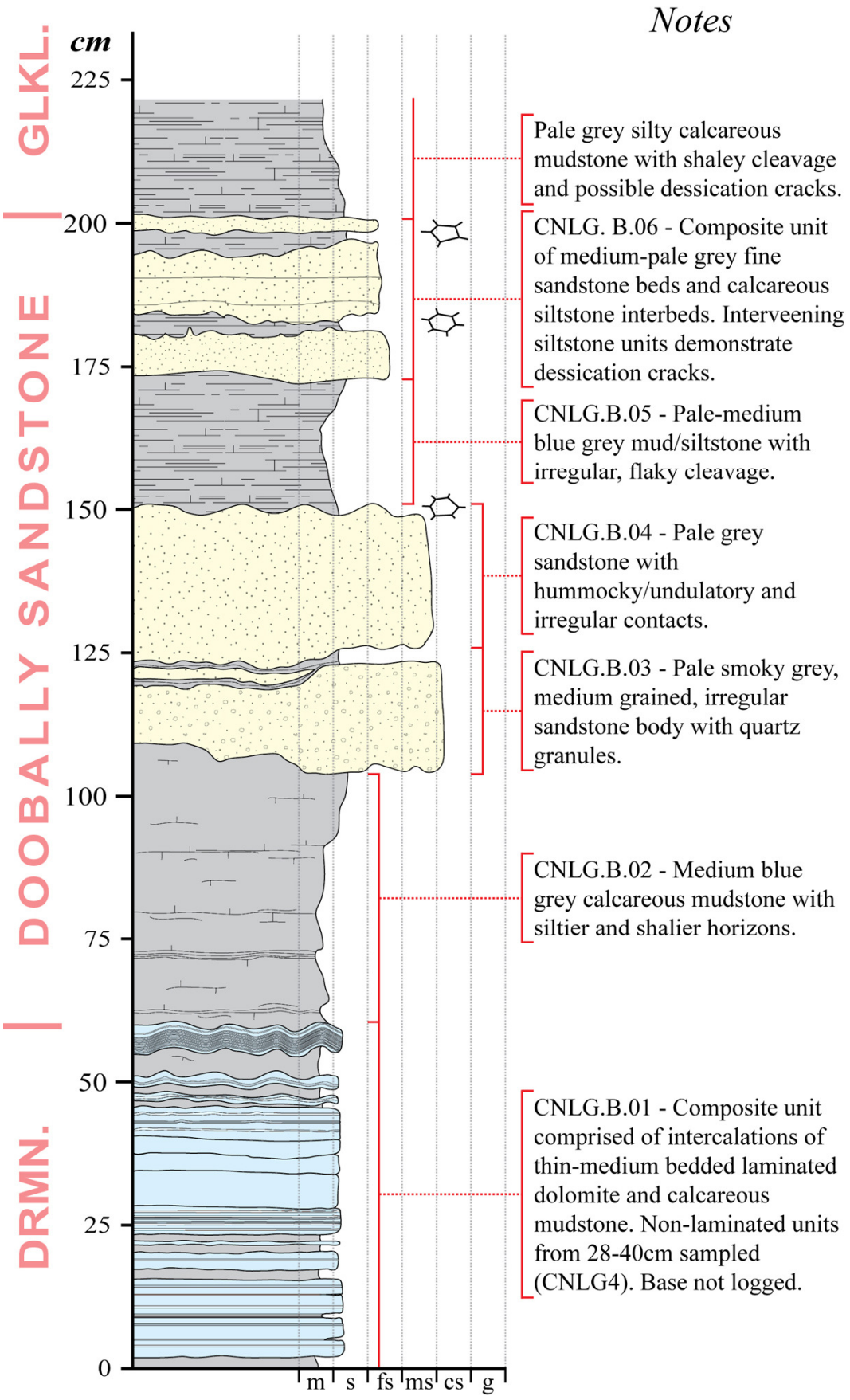

Fig. 2.3.2f Log of the Drummangarvagh-Doobally-Glenkeel Mbrs. contacts, CNLG.

Key as in Fig. 2.2.1e. The contact between: (1) the Drummangarvagh and Doobally Sst. Members is at 58.5cm (2) the Doobally Sst. and the Glenkeel Members is at 200.5cm.

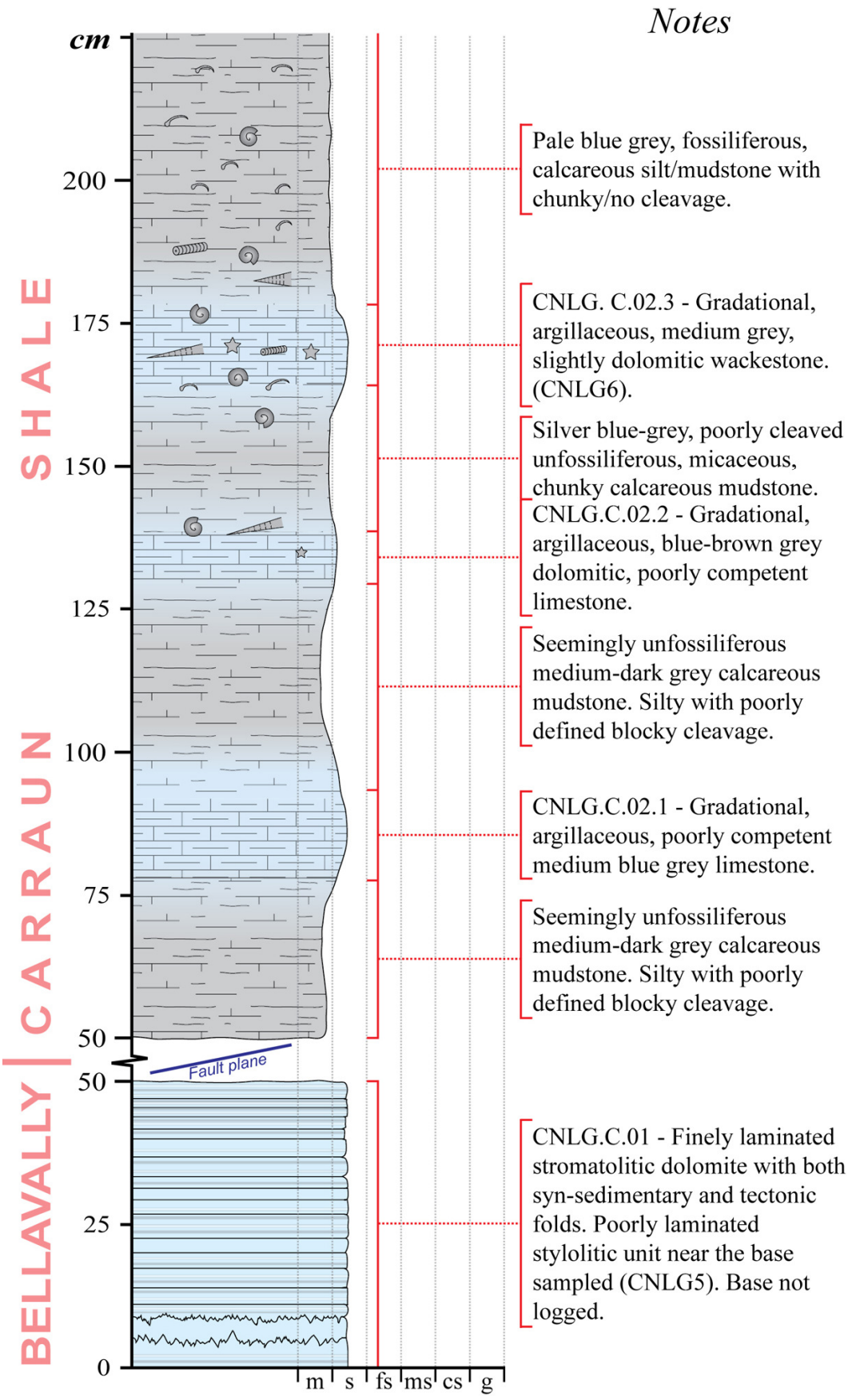

Fig. 2.3.2g Log of the Bellavally-Carraun Shale contact in the CNLG Section.

Key as in Fig. 2.2.1e. The Corry Member (Bellavally Fm.)-Derreens Lmst. Member (Carraun Shale Fm.) contact is locally faulted. Bed C.02.3 represents the Derrybofin Bed.

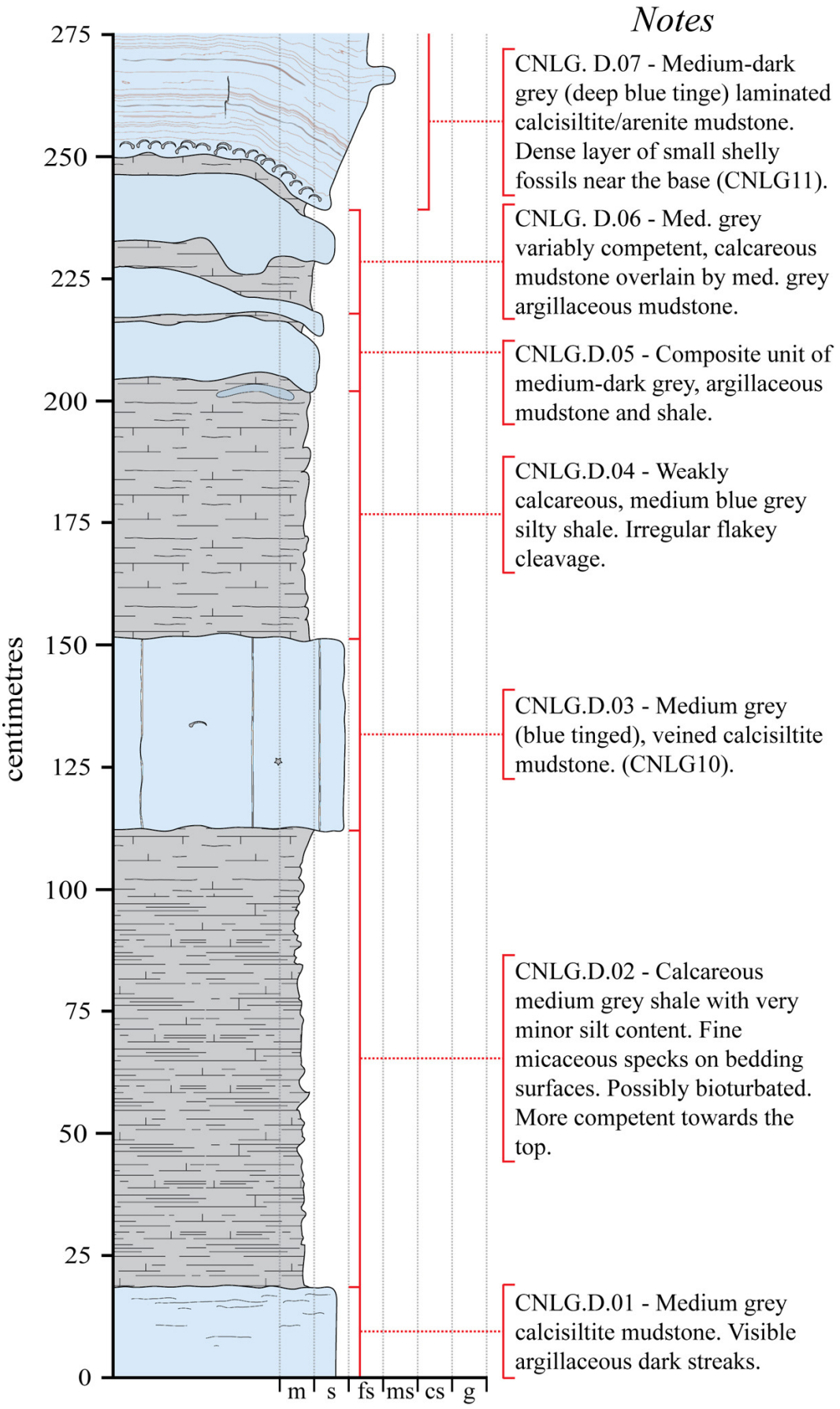

Fig. 2.3.2h Log of the Tawnyunshinagh Member, Carraun Shale Fm., CNLG Section.
Key as in Fig. 2.2.1e. Continued overleaf.

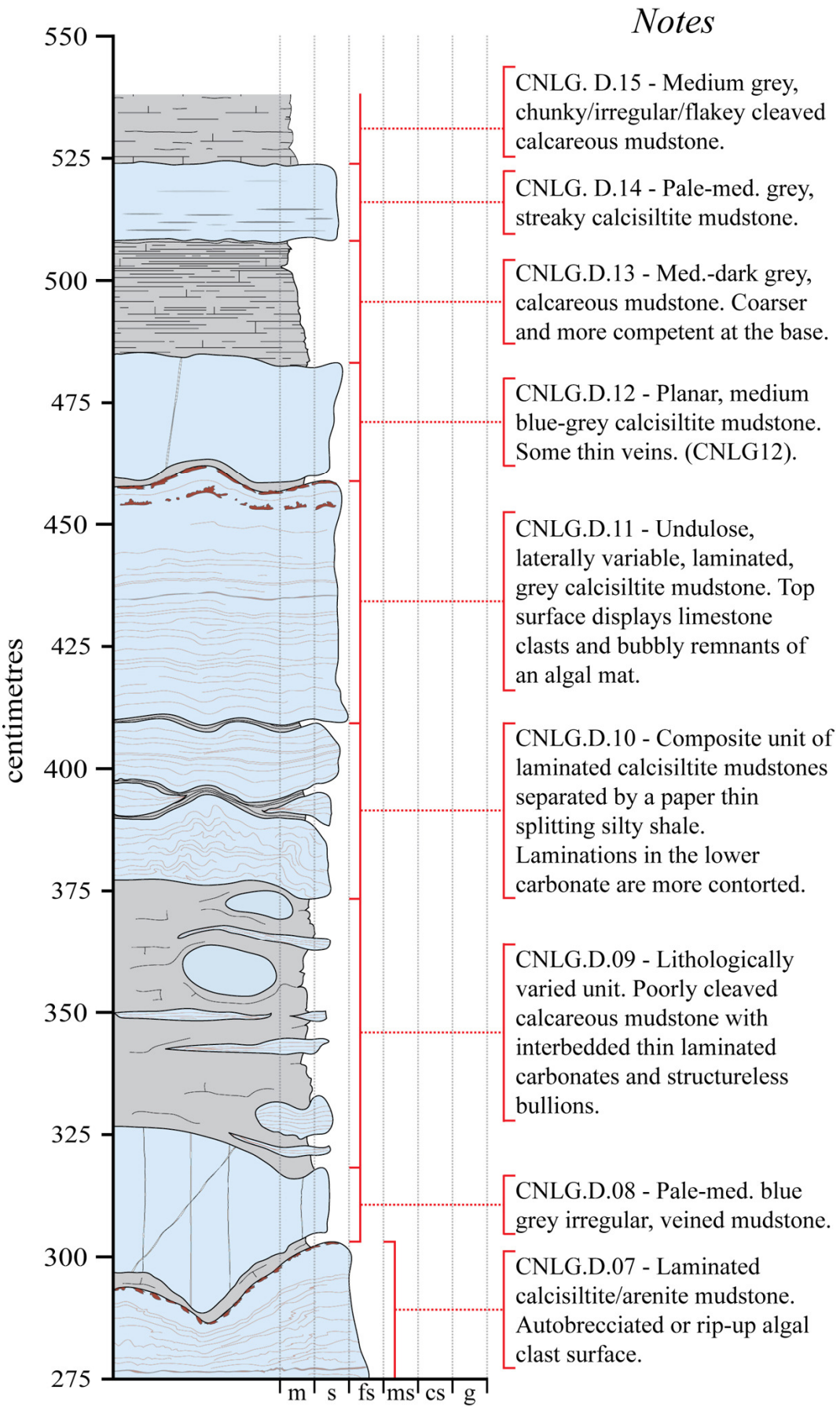

Fig 2.3.2h Continued. The Tawnyunshinagh Mbr. begins 249.5cm above the log base and ends 456cm up at a breccia surface. Probable algal mat remnants are of particular note.

Fig. 2.3.2i Base of the Carraun/Lugasnaghta Section.

View upstream to the first outcrop of the section. Microfossil samples CNLG1, CNLG2 and CNLG3 were taken from the beds marked by dashed white lines. Note the obvious deformation of bedding. Hammer circled for scale.

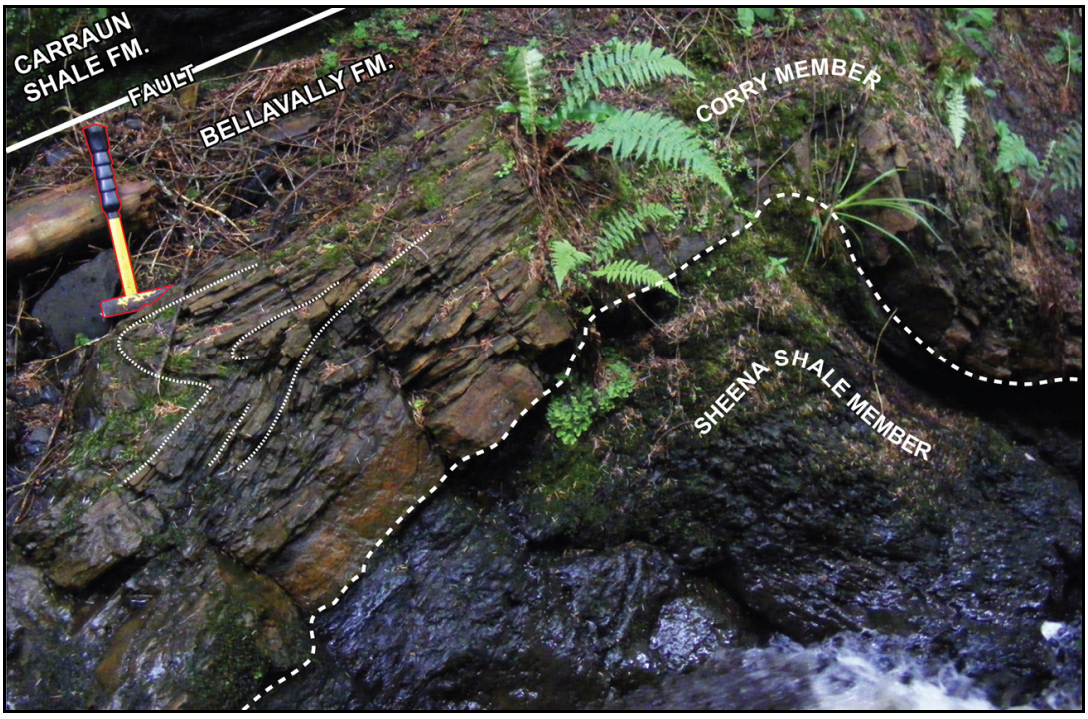

Fig. 2.3.2j Sheena Shale-Corry Member contact in the Carraun/Lugasnaghta Section.

The thicker orange/brown horizon marking the bottom of the Corry Member was sampled for microfossils (CNLG5). Note the small, overturned fold in the laminites below and to the right of the hammer head (fine dashed white line). Hammer (highlighted in red) for scale.

Fig. 2.3.2k Notable fossils and structures in the Carraun/Lugasnaghta Section.

(i) *View of the SE bank exposing complex folding (highlighted in red and white dashed lines) above the Doobally Sst. Mbr., Bellavally Fm. Field of view is ~8m wide.* ***(ii)*** *Unusual carbonate nodule in the Lugasnaghta Sh. Mbr., Bellavally Fm. with a distinct honeycomb texture.* ***(iii)*** *Sectional view of beekite-like structures preserved in the Tawnyunshinagh Lmst. Mbr., Carraun Shale Fm.* ***(iv)*** *Large Posidonia fossil from the Carraun Sh. Fm., above the Tawnyunshinagh Lmst. Mbr.* ***(v)*** *Probable partially collapsed fragments of large orthoconic nautiloid test (highlighted in yellow), found on a loose bullion face in the Carraun Sh. Fm.* ***(vi)*** *Sandstone dykes (highlighted by white dashed lines) cutting the Black Mountain Sh. Mbr., Dergvone Sh. Fm. Note the persistence of the thin dykelets.*

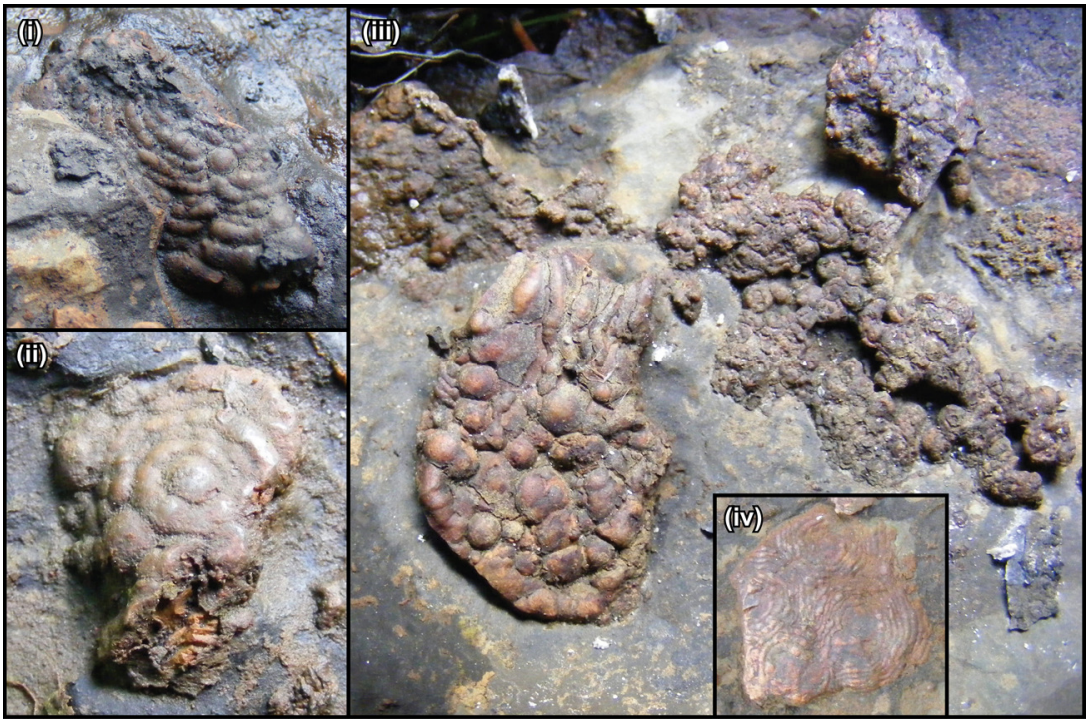

Fig. 2.3.2l Beekite-like structures on the surface of the Tawnyunshinagh Lmst. Mbr.

A selection of macroscopic views of the probable algal structures exposed on the upper breccia surface of the member. ***(i)*** *– 2cm tall structure,* ***(ii)*** *– 1.5cm tall structure,* ***(iii)*** *– field of view is 4cm across,* ***(iv)*** *– field of view is 2.5cm wide.*

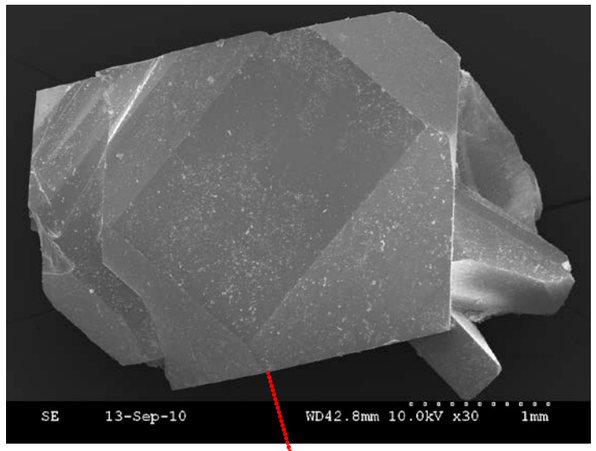

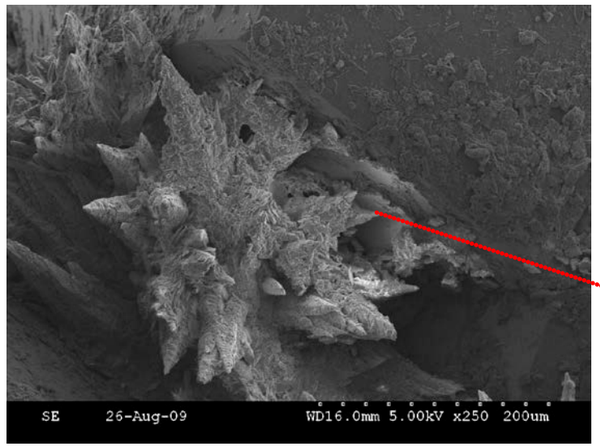

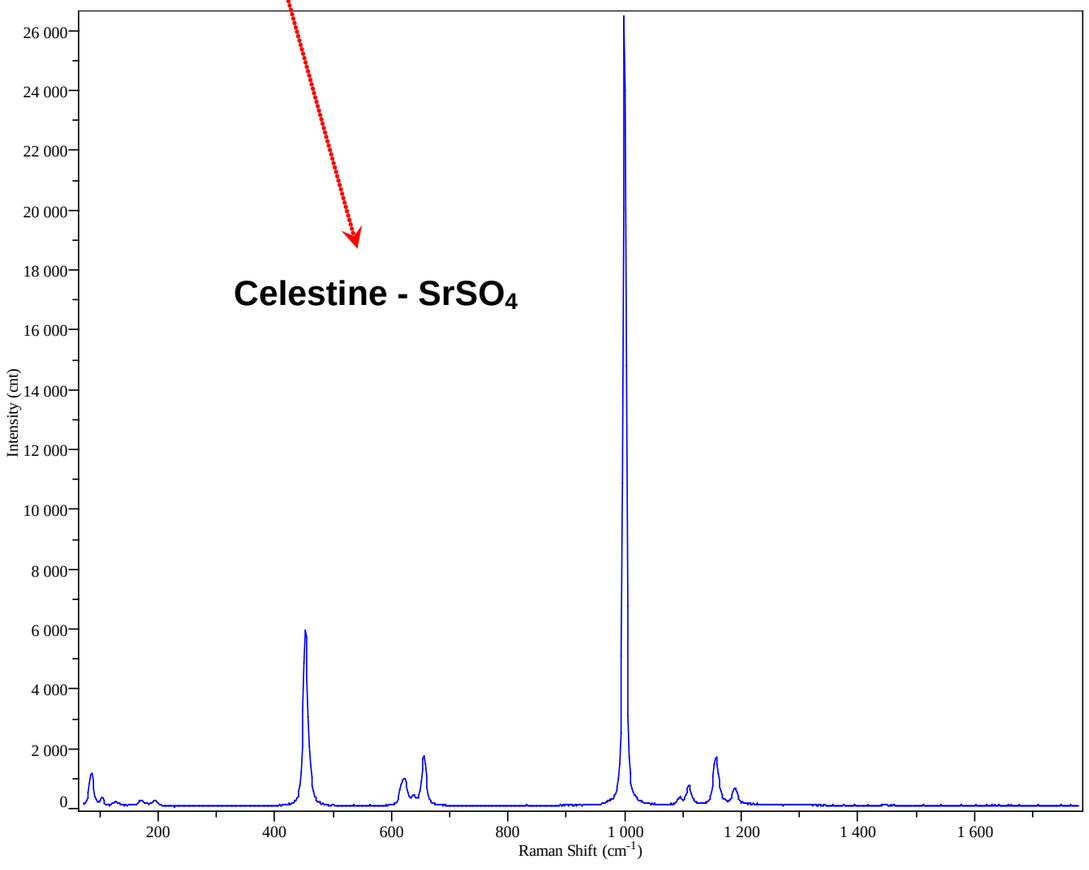

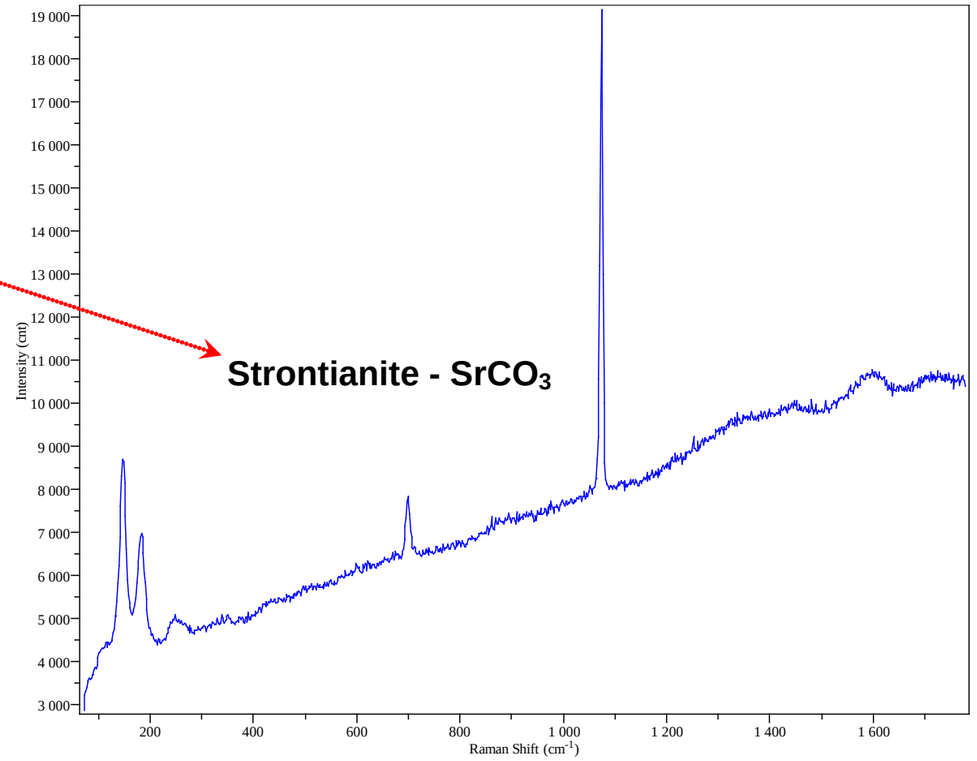

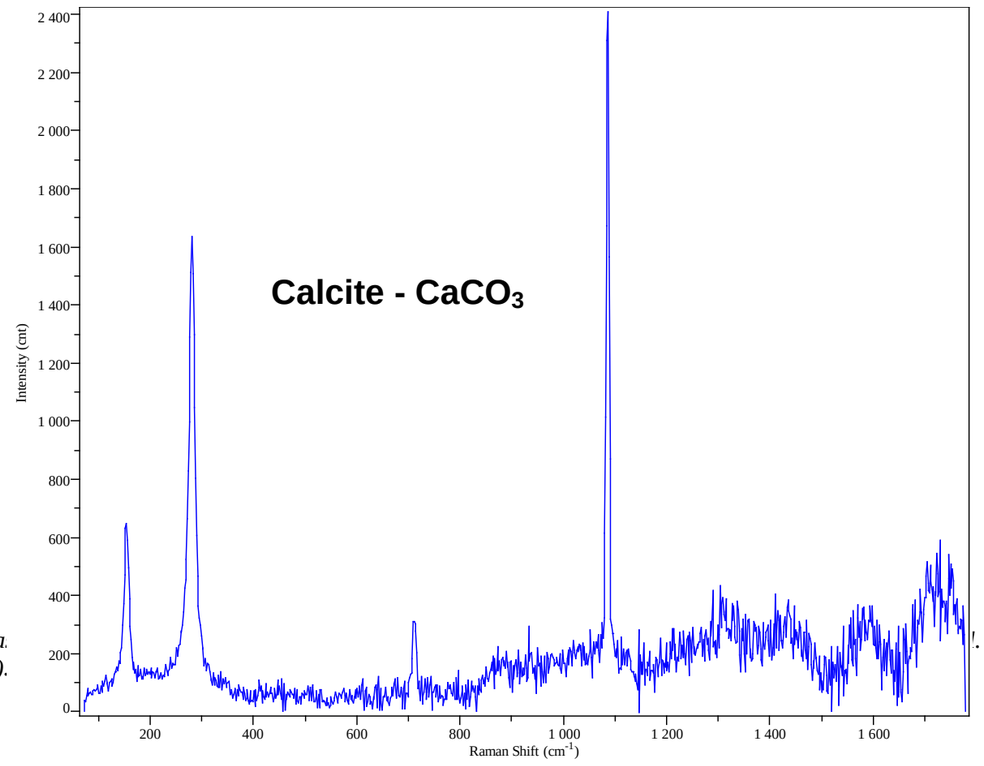

Fig. 2.4a Results of macrocell mineral investigations.

Images in the top left-hand corner of the page are taken with an SEM and do not represent the exact mineral used during La
The spectrums represent classic peaks for the minerals celestine, strontianite and calcite respectively (clockwise from above).

Fig. 2.4b Comparison of a modern algal mat and the Tawnyunshinagh Lmst. Mbr.

(i) *Displays a modern algal mat that has been exposed and desiccated, forming distinctive cracks and curled edges.* ***(ii)*** *Structures on the surface of the Tawnyunshinagh Limestone Member (Carraun Shale Formation) which are superficially comparable to those in (i) and are therefore possibly analogous in origin.*

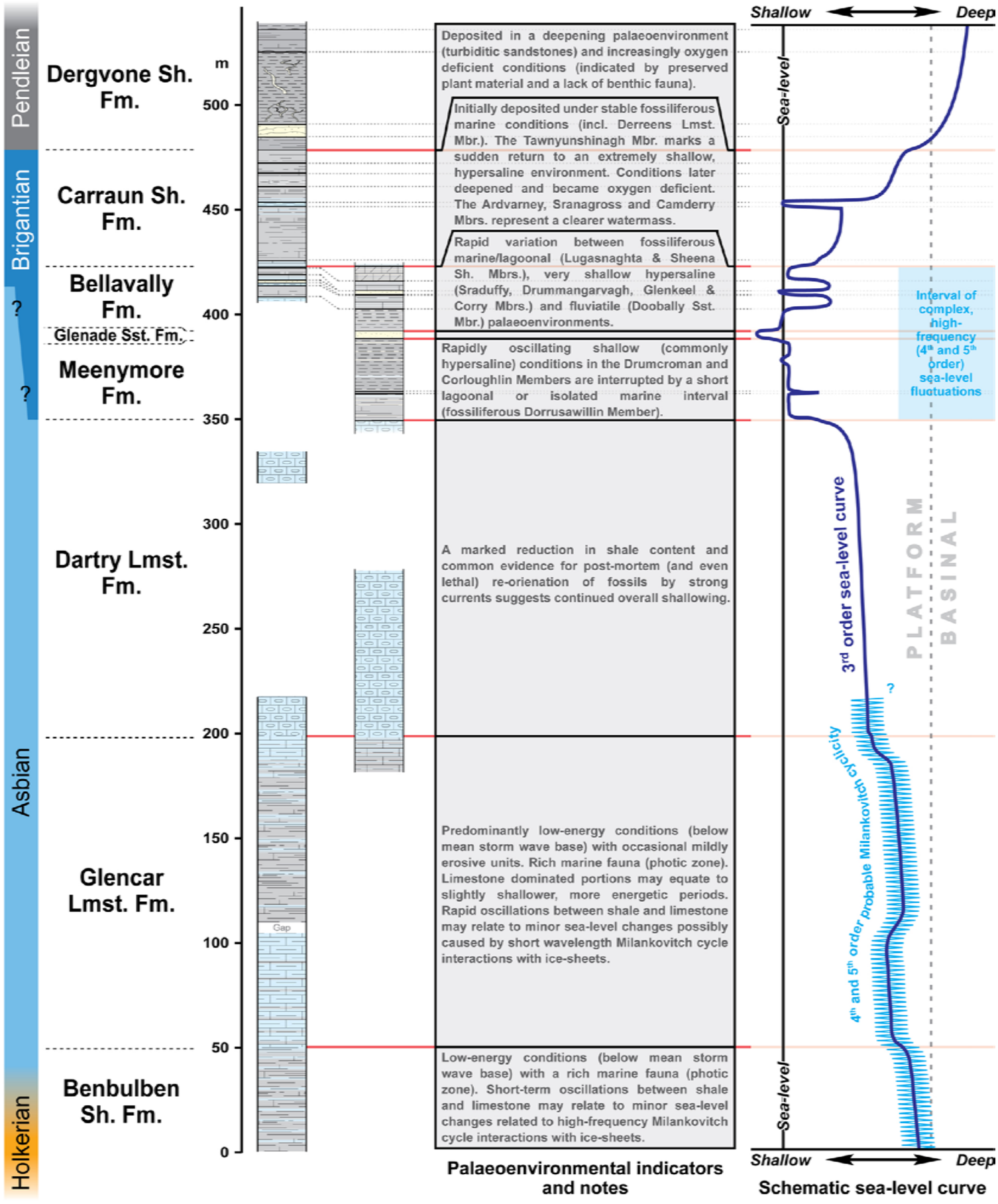

Fig. 2.4c Interpretative sea-level curve for the late Viséan to Serpukhovian stratigraphy in NW Ireland.

Stratigraphic columns are derived from investigation of the Tievebaun (Section 2.2.1), Glencar (Section 2.2.2), Glenade (Section 2.2.3). Aghagrania (Section 2.3.1) and Carraun/Lugasnaghta (Section 2.3.2) Sections. The sea-level curve produced is schematic and the magnitudes of shifts were not measured exactly. The 4th and 5th order cyclicity illustrates the patterned development of limestone and shale that is discussed in Section 2.5.

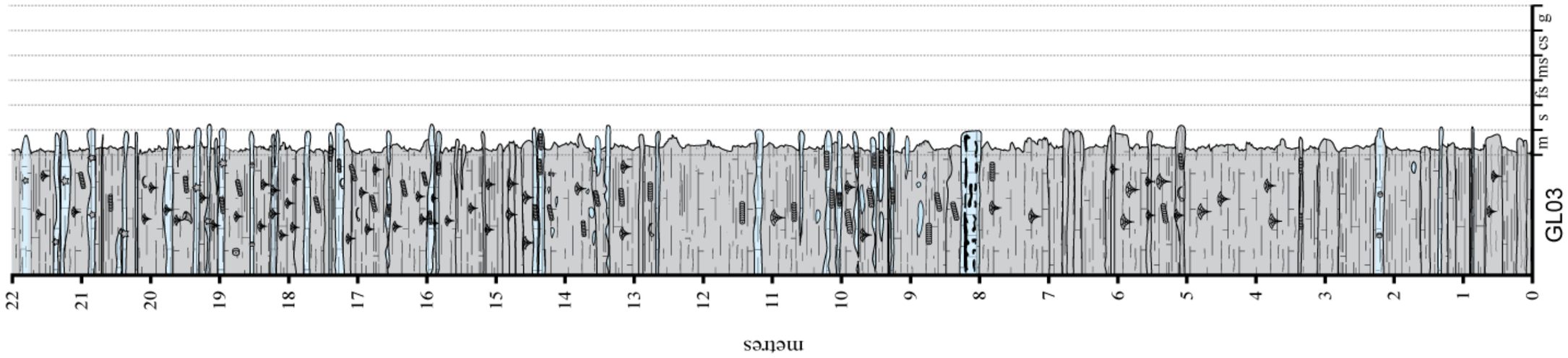

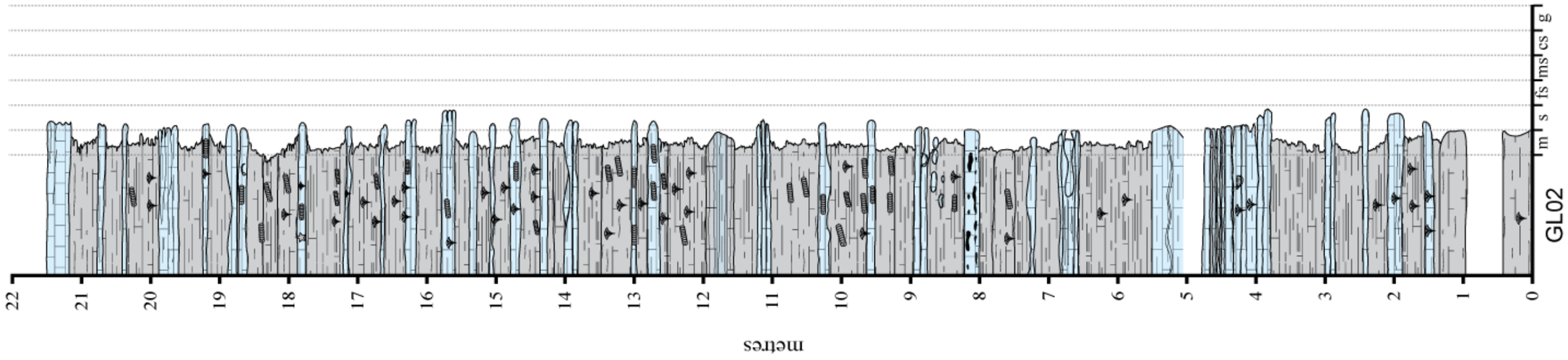

Fig. 2.5a Correlation of lithologies in the Glencar Limestone Formation.

This figure demonstrates the correlation (in red) of sections GL02 and GL03 over a horizontal distance of 690m using the cherty bed at 8m as a marker horizon. Note that both logs have been arbitrarily zeroed. Key is as in Fig. 2.2.1e.

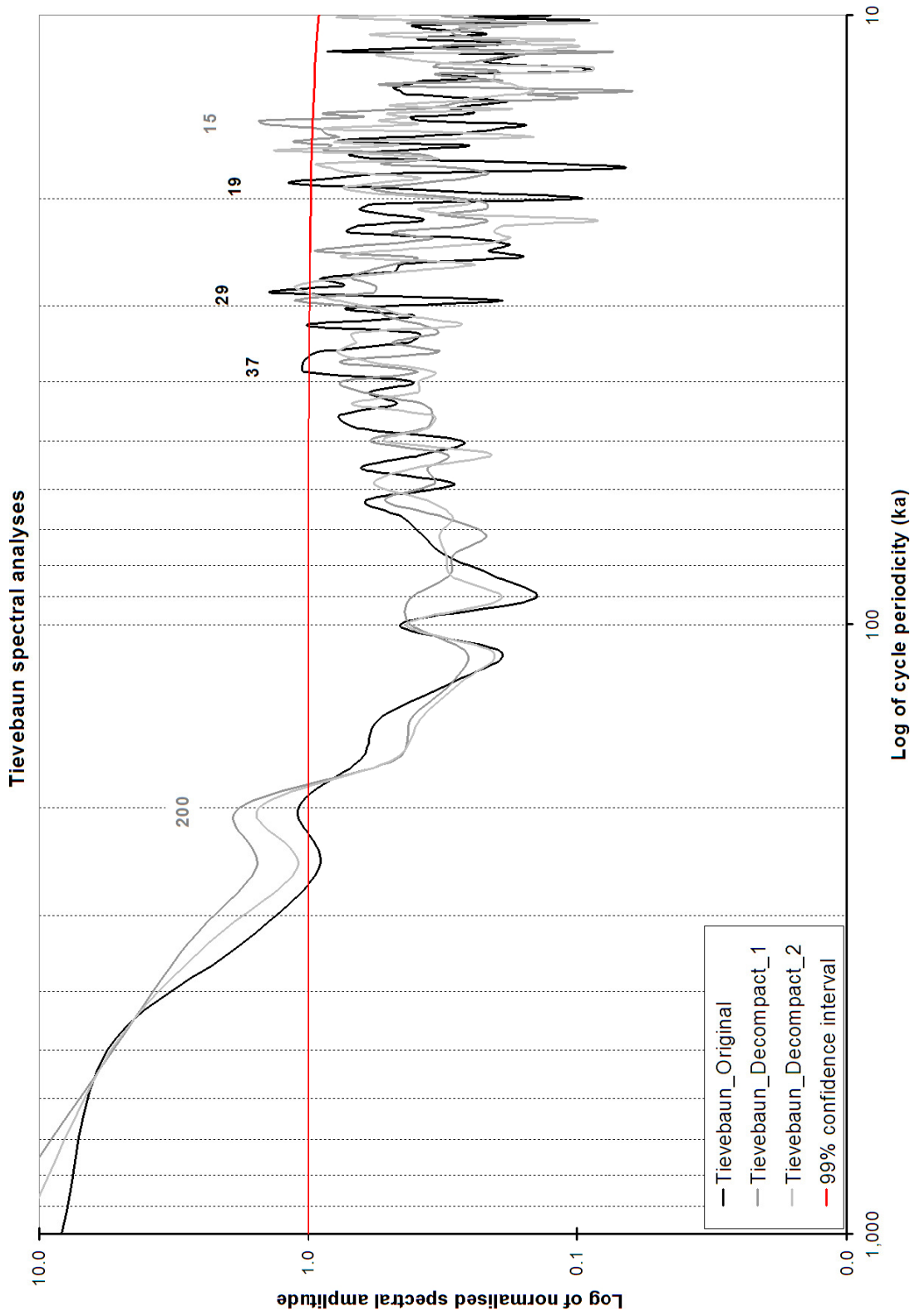

Fig. 2.5b Power spectra for the three decompaction models of the Tievebaun Section.

Grey lines (see key in bottom left of graph) represent the three models of decompaction for the Tievebaun Section. The corresponding cycle periodicity is statistically significant where its spectrum plots above the red line. Numbers above significant peaks give the periodicity in ka of that peak.

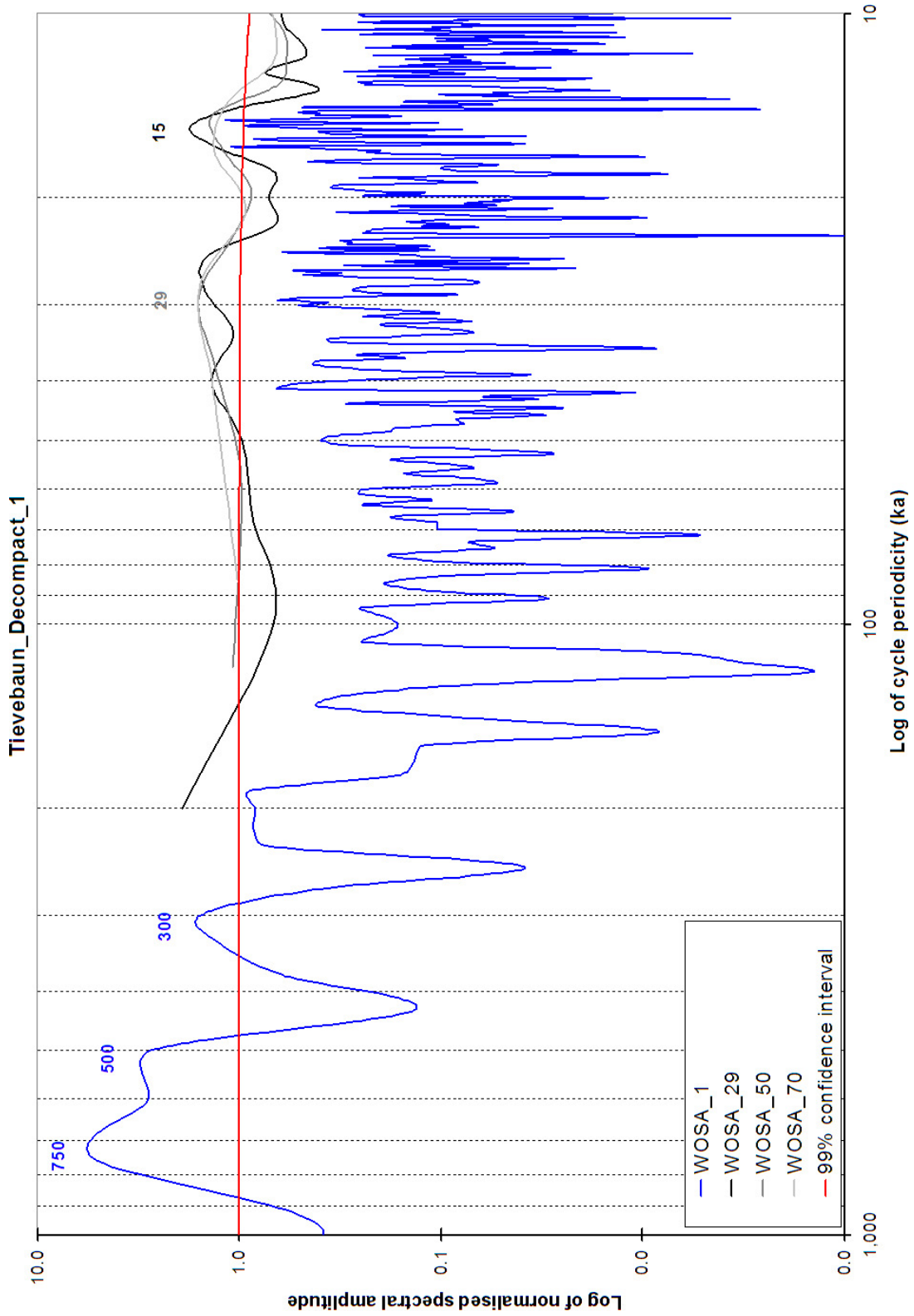

Fig. 2.5c Power spectra for various WOSA applied to Tievebaun_Deccompact_1.

The lines represent the different WOSA conditions as shown in the key (bottom left of graph). Numbers above significant peaks indicate the cycle periodicity of the appropriate peak. Note that the WOSA_1 spectrum continues to 3Ma, increasing at a steady state from the trough at 1Ma, but was excluded from the plot since it reduced the detail of the other plots.

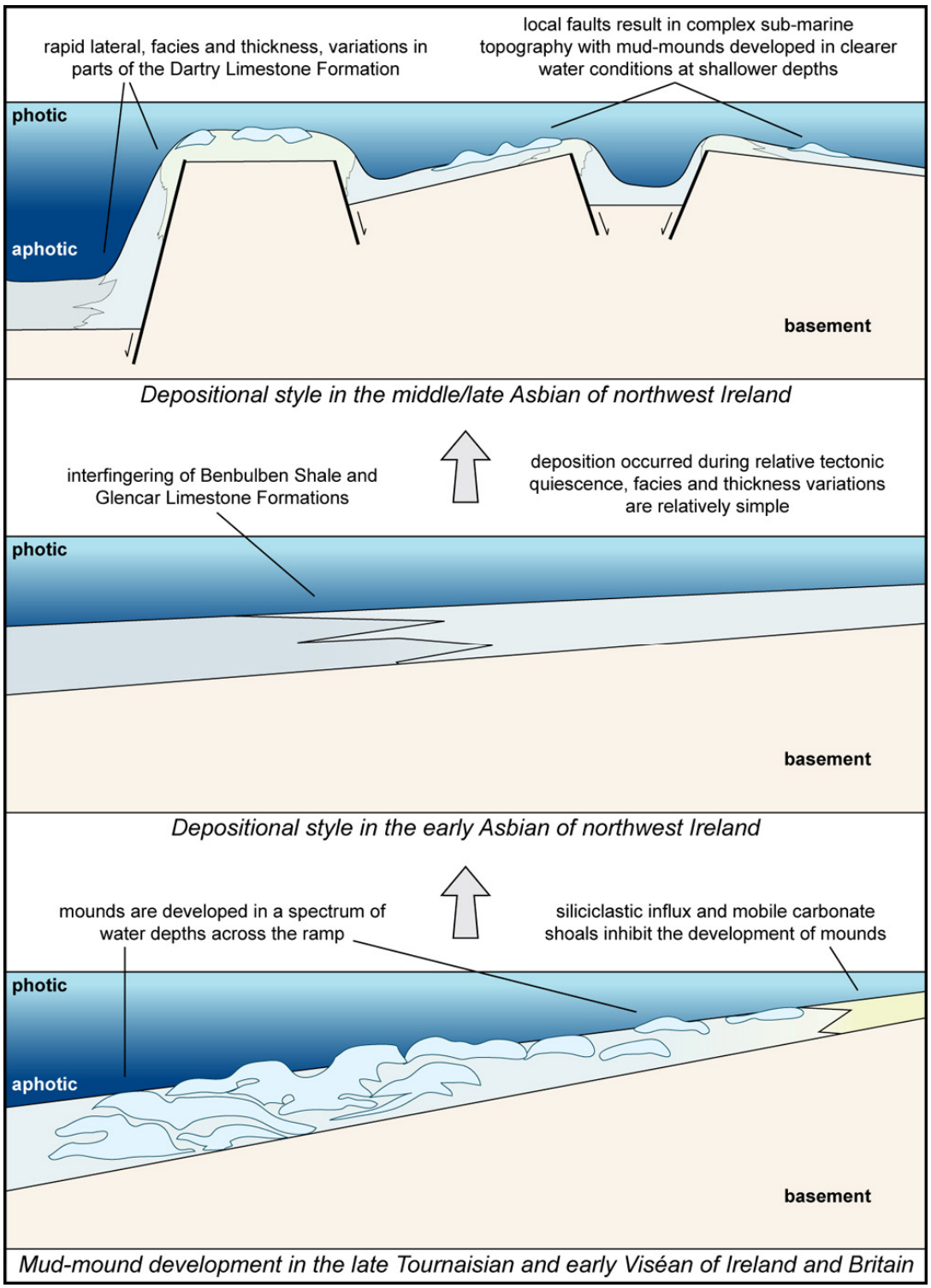

Fig. 2.6 Evolution of depositional setting for the mid-late Viséan of NW Ireland.
Based on Bridges et al. (1995).

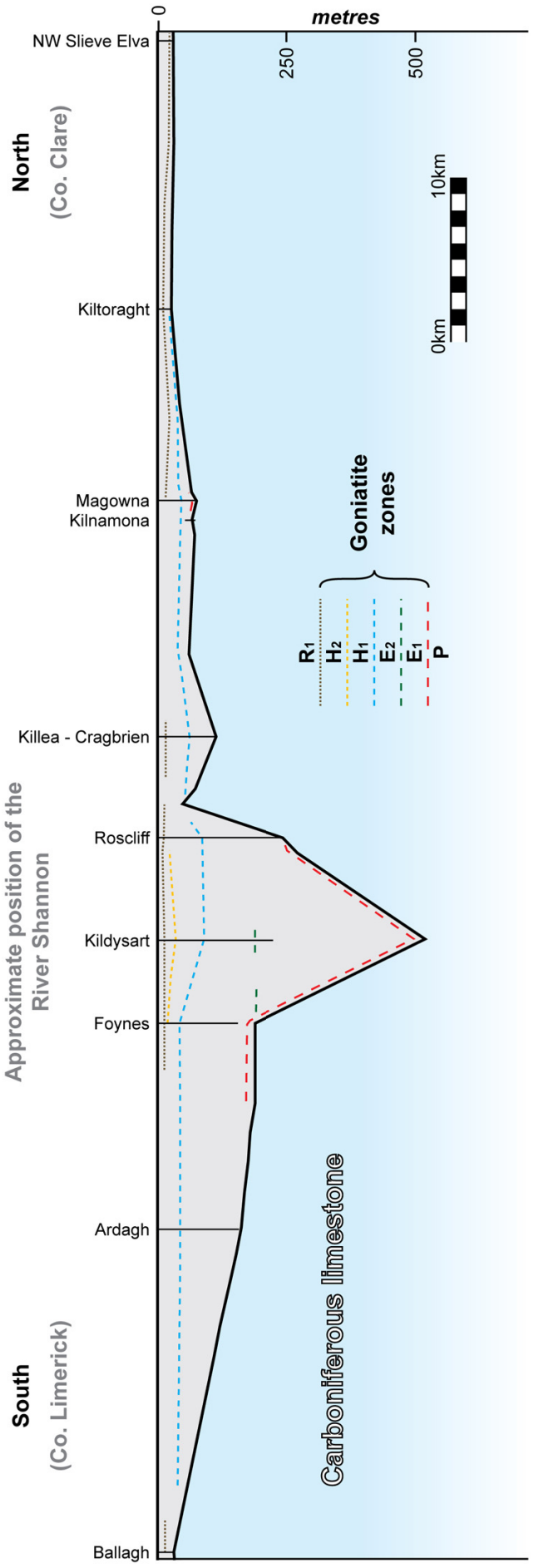

Fig. 3.1 Lateral variation across the Shannon Basin.
The figure demonstrates the chronostratigraphic discordance of the post Viséan limestone sequence from north to south across the basin axis. The thickest and most continuous depositional record is found in the basin axis with goniatite zones obviously onlapping the basin margins as the basin filled. Modified from Hodson and Lewarne (1961).

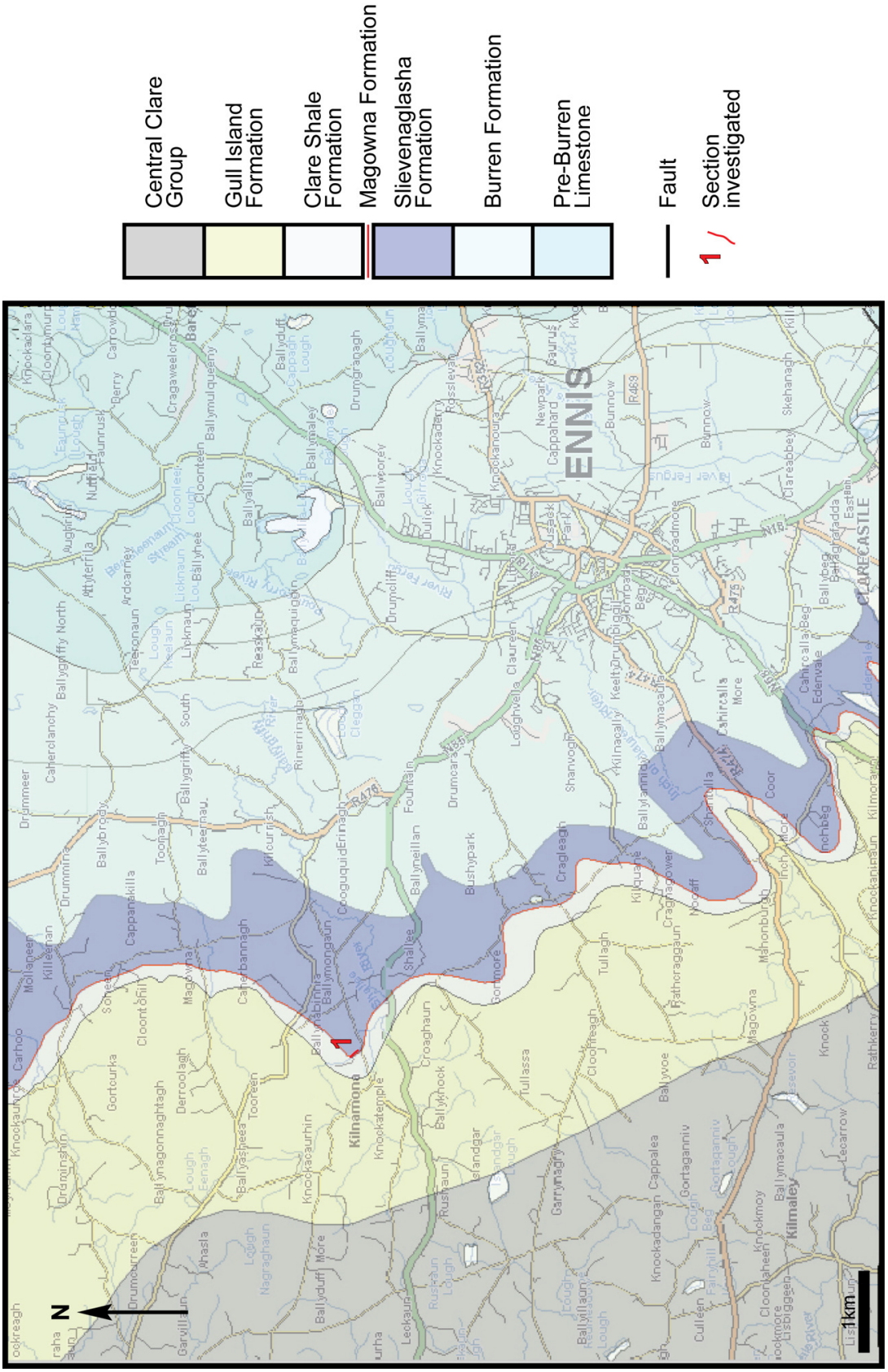

Fig. 3.2.1a Location map for the Kilnamona Section in southwest Ireland.

The thicker red line indicates the portion of the stream that was investigated herein. Overlain on the Ordnance Survey of Ireland map is a simplified version of the 1:100,000 scale geology as mapped by the Geological Survey of Ireland.

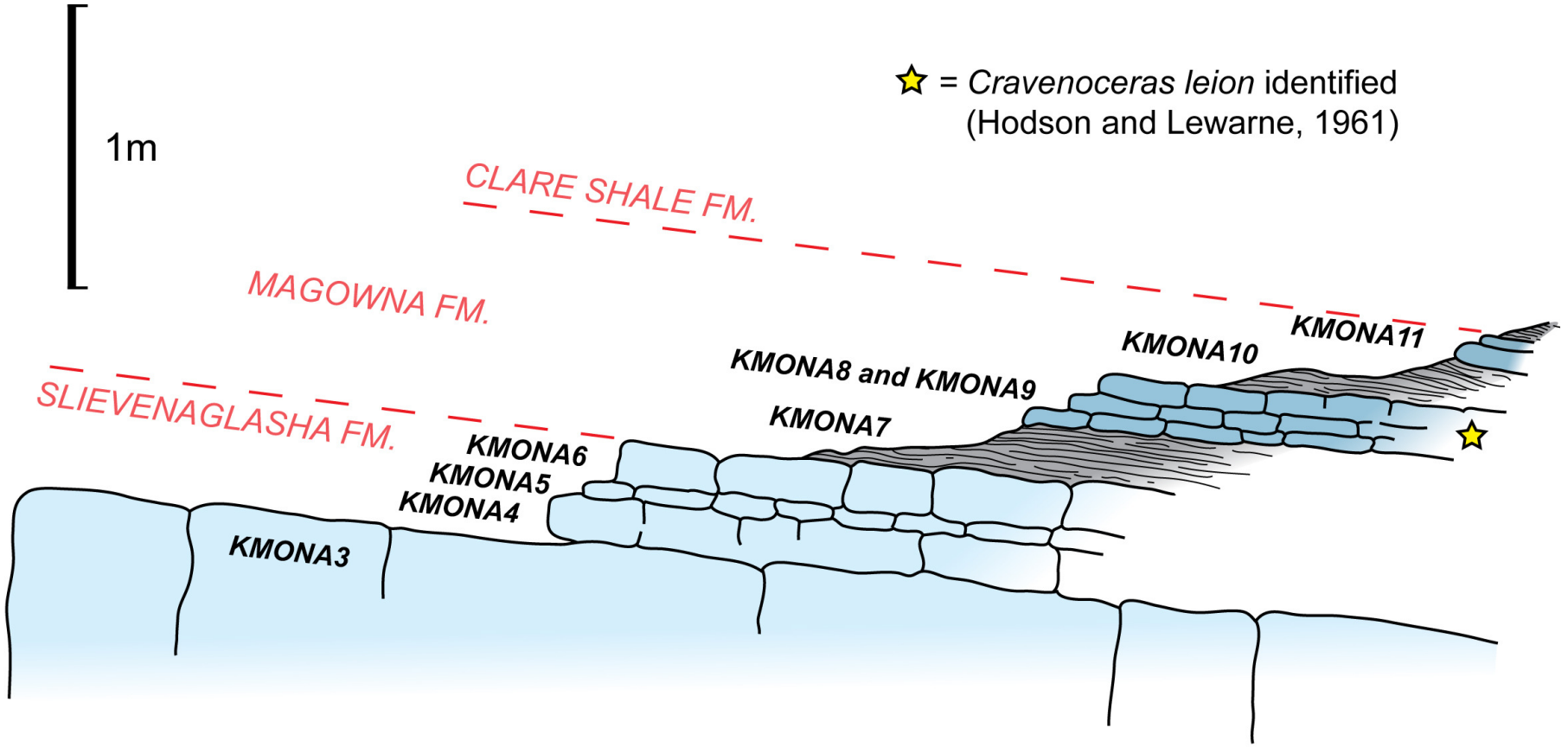

Fig. 3.2.1b Sketch of the Kilnamona Section.

The figure is a reasonably accurate graphical representation of the cross sectional geology exposed in the Kilnamona Section. The image is modified from figure four of Skompski et al. (1995).

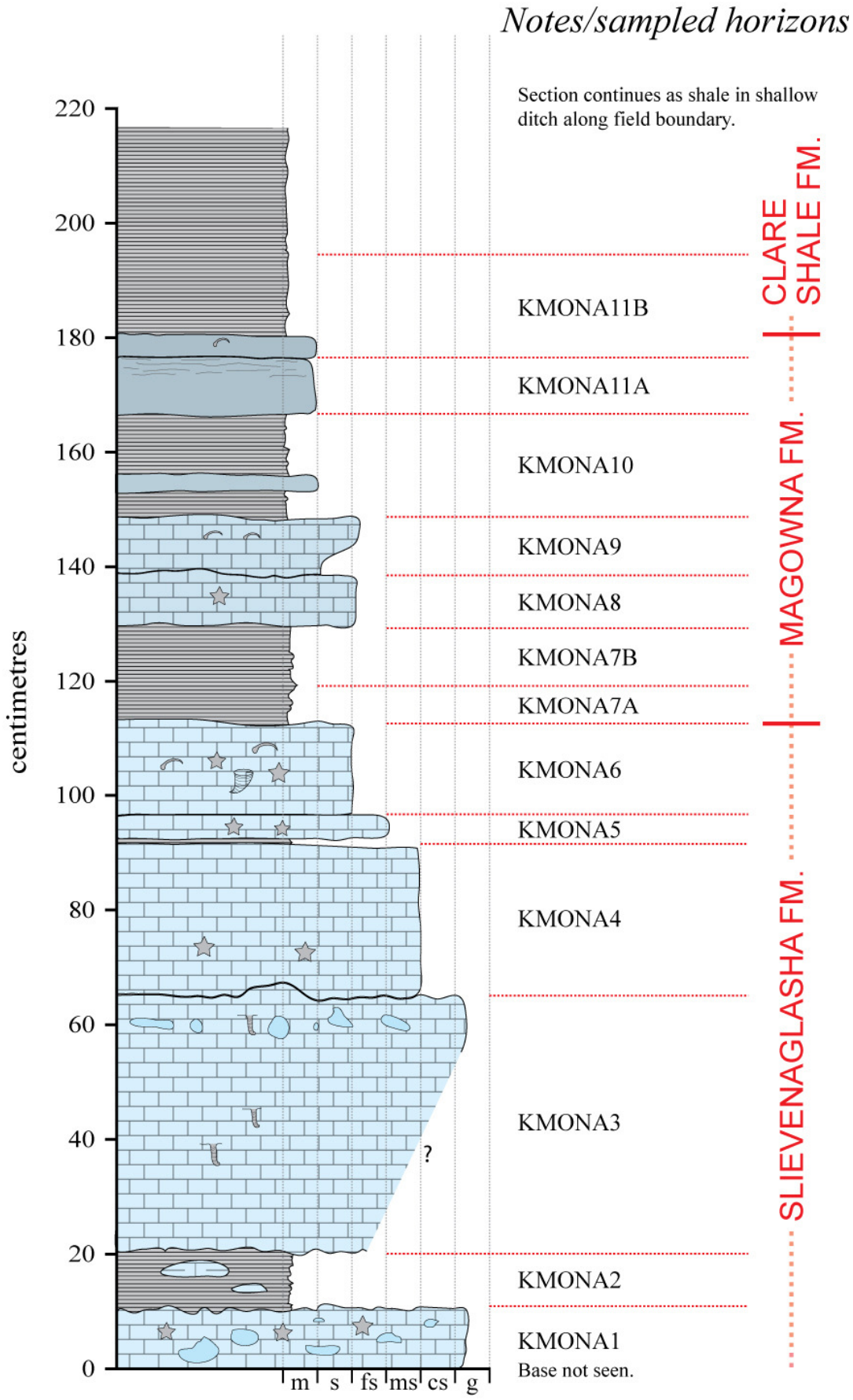

Fig. 3.2.1c Log of the Kilnamona Section.

Key as in Fig. 2.2.1e.

Fig. 3.2.1d Base of the Kilnamona Section.

View upstream towards the start of the logged section, with unit boundaries defined by dashed white lines. Bed KMONA3 can be traced downstream along the west bank, although no lower stratigraphical units are exposed. Note the hammer for scale.

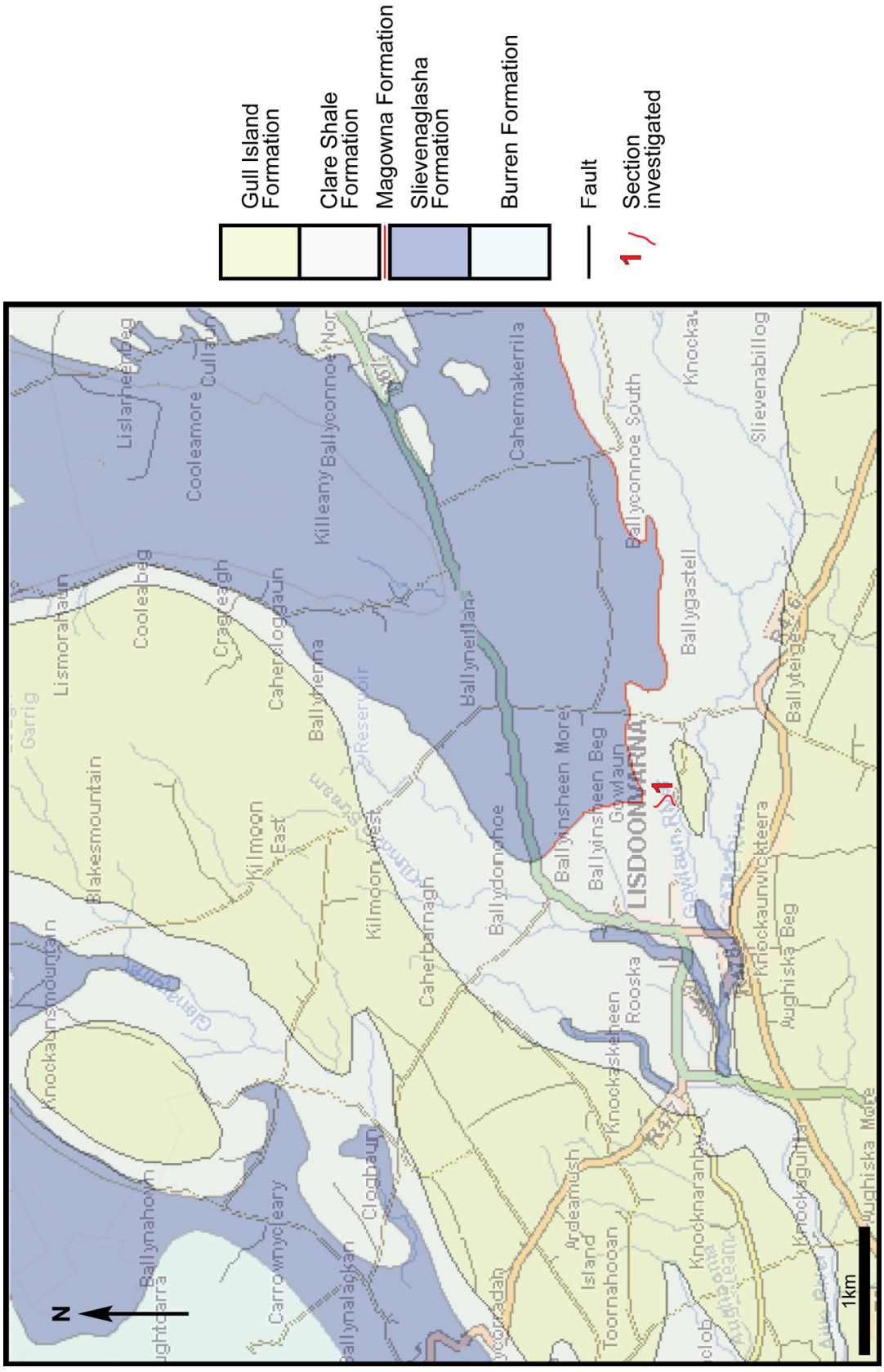

Fig. 3.2.2a Location map for the St. Brendan's Well Section in southwest Ireland.

The thicker red line indicates the portion of the Gowlaun River that was investigated herein. Overlain on the Ordnance Survey of Ireland map is a simplified version of the 1:100,000 scale geology as mapped by the Geological Survey of Ireland. Note that the boundaries as shown by the GSI are slightly inaccurate locally.

Fig. 3.2.2b Overview of the St. Brendan's Well Section exposure.

View upstream towards the prominent bank cut exposing the Clare Shale Formation. Formational boundaries are highlighted by dashed white lines. Hammer for scale is circled in black.

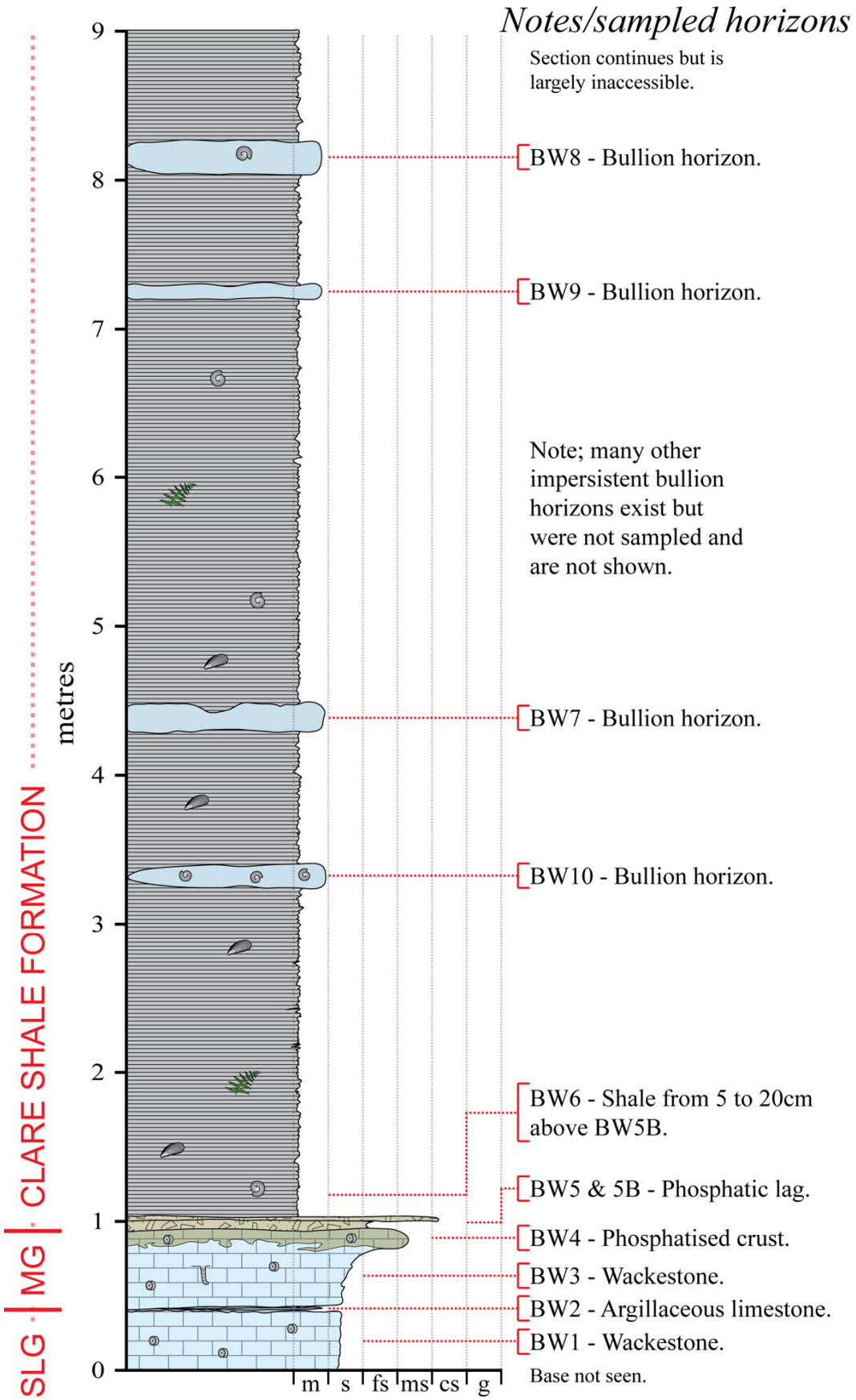

Fig. 3.2.2c Log of the St. Brendan's Well Section.

Key as Fig. 2.2.1e. The distribution of fossils in the shale is schematic. SLG = Slievenaglasha Fm., MG = Magowna Fm. Bullion horizons labelled in order of discovery.

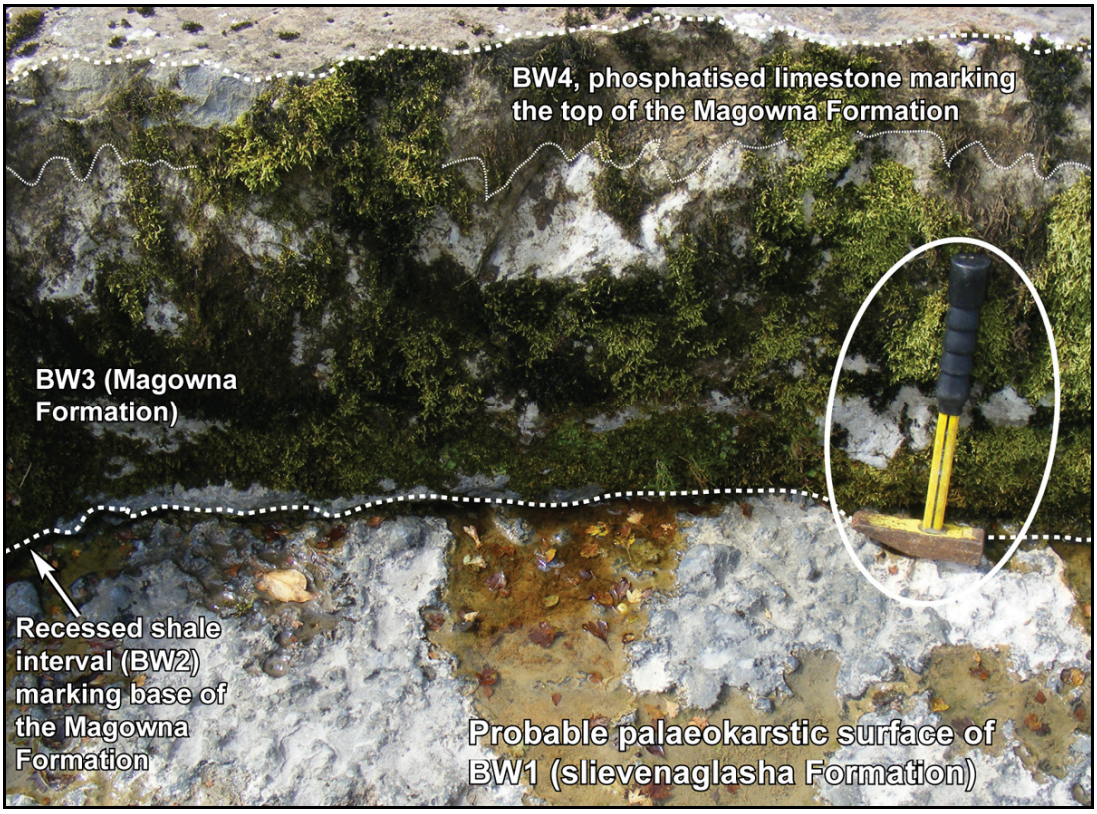

Fig. 3.2.2d Detail of the Slievenaglasha-Magowna contact, St. Brendan's Well Section.

View obliquely downstream towards the Slievenaglasha-Magowna contact (lower dashed white line). Note the probable weakly developed palaeokarstic irregularity of the top of BW1 in the bottom of the photograph which can be traced right up to, and under, the overlying unit. The hammer (for scale) is circled in white.

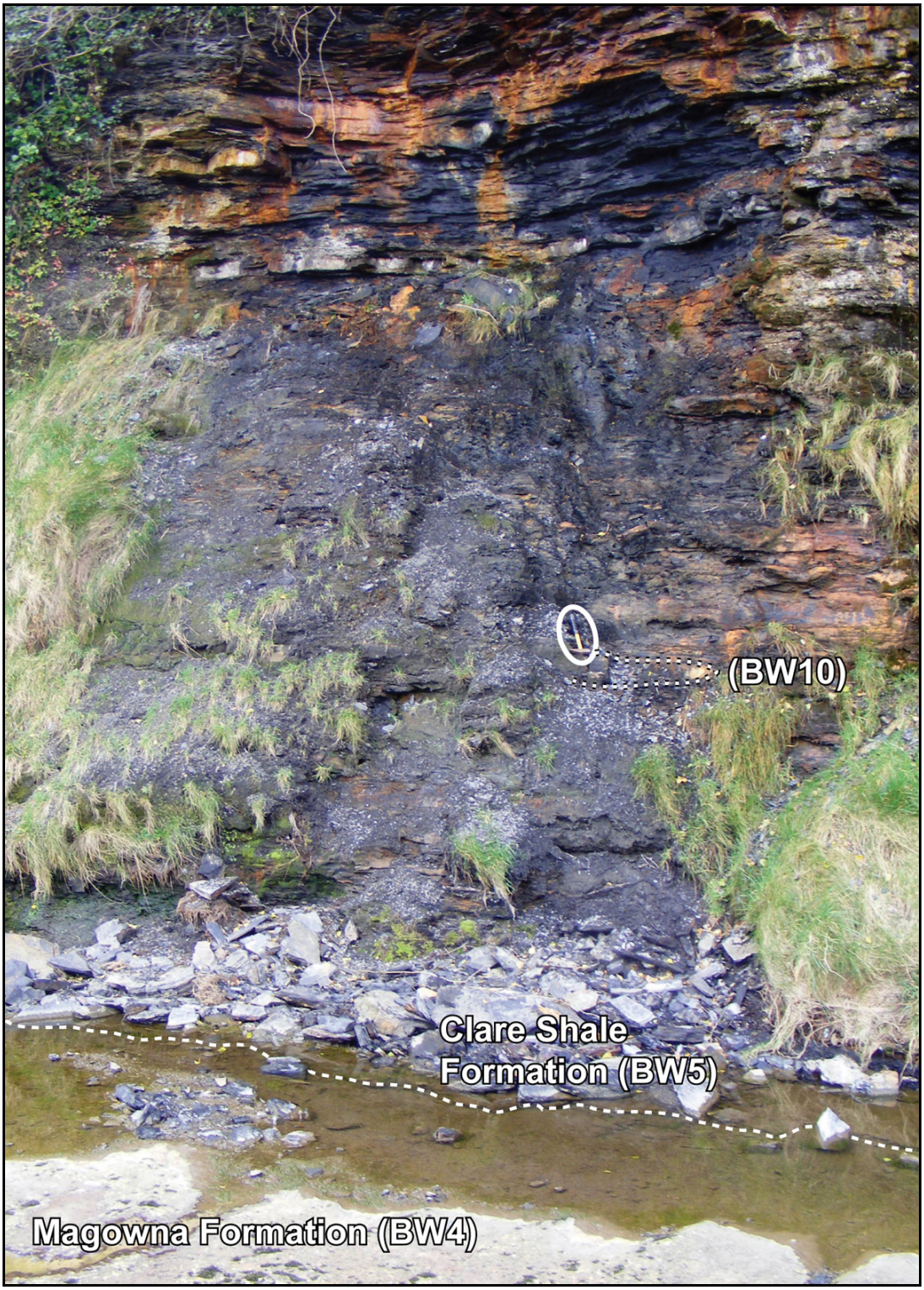

Fig. 3.2.2e The Clare Shale Formation in the St. Brendan's Well Section, Co. Clare.

The bedding plane in the foreground is the top surface of the limestone bed BW4, marking the top of the Magowna Formation. Just below the loose rock at the base of the bank cut, a small step is visible in the water; this represents the exposure of the phosphatic conglomerate (BW5) and the base of the Clare Shale Formation. The hammer in the centre of the photograph (circled in white for scale) rests on the bullion horizon BW10.

Fig. 3.4 Extensive exposure of the possible palaeokarst, St. Brendan's Well Section.

View upstream along the upper surface of the Slievenaglasha Formation (BW1). Note that the shallow white channels in the bedding surface represent modern dissolution due to drainage from the overburden to the right of the image. The hammer (for scale) is circled in white.

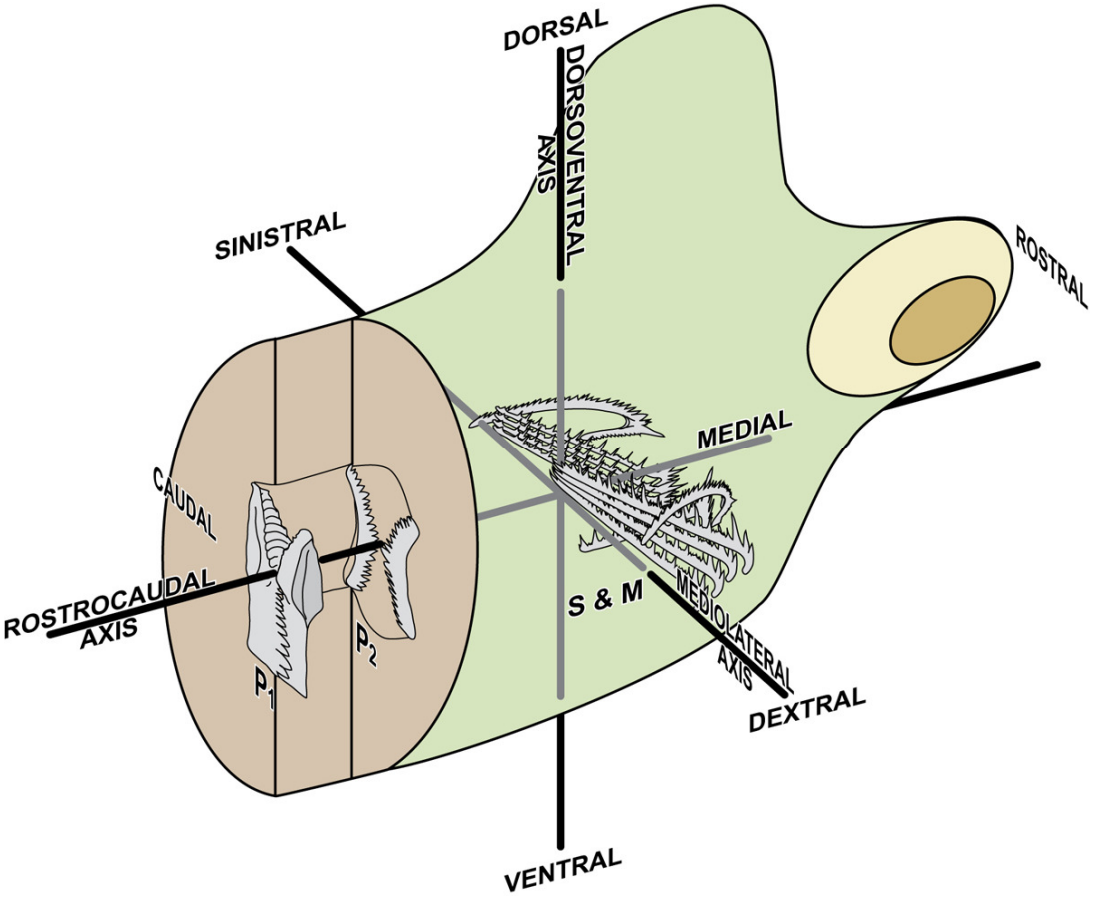

Fig. 4.2a Topological terminology used in conodont apparatus descriptions.
Modified from Purnell et al. (2000).

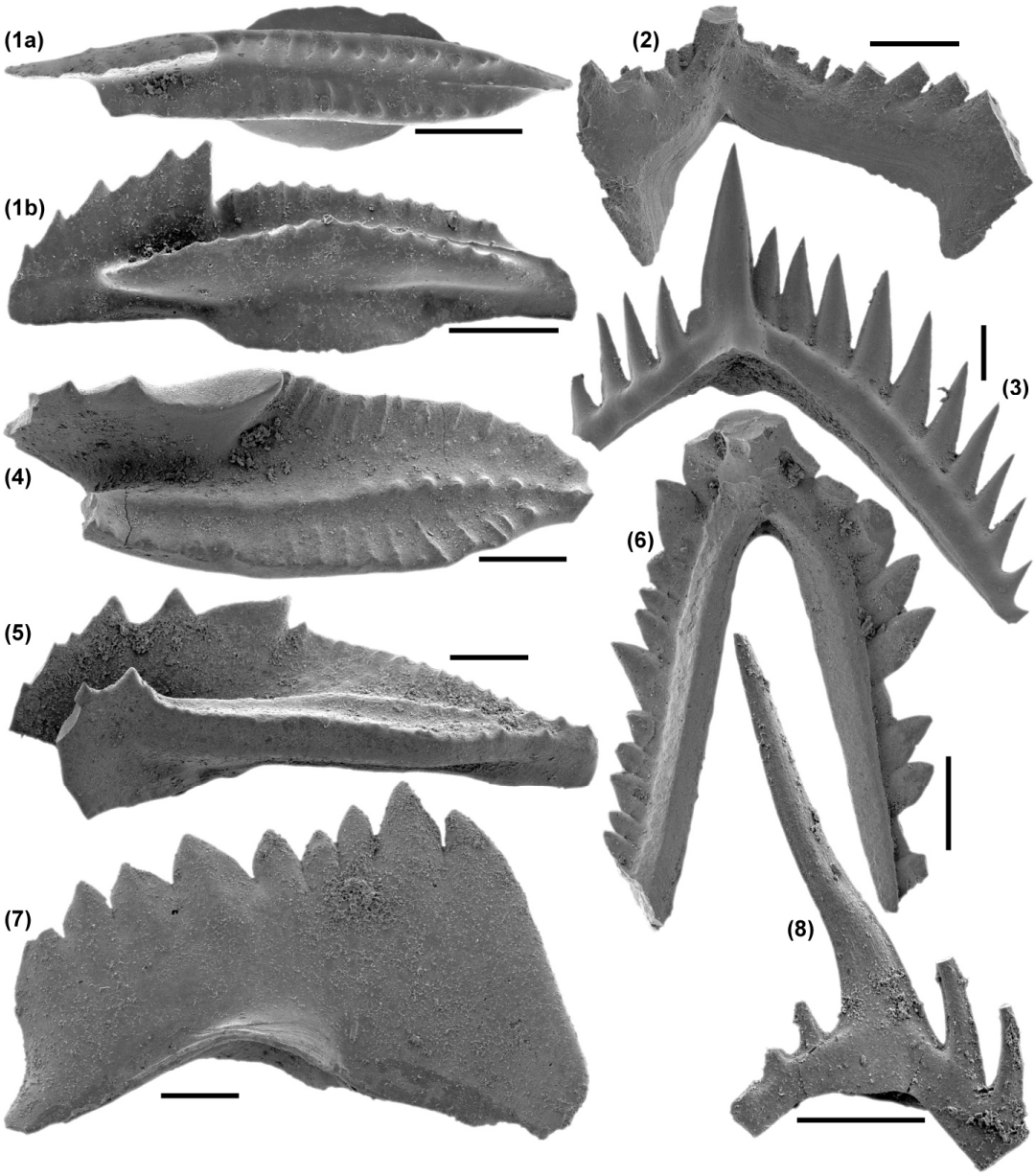

Fig. 4.2b Assorted uncommon conodont genera.

Black scale bars represent 200μm. ***(1a & 1b)*** *Oral and oblique-lateral view of a C. naviculus P_1-element - AGHA4, MB.23B.1.* ***(2)*** *Lateral view of a Hindeodus S-element – BW1, MB.11C.24.* ***(3)*** *Lateral view of an Idioprioniodus element - CNLG1, MB.24A.2.* ***(4)*** *Oral view of a M. bipluti P_1-element - CNLG7, MB.24B.2.* ***(5)*** *Oblique-lateral view of a M. bipluti P_1-element – CNLG7, MB.24B.1.* ***(6)*** *Lateral view of a Synclydognathus S-element - AGHA4, MB.23B.2.* ***(7)*** *Lateral view of a Hindeodus P_1-element. Note that (though worn) the basal cavity extends to the dorsal termination of the element - KMONA4, MB.10A.12.* ***(8)*** *Lateral view of an Idioprioniodus element - AGHA3.2, MB.23A.2.*

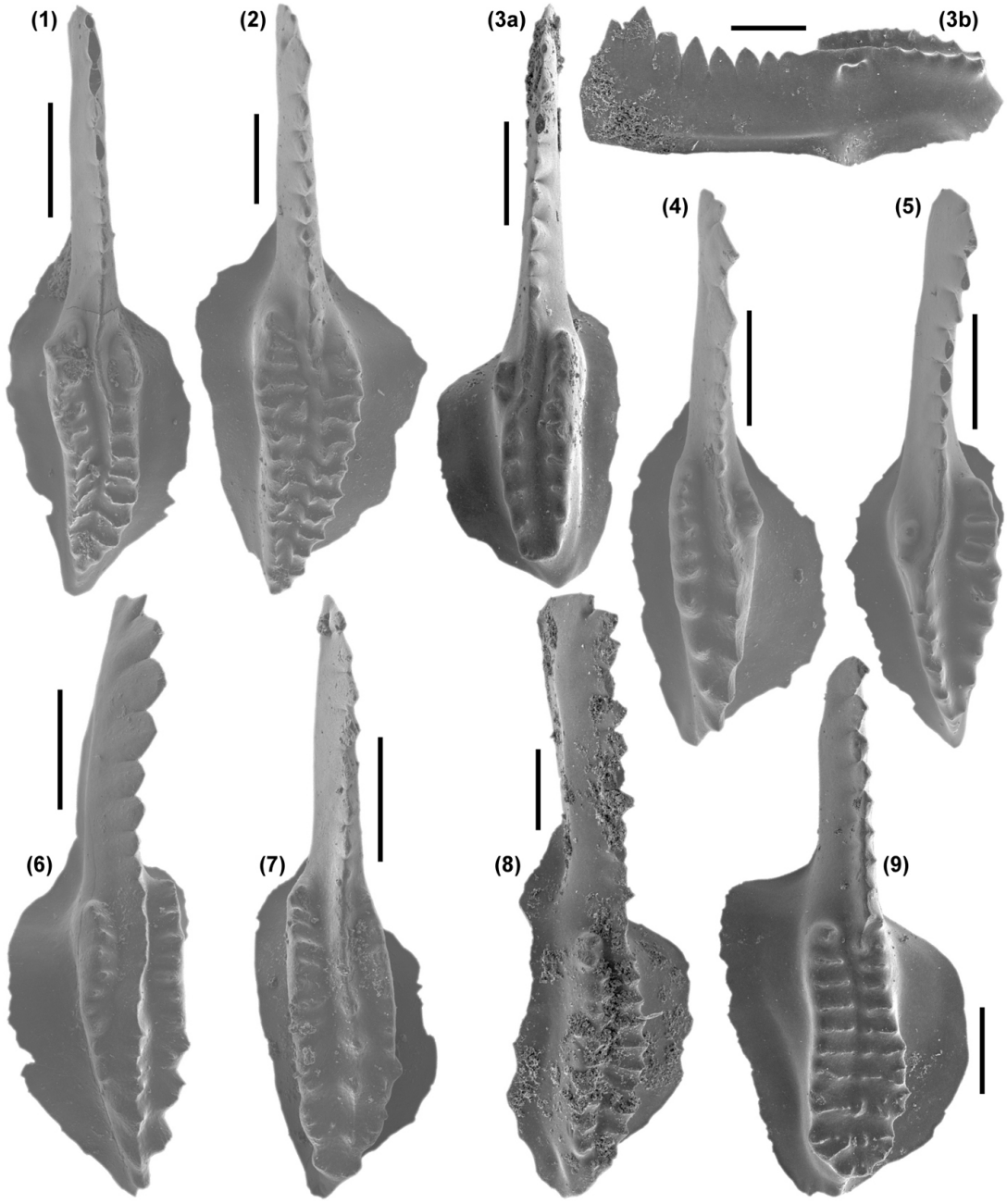

Fig. 4.2c Bashkirian conodonts from the Clare Shale Formation.

All scale bars (black lines) represent 200µm. ***(1)*** *Oral view of a D. lateralis P_1-element - BW10, MB.13A.11.* ***(2)*** *Oral view of a D. lateralis P_1-element - BW10, MB.13A.31.* ***(3a & 3b)*** *Oral and (slightly) oblique oral-rostral view of a D. noduliferous P_1-element - BW8, MB.12C.3.* ***(4)*** *Oral view of a D. noduliferous japonicus? P_1-element - BW10, MB.13A.12.* ***(5)*** *Oral view of a D. noduliferous japonicus? P_1-element - BW10, MB.13A.20.* ***(6)*** *Oral view of a D. noduliferous inaequalis? P_1-element - BW10, MB.13A.18.* ***(7)*** *Oral view of a Neognathodus symmetricus? P_1-element - BW10.* ***(8)*** *Oral view of an Idiognathoides P_1-element - BW8, MB.12C.4.* ***(9)*** *Oral view of an Idiognathoides P_1-element - BW8, MB.12C.1.*

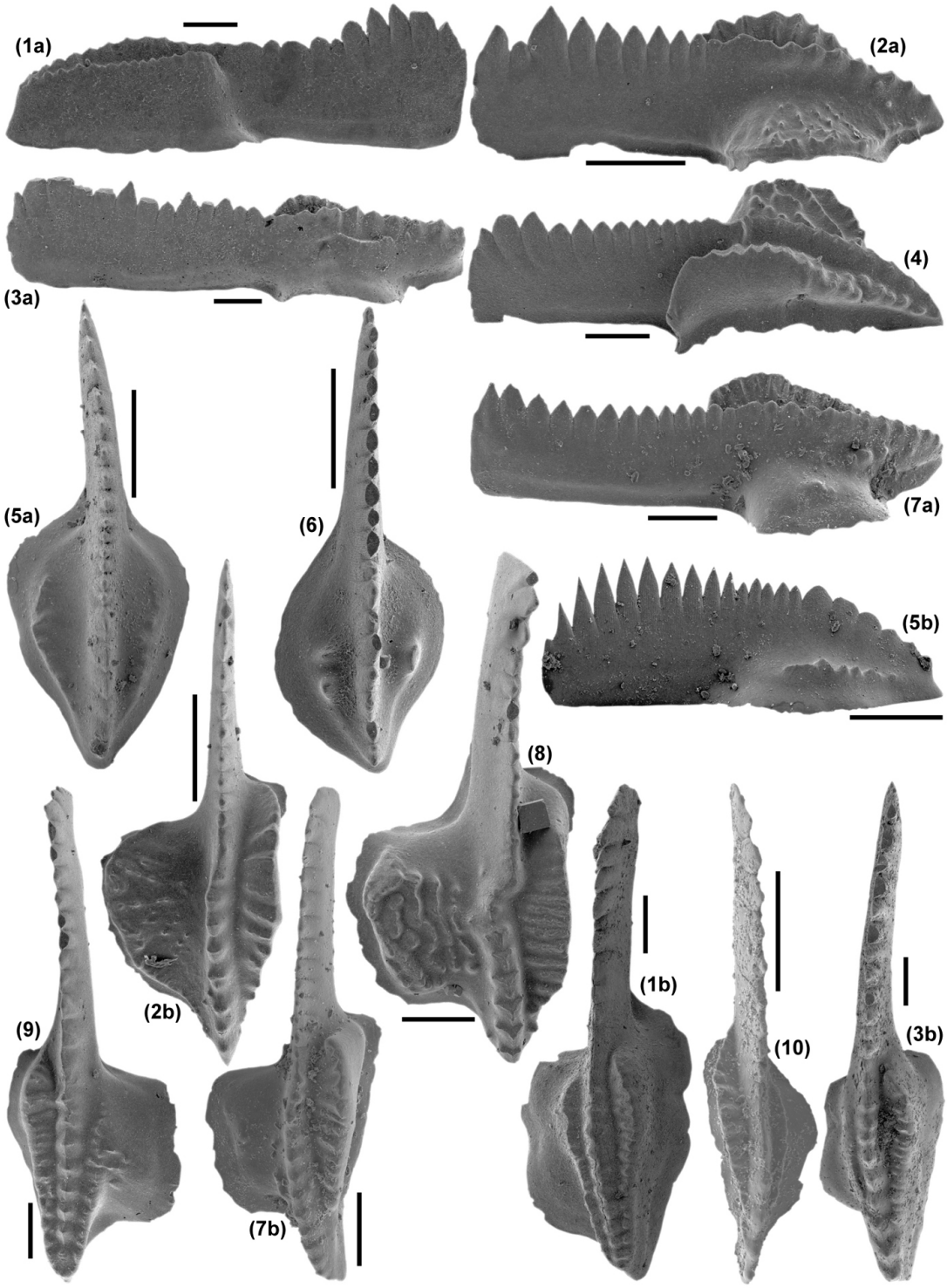

Fig. 4.2d P_1 conodonts of the genus Gnathodus.

Black scale bars represent 200µm. ***(1a &1b)*** *Caudal and oral views of a G. girtyi P_1-element - BW1, MB.11C.10.* ***(2a & 2b)*** *Rostral and oral views of a G. bilineatus P_1-element - BW4, MB.BW4.15.* ***(3a & 3b)*** *Caudal and oral view of a G. girtyi collinsoni? P_1-element - KMONA4, MB.10A.5.* ***(4)*** *Oblique oral-caudal view of a G. bilineatus P_1-element – BW4, MB.BW4.13.* ***(5a &5b)*** *Oral and lateral views of a G. homopunctatus P_1-element - CNLG1, MB.24A.3.* ***(6)*** *Oral view of a G. homopunctatus P_1-element - BW4, MB.BW4.29.* ***(7a & 7b)*** *Rostral and oral views of an G. bilineatus-G. girtyi intermediate - CNLG1, MB.6C.3.* ***(8)*** *Oral view of a G. bilineatus P_1-element with a distinct carinal kink - BW4, MB.BW4.16.* ***(9)*** *Oral view of an intermediate G. bilineatus-G. girtyi P_1-element - BW4, MB.BW4.24.* ***(10)*** *Oral view of a G. girtyi P_1-element - KMONA5, MB.KMONA5.6.*

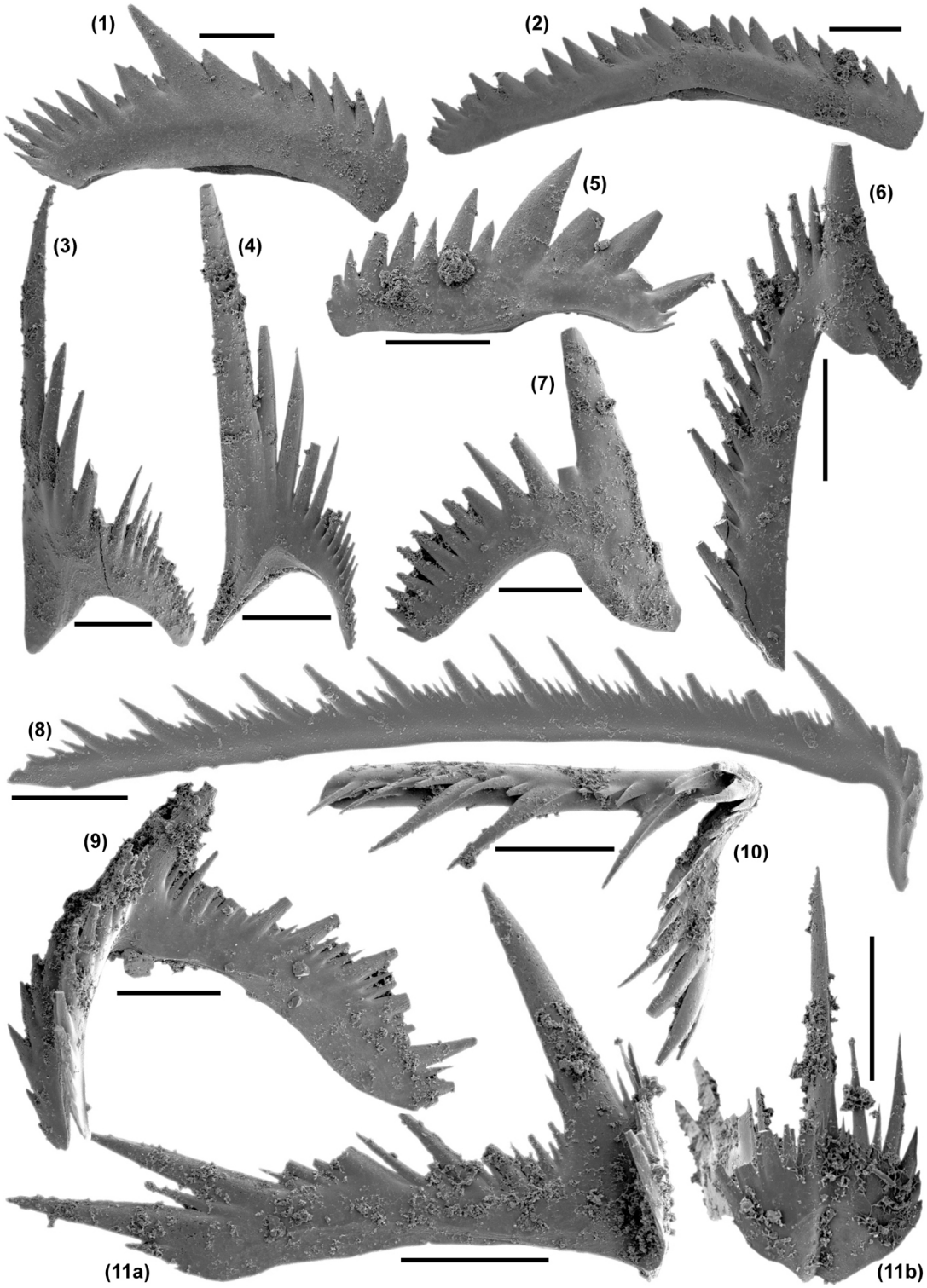

Fig. 4.2e Various P_2-, M- and S- elements.

Black scale bars represent 200µm. ***(1)*** *Lateral view of a possible Lochriea P_2-element - CNLG19, MB.26.13.* ***(2)*** *Lateral view of a Gnathodus P_2-element - CNLG15, MB.25C.8.* ***(3 & 4)*** *Lateral views of Lochriea M-elements – both CNLG19, MB.26.20, MB.26.23.* ***(5)*** *Lateral view of a Lochriea P_2-element - CNLG19, MB.26.14.* ***(6)*** *Lateral view of a Gnathodus M-element - CNLG19, MB.26.12.* ***(7)*** *Lateral view of a Kladognathus M-element - CNLG19, MB.26.21.* ***(8)*** *Lateral view of an isolated S-element of unknown affinity - BW10, MB.13A.9.* ***(9)*** *Lateral view of an S_0-element of unknown affinity - CNLG19, MB.26.10.* ***(10)*** *Oral view of an element of unknown affinity - CNLG19, MB.26.22.* ***(11a & b)*** *Lateral and rostral views of an S_0-element of unknown affinity - CNLG19, MB.26.11.*

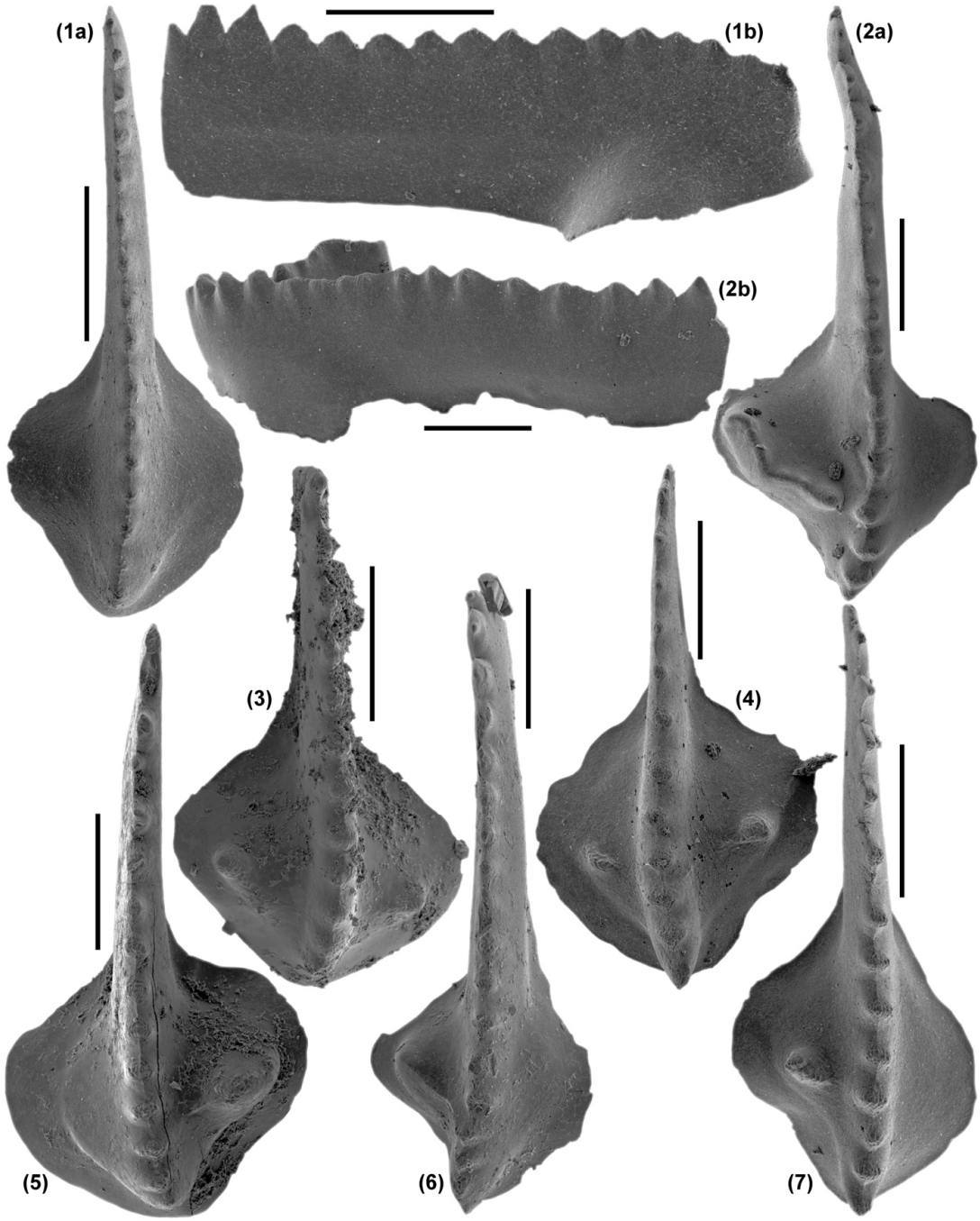

Fig. 4.2f P_1 conodonts of the genus Lochriea (I).

Black scale bars represent 200µm. ***(1a & b)*** *Oral and lateral views of a L. commutata element - BW4, MB.BW4.38.* ***(2a & b)*** *Oral and lateral vies of a L. monocostata element - BW4, MB.BW4.60.* ***(3 & 4)*** *Oral views of L. nodosa elements - CNLG19, MB.26.3 and BW4, MB.BW4.50 respectively.* ***(5 & 7)*** *Oral views of L. mononodosa elements - CNLG15, MB.25C.1 and BW4, MB.BW4.37 respectively.* ***(6)*** *Oral view of a L. monocostata element - KMONA9, MB.11B.2.*

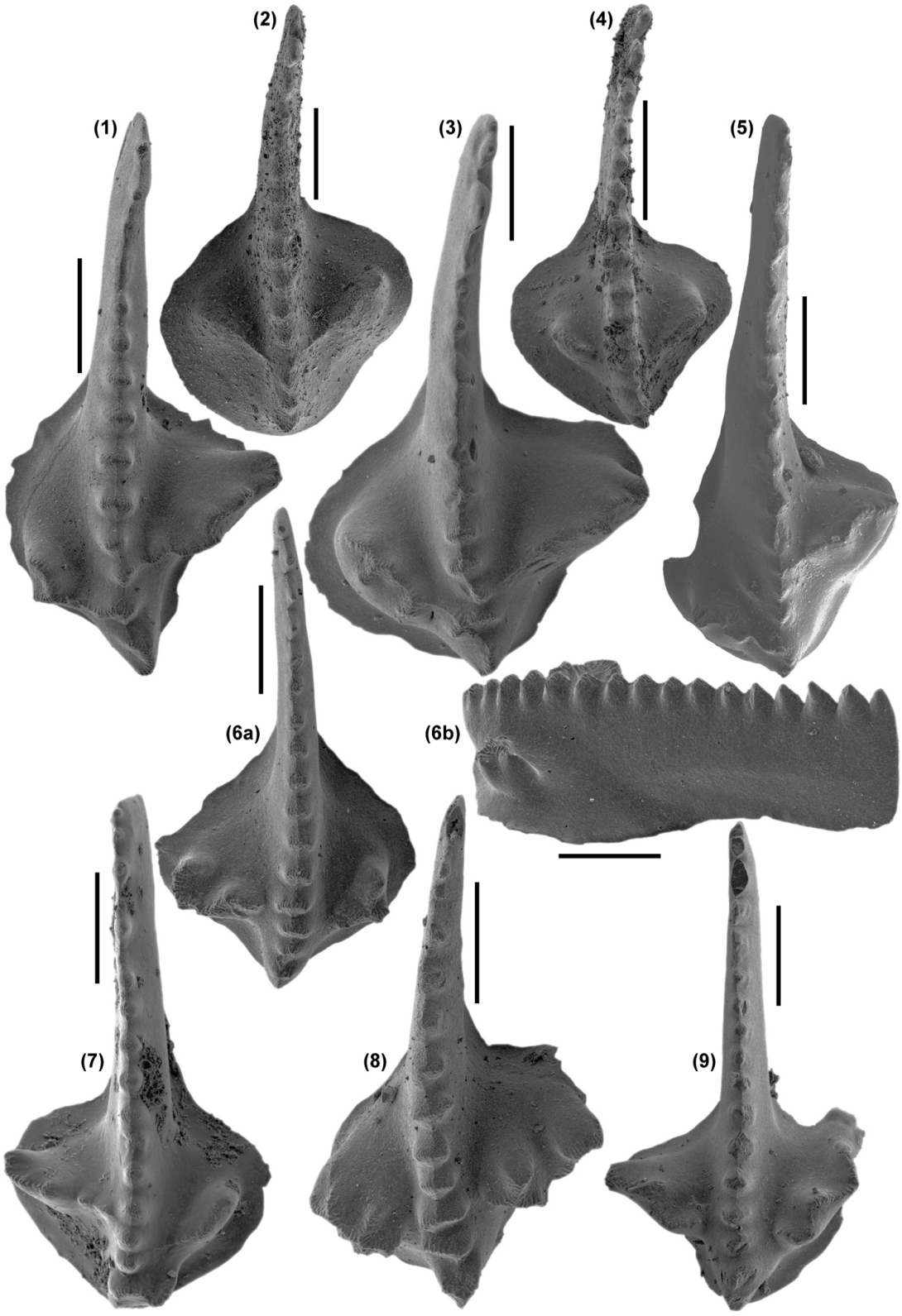

Fig. 4.2g P_1 conodonts of the genus Lochriea (II).

Black scale bars represent 200µm. ***(1, 3 & 5)*** *Oral views of L. cruciformis elements - BW4, MB.BW4.62, BW4, MB.BW4.76 and KMONA5, MB.KMONA5.21 respectively.* ***(2 & 4)*** *Oral views of L. costata elements - KMONA3, MB.9C.6 and CNLG19, MB.26.17 respectively.* ***(6a & b)*** *Oral and lateral views of a L. ziegleri element - BW4, MB.BW4.46.* ***(7, 8 & 9)*** *Oral views of L. ziegleri elements - CNLG15, MB.25C.4, BW4, MB.BW4.52 and BW4, MB.BW4.72 respectively.*

Fig. 4.2h Conodont S-element clusters.

Black scale bars represent 200µm. ***(1)*** *S- and M-element cluster of unknown affinity - CNLG19, MB.26.25.* ***(2-5)*** *S-element clusters of unknown affinity - CNLG19, MB.26.29, MB.26.27, MB.26.26 and MB.26.28 respectively.*

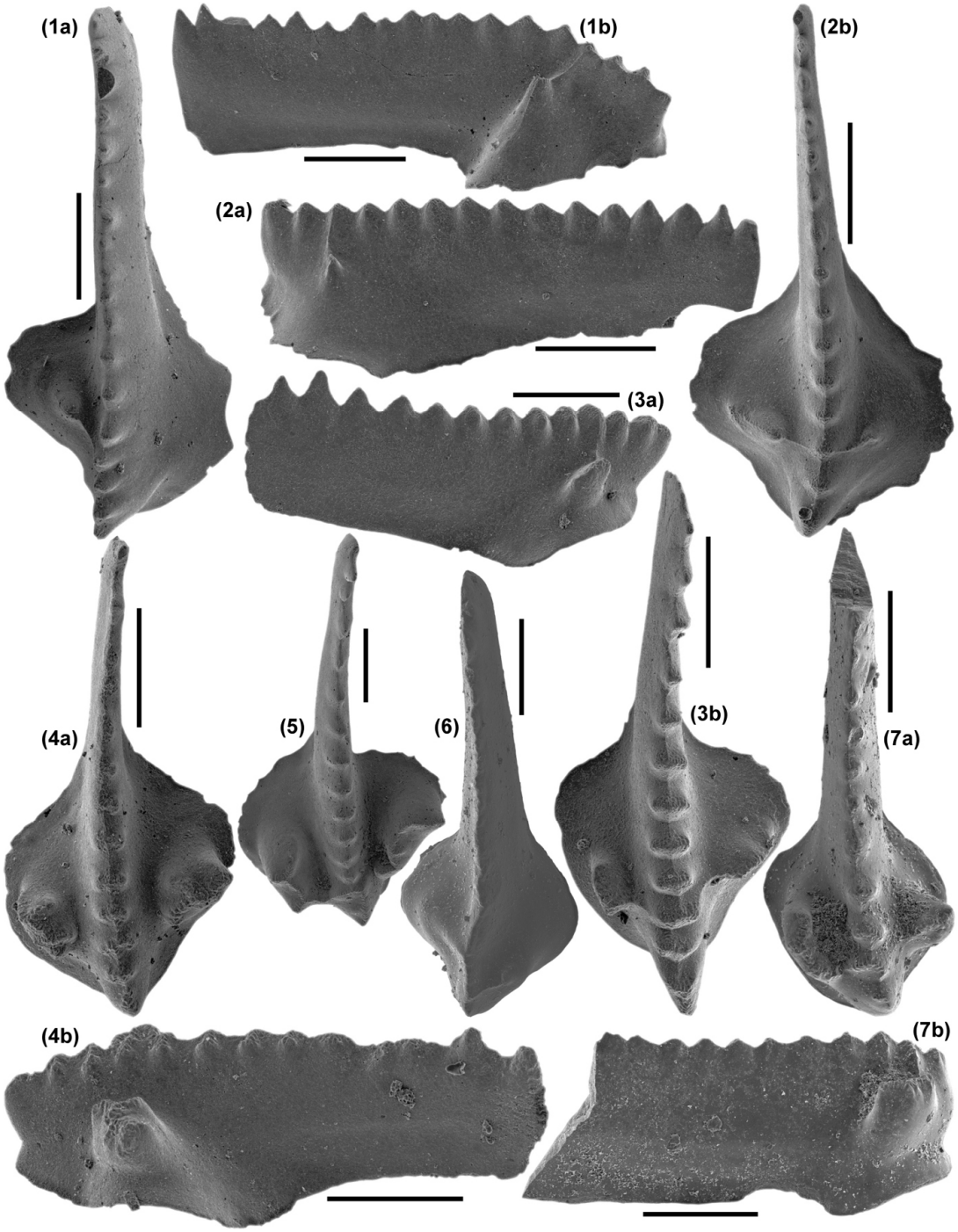

Fig. 4.3a Transitional P_1-elements of the genus Lochriea.

Black scale bars represent 200µm. ***(1a & b)*** *Oral and lateral views of a transitional L. mononodosa to L. monocostata form - BW4, MB.BW4.31.* ***(2a & b)*** *Lateral and oral views of a transitional L. nodosa to L. costata form - BW4, MB.BW4.47.* ***(3a & b)*** *Lateral and oral views of a transitional L. nodosa to L. cruciformis form - BW4, MB.BW4.40.* ***(4a & b)*** *Oral and lateral views of a transitional L. nodosa to L. ziegleri form - BW4, MB.BW4.32.* ***(5)*** *Oral view of a transitional L. ziegleri to L. cruciformis form – KMONA8, MB.11A.30.* ***(6)*** *Oral view of a transitional L. commutata to L. costata form - KMONA5, MB.KMONA5.30.* ***(7a & b)*** *Oral and lateral views of a transitional L. nodosa to L. ziegleri form - CNLG14, MB.8A.3.*

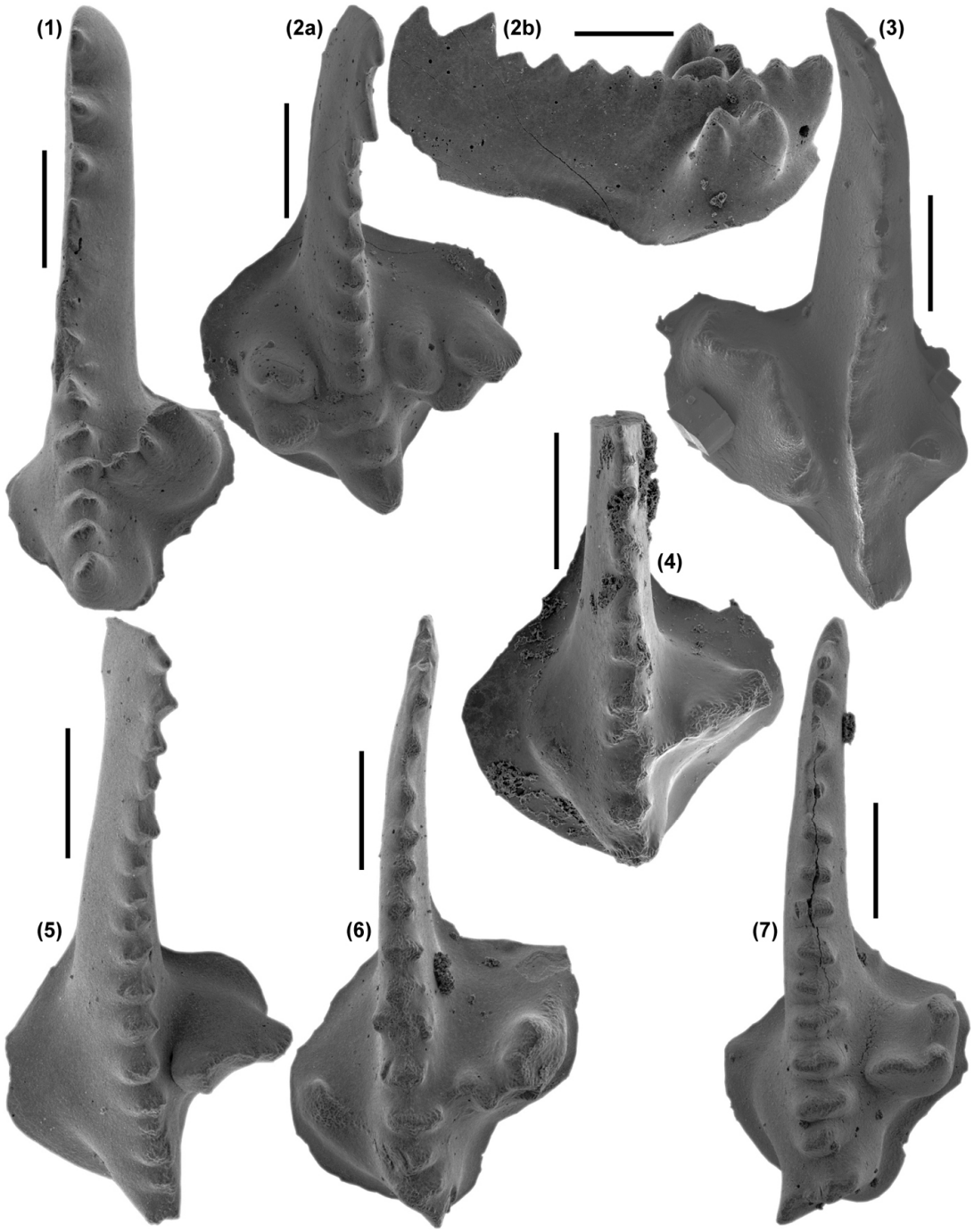

Fig. 4.3b Transitional and taxonomically difficult Lochriea P_1-elements.

Black scale bars represent 200µm. ***(1)*** *Oral view of a difficult to classify element that is morphologically between L. monocostata and L. cruciformis - BW4, MB.BW4.51.* ***(2a & b)*** *Oral and lateral views of a complex Lochriea form that may represent some variant of L. senckenbergica - KMONA8, MB.11A.44.* ***(3)*** *Oral view of a Lochriea element with asymmetric complexity of its lateral ornament - BW3, MB.12B.19.* ***(4)*** *Oral view of an asymmetrically complex element, note the slightly raised rough area on the underdeveloped side of the platform - CNLG15, MB.25C.9.* ***(5)*** *Oral view of an asymmetrically complex Lochriea platform, possibly representing a slightly evolved L. monocostata - BW4, MB.BW4.42.* ***(6)*** *Oral view of an asymmetrically complex element which may represent a transitional form between L. nodosa and L. ziegleri - BW4, MB.BW4.58.* ***(7)*** *Oral view of an asymmetrically complex element, note the pronounced bend in the dorsal termination of the carina - BW4, MB.BW4.75.*

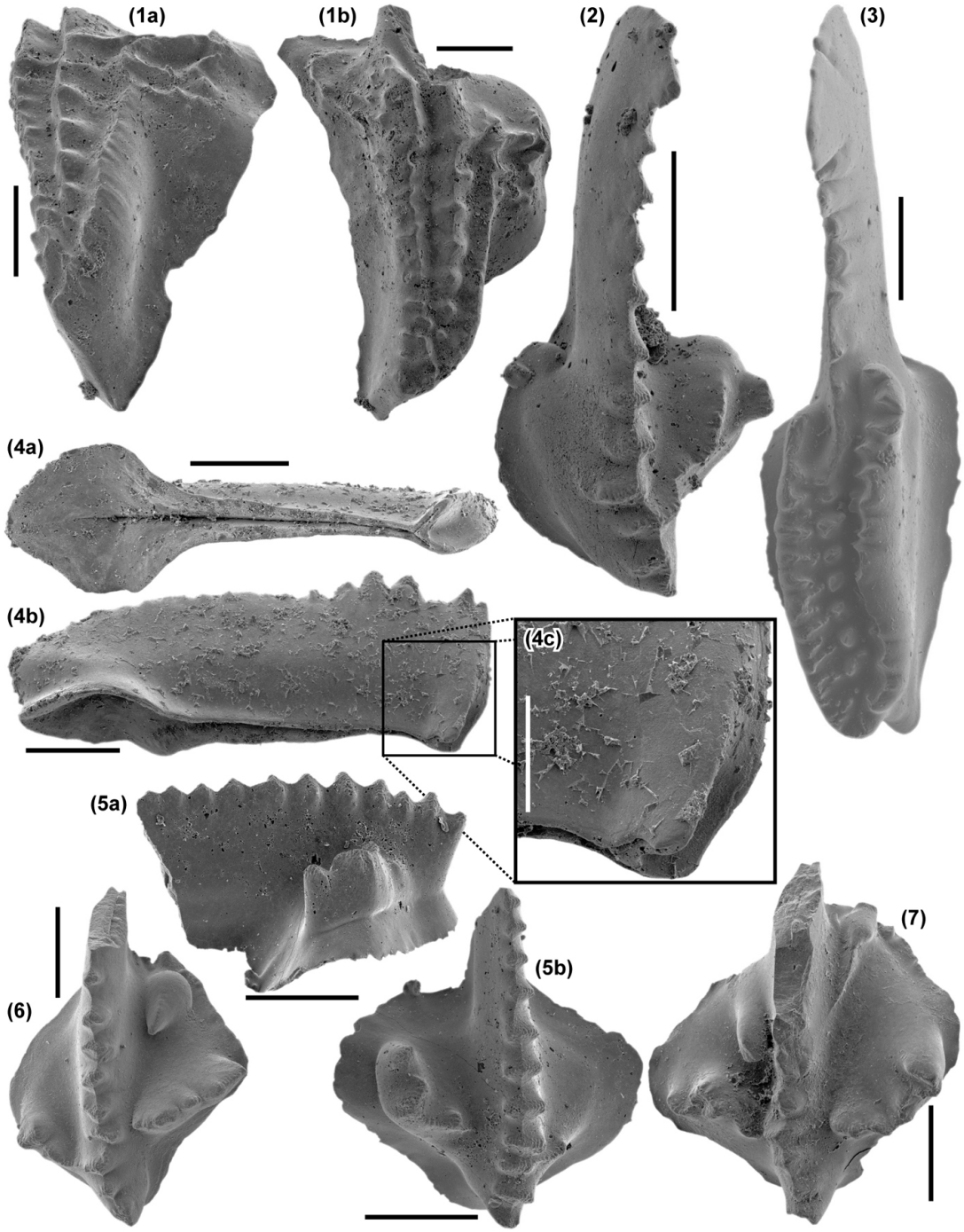

Fig. 4.3c Abnormal P_1-elements of the genera Lochriea and Gnathodus.

Black and white scale bars represent 200µm and100µm respectively. ***(1a & b)*** *Oblique oral views of a G. girtyi element with an irregular ornament descending from the ventral end of the rostral parapet - BW4, MB.BW4.27.* ***(2)*** *Oral view of an unusual Lochriea element. Not only is the platform asymmetrically complex, but isolated, non-functional phosphatic "warts" are found near the basal margin - KMONA8, MB.11A.17.* ***(3)*** *Oral view of a Declinognathodus element which exhibits a concave oral surface and over-steepening of parapets - BW10, MB.13A.24.* ***(4a, b & c)*** *Aboral, lateral and macro views of a L. commutata element with partial blade bifurcation - KMONA4, MB.10A.2.* ***(5a & b)*** *Lateral and oral views of an asymmetrically complex Lochriea element with a small phosphatic "wart" on the ventral margin of the platform base - KMONA8, MB.11A.33.* ***(6 & 7)*** *Oral views of incomplete L. ziegleri elements with distinct abnormal phosphatic growths at the juncture of the free blade and platform - both BW4, MB.BW4.65, MB.BW4.61.*

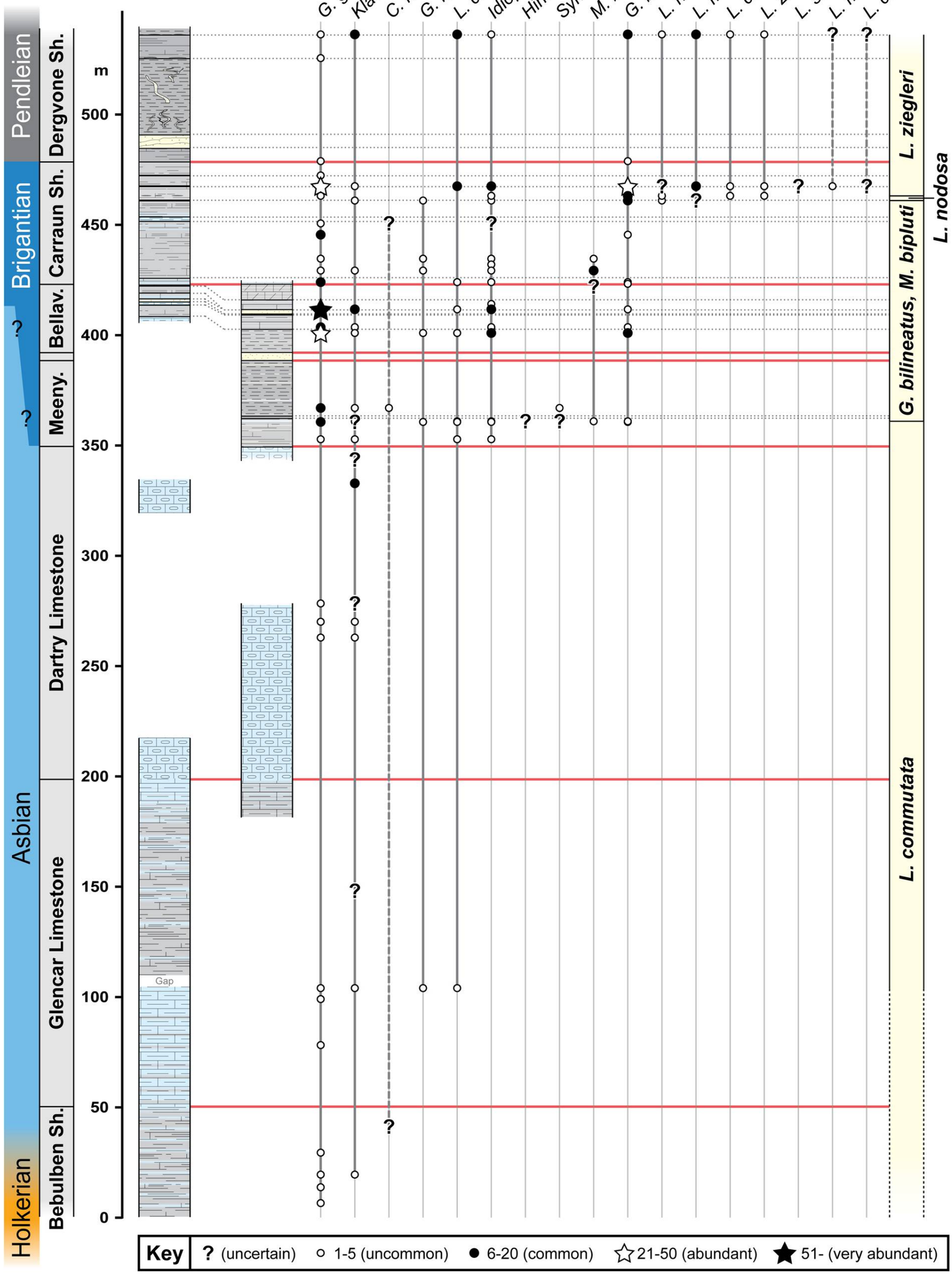

Fig. 4.4a Conodont biostratigraphy in NW Ireland Sections.
Red lines indicate formational boundaries (formations listed in the grey column on the left). Note that the Glenade Sandstone is not named. Dotted grey lines indicate member boundaries. Lithological columns are derived from the: Tievebaun, Glencar, Glenade, Aghagrania and Carraun/Lugasnaghta Sections. Abundances are per 2kg. Conodont Biozones are provided in the yellow column on the right.

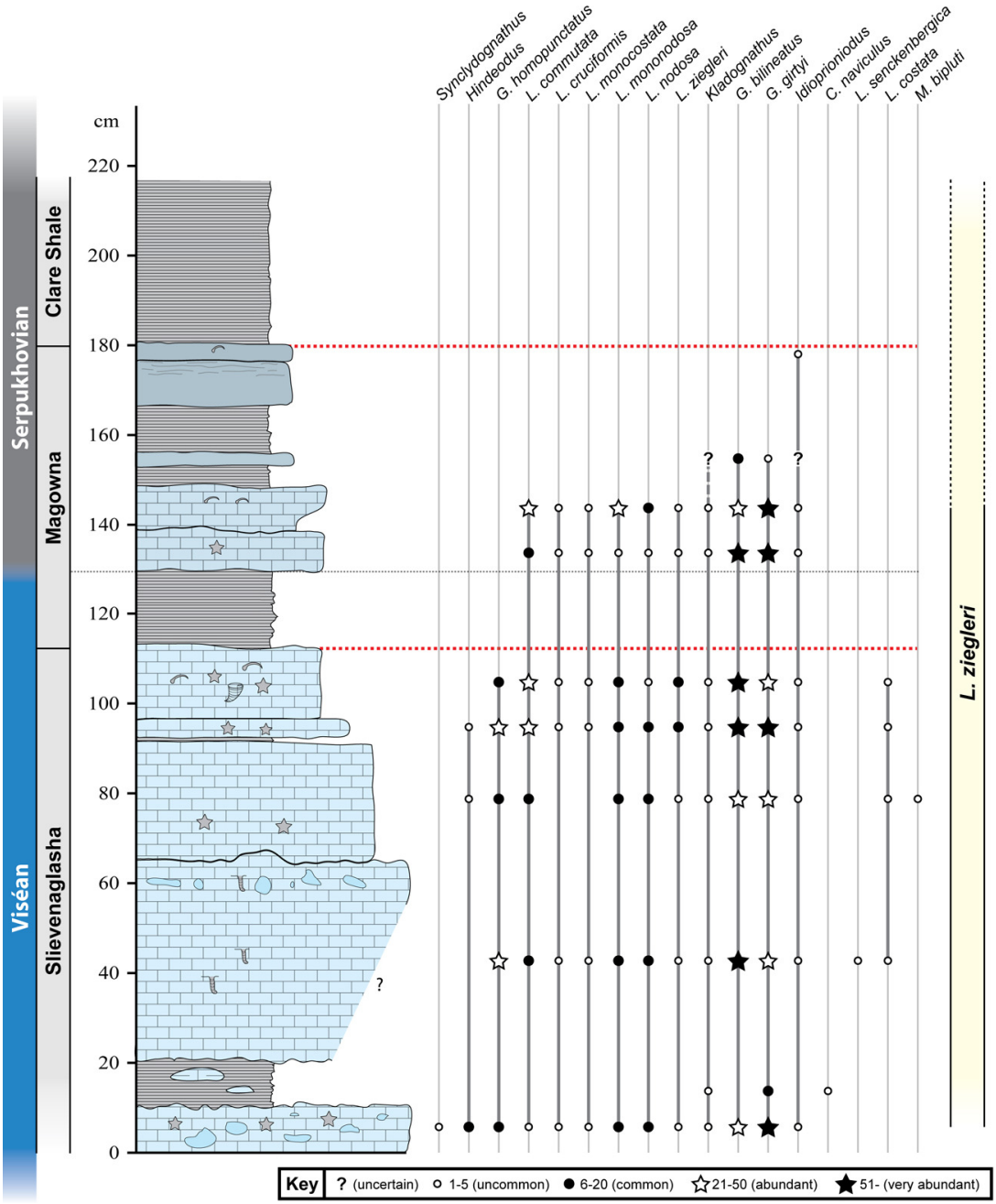

Fig. 4.4b Conodont biostratigraphy of the Kilnamona Section.

Red lines indicate formational boundaries (formations are indicated in the grey column on the left). The single black line represents the likely position of the currently recognised Viséan-Serpukhovian boundary. The proposed conodont Biozone of the sequence is shown in the faint yellow column on the right. Abundances are per 2kg.

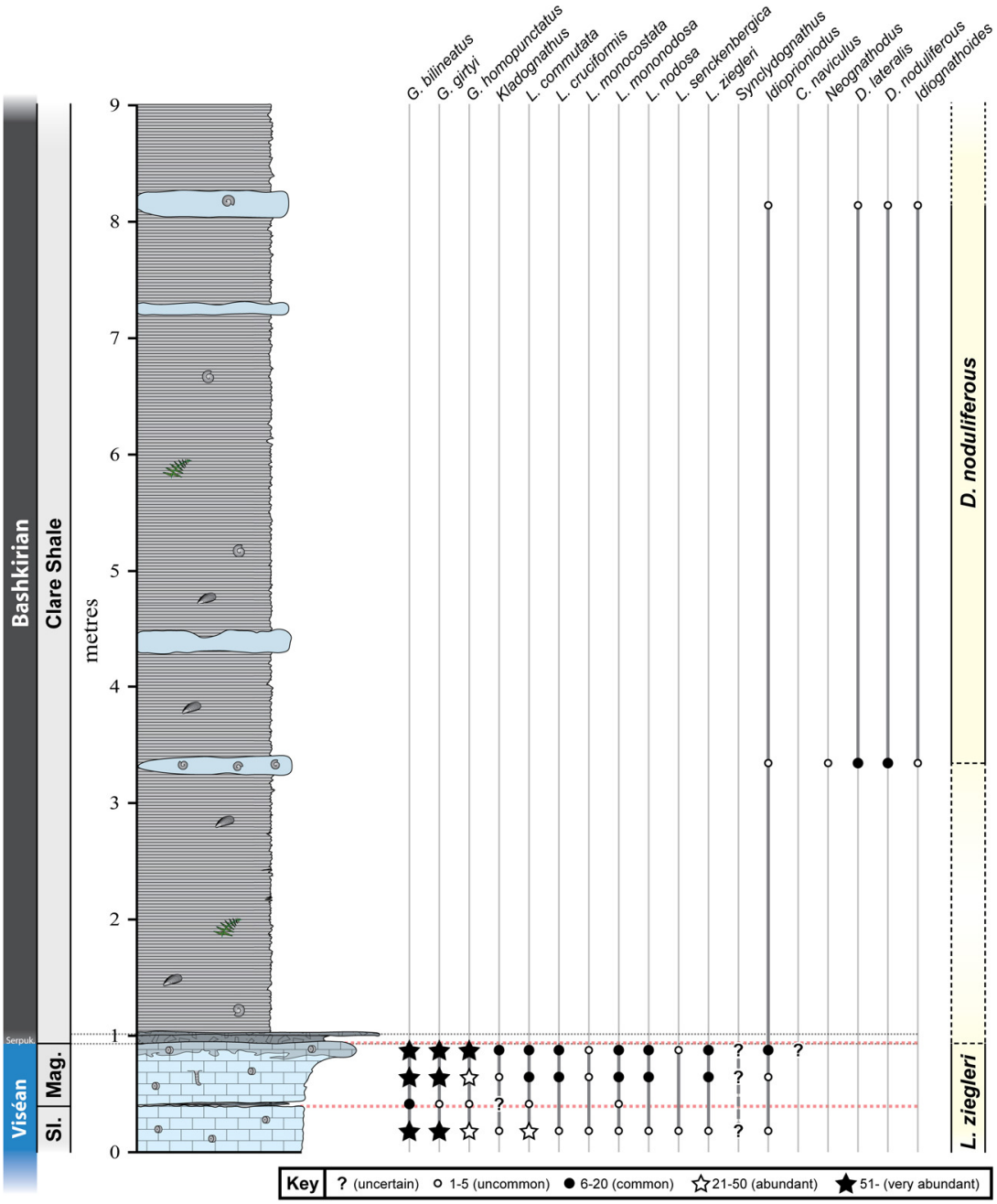

Fig. 4.4c Conodont biostratigraphy of the St. Brendan's Well Section.

Red lines indicate formational boundaries (formations are indicated in the grey column on the left, Sl. = Slievenaglasha and Mag. = Magowna). Black lines represent the likely position of the Viséan-Serpukhovian (as currently recognised) and Serpukhovian-Bashkirian boundaries. The conodont Biozones recognised are shown in the pale yellow column on the right. Abundances are per 2kg.

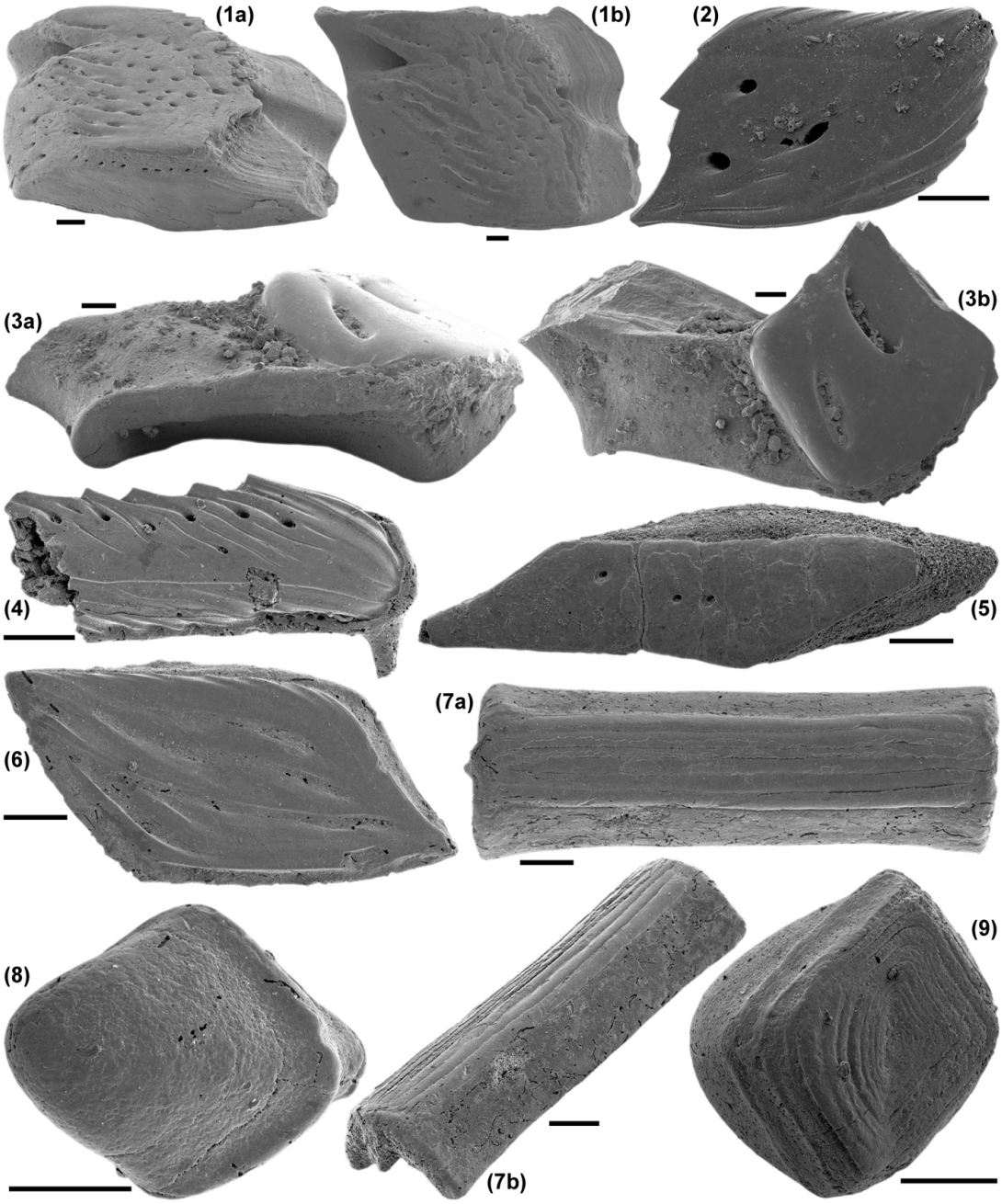

Fig. 4.5a Actinopterygian and Acanthodian scales.

Black scale bars represent 200µm. ***(1a & b)*** *Oblique and upper-surface views of a particularly thickened rhomb shaped Actinopterygian scale - DAGN1, MB.5A.2.* ***(2)*** *Upper-surface of a rhomb-shaped Actinopterygian scale - KMONA3, MB.9C.19.* ***(3a & b)*** *Oblique-lateral and upper-surface views of a rhomb-shaped Actinopterygian scale which has an especially elongate and complex base - GLTV16, MB.2A.10.* ***(4)*** *Upper-surface of an incomplete, elongate rectangular Actinopterygian scale with a distinct articulating process - KMONA6, MB.10C.42.* ***(5)*** *Upper-surface of a spear-shaped Actinopterygian scale - KMONA3, MB.9C.23.* ***(6)*** *Upper-surface of a rhomb-shaped Actinopterygian scale - KMONA5, MB.10B.13.* ***(7a & b)*** *Upper-surface and oblique views of a beading-type Actinopterygian scale - KMONA4, MB.10A.19.* ***(8 & 9)*** *Basal and oblique upper-surface views of Acanthodian scales, note the faint ornament in (9) - KMONA5, MB.10B.17 and KMONA4, MB.10A.4 respectively.*

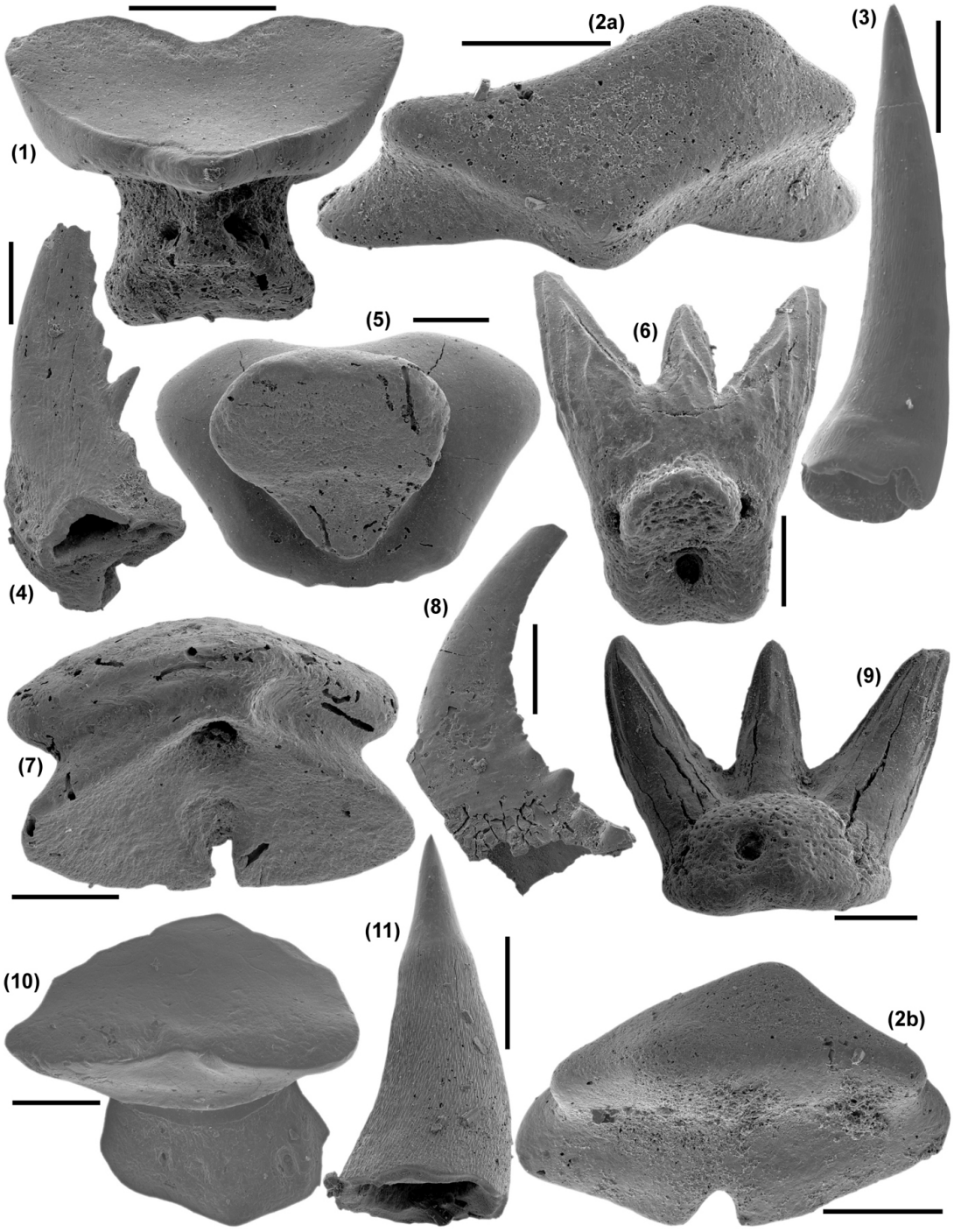

Fig. 4.5b Assorted chordate microremains.

Black scale bars represent 200µm. ***(1, 5 & 10)*** *Posterior, basal and oblique-anterior views of Ginteria teeth - KMONA6, MB.10C.23, KMONA6, MB.10C.7 and BW3, MB.12B.26 respectively.* ***(2a & b)*** *Oblique posterior and upper-surface views of Cooleyella teeth - AGHA4, MB.5C.20.* ***(3 & 11)*** *Lateral views of Palaeoniscid teeth, note the constriction near the top of the elements representing the acridine tip - KMONA5, MB.KMONA5.7 and AGHA4, MB.23B.3 respectively.* ***(4 & 8)*** *Lateral views of probable Conopiscius dental elements - both AGHA4, MB.5C.18 and MB.5C.13 respectively.* ***(6 & 9)*** *Basal-anterior and posterior view of Xenacanthus teeth - KMONA5, MB.10B.19 and KMONA3, MB.9C.22 respectively.* ***(7)*** *Basal-posterior view of a Cooleyella tooth - KMONA6, MB.10C.9.*

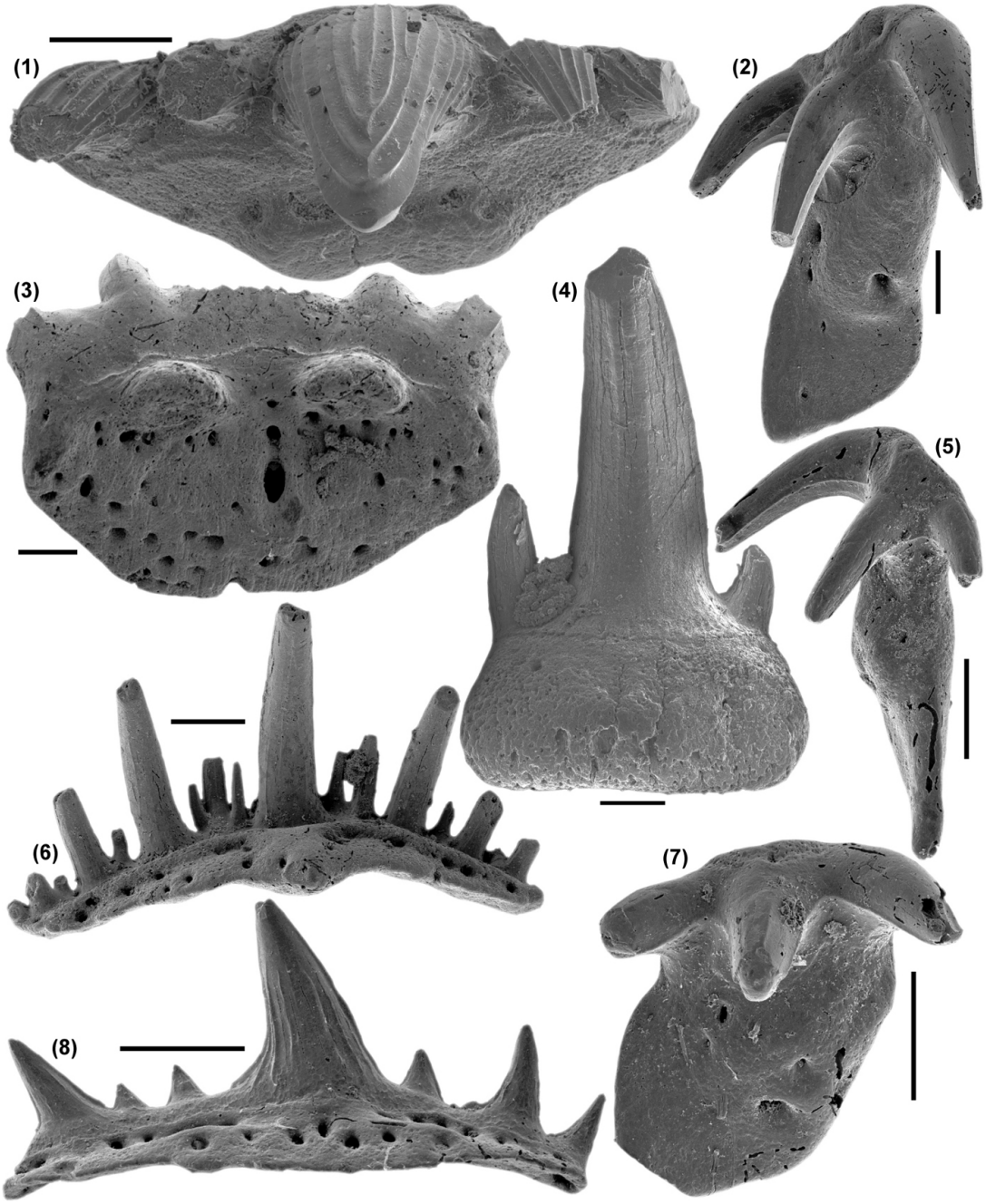

Fig. 4.5c Cladodont and Thrinacodus Chondrichthyan teeth.

Black scale bars represent 200µm. ***(1, 3, 4, 6 & 8)*** *Oral, aboral and three posterior views of various cladodont morphologies - GLTV39, MB.4B.1, KMONA5, MB.10B.21, BW3, MB.12B.8, KMONA3, MB.9C.16 and KMONA5, MB.10B.12 respectively.* ***(2, 5 & 8)*** *Oral, lateral and oral views of slightly different Thrinacodus teeth forms - all from KMONA5, MB.10B.34, MB.10B.28 and MB.10B.23 respectively.*

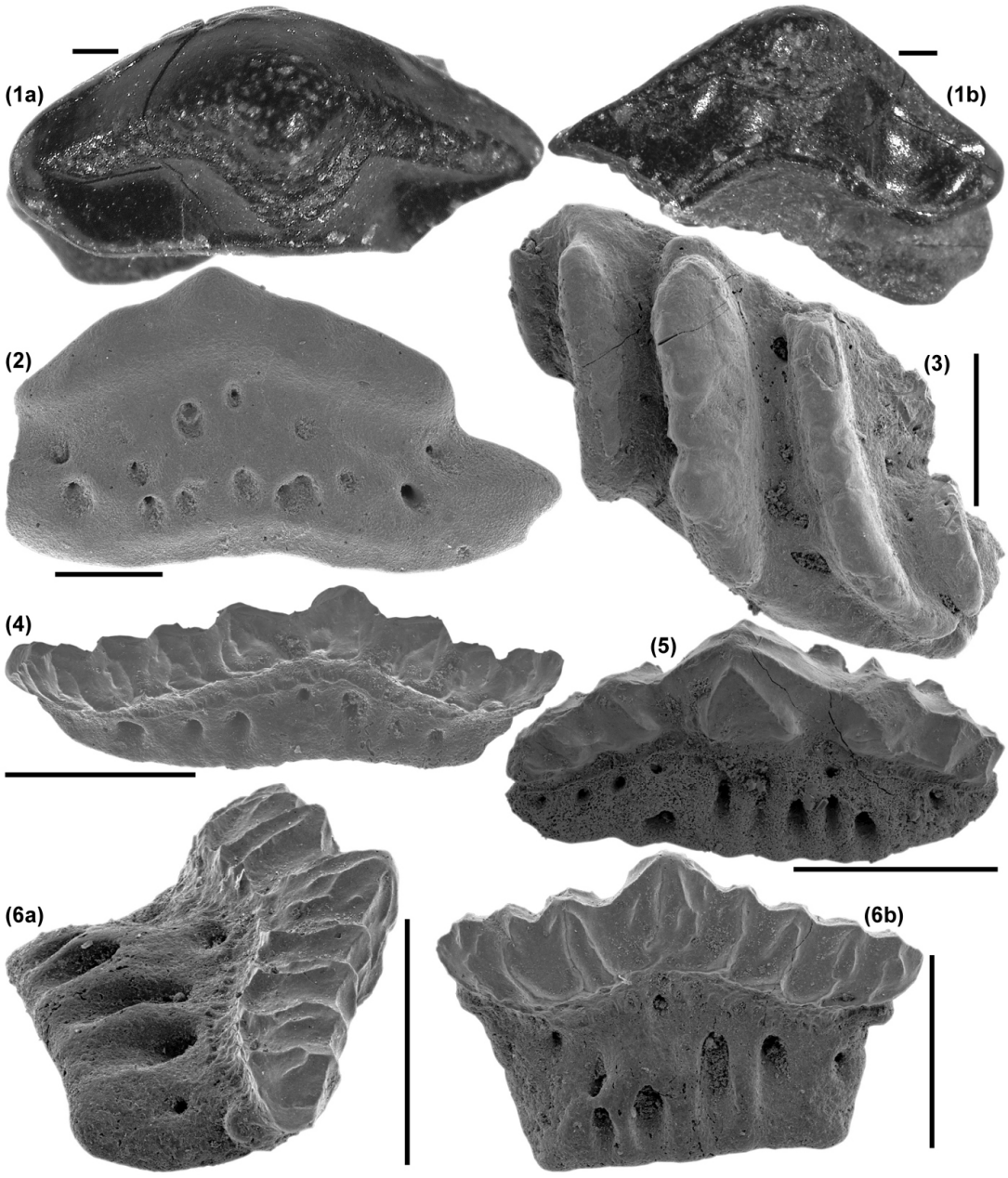

Fig. 4.5d Orodus, Lissodus and Protacrodus bar-like teeth.

Black scale bars represent 500μm. ***(1a & b)*** *Oral and posterior views of a large orodont tooth imaged under a binocular microscope - Dorrusawillin handsample.* ***(2)*** *Oral-posterior view of a Lissodus tooth - CNLG8, MB.7A.1.* ***(3)*** *Oral view of a possible Lissodus tooth plate - KMONA5, MB.10B.2.* ***(4 & 5)*** *Oral views of various protacrodont teeth forms - KMONA5, MB.KMONA5.33 and AGHA4, MB.5C.7 respectively.* ***(6a & b)*** *Lateral and oral views of a protacrodont tooth - KMONA5, MB.10B.10.*

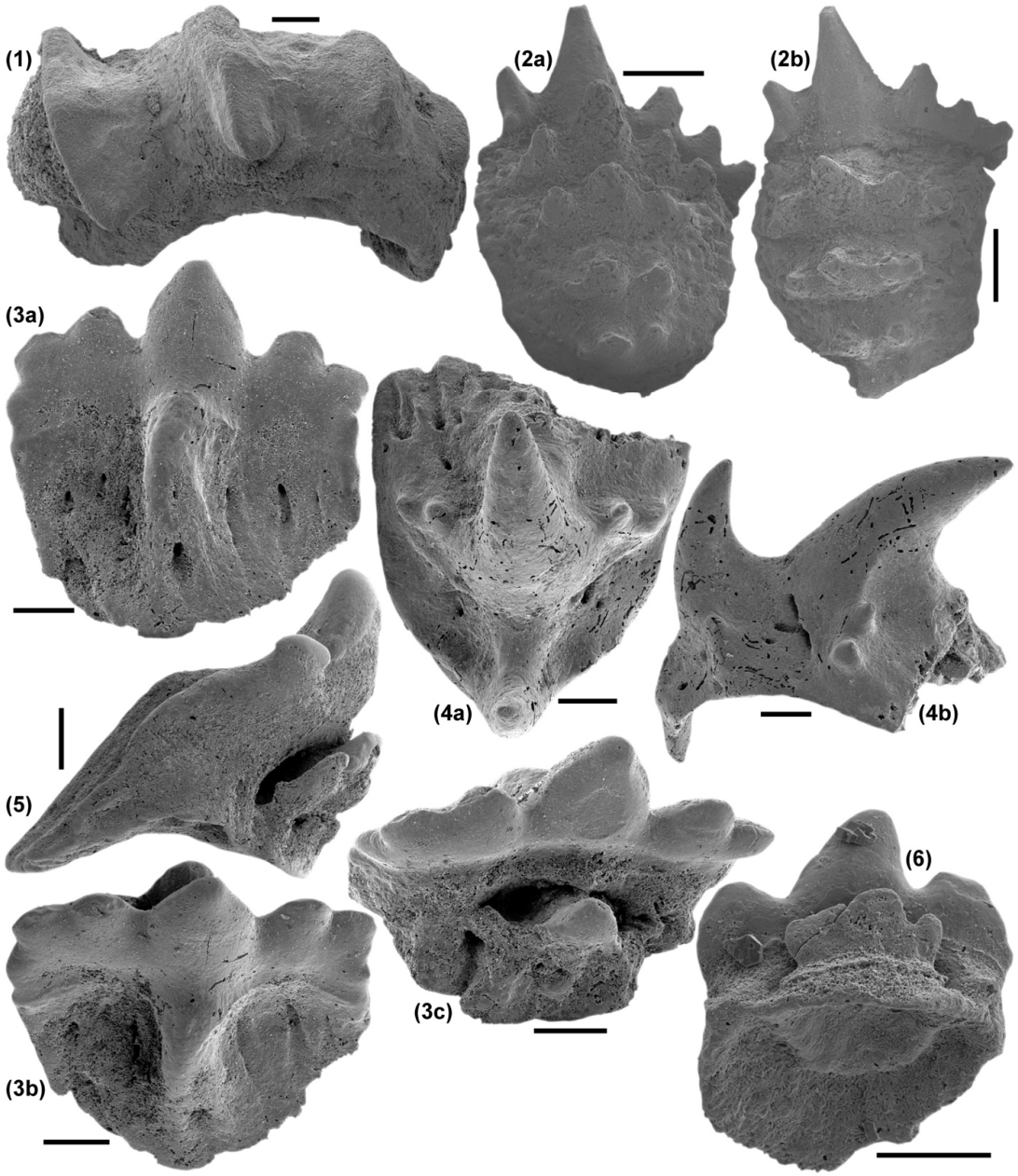

Fig. 4.5e Chondrichthyan teeth whorls and families.

Black scale bars represent 200µm. ***(1)*** *Oblique-lateral view of a possible Lissodus tooth whorl - CNLG13, MB.7C.2.* ***(2a & b)*** *Oral posterior and oral view of a tooth whorl - BW3, MB.12B.2.* ***(3a, 3b, 3c, 5 & 6)*** *Posterior, oral, anterior-oral, lateral and basal-anterior views of the most common tooth family morphology - KMONA4, MB.10A.3, KMONA4, MB.10A.8 and GLTV16, MB.2A.2 respectively.* ***(4a & b)*** *Oral and lateral views of an incomplete tooth whorl of unknown affinities - KMONA5, MB.10A.9.*

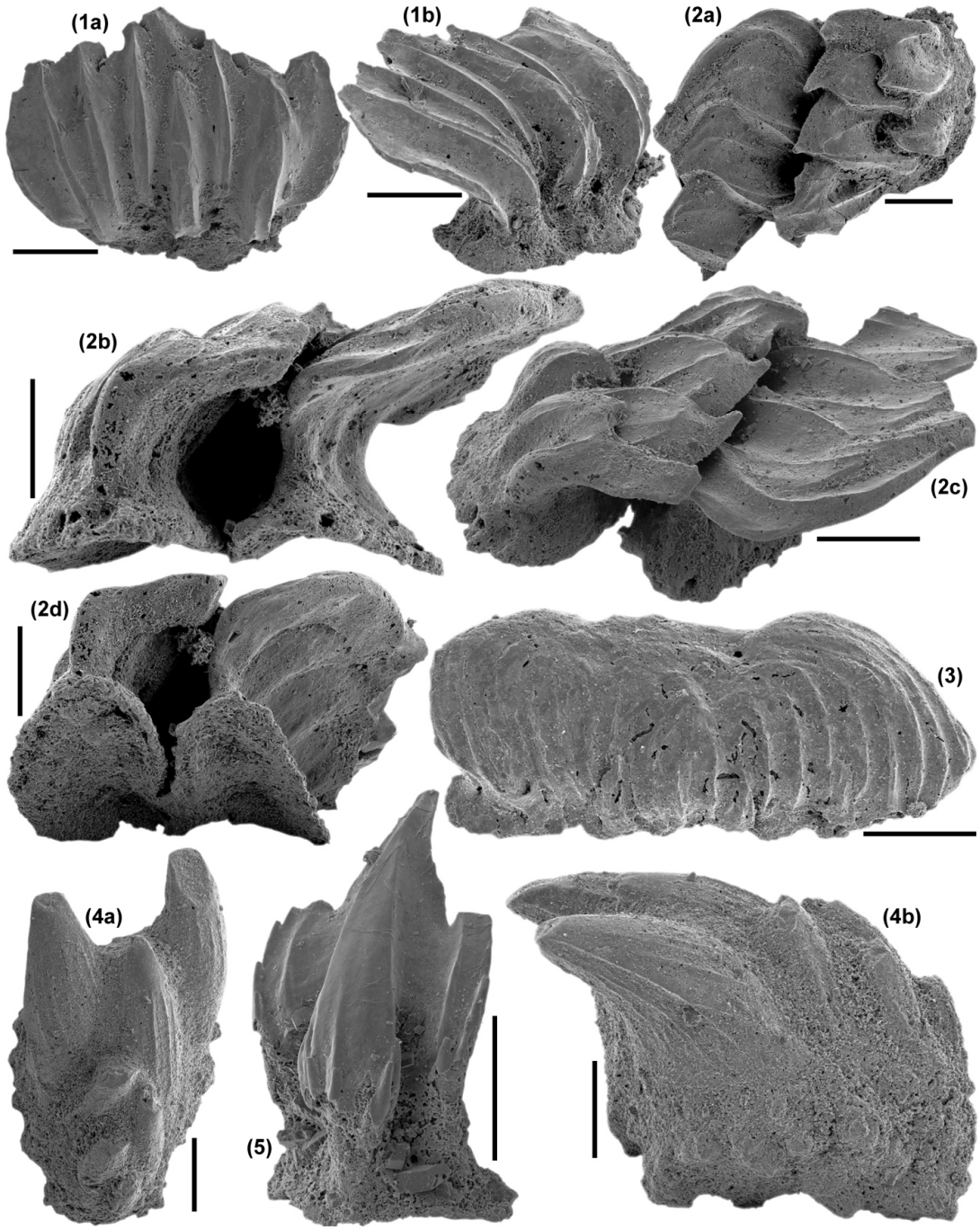

Fig. 4.5f Chondrichthyan denticles.

Black scale bars represent 200µm. ***(1a & b)*** *Crown and oblique lateral views of a "ctenacanth"-type denticle - AGHA4, MB.5C.5.* ***(2a, b, c & d)*** *Crown, lateral, oblique-crown and oblique-basal views of an articulated pair of "ctenacanth"-type denticles - AGHA4, MB.5C.25.* ***(3)*** *Crown view of an elongate "ctenacanth"-type denticle - KMONA6, MB.10C.41.* ***(4a & b)*** *Crown and lateral views of a "mucous-membrane"-type denticle - AGHA10, MB.6B.7.* ***(5)*** *Anterior view of a "listracanthus"-type denticle - AGHA4, MB.5C.30.*

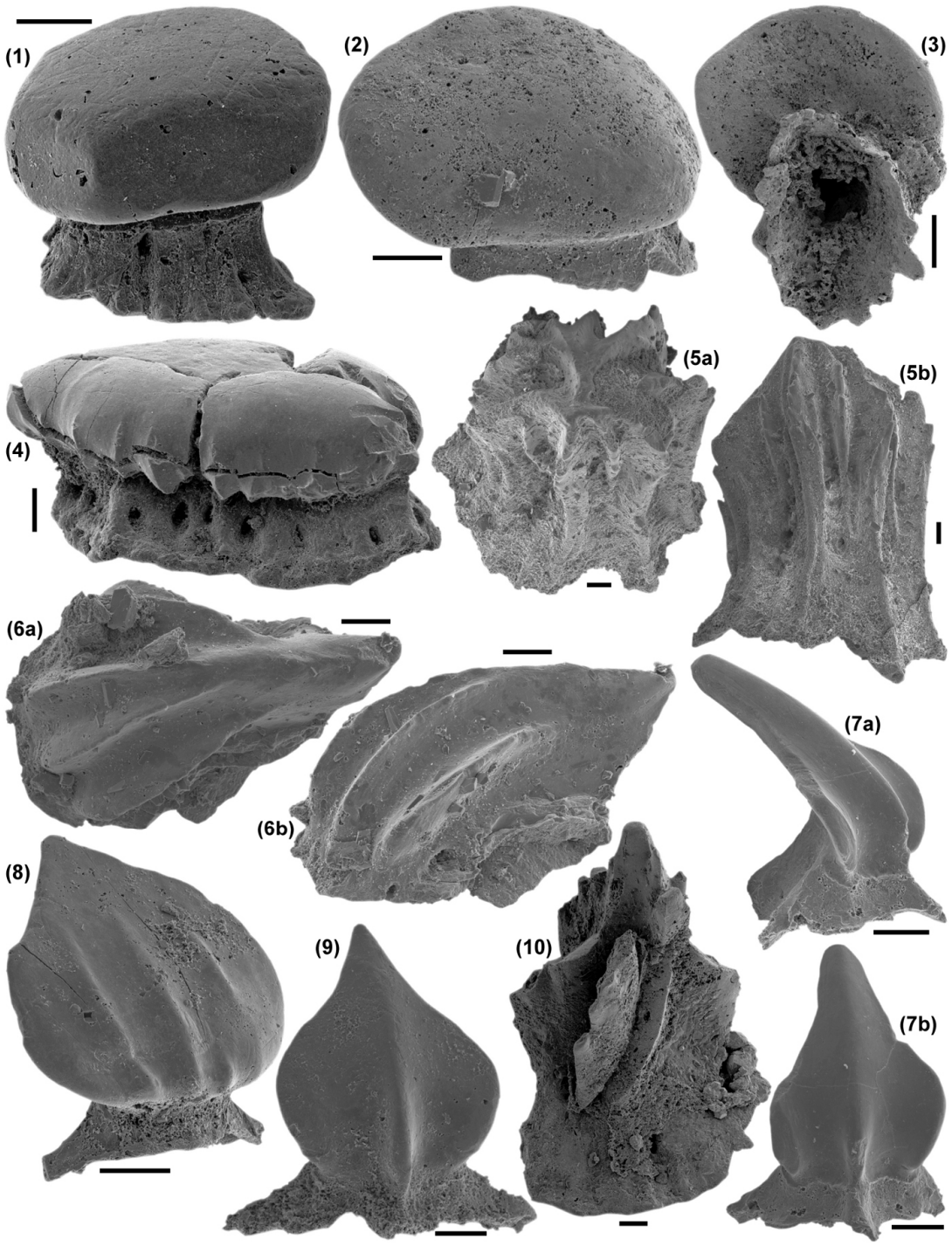

Fig. 4.5g Chondrichthyan hybodont denticles.

Black scale bars represent 100µm. ***(1, 2, 3 & 4)*** *Lateral, upper-surface, basal and oblique views of various "button/mushroom" hybodont denticle morphologies - KMONA3, MB.9C.27, AGHA4, MB.5C.3, GLTV13, MB.1A.6 and KMONA6, MB.10C10 respectively.* ***(5a & 5b)*** *Upper-surface and lateral views of a "flame"-like denticle - GLTV22, MB.3B.1.* ***(6a & b)*** *Upper-surface and lateral views of a "thorn"-like denticle - GLTV23, MB.3C.1.* ***(7a, b, 8 & 9)*** *Variously oblique lateral-anterior views of three different lanceolate denticles - GLTV18, MB.3A.3, AGHA4, MB.5C.11 and GLTV18, MB.3A.4 respectively.* ***(10)*** *Oblique-lateral view of a "flame"-like denticle - KMONA1, MB.9B.15.*

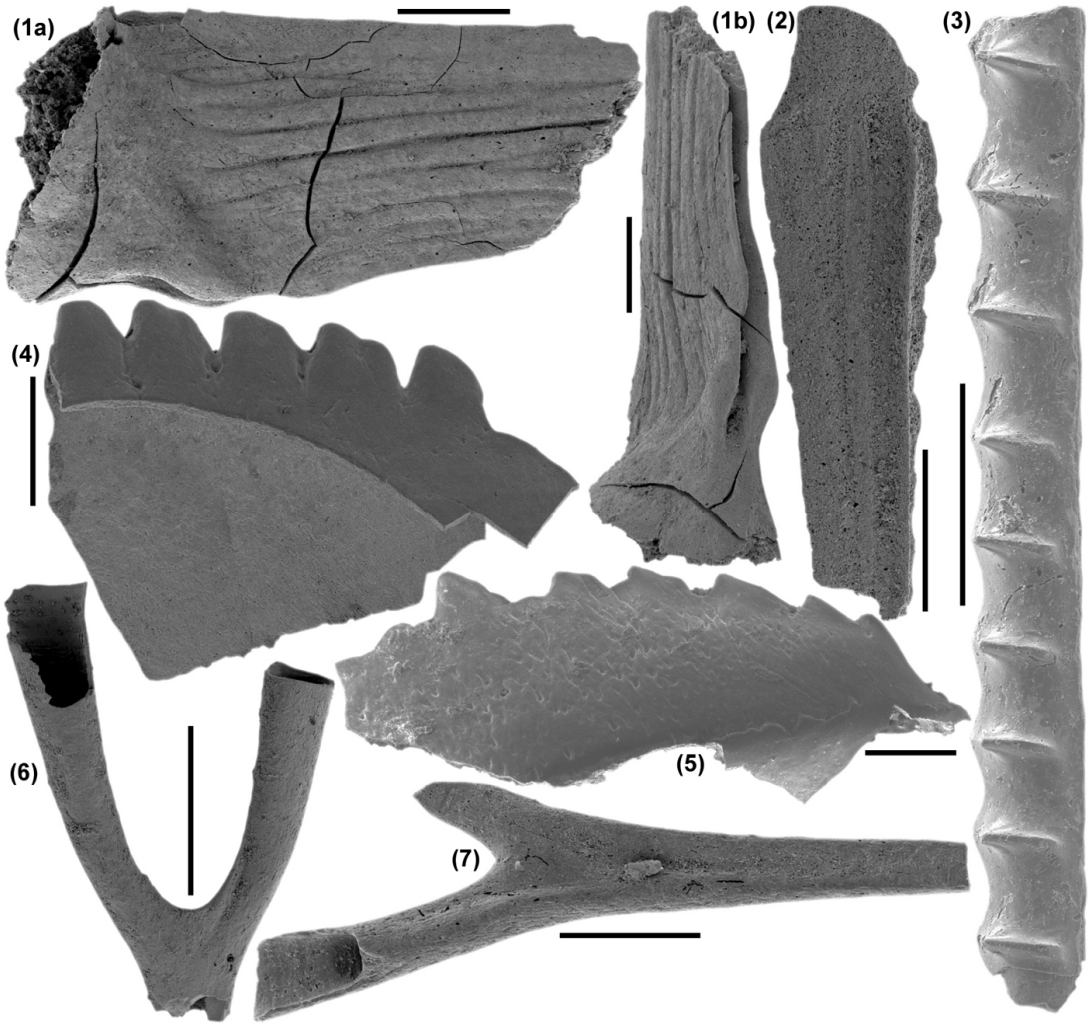

Fig. 4.5h Osteichthyan and assorted vertebrate microremains.

Black scale bars represent 500µm. ***(1a, b & 2)*** *Various lateral views of possible gill raking or Actinopterygian bone structures - GLTV14, MB.1B.1 and AGHA10, MB.6B.2 respectively.* ***(3)*** *Upper-surface view of an isolated bar-element - KMONA5, MB.KMONA5.34.* ***(4 & 5)*** *Lateral views of unknown hollow serrated ridge structures - BW4, MB.BW4.1 and BW3, MB.12B.1 respectively.* ***(6 & 7)*** *Lateral views of "catapult"-structures of unknown affinity - CNLG14, MB.25B.1 and KMONA5, MB.10B.27 respectively.*

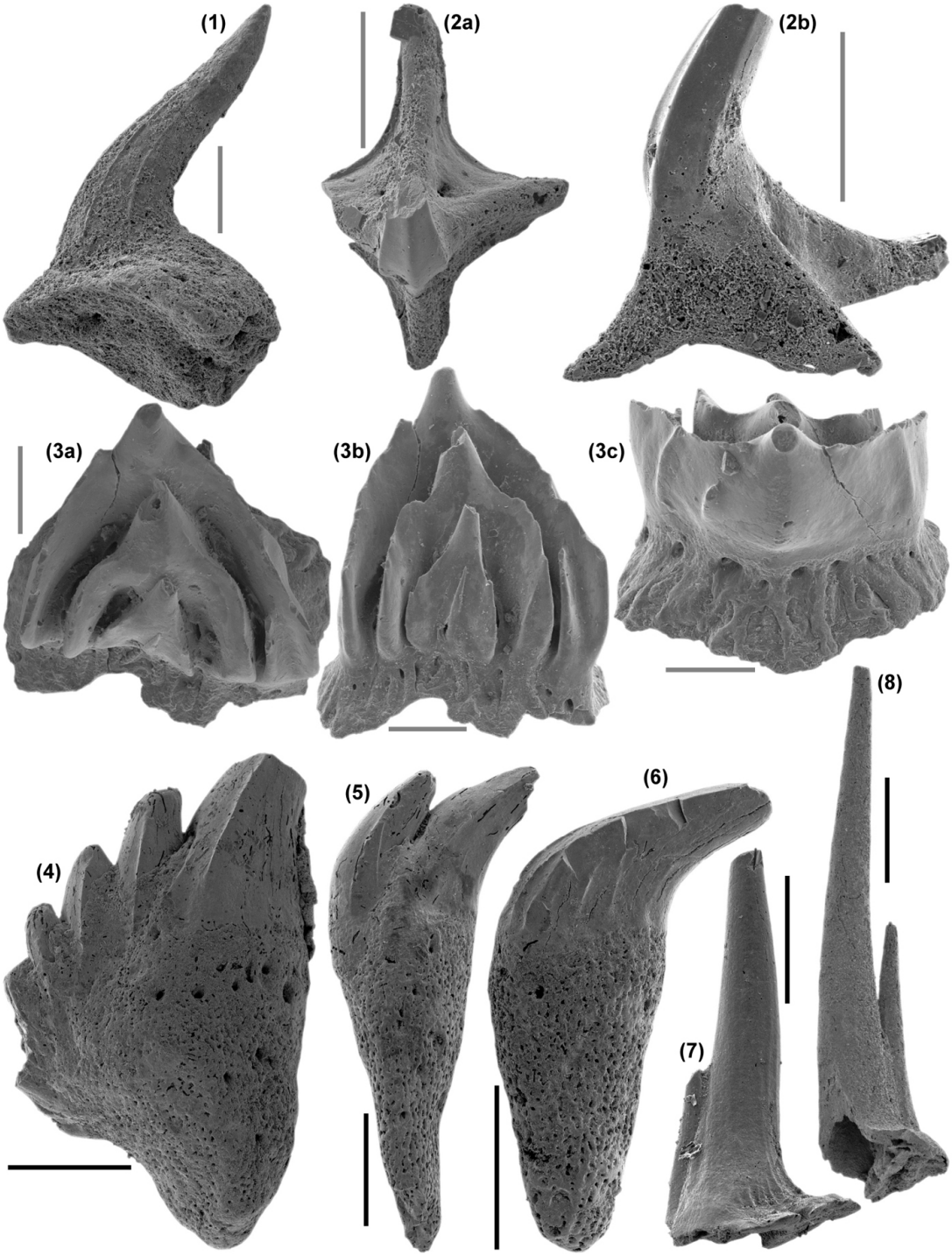

Fig. 4.5i Microvertebrate denticles of unknown affinity.

Black scale bars represent 500µm, whilst grey scale bars (1-3) are equivalent to 200µm. ***(1, 2a & b)*** *Lateral, upper-surface and lateral-anterior views of "thorn"-like denticle morphologies - CNLG9, MB.9A.1 and AGHA4, MB.5C.31 respectively.* ***(3a, b & c)*** *Upper-surface, anterior and posterior views of a chondrichthyan "nested" denticle - GLTV18, MB.3A.2.* ***(4, 5 & 6)*** *Lateral views of rooted denticle forms - KMONA1, MB.9B.17, KMONA5, MB.10B.3 and KMONA6, MB.10C.35 respectively.* ***(7 & 8)*** *Lateral views of skirted-cusp denticles of unknown affinity - KMONA5, MB.10B.38 and KMONA4, MB.10A.18 respectively.*

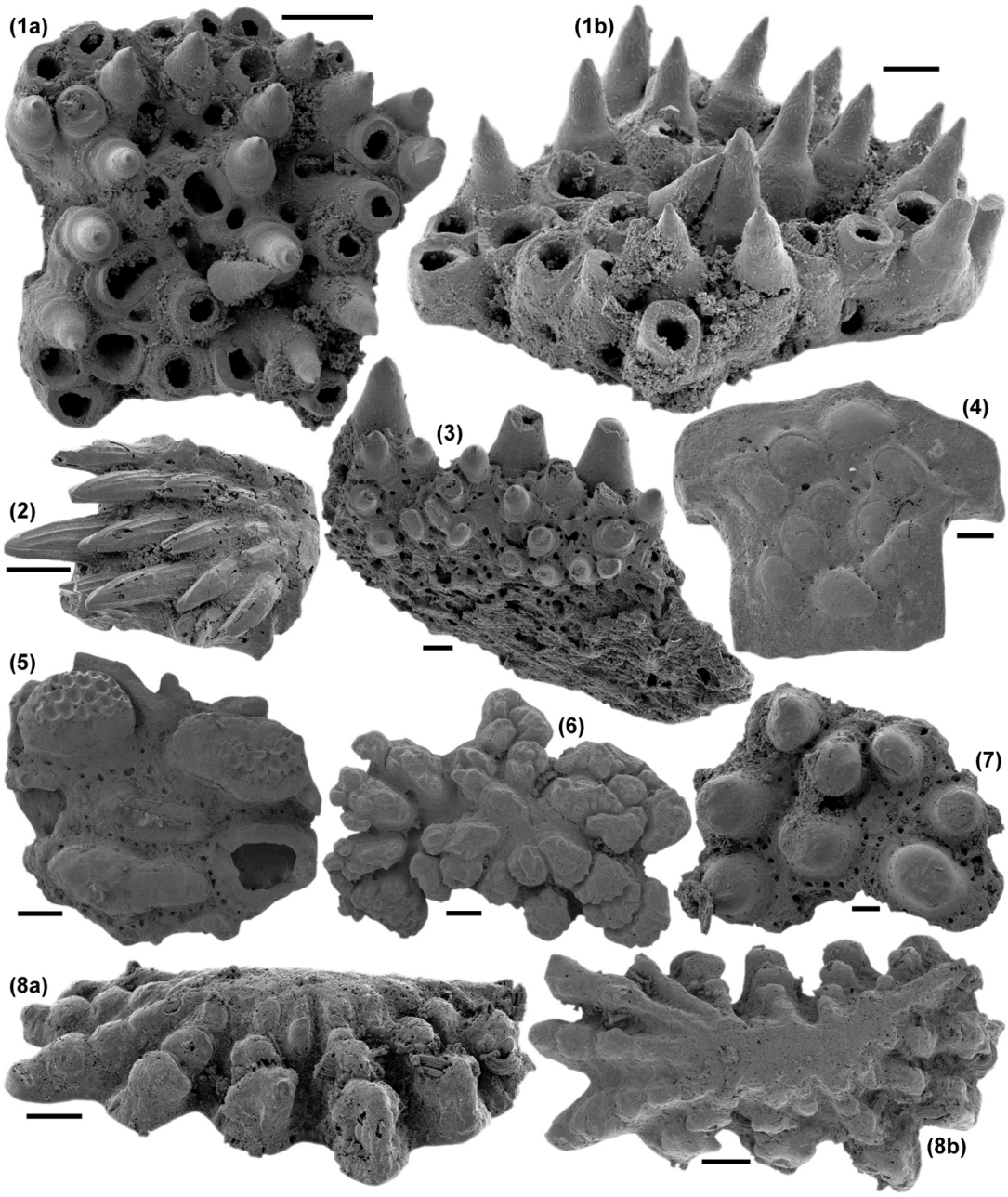

Fig. 4.5j Microvertebrate plates of unknown affinity.

Black scale bars represent 200µm. ***(1a & b)*** *Upper-surface and oblique views of a simple conically cusped plate - AGHA4, MB.5C.14.* ***(2 & 3)*** *Upper surface views of reclined cusped plates - KMONA5, MB.10B.32 and KMONA1, MB.9B.19 respectively.* ***(4, 5 & 7)*** *Upper-surface views of noded plate bodies of unknown affinity - KMONA5, MB.10B.26, DAGN1, MB.5A.1 and AGHA4, MB.5C.10 respectively.* ***(6, 8a & b)*** *Upper-surface, lateral and upper-surface views of examples of "stellar" plate morphologies - BW4, MB.BW4.8 and KMONA4, MB.10A.21 respectively.*

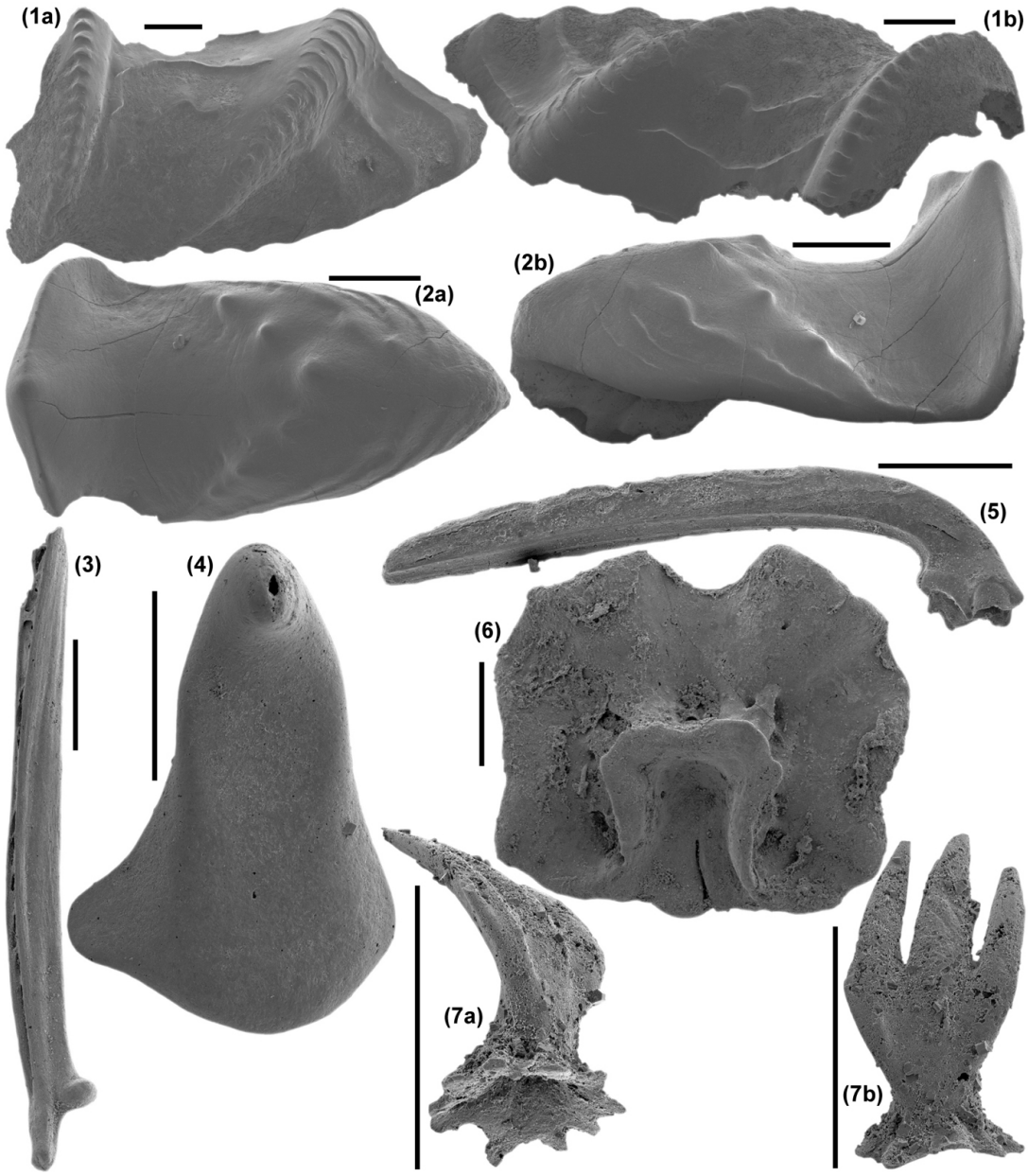

Fig. 4.5k Microvertebrate bodies of unknown affinity.

Black scale bars represent 500µm. ***(1a, & b)*** *Upper-surface and oblique views of a fragment of possible conulariid material - BW3, MB.12B.23.* ***(2a & b)*** *Upper-surface and lateral views of an unknown, possible denticle - BW3, MB.12B.10.* ***(3 & 5)*** *Lateral views of unknown distinct bar or spine elements - both CNLG14, MB.8A.1 and MB.8A.2 respectively.* ***(4)*** *Upper-surface views of a possible worn denticle of unknown affinity - AGHA4, MB.5C.19.* ***(6)*** *View of an unusual unidentifiable microvertebrate element - KMONA4, MB.10A.17.* ***(7a & b)*** *Basal-lateral and anterior views of a tri-cusped denticle of unknown origin - AGHA4, MB.5C.27.*

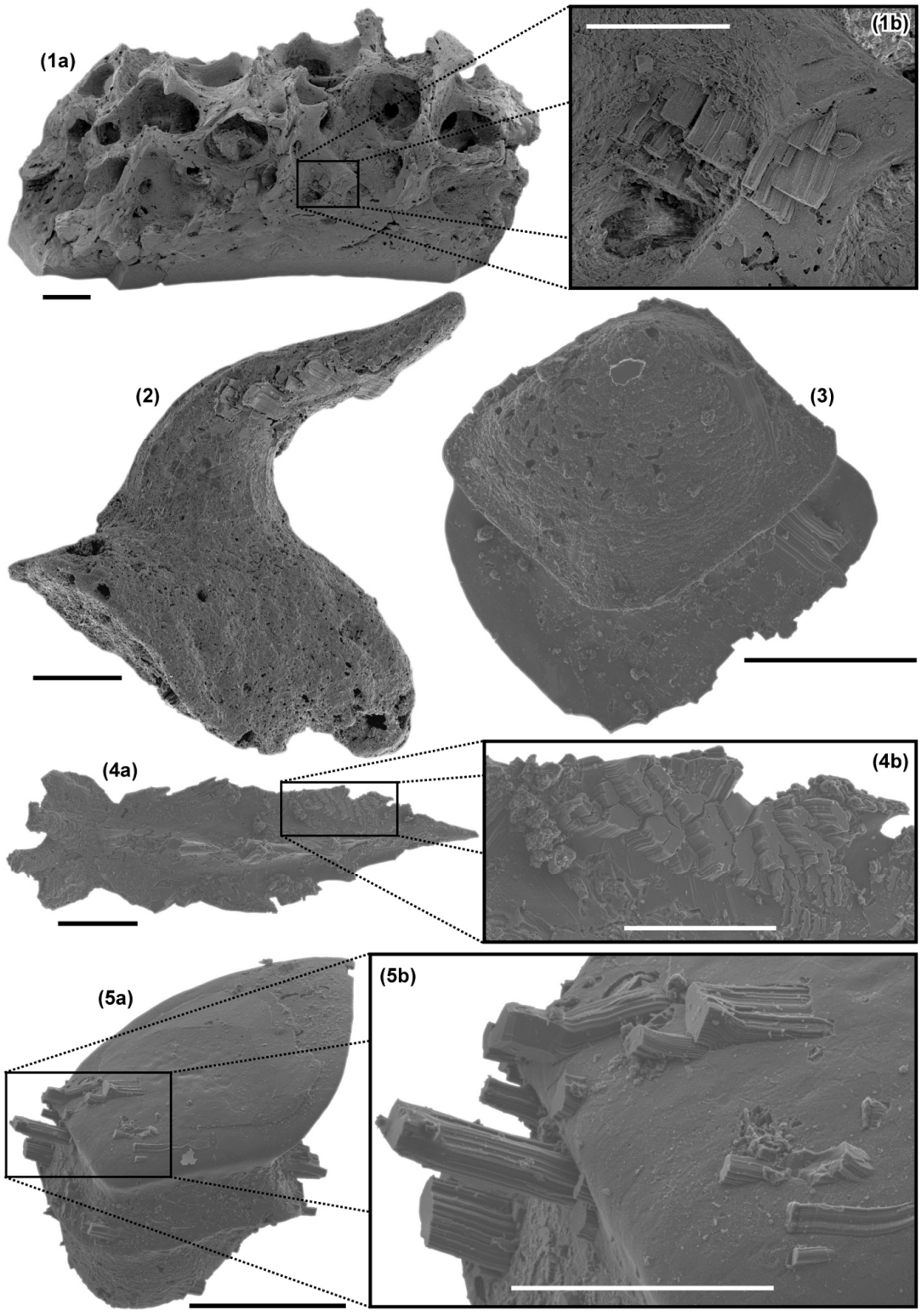

Fig. 4.6a Overgrowths on ichthyolith elements.

Black scale bars = 200µm and white scale bars = 100µm. ***(1a & 1b)*** *Oblique view of the porous internal tissue of an unknown ichthyolith. Area within box is shown in detail in (1b) - GLTV15, MB.1C.3.* ***(2)*** *Lateral-posterior view of unknown ichthyolith with overgrowths on cusp - KMONA8, MB.11A.8.* ***(3)*** *Basal view of an acanthodian denticle with overgrowths on underside of crown plate - BW10, MB.13A.8.* ***(4a & 4b)*** *Dorsal view of a particularly degraded unknown ichthyolith. Overgrown area within the box is shown in detail in (4b) - BW10, MB.13A.1.* ***(5a & 5b)*** *Oblique-dorsal view of an acanthodian denticle. Boxed area shown in detail in (5b) - BW10, MB.13A.2.*

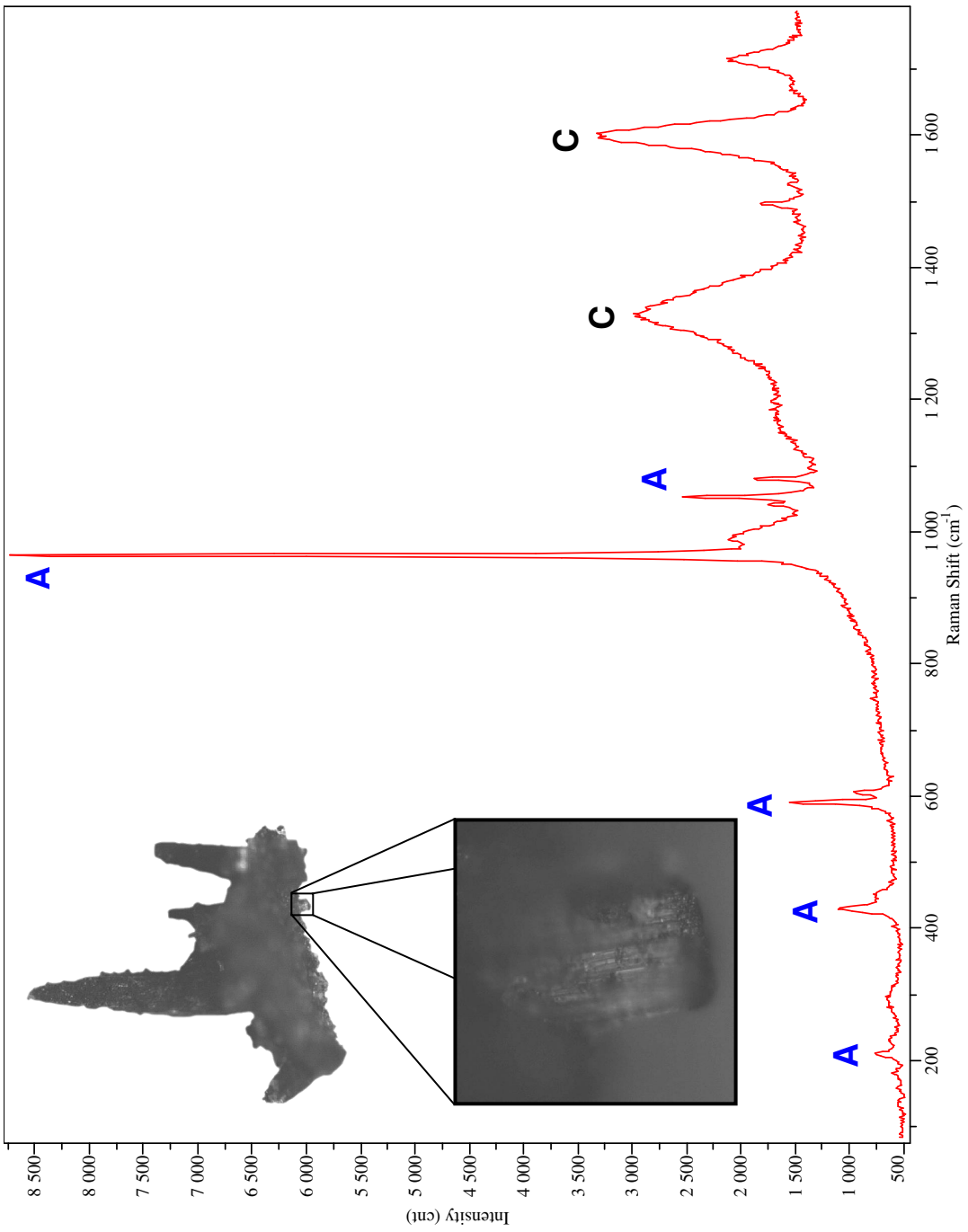

Fig. 4.6b Raman spectrum of an ichthyolith overgrowth.

Inset pictures show the cladodont analysed as seen by the Laser Raman. The image below the cladodont shows an enlargement of the area within the black box on the cladodont. This enlargement is of one of the overgrowths that were analysed and its spectrum is shown. Peaks labelled with a blue "A" are typical of apatite whilst peaks labelled with a black "C" are characteristic of pyrolitic (altered under heat) carbon.

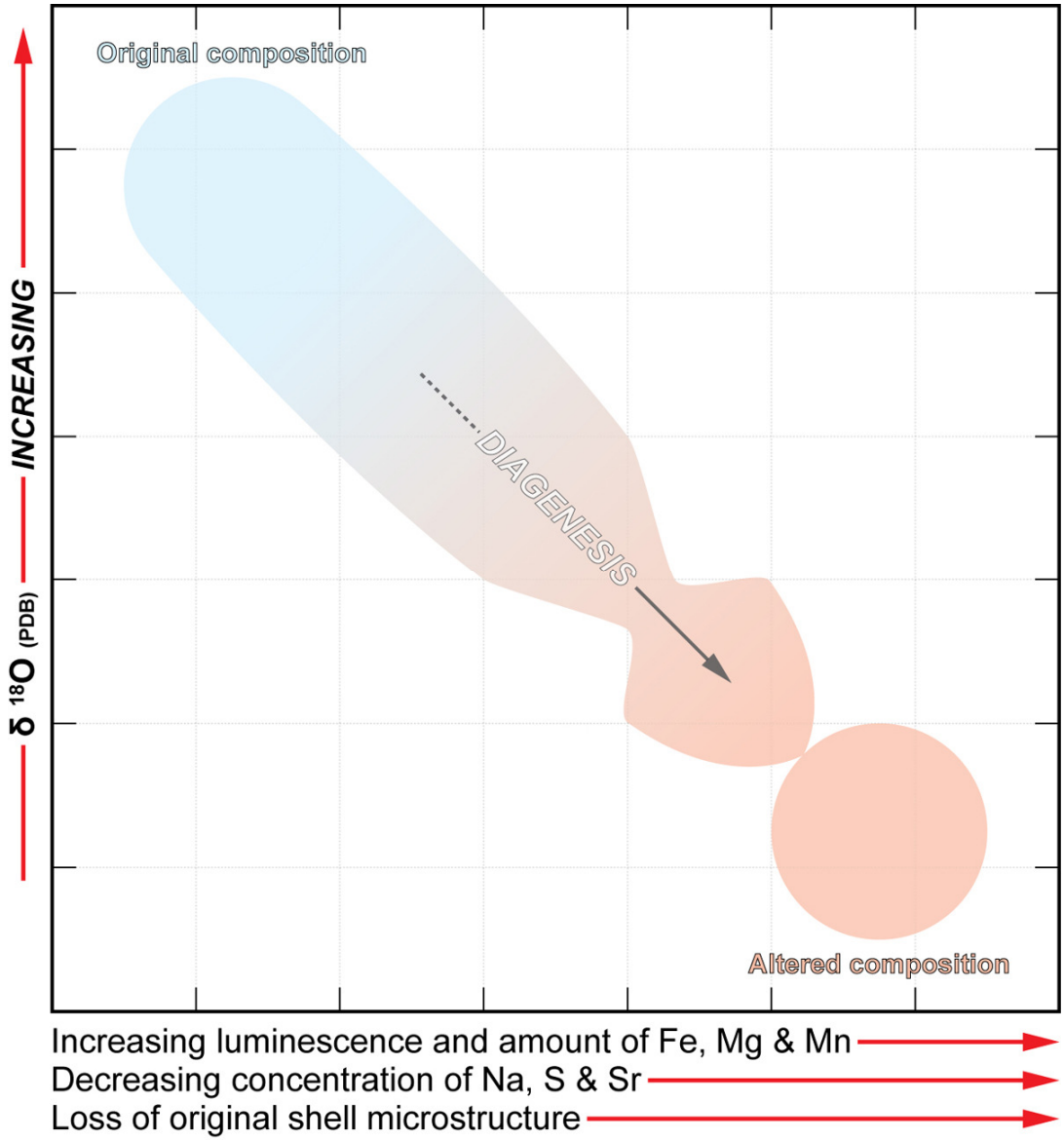

Fig. 5.1.2a Effect of diagenetic alteration on brachiopod calcite characteristics.

The figure shows the effect of diagenesis and interaction with meteoric waters on the physical and geochemical characteristics of brachiopod calcite.

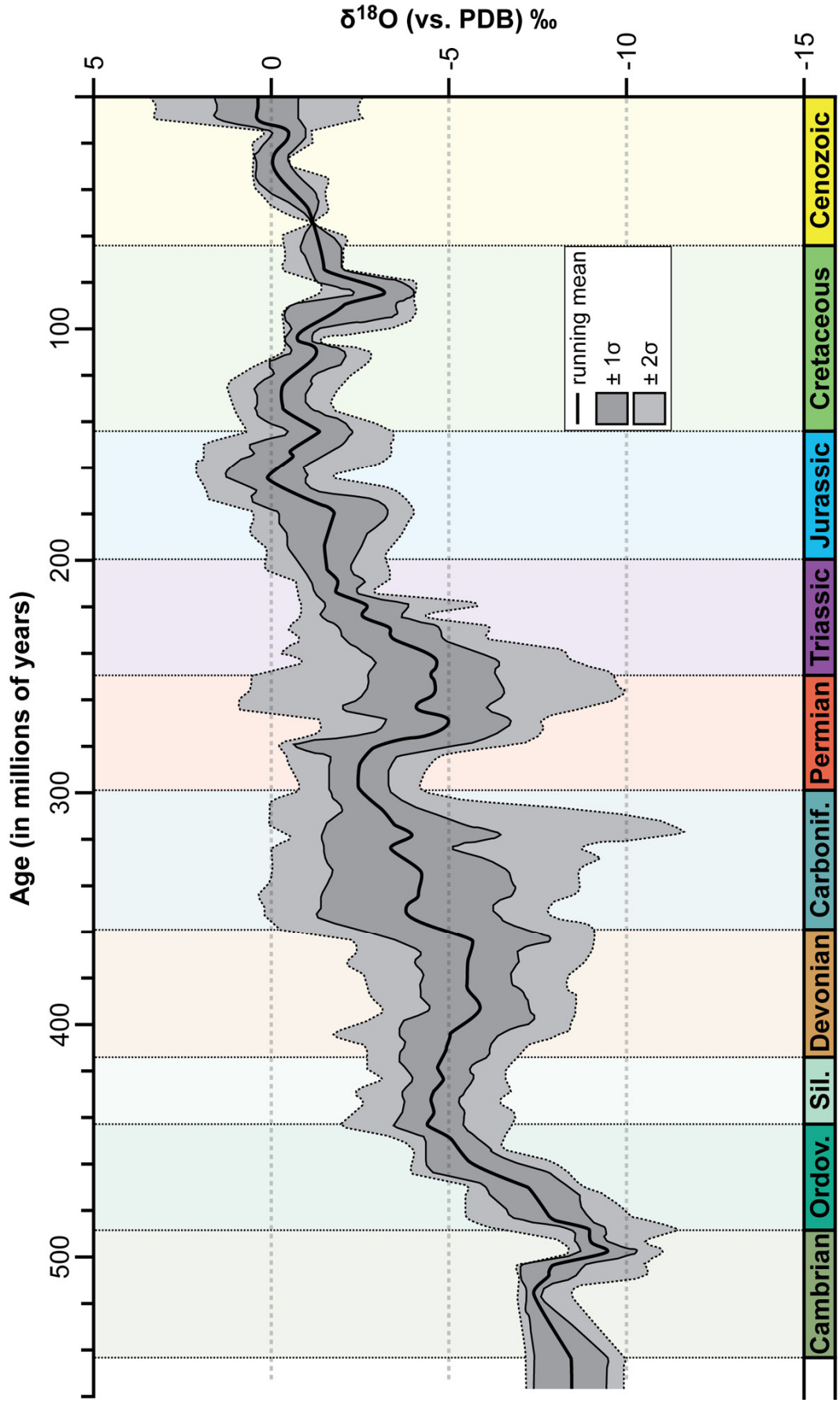

Fig. 5.1.2b Secular change in Phanerozoic $\delta^{18}O$ record derived from brachiopods.
Modified from Veizer et al. (1999) with colours according to the CGMW.

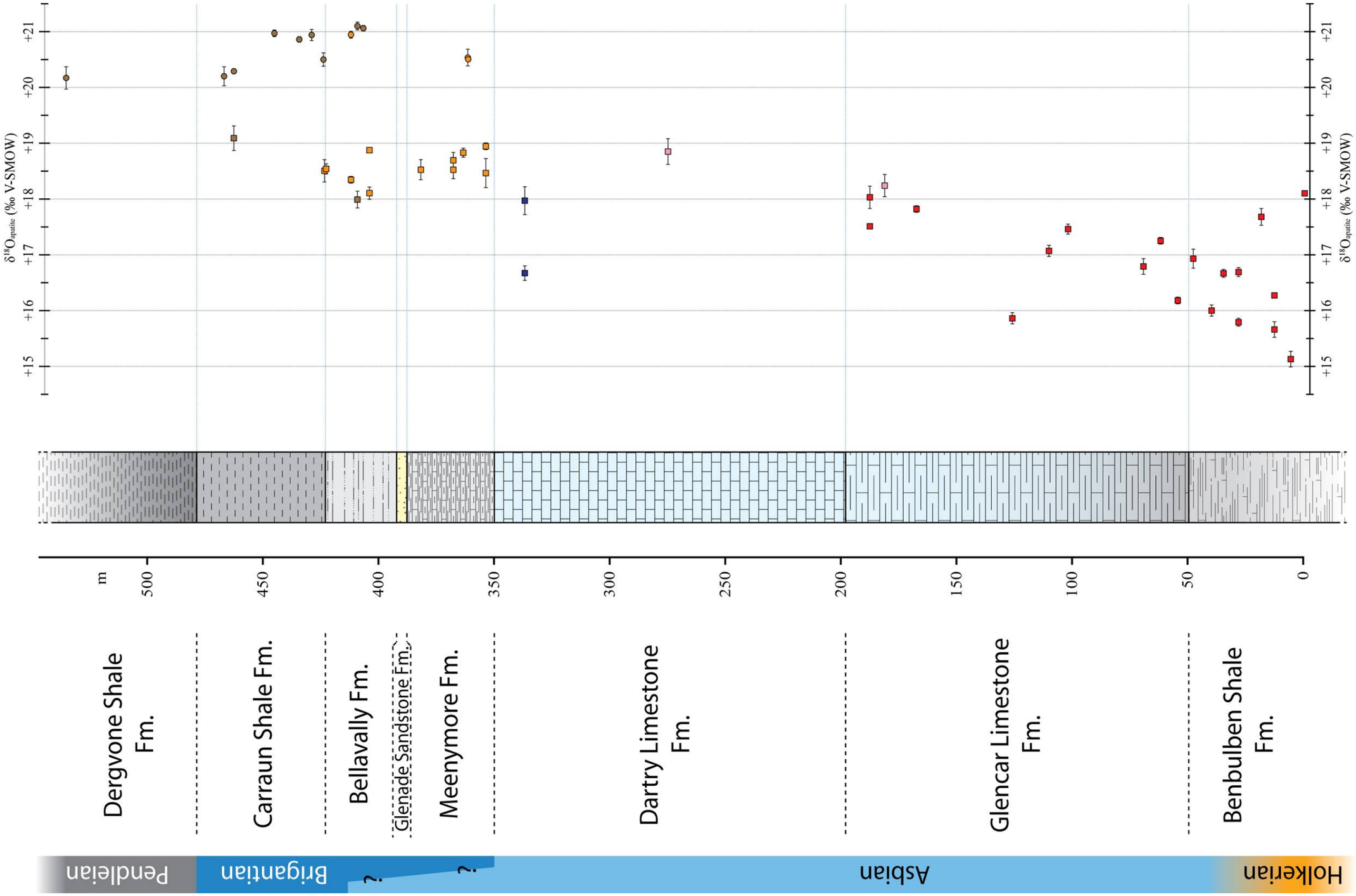

Fig. 5.2.1a $\delta^{18}O$ record of phosphatic analyses in northwest Ireland.

Filled squares represent analyses conducted on ichthyoliths while filled circles represent analyses of conodont elements. The various colours of the data signify which section the analyte was extracted from. Red – Tievebaun, Pink – Glencar, Blue – Glenade, Orange – Aghagrania and Brown – Carraun/Lugasnaghta. The data appears to show an increase in the $\delta^{18}O$ value up the stratigraphy. Note also the offset between fish and conodont data.

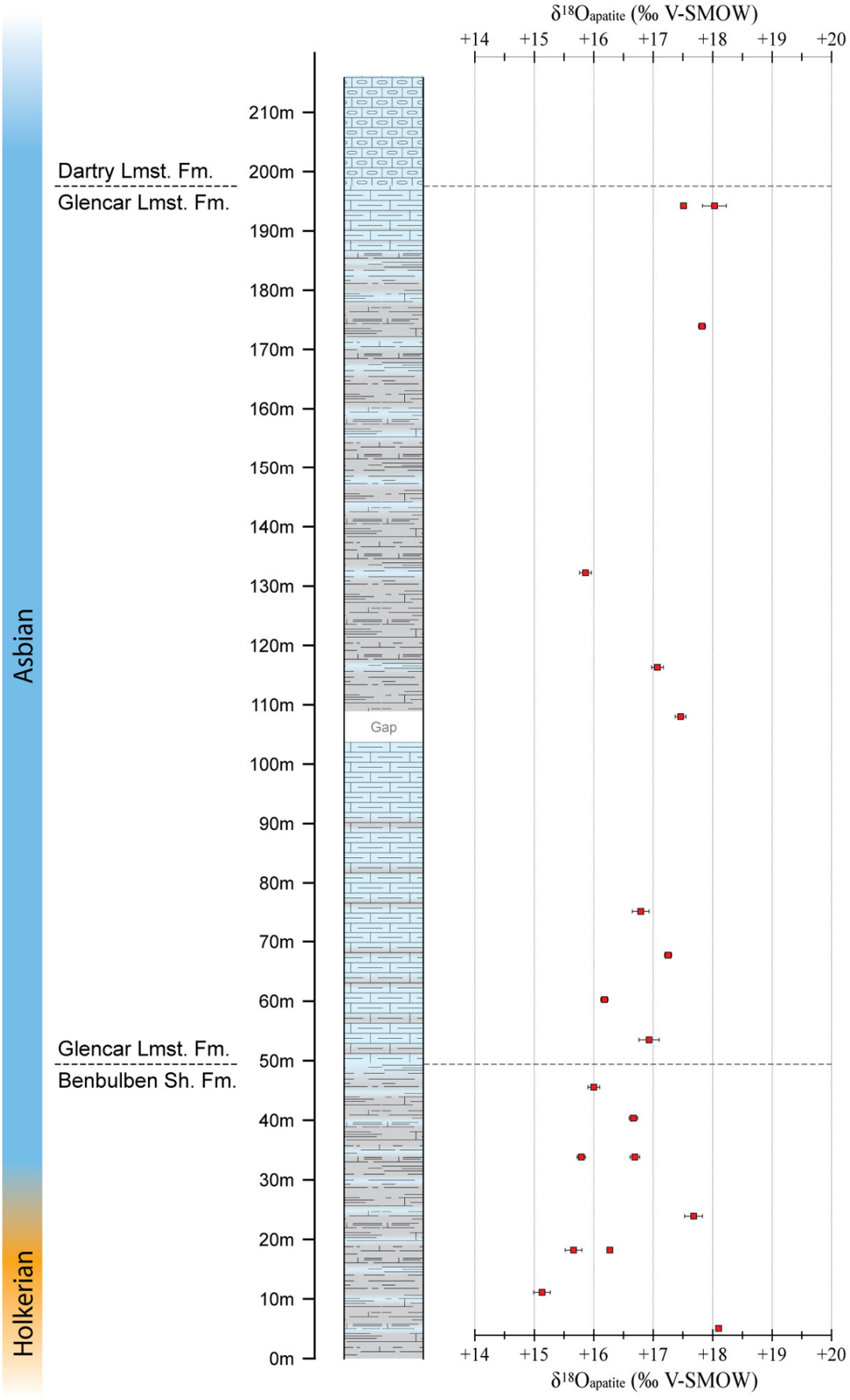

Fig. 5.2.1b $\delta^{18}O$ record of fish apatite from the Tievebaun Section.

Data point bars represent 1σ. An overall increase in $\delta^{18}O$ values is seen up the section.

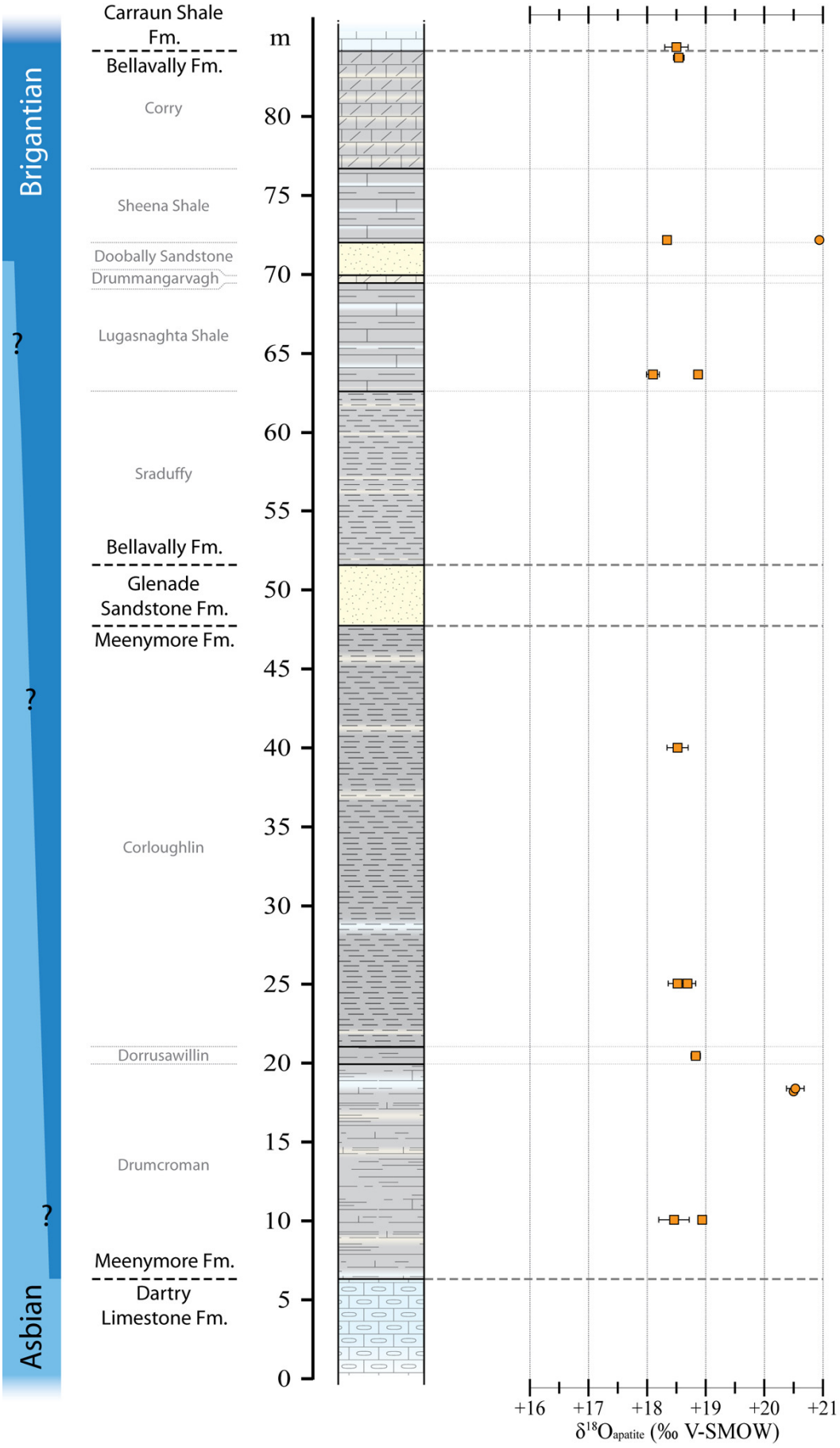

Fig. 5.2.1c $\delta^{18}O$ record of ichthyoliths (squares) and conodonts (circles), AGHA Section.

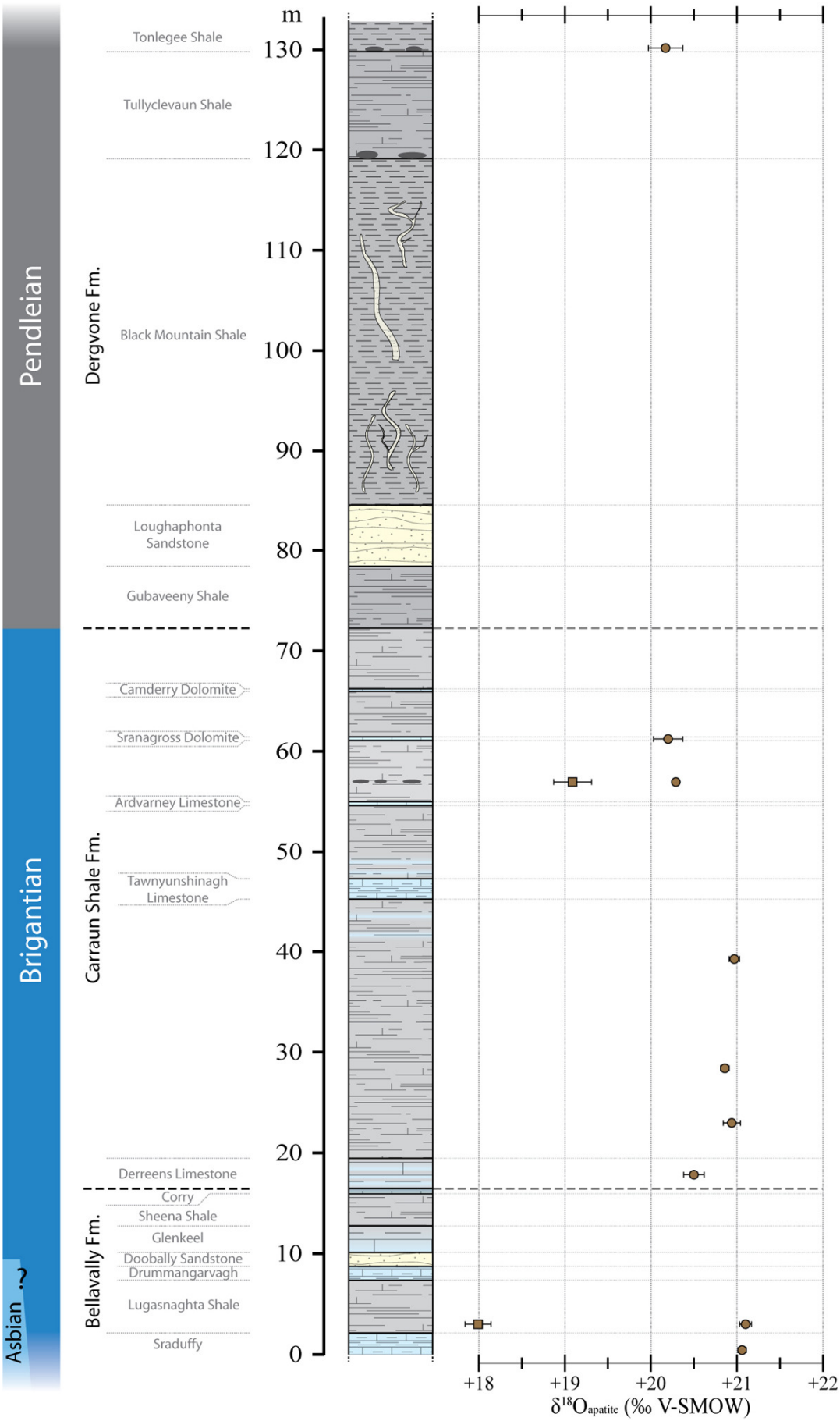

Fig. 5.2.1d $\delta^{18}O$ record of ichthyoliths (squares) and conodonts (circles), CNLG Section.

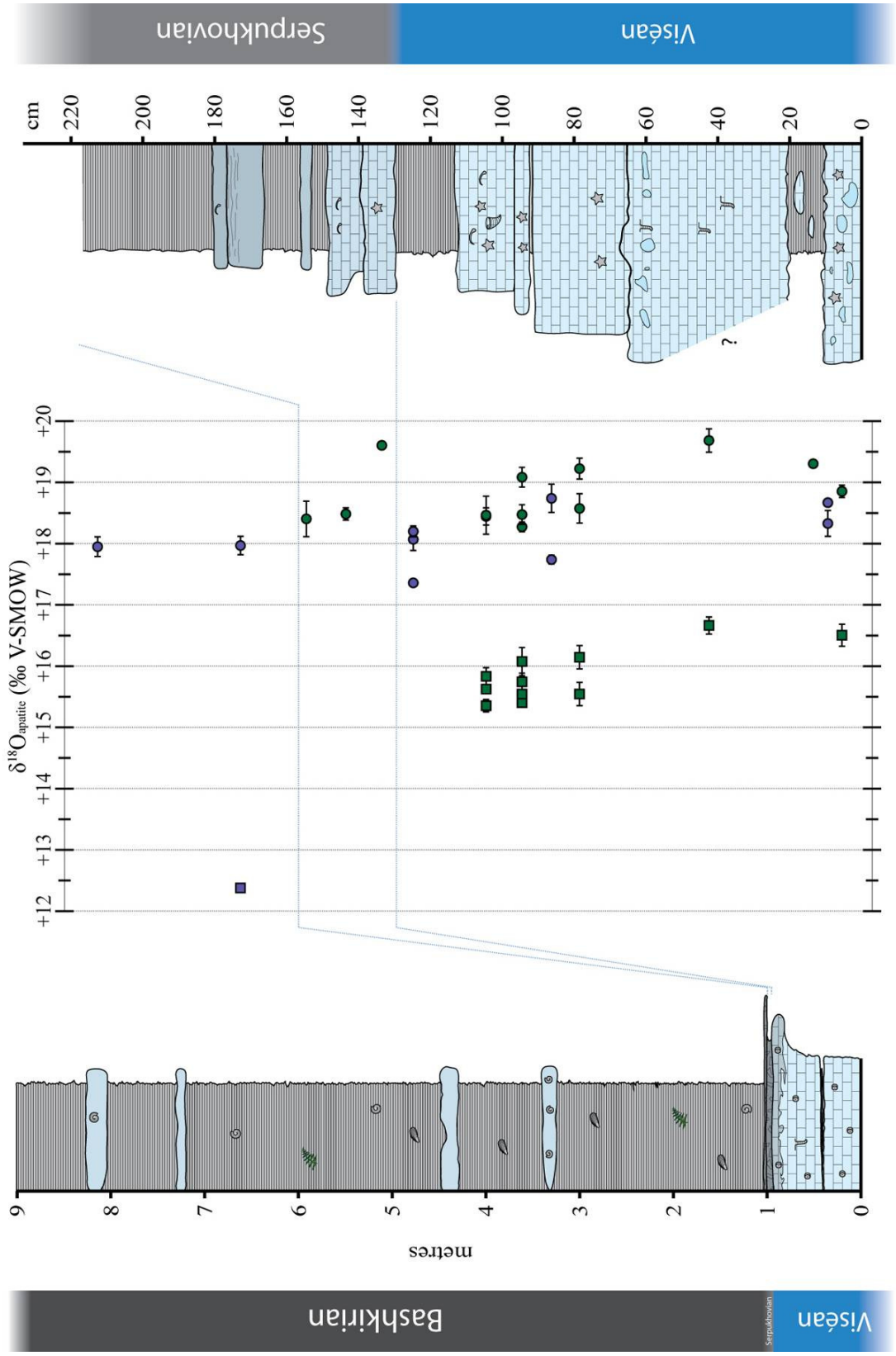

Fig. 5.2.2a $\delta^{18}O$ record of phosphatic microfossils in two western Ireland sections.

The graphic represents the probable correlation of sections studied in Co. Clare. Results from the St. Brendan's Well Section (left), in purple, are expanded or collapsed to match the Kilnamona Section (in green) scale. Circles = conodont, squares = ichthyoliths and error bars = 1σ.

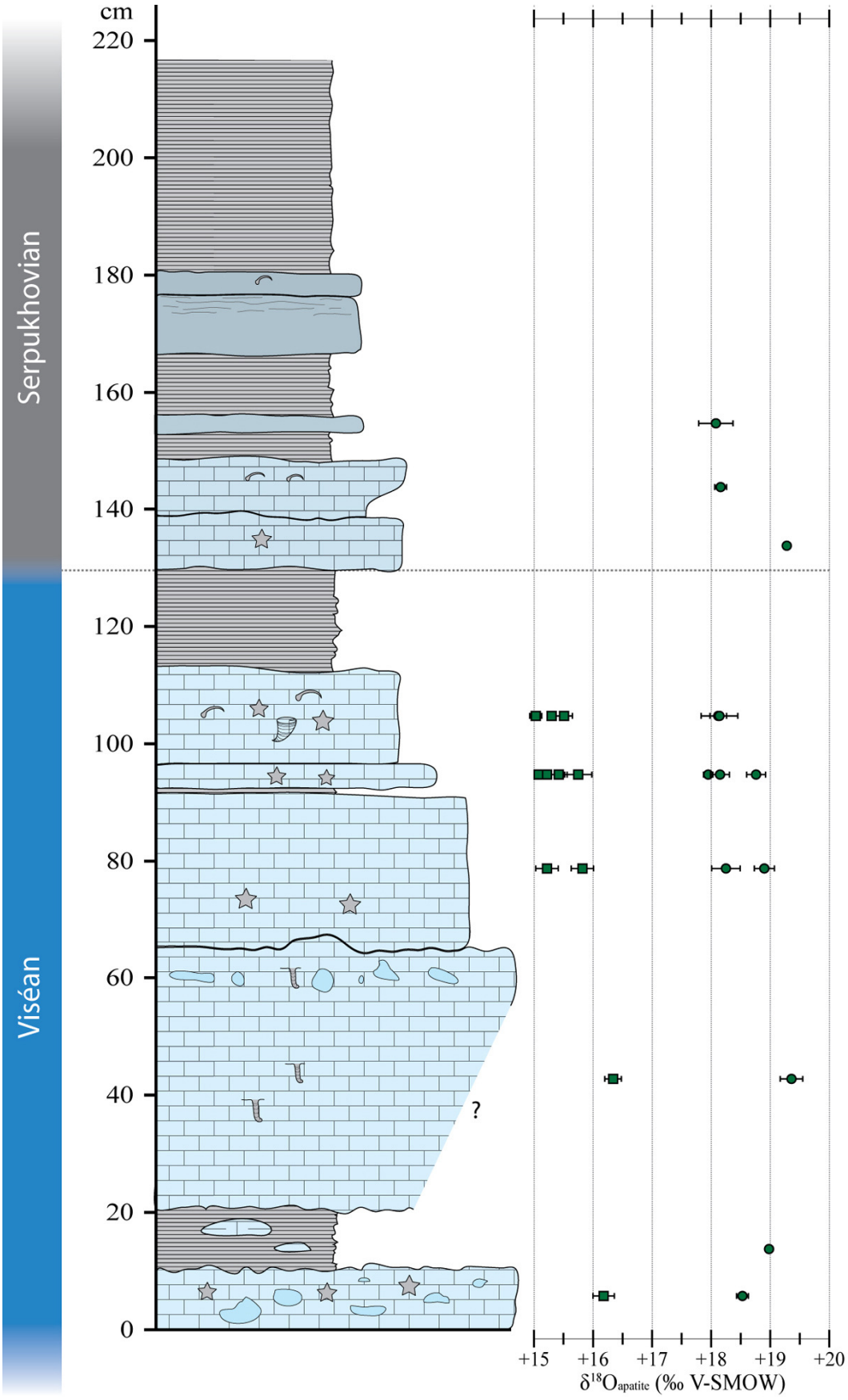

Fig. 5.2.2b $\delta^{18}O$ record of fish and conodont dental elements, Kilnamona Section.

Squares represent ichthyolith analyses, circles represent conodont analyses and error bars represent 1σ of the data. Note how the fish and conodont trends are essentially parallel.

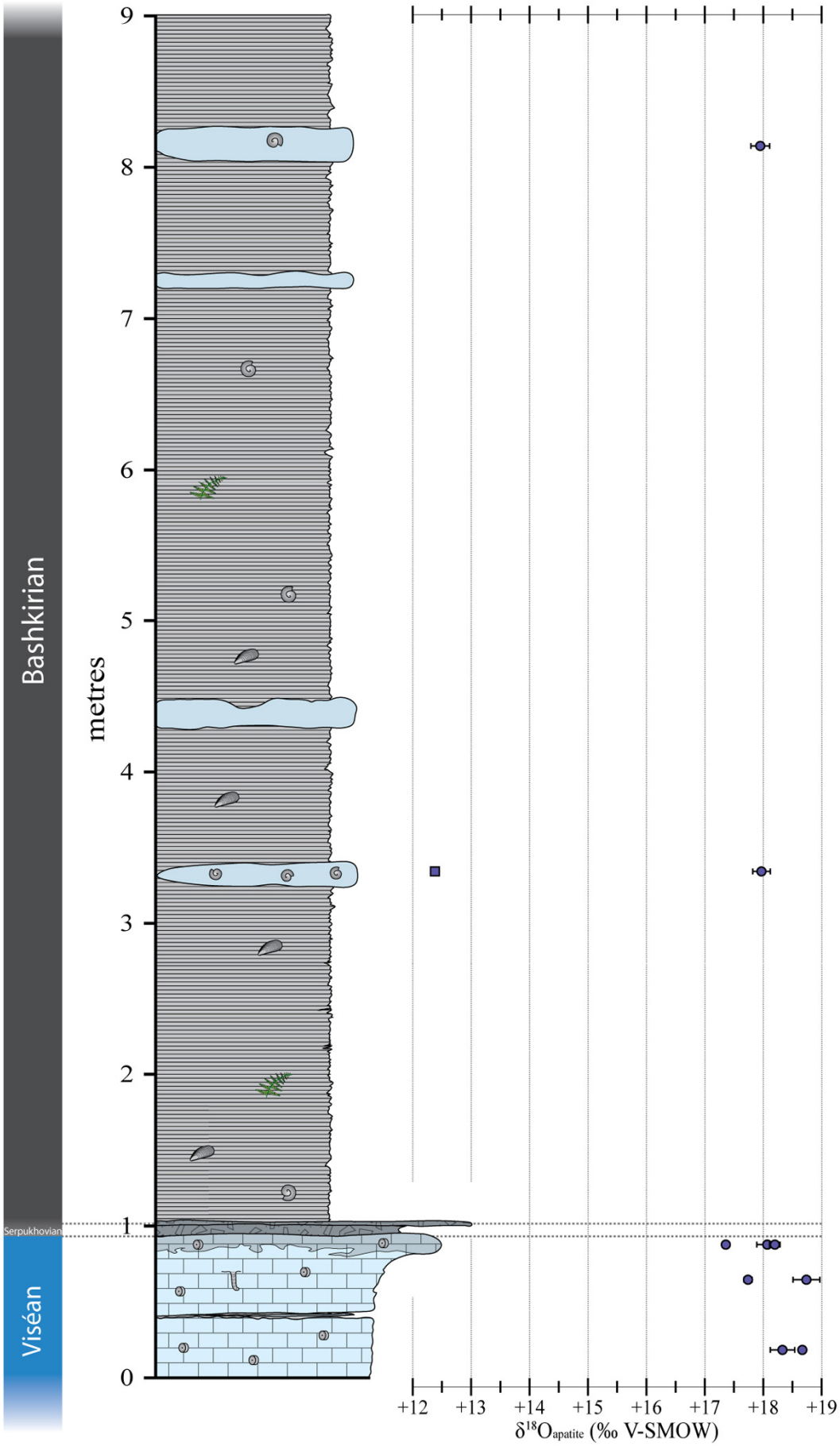

Fig. 5.2.2c $\delta^{18}O$ record of fish (square) and conodont (circles) remains, BW Section.

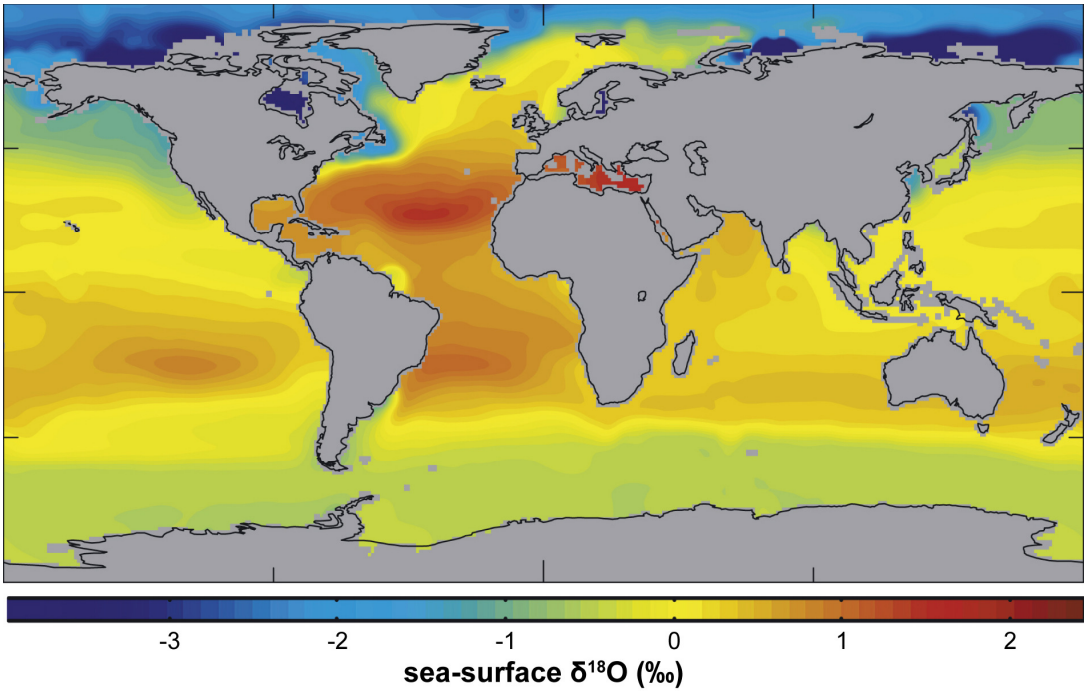

Fig. 5.3.1.2 Map of the worlds present sea-surface $\delta^{18}O$ values.

The surface variation in $\delta^{18}O$ values, due to differences in freshwater input and rates of evaporation, is shown. Note the irregularities in the general latitudinal pattern that exist due to large river systems (Amazon River – northeast coast of S. America, Ganges/Brahmaputra Rivers – Bay of Bengal) or ocean currents (eastern seaboard of Canada – Labrador Current vs. western coast of Europe – The Gulf Stream). Modified from LeGrande & Schmidt (2006).

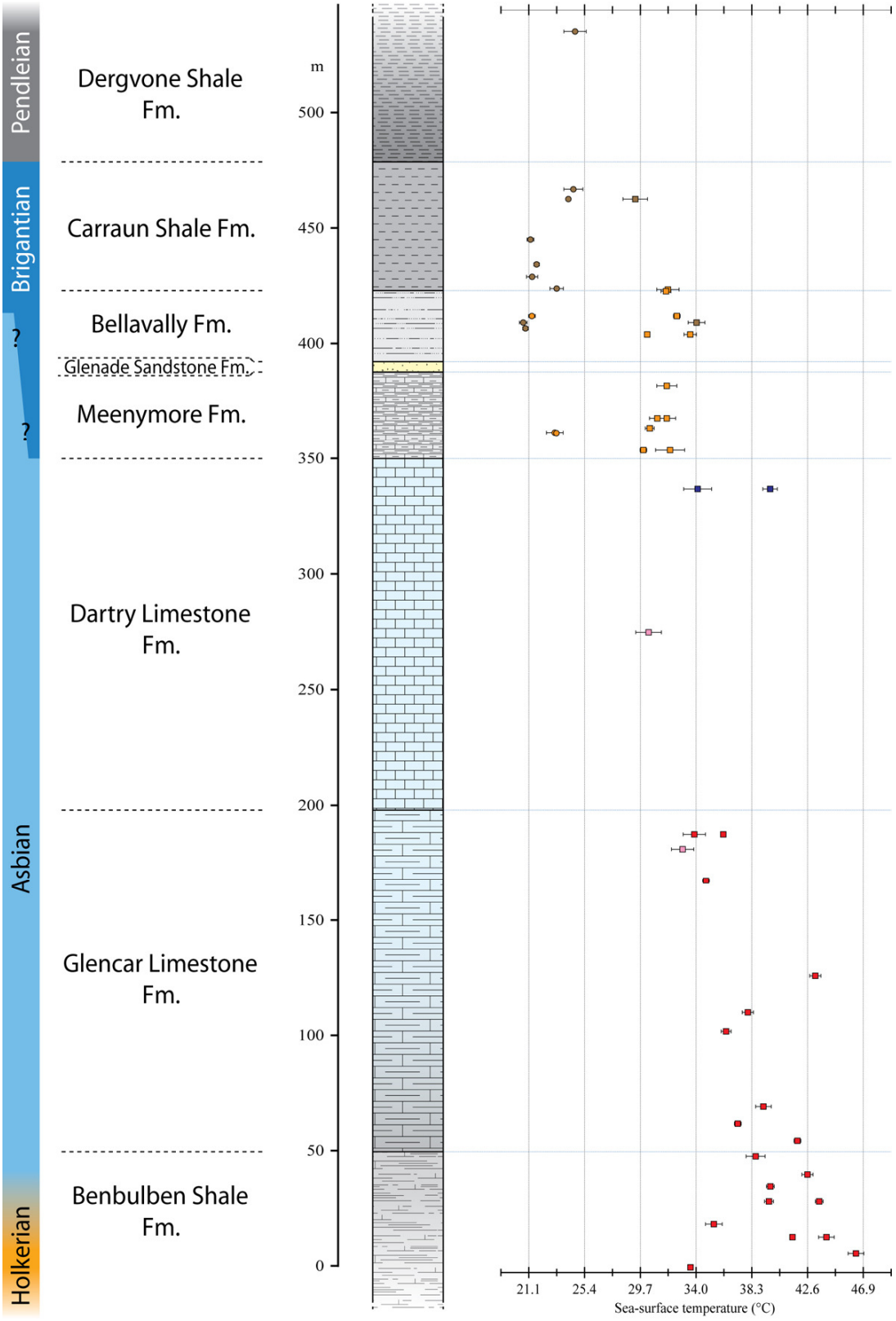

Fig. 5.3.1.4a Palaeotemperature derivations from $\delta^{18}O$ values, NW Ireland Sections.

This figure demonstrates the isotopic data from the northwest sections plotted on a SST palaeotemperature scale derived from the isotopic values of the analyses.

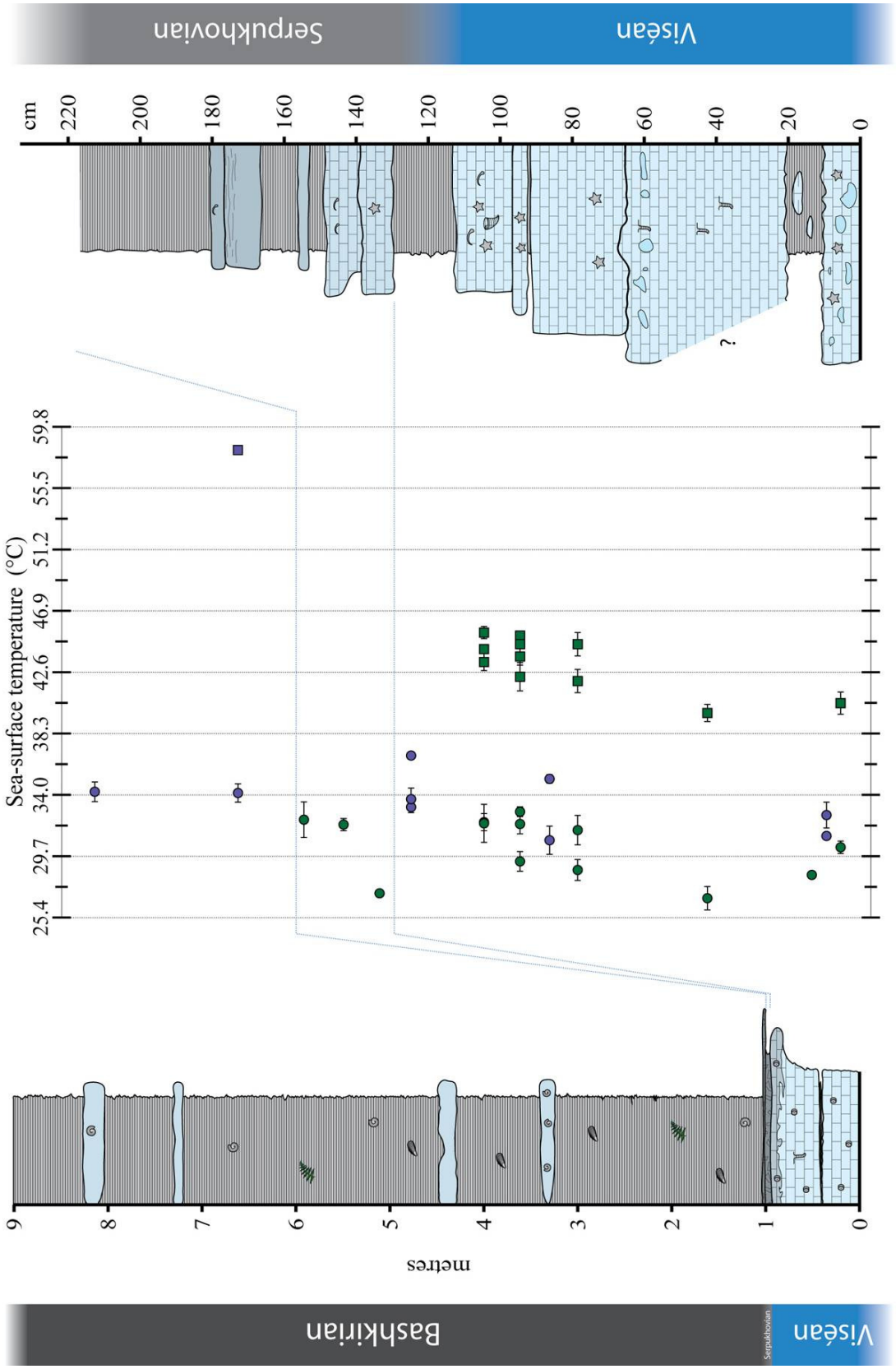

Fig. 5.3.1.4b Palaeotemperature derivations from $\delta^{18}O$ values, Burren Platform Sections.
This figure demonstrates the isotopic data from the Shannon Basin sections plotted on a SST palaeotemperature scale derived from the isotopic values of the analyses.

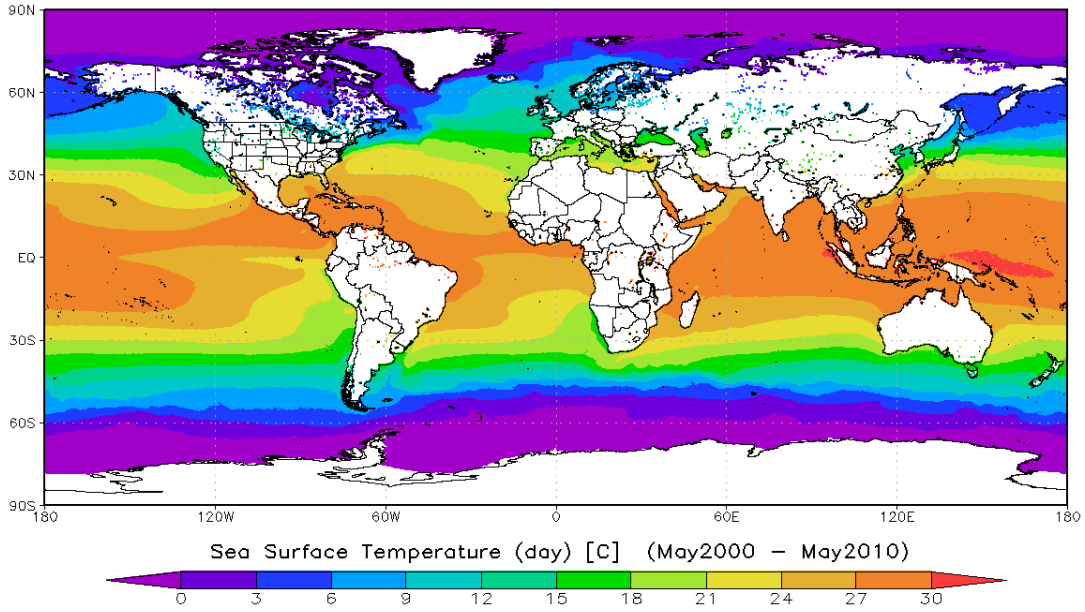

Fig. 5.3.2a Map of the 10-year average, modern, daytime sea-surface temperature.

Isolation of water bodies (contrast the Mediterranean with. the Red Sea or Black Sea) and the effects of ocean currents (Labrador – E Canada and Benguela – SW Africa) allow significant differences in temperature to develop over short distances. Image produced with the Giovanni online data system, developed and maintained by the NASA GES DISC.

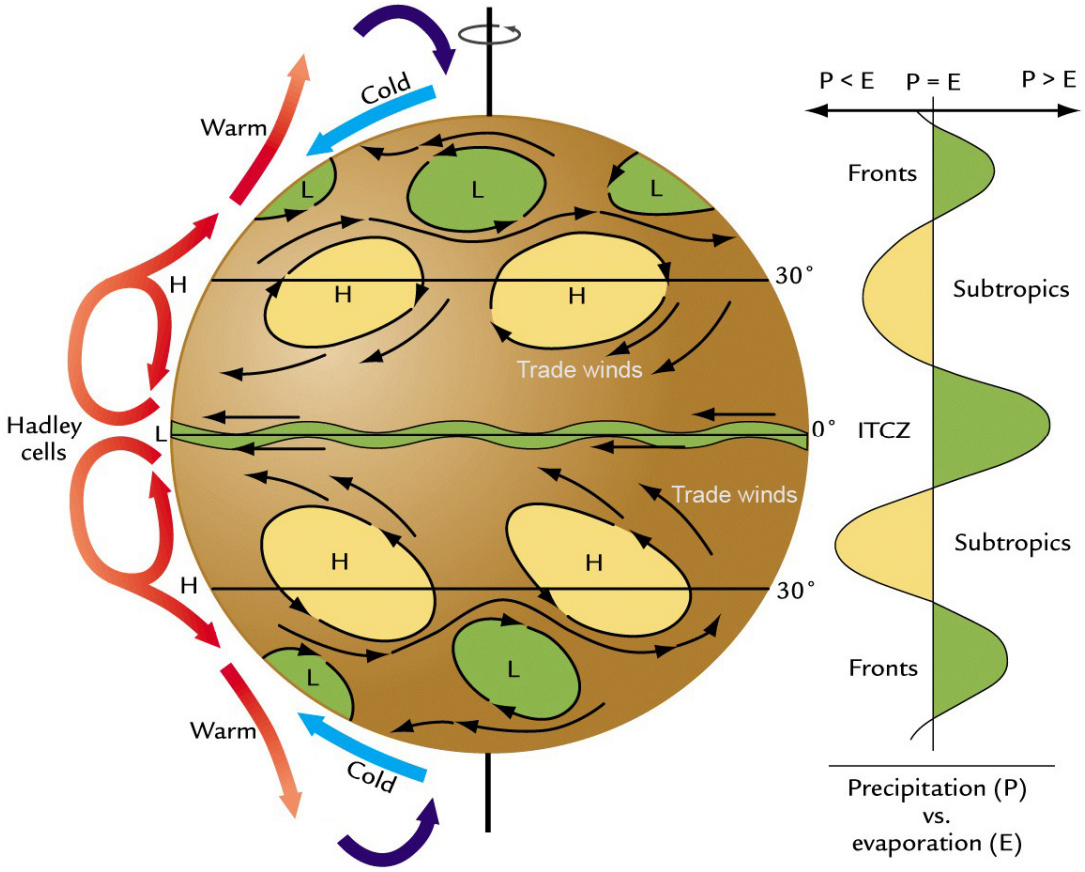

Fig. 5.3.2b Atmospheric circulation patterns and the ITCZ.

The atmospheric circulation patterns on a generalised globe are shown. Thin black arrows illustrate dominant wind directions. Modified from Ruddiman (2001).

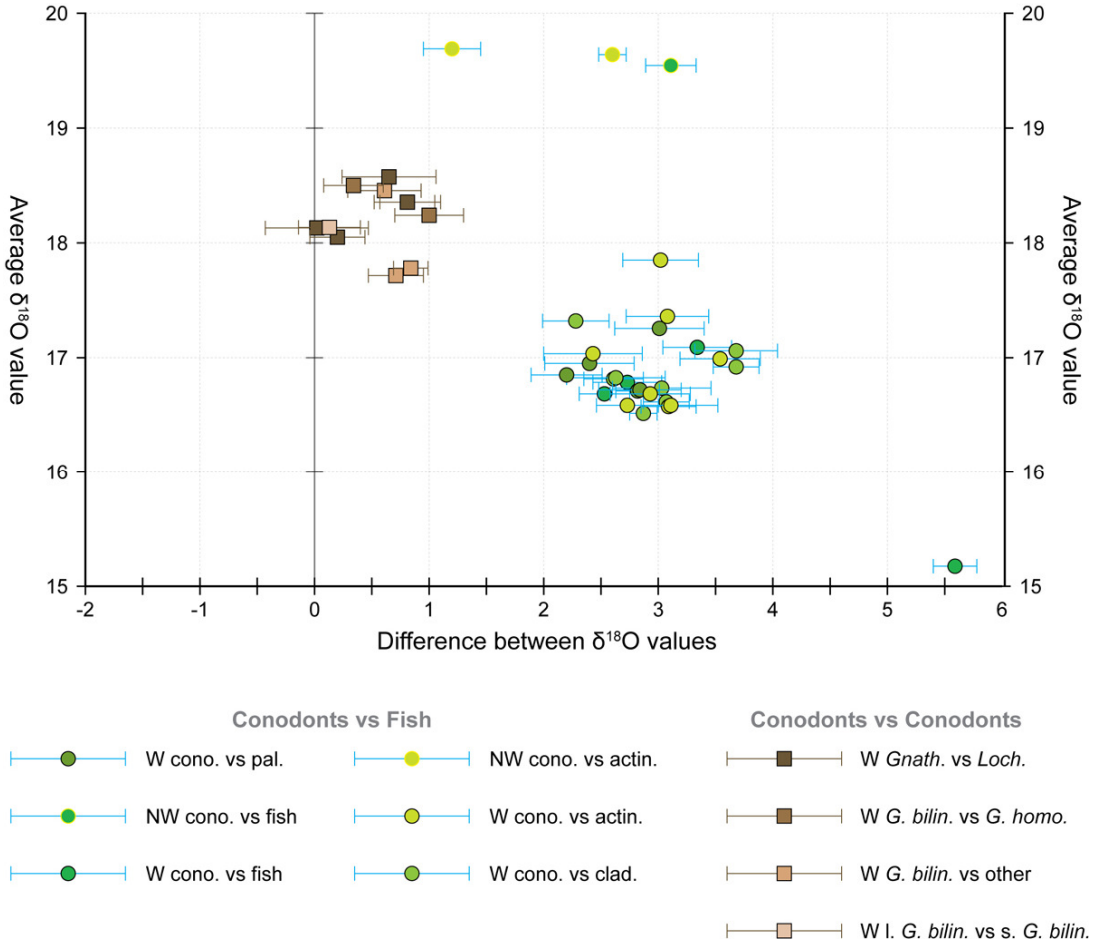

Fig. 5.3.3a Intra-conodont and conodont-fish $\delta^{18}O$ value variations.

The graph attempts to clarify how conodont analyses compare to other conodont and fish results from the same horizon. Each different colour represents the comparison of different species of conodonts or fish as listed in the key. A yellow outline to the circles represents data from northwest Ireland, while a black outline indicate the data comes from the Shannon Basin. The x-axis records the value obtained after subtracting the $\delta^{18}O$ value of the secondary element from the primary element listed. The y-axis represents the average $\delta^{18}O$ value of the two elements that are being compared. Error bars on the data points account for the possible maximum and minimum differences if the standard deviations of each element are taken into account. All the conodont vs. conodont values plot slightly in the positive field, possibly suggesting that G. bilineatus is slightly enriched in $\delta^{18}O$ relative to most conodonts. Conodont vs. fish values plot predominantly around the +3 differential line suggesting some stability and consistency of offset. In the key, W = Shannon Basin, NW = northwestern study area, cono. = undifferentiated conodont analysis, pal. = palaeoniscid teeth analysis, actin. = actinopterygian scale analysis, clad. = cladodont analysis, Gnath. = undifferentiated Gnathodus analysis, Loch. = undifferentiated Lochriea analysis, G. bilin. = Gnathodus bilineatus analysis, G. homo. = Gnathodus homopunctatus analysis, other = undifferentiated conodont analysis, l. = large platform elements and s. = small platform elements.

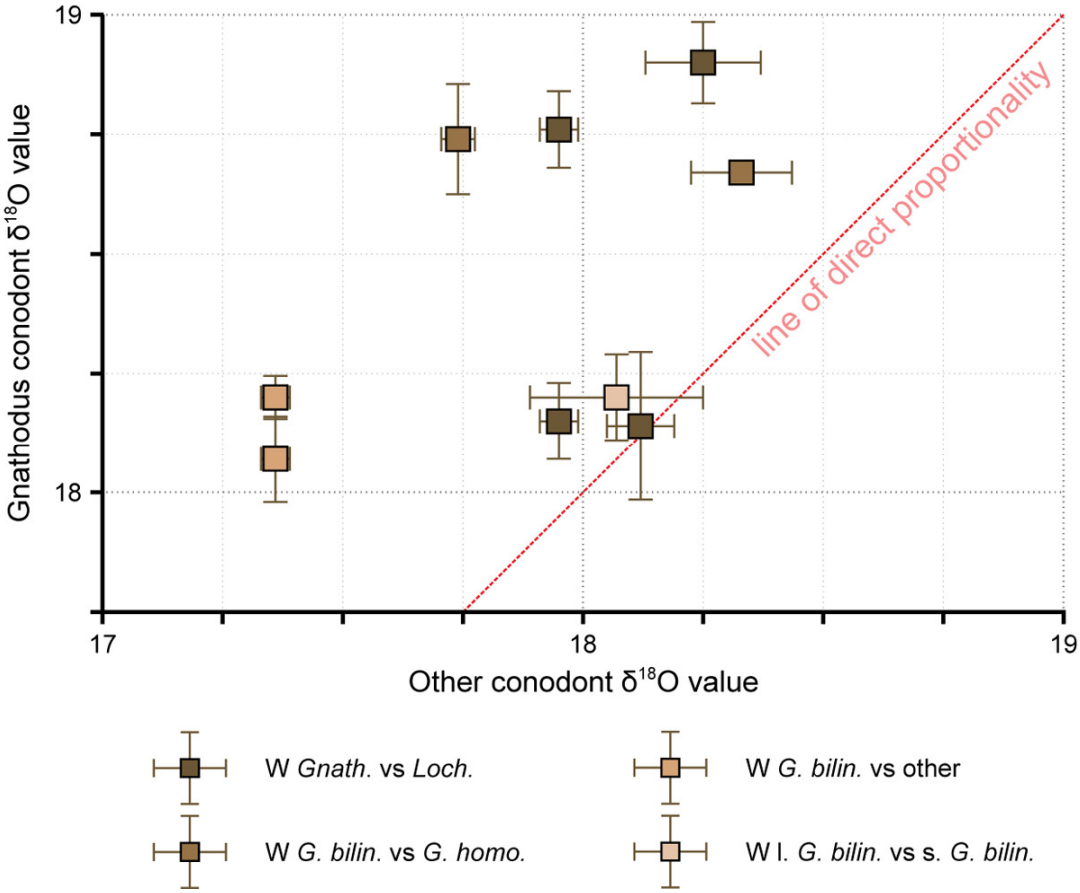

Fig. 5.3.3b Comparison of multiple conodont $\delta^{18}O$ analyses.
Plotted in ‰ relative to V-SMOW. Note that Gnathodus values are consistently higher.

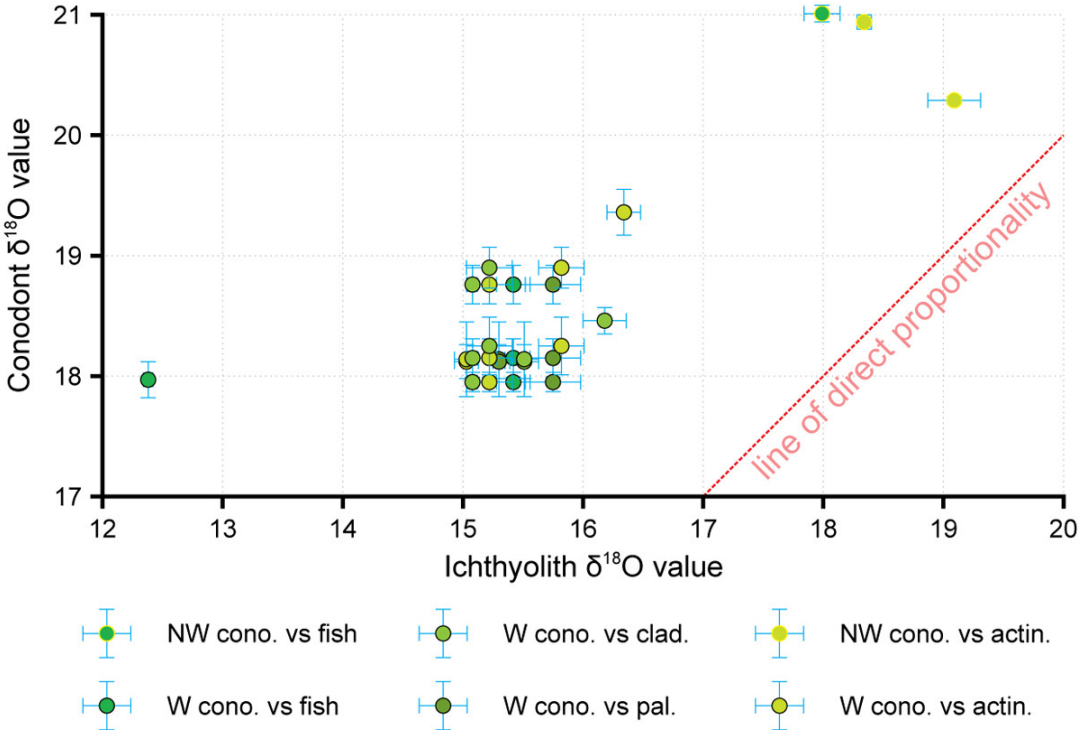

Fig. 5.3.3c Comparison of conodont and ichthyolith $\delta^{18}O$ analyses.
Values plotted in ‰ relative to V-SMOW. Note the clustering of data with a distinct offset.

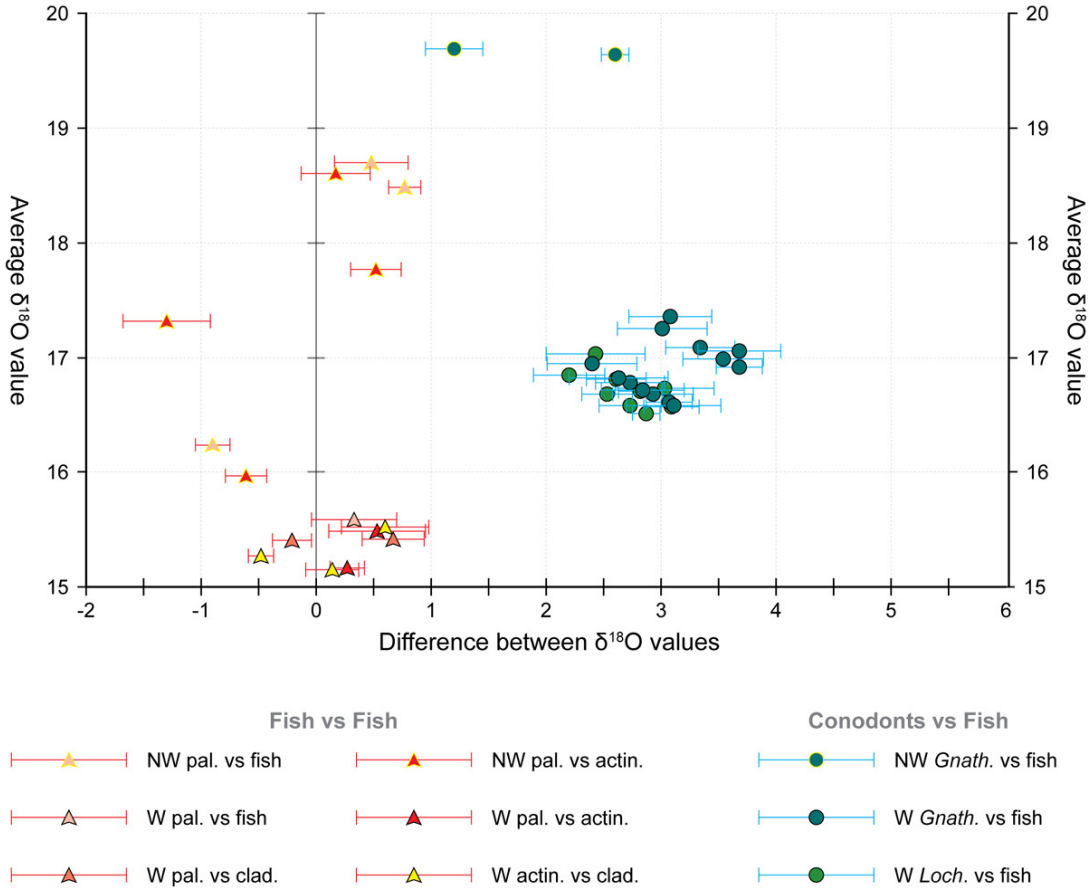

Fig. 5.3.3d Intra-fish and conodont-fish $\delta^{18}O$ variations.

The graph attempts to clarify how fish and conodont analyses compare to other fish results from the same horizon. Each different colour represents the comparison of different species of conodonts or fish as listed in the key. A yellow outline to the circles represents data from northwest Ireland, while a black outline indicate the data comes from the Shannon Basin. The x-axis records the value obtained after subtracting the $\delta^{18}O$ value of the secondary element from the primary element listed. The y-axis represents the average $\delta^{18}O$ value of the two elements that are being compared. Error bars on the data points account for the possible maximum and minimum differences if the standard deviations of each element are taken into account. The fish vs. fish values, although scattered, have a mean about the zero difference line, indicating no consistent offset between individual fish species. Gnathodid conodonts tend to have a greater offset against fish analyses than Lochriea conodonts. This can probably be attributed to G. bilineatus being slightly enriched in ^{18}O, as seen in Fig. 5.3c. In the key, W = Shannon Basin, NW = northwestern study area, cono. = undifferentiated conodont analysis, pal. = palaeoniscid teeth analysis, actin. = actinopterygian scale analysis, clad. = cladodont analysis, Gnath. = undifferentiated Gnathodus analysis, Loch. = undifferentiated Lochriea analysis, G. bilin. = Gnathodus bilineatus analysis, G. homo. = Gnathodus homopunctatus analysis, other = undifferentiated conodont analysis, l. = large platform elements and s. = small platform elements.

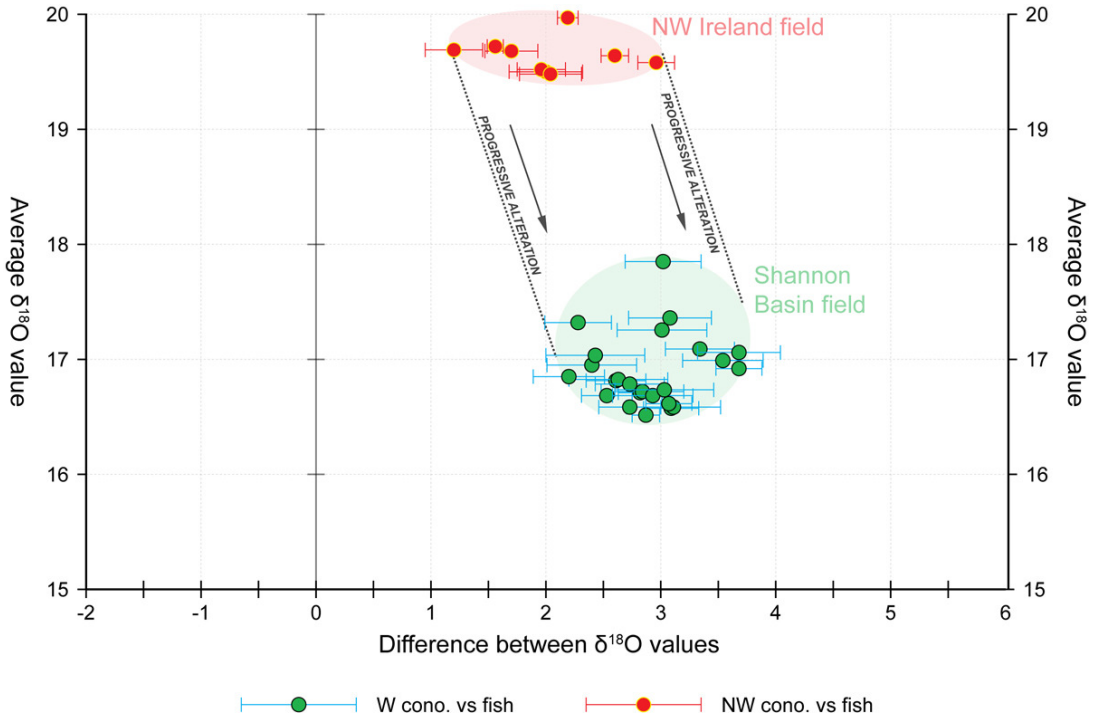

Fig. 5.3.3e Difference in the conodont-fish offset between study areas.

The figure plots the conodont vs. fish data for the northwest sections (derived both from same sample comparisons and stratigraphically adjacent $\delta^{18}O$ value comparisons) and the Shannon Basin sections (derived purely from same sample comparisons from the Kilnamona Section) Acanthodian data has been excluded. Distinct fields are identified with less of a difference between conodonts and fish in the northwest than in the Shannon Basin. The greater offset identified in the Shannon Basin may represent progressive alteration. Key as in Fig. 5.3.3a and Fig. 5.3.3d.

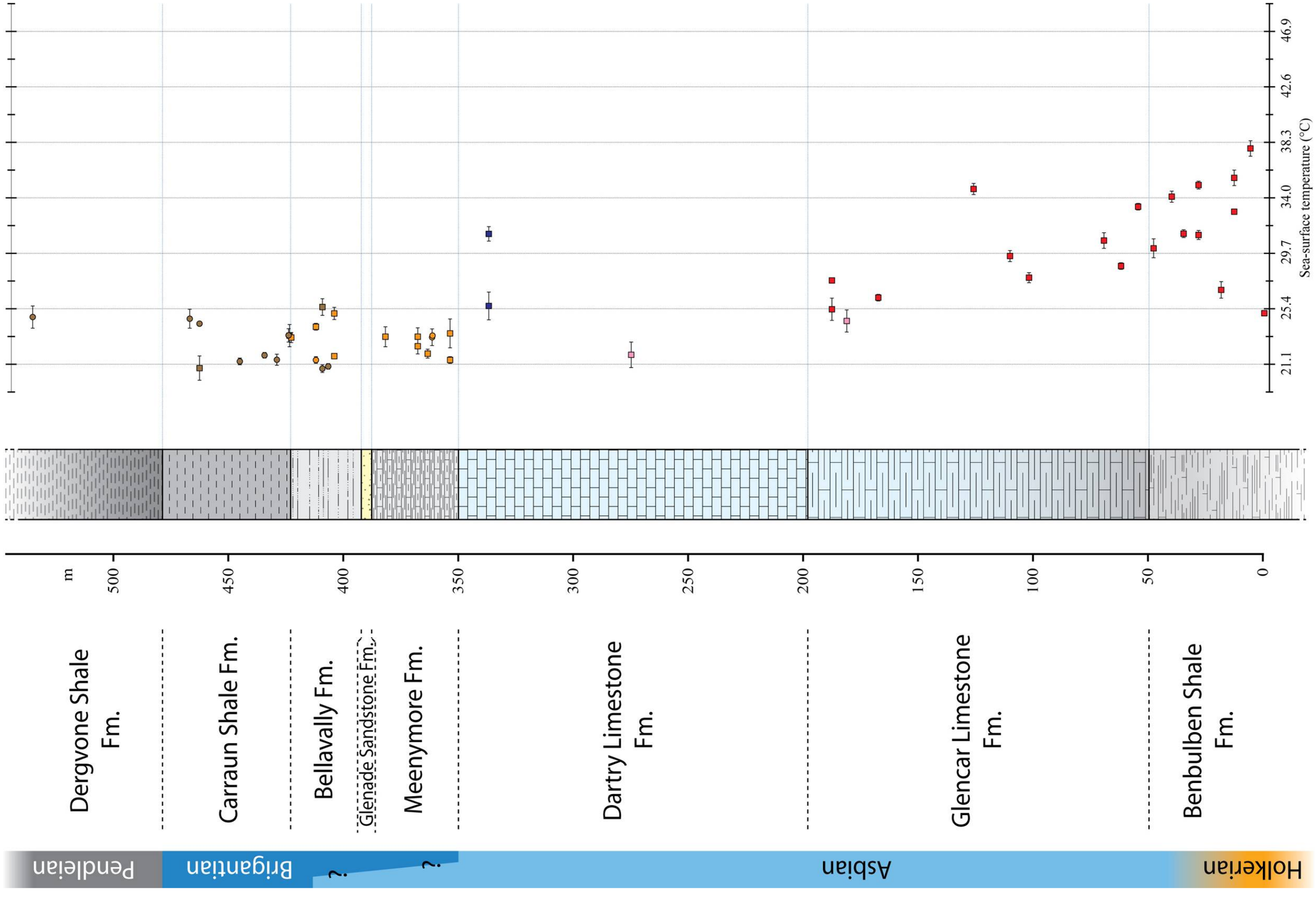

Fig. 5.3.3f Isotopic trends of northwestern sections with adjusted fish results.

This figure demonstrates the isotopic data from the NW sections plotted on a palaeo-SST scale. All fish analyse have been shifted by 2‰ in an attempt to return them to their original isotopic composition.

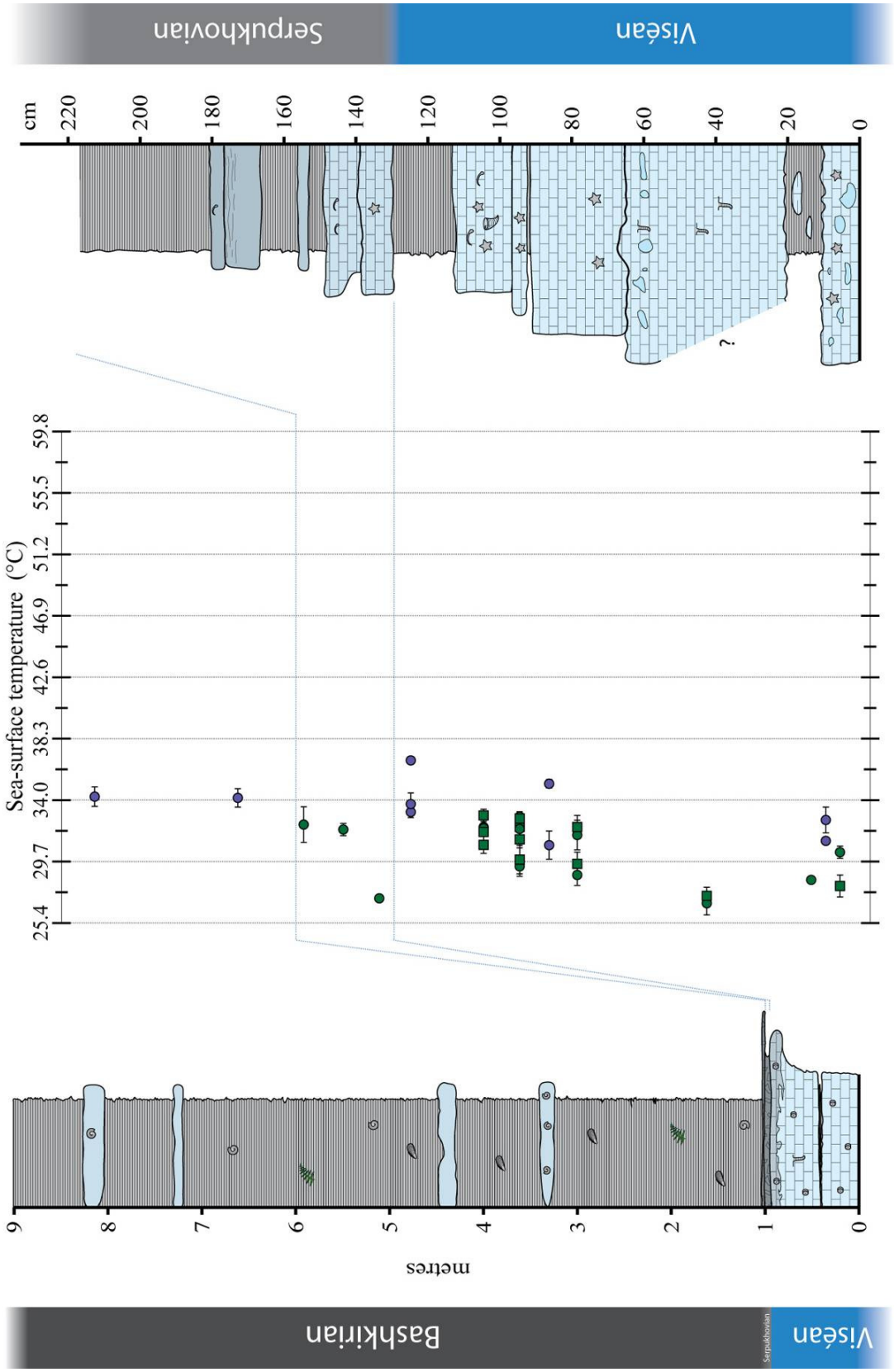

Fig. 5.3.3g Isotopic trends from Shannon Basin sections with adjusted fish results.

This figure demonstrates the isotopic data from the Shannon Basin sections plotted on a SST palaeotemperature scale derived from the isotopic values of the analyses. In this plot all fish analyse have been shifted by 2.9‰ in order to attempt to return them to their original isotopic composition.

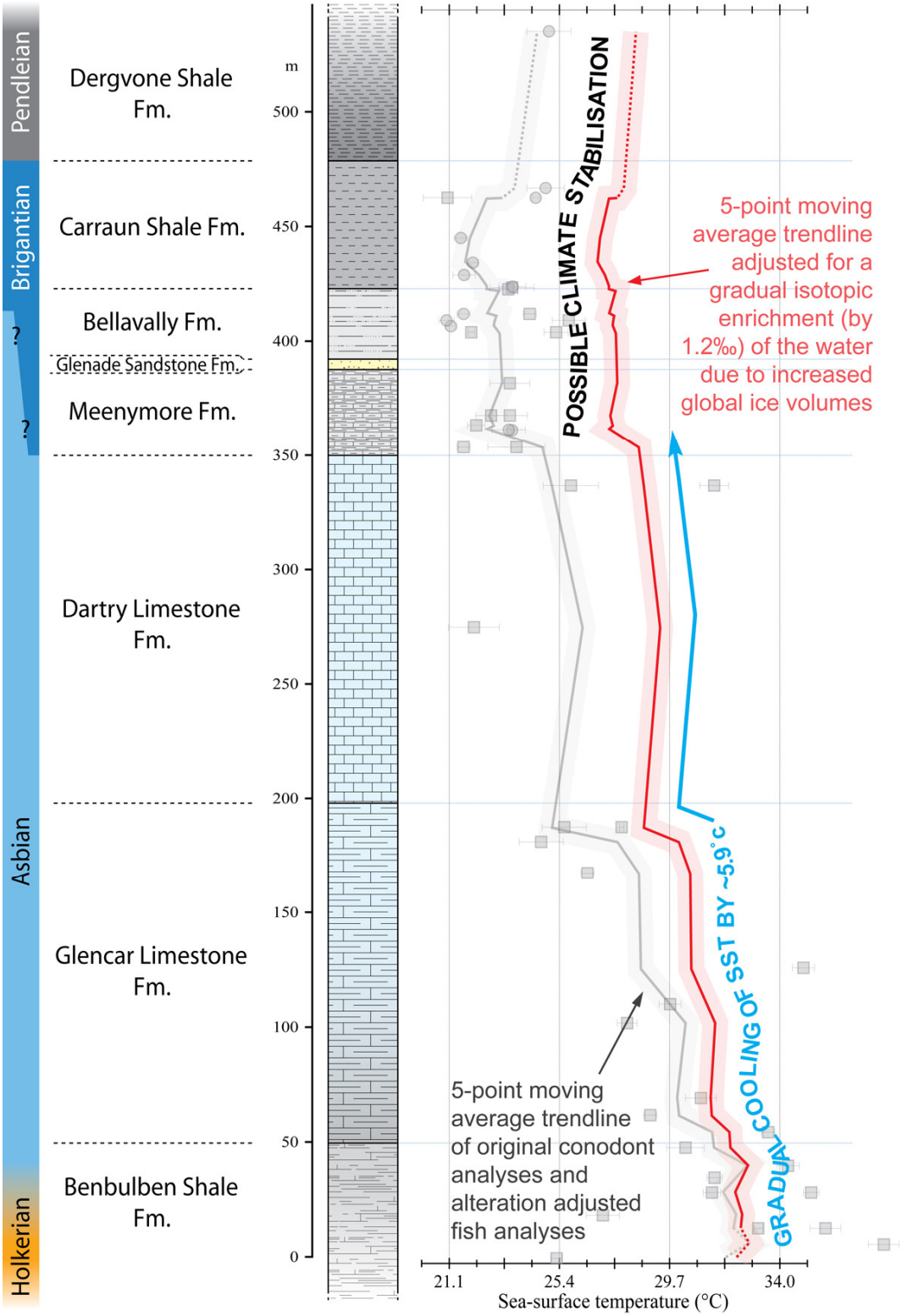

Fig. 5.3.4 Palaeoclimatic reconstruction of the late Viséan to early Serpukhovian.

The pale grey line (5-point moving average trendline for the adjusted NW analyses) suggests the cooling that the data implies if the entire $\delta^{18}O$ shift is attributed to changes of SST. The red line (5-point trendline adjusted for a 1.2‰ shift in palaeo-seawater) suggests a maximum cooling of ~5.9ºC from the uppermost Holkerian before the climate began to stabilise and possibly warm slightly in the early Serpukhovian. Dashed lines represent the probable continuation of the trendline but where a 5-point average is no longer possible.

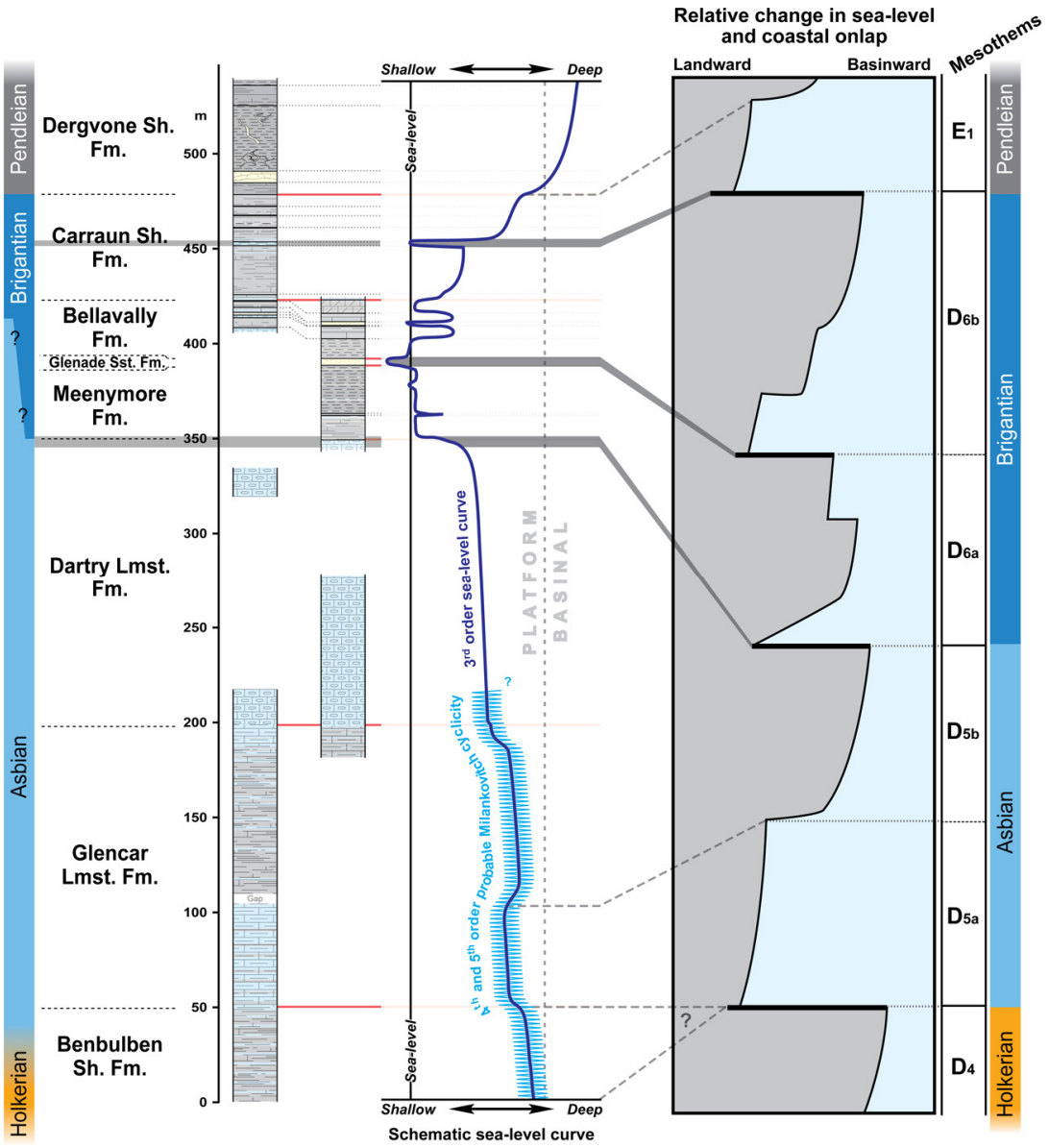

Fig. 6.1.1 Correlation of Viséan mesothems with the 3rd order sea-level of NW Ireland.

Lithostratigraphic columns are derived from the Tievebaun, Glencar, Glenade, Aghagrania and Carraun/Lugasnaghta Sections respectively. The sequence stratigraphic, mesothem data on the right is taken from Ross & Ross (1987). Correlations between the sea-level curve produced for NW Ireland and the curve of Ross & Ross (1987) are those proposed in the text. Note the continuation of the D_5/D_6 and D_6/E_1 correlations to the chronostratigraphic column for NW Ireland, illustrating the possible disparities between the original proposed event timings of Ross & Ross (1987).

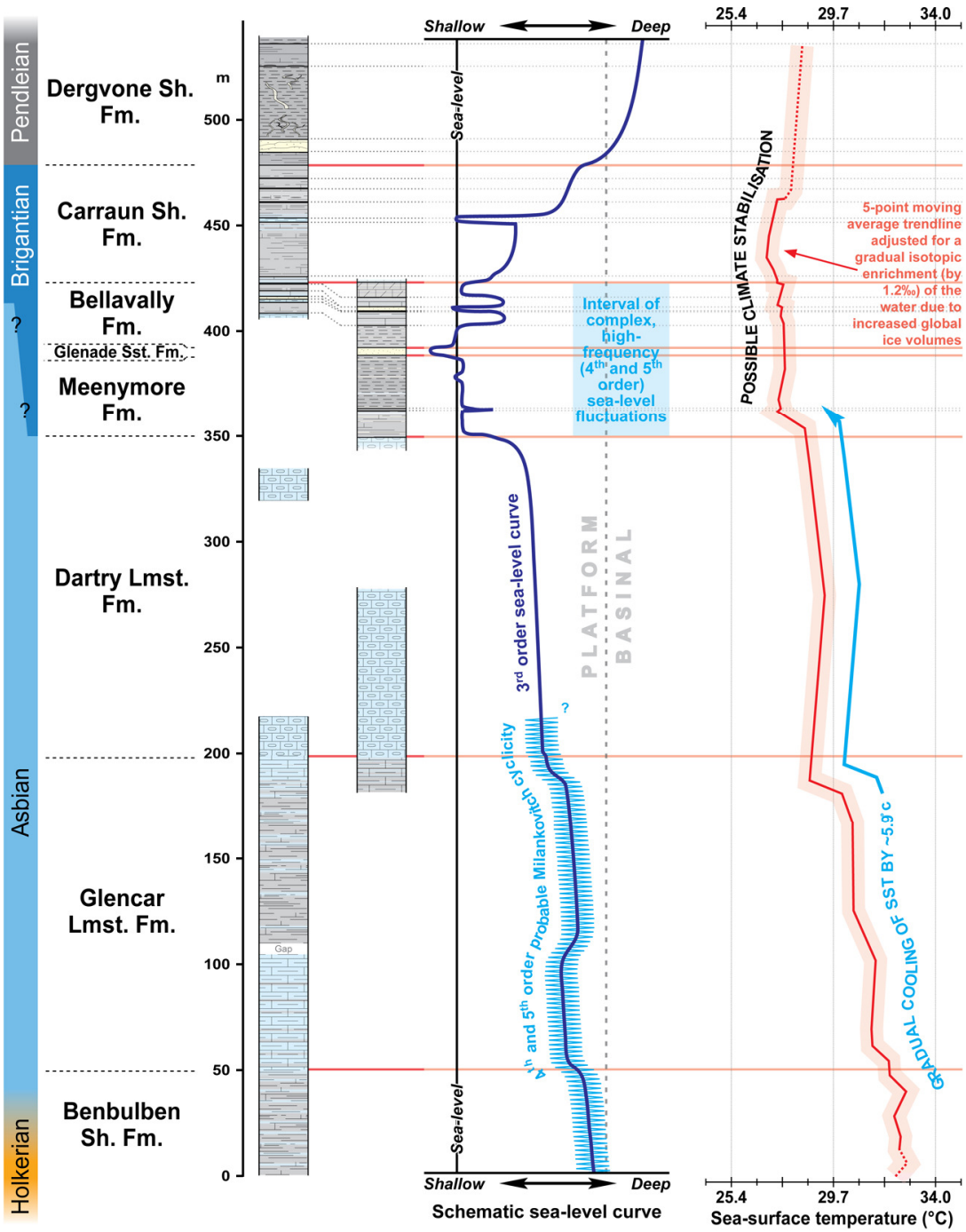

Fig. 6.2a Correlation of isotopic and sea-level curves for NW Ireland.

Lithological columns represent (in ascending order) the Tievebaun, Glencar, Glenade, Aghagrania and Carraun/Lugasnaghta Sections. Refer to Figs. 2.2.1d, 2.2.1e, 2.3.1d and 2.3.2d for the detailed stratigraphy as well as the names of members and lithological keys. The dark blue curve on the left represents an interpretation of 3rd order sea-level change with pale blue, high-frequency oscillations overlain (Chapter 2). The red line represents the temperature variation derived from the isotopic analysis of biogenic apatite (Chapter 5).

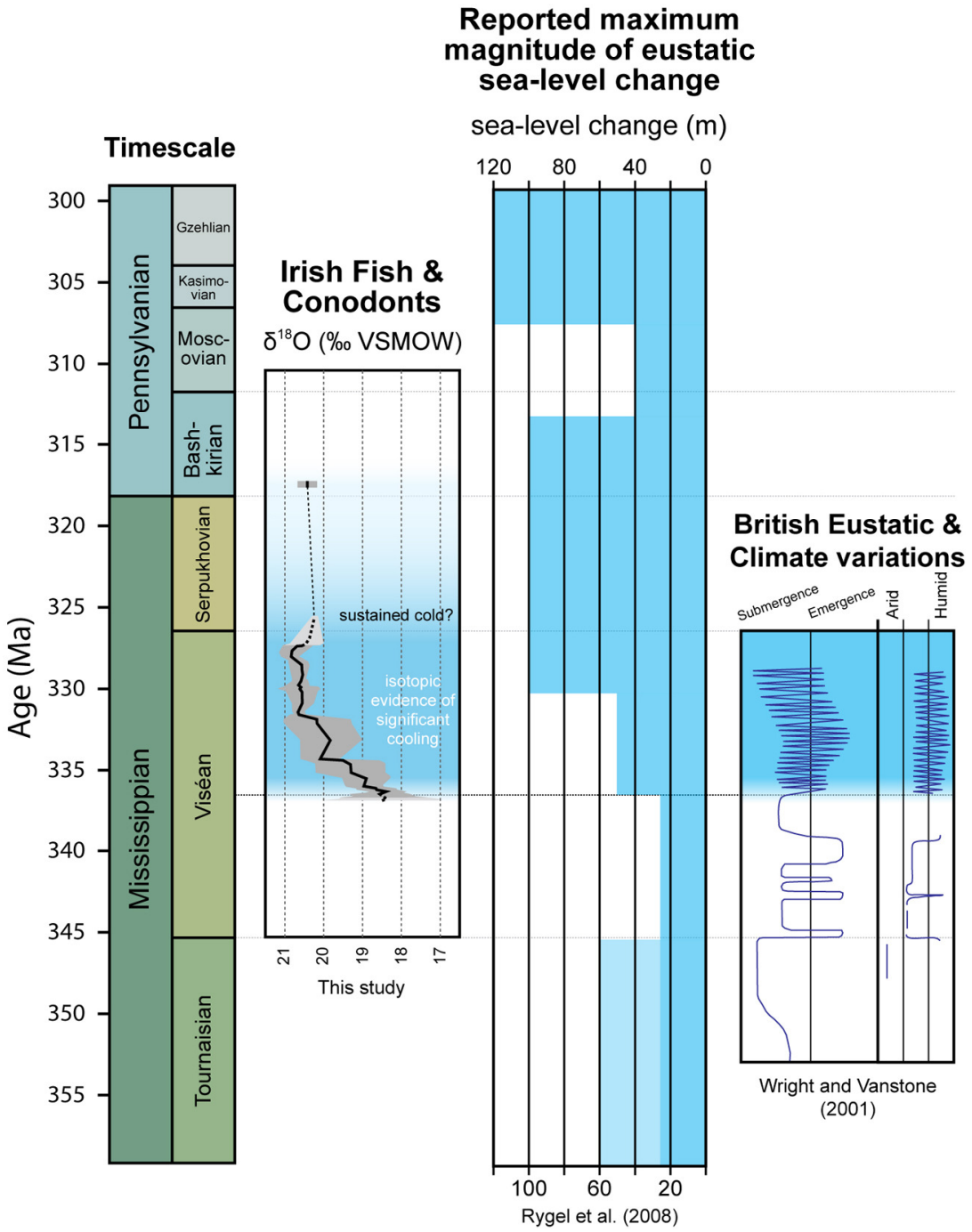

Fig. 6.2b Correlation of isotopic curve with published Carboniferous eustasy data.

Dashed grey lines in the background represent Stage boundaries, whilst the black dashed line indicates the position of the Holkerian-Asbian boundary. All data are plotted relative to the timescale in Rygel et al. (2008).

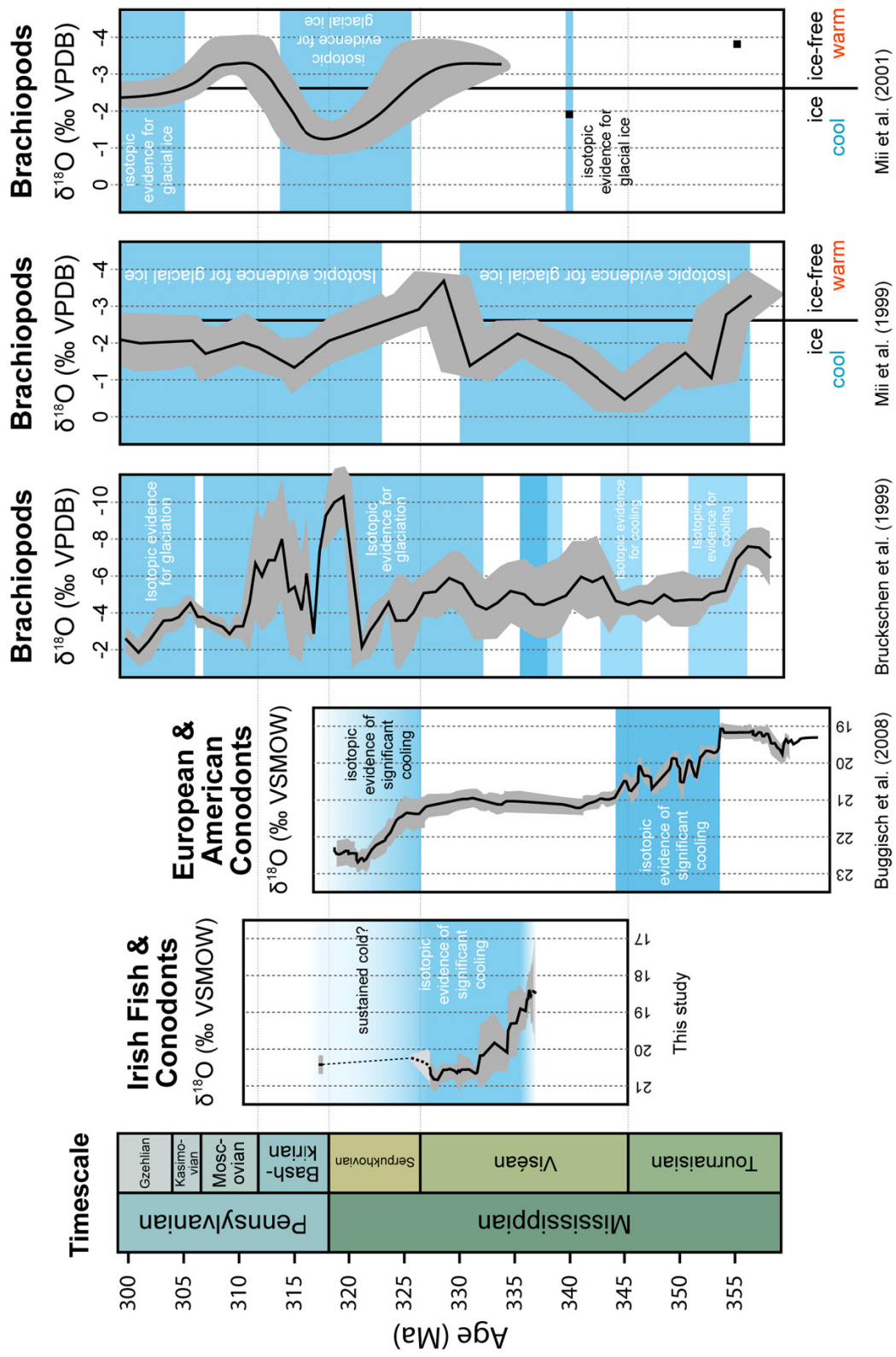

Fig. 6.2c Comparison of Carboniferous isotopic datasets.

The work of Bruckschen et al. (1999) is plotted at a different isotopic scale to the others. Black lines represent moving averages of the data, whilst grey areas around the trends represent one standard deviation of the data. Dashed grey lines in the background correspond to Stage boundaries. Blue filled areas represent the intervals recognised by the authors of the specific work as being glacial. All isotopic curves are plotted relative to the timescale of Rygel et al. (2008).

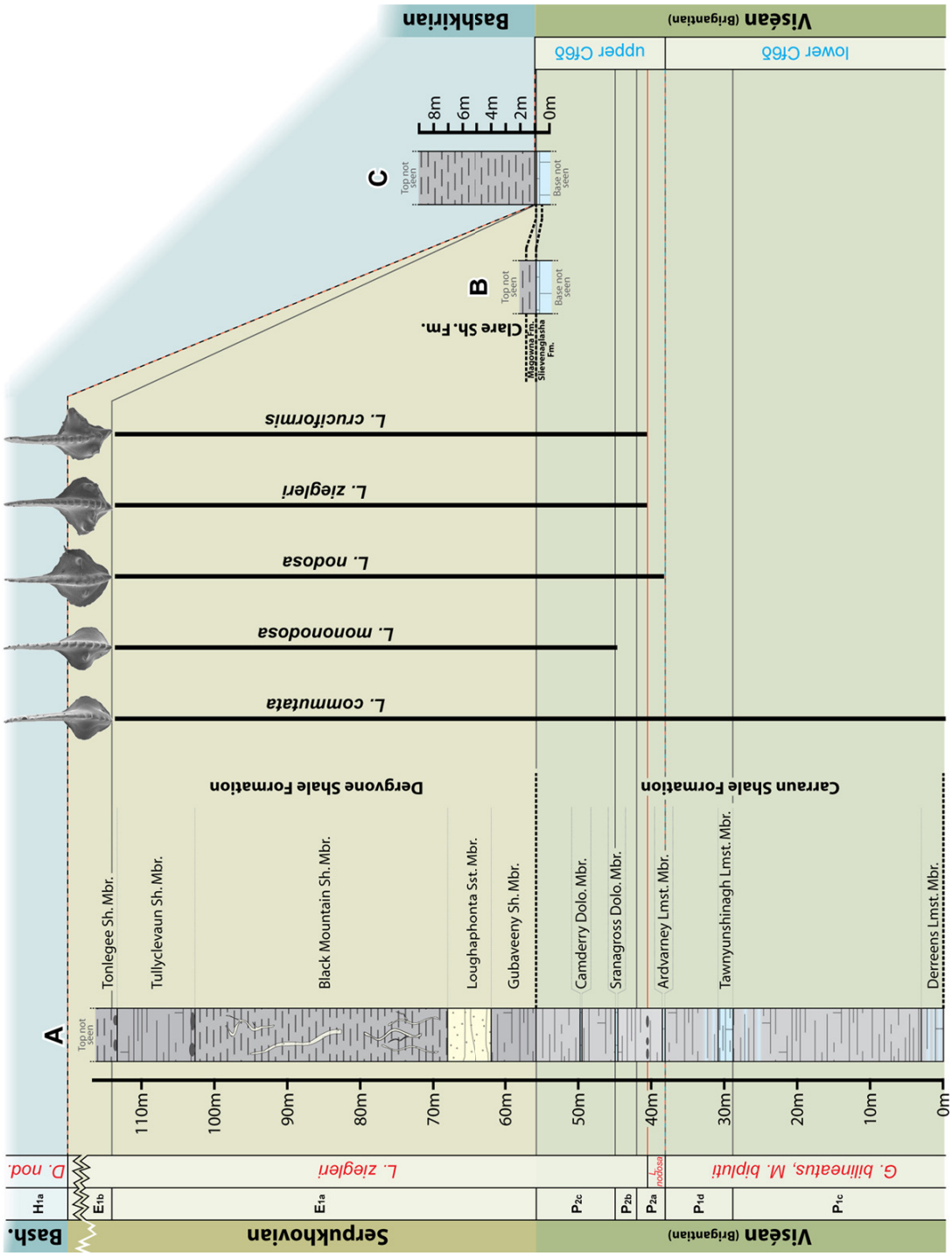

Fig. 6.4 The biostratigraphy of the Lochriea lineage in Ireland.

Section A represents the Carraun/Lugasnaghta Section in NW Ireland, whilst B and C are the Kilnamona and St. Brendan's Well Sections respectively. The ammonoid and conodont biozones (black and red respectively) are shown on the left whilst the foraminiferal biozones are demonstrated on the right in blue. Only the confirmed occurrences of conodonts are shown. Stage colours are according to the CGMW. Note the break in the litho- and chronological scales on the left.

APPENDICES

Appendix A - Rock digestion/disaggregation method.

Appendix B - Digital spectral analysis of the Tievebaun Section.

Appendix C - Bulk-apatite preparation procedure for stable isotope analysis.

Appendix D - Microfossil sample locations in NW Ireland sections.

Appendix E - Microfossil sample locations in Co. Clare, western Ireland sections.

Appendix F - Catalogue of the invertebrate microfauna recovered.

Appendix G - Samples for stable isotope analyses.

Appendix H - SEM stub maps and museum number.

APPENDIX A –

Rock digestion/disaggregation method

A variety of both chemical and physical methods were utilised to break down rock samples which were selected for microfossil processing. All samples (except fissile shales) were returned to the laboratory and immersed in a bucket containing a hot, dilute bleach solution for 24-48hrs. Samples were subsequently removed, washed and scrubbed to remove loose clay, and organic mosses and lichens. After drying, the rocks were re-examined and any previously obscured lithological features were recorded. Samples were broken down into pieces (no larger than ~5cm) in order to increase reactive surface areas and therefore the speed of sample breakdown. Fissile shale samples were always dug out from outcrop and did not require the removal of recent organics or mechanical breakdown. At this point processing methodologies diverged for each sample depending on its specific lithological characteristics. Initial sample sizes were maintained as close to 2kg as possible. Tables, listing the chemicals utilised as well as the initial and final weights for each sample (note that some samples were run more than once) follow the methodologies below.

Carbonates

(1) Rock fragments were placed into an open-structured basket within a bucket to allow the sample to be suspended above the bucket base. Numerous holes in the basket facilitated circulation of an acid mixture around the sample and also small, non-digestible material (released during reaction) to fall to the base of the bucket. Microfossils, once at the bucket base, are relatively sheltered from both acid etching and mechanical damage due to solution stratification and a coating of argillaceous material.

(2) A buffered, dilute formic acid solution was constructed according to both the lithological composition and mass of the microfossil sample to be immersed. Typically a 6% acid solution was constructed by mixing 11 parts water with 2 parts of buffer and adding 1 part 85% formic acid (lower concentration facilitates the ionisation of the acid by the water, and thus increases the

efficiency of the acid; Stone, 1987). Some samples were also treated with acetic acid, in a similar fashion to formic acid, during experimentation. Buffer solutions were obtained by filtering the reacted fluid from a previous run. Where samples were especially argillaceous or silicified, reduced volumes of acid were added but the temperature was increased by the use of hot water. Pure limestone samples were occasionally subjected to greater volumes of more concentrated acid solutions (up to 8%). The volume of acid solution to construct was calculated by taking the sample weight, in grams, and dividing by four. The resulting value represents the volume of 1 part of the mixture in millilitres. Greater or lesser volumes of solution were constructed by using a larger or smaller fraction of the sample weight (maximum = ½, minimum = ⅛).

(3) After 24-48hrs a portion of the solution was removed for use as buffer while any solids were subjected to washing and sieving (discussed below). Significant residues that required further acid digestion were weighed and treated as described above.

Shales (calcareous, organic-rich etc.)

Occasionally, particularly argillaceous limestone residues were subjected to some similar steps as outlined below in order to tackle thick, smothering coatings of mud on restite clasts.

(1) Samples were broken loosely by hand into open, heat resistant containers and dried in an oven at 70ºC.

(2) Samples were covered in boiling water and allowed to expand and disaggregate. Resulting residues were sieved (discussed below), while coarse materials were returned for repeated oven desiccation and soaking expansion until completely disaggregated.

Samples that failed to breakdown in this manner were examined and simplistically categorised as being either carbonate bound or organically bound. Calcareous cements were treated with mild formic acid solutions intermittently between dryings, while binding organics were broken down with sparing amounts of hydrogen peroxide (H_2O_2).

Sieving and microfossil picking

Sediments were gently washed through 2mm, 0.5mm and 0.125mm meshed (20cm internal diameter) sieves. Anything retained in the 2mm mesh sieve was returned for further breakdown. Anything smaller than 0.125mm was not retained since material this small would have been labour intensive to examine and in any case phosphatic microfossils recovered would have been of little assistance in meeting the mass requirements of stable isotopic analysis undertaken herein. Residues retained in the 0.5mm and 0.125mm mesh sieves were carefully washed into labelled filter papers and dried in an oven at ~70ºC. Residue from the 0.125-0.5mm fraction was further separated using a 0.25mm mesh sieve, thus resulting in 3 fractions: fine = 0.125-0.25mm, medium = 0.25-0.5mm and coarse = 0.5-2mm, which were stored in size-sorted, labelled, 120ml-capacity wide-neck glass jars with Bakelite screw tops. A final, very coarse residue fraction comprised any residue remaining from rock processing once sample sizes were less than ~50g as well as any residue which simply could not be broken down, e.g. chert masses.

Residues from samples that were especially voluminous were elected for density separation. A portion of the residue was examined (as normal) in order to both maintain some inspection standard across all samples and investigate siliceous and other “light” fossils and features of interest. Remaining residues were immersed in a dilute acid solution (to remove any carbonate and liberate calcium) for no more than a few hours to prevent damage to phosphatic microfossils. Residues were than washed repeatedly with distilled water to flush out any calcium that would react with the heavy liquid – sodium polytungstate ($3Na_2WO_4.9WO_3.H_2O$). The exact methodology of density separation employed herein broadly follows that detailed by Savage (1988).

All fractions (except the fines) were examined and described using a ZEISS Stemi DV4 binocular microscope. The phosphatic microfossils recovered are described in detail in Chapter 4, whilst a brief description of other (mainly siliceous and pyritic) fossils and structures of note can be found in Appendix F.

S.	Fm.	Sample & Lithology	Original weight (g)	Final weight (g)	Method
Tievebaun	Dartry Limestone	**GLTV43 –** Cherty mudstone	2003	192	Formic acid, H_2O_2
		GLTV42 – Cherty mudstone	2002	260	Formic acid, H_2O_2
		GLTV41 – Cherty mudstone	2000	524	Formic acid, H_2O_2
	Glencar Limestone	**GLTV40 –** Wackestone	2000	350	Formic acid, H_2O_2
		GLTV39 – Mudstone/Wackestone	2000	82	Formic acid, H_2O_2
		GLTV18532.5NOD – Carbonate nodule	1855	87	Formic acid
		GLTV38 – Lensoidal mudstone	2000	56	Formic acid, H_2O_2
		GLTV37 – Crinoidal wackestone	2000	350	Formic acid, H_2O_2
		GLTV36 – Dolomitic mudstone	2000	50	Formic acid, H_2O_2
		GLTV35 – Mudstone	2000	50	Formic acid, H_2O_2
		GLTV34 – Wackestone	2000	40	Formic acid, H_2O_2
		GLTV33 – Calcilutite mudstone	2000	10	Formic acid, H_2O_2
		GLTV32 – Wackestone	2000	45	Formic acid, H_2O_2
		GLTV31 – Cherty mudstone	2000	241	Formic acid, H_2O_2
		GLTV30 – Argillaceous mudstone	2000	120	Formic acid, H_2O_2
		GLTV29 – Mudstone	2030	20	Formic acid, H_2O_2
		GLTV28 – Calcilutite mudstone	1000	10	Formic acid, desiccation
		GLTV27 – Calcilutite mudstone	2050	65	Formic acid, H_2O_2
		GLTV26 – Crinoidal wackestone	1000	90	Formic acid, desiccation
		GLTV25 – Wackestone/mudstone	1525	10	Formic acid, desiccation
		GLTV24 – Muddy wackestone	2000	10	Formic acid, desiccation
		GLTV23 – Wackestone	2020	10	Formic acid, desiccation
		GLTV22 – Mudstone	2000	10	Formic acid, desiccation
		GLTV21 – Wackestone	2020	61	Formic acid, H_2O_2
		GLTV20 – Mudstone/wackestone	2000	~80	Formic acid

S.	*Fm.*	*Sample & Lithology*	*Original weight (g)*	*Final weight (g)*	*Method*
Tievebaun	**Benbulben Shale**	**GLTV19 –** Mudstone/wackestone	1985	72	Formic acid, H_2O_2
		GLTV18 – Wackestone	2000	30	Formic acid
		GLTV17 – Crinoidal wackestone	2000	10	Formic acid, desiccation
		GLTV16 – Crinoidal wackestone	2000	40	Formic acid
		GLTV15 – Wackestone/packstone	1800	10	Formic acid
		GLTV1600NOD – Carbonate nodule	928	58	Formic acid
		GLTV14 – Wackestone	2000	50	Formic acid
		GLTV950NOD – Carbonate nodule	1218	33	Formic acid
		GLTV13 – Wackestone	1500	10	Formic acid, desiccation, H_2O_2
		GLTV12 – Wackestone	2000	90	Formic acid

S.	*Fm.*	*Sample & Lithology*	*Original weight (g)*	*Final weight (g)*	*Method*
Glenade	**Dartry Lmst.**	**DAGN1 –** Wackestone	2005	56	Formic acid
		DAGN2 – Crinoidal wackestone	2005	63	Formic acid

Glencar	**Dartry Limestone**	**DAGL15 –** Argillaceous mudstone	2002	331	Formic acid
		DAGL14 – Cherty mudstone	2001	431	Formic acid
		DAGL13 – Cherty mudstone	2003	347	Formic acid
		DAGL12 – Cherty wackestone	2003	1315	Formic acid, H_2O_2
		DAGL11 – Cherty wackestone	2003	290	Formic acid
		DAGL10 – Cherty mudstone	2005	1171	Formic acid, H_2O_2
		DAGL9 – Cherty wackestone	2002	280	Formic acid, acetic acid
		DAGL8 – Mudstone	2006	18	Formic acid, acetic acid
		DAGL7 – Mudstone	2001	53	Formic acid, acetic acid
		DAGL6 – Cherty wackestone	2003	643	Formic acid, H_2O_2
		DAGL5 – Cherty mud/wackestone	2006	1028	Formic acid, H_2O_2
	Glencar Limestone	**DAGL4 –** Calcisiltite wackestone	2004	420	Formic acid, acetic acid, H_2O_2
		DAGL3 – Wackestone	2002	830	Formic acid, H_2O_2
		DAGL2 – Argillaceous mudstone	2005	156	Formic acid, acetic acid, H_2O_2
		DAGL1 – Mudstone	2006	180	Formic acid, H_2O_2

S.	*Fm.*	*Sample & Lithology*	*Original weight (g)*	*Final weight (g)*	*Method*
Aghagrania	**C. S.**	**AGHA13 –** Lime-clast wackestone	2007	27	Formic acid
	Bellavally	**AGHA12 –** Argillaceous mudstone	2002	39	Formic acid
		AGHA11 – Calcareous mudstone	1730	~708	Formic acid, desiccation, H_2O_2, sodium polytungstate
		AGHA10 – Wackestone	4010	60	Formic acid
		AGHA9 – Wackestone	2002	63	Formic acid
		AGHA8 – Mudstone	2003	28	Formic acid
	Meenymore	**AGHA7 –** Calcisiltite mudstone	2002	45	Formic acid
		AGHA6 – Calcilutite mudstone	2008	33	Formic acid
		AGHA5 – Laminated mudstone	2003	22	Formic acid, H_2O_2
		AGHA4 – Argillaceous wackestone	2000	96	Formic acid, H_2O_2
		AGHA3.2 – Bioturbated? mudstone	3862	128	Formic acid
		AGHA3.1 – Bioturbated? mudstone	2869	139	Formic acid
		AGHA2 – Chert bound mudstone	2000	62	Formic acid
		AGHA1 – Wackestone	2000	45	Formic acid
		AGHA.A11 – Calcilutite mudstone	2000	60	Formic acid
	Dartry Lmst.	**AGHA.A2 –** Crinoidal wackestone/packstone	2002	33	Formic acid
		AGHA.CAV.1 – Cherty wackestone	2002	743	Formic acid

S.	Fm.	Sample & Lithology	Original weight (g)	Final weight (g)	Method
Carraun/Lugasnaghta	Dergvone Shale	**CNLG19 –** Wackestone bullion	3347	267	Formic acid
		CNLG18 – Mudstone bullion	2004	1974	Formic acid, desiccation, H_2O_2
		CNLG17 – Poorly cleaved shale	2005	1260	Formic acid, desiccation, H_2O_2
	Carraun Shale	**CNLG16 –** Large dolomite bullion	2002	32	Formic acid
		CNLG15 – Calcisiltite mudstone	4006	74	Formic acid
		CNLG14 – Mudstone bullion	2001	24	Formic acid
		CNLG13 – Calcisiltite mudstone	2005	31	Formic acid
		CNLG12 – Calcisiltite mudstone	2003	150	Formic acid
		CNLG11 – Shell layer in a laminite	2002	45	Formic acid
		CNLG10 – Calcisiltite mudstone	2000	57	Formic acid
		CNLG9 – Calcisiltite mudstone	2007	41	Formic acid
		CNLG8 – Calcilutite mudstone	2002	56	Formic acid
		D.K. CNLG ABV. DERREENS – Fossiliferous shale	2001	6	Formic acid, desiccation, H_2O_2, sodium polytungstate
		CNLG7 – Calcilutite mudstone	2594	81	Formic acid
		CNLG6 – Calcilutite wackestone	2000	37	Formic acid
	Bellavally	**CNLG5 –** Laminated mudstone	2005	109	Formic acid
		D.K. CNLG SHEENA – Fossiliferous shale	2013	15	Formic acid, desiccation, H_2O_2
		CNLG4 – Laminated mudstone	2000	22	Formic acid
		D.K. CNLG.A – Fossiliferous shale	2010	6	Formic acid, desiccation, H_2O_2, sodium polytungstate
		CNLG3 – Laminite and macrocell	2000	1091	Formic acid
		CNLG2 – Laminite and macrocell	2001	107	Formic acid
		CNLG1 – Argillaceous wackestone	3134	61	Formic acid

S.	*Fm.*	*Sample & Lithology*	*Original weight (g)*	*Final weight (g)*	*Method*
St. Brendan's Well	**Clare Shale**	**BW8 –** Carbonate bullion	6006	~117	Formic acid, H_2O_2
		BW9 – Carbonate bullion	2000	~80	Formic acid, desiccation
		BW7 – Carbonate bullion	2000	301	Formic acid, H_2O_2
		BW10 – Carbonate bullion	4009	~118	Formic acid
		BW6 – Shale	2163	10	Desiccation, H_2O_2, sodium polytungstate
		BW5B – Phosphatic lag	2000	1967	Formic acid
		BW5 – Phosphatic lag	2000	1898	Formic acid
	Magowna	**BW4 –** Phosphatised limestone	6027	60	Formic acid
		BW3 – Crinoidal wackestone	6435	~45	Formic acid
		BW2 – Argillaceous limestone	2309	10	Formic acid
	SLG	**BW1 –** Crinoidal wackestone	6283	49	Formic acid
Kilnamona	**Magowna**	**KMONA11B –** Calcareous mudstone	2009	~500	Formic acid, H_2O_2
		KMONA11A – Calcareous mudstone	2006	~1000	Formic acid, H_2O_2
		KMONA10 – Calcareous mudstone	2004	~600	Formic acid, H_2O_2
		KMONA9 – Wackestone	2004	~600	Formic acid, H_2O_2
		KMONA8 – Crinoidal wackestone	2009	~300	Formic acid, H_2O_2
	Slievenaglasha	**KMONA6 –** Crinoidal wackestone	2003	50	Formic acid
		KMONA5 – Crinoidal wackestone	2002	53	Formic acid
		KMONA4 – Crinoidal wackestone	2001	50	Formic acid
		KMONA3 – Crinoidal wackestone	2004	47	Formic acid
		KMONA2 – Wackestone nodules	1115	50	Formic acid
		KMONA1 – Crinoidal wackestone	2004	51	Formic acid

APPENDIX B –

Digital spectral analysis of the Tievebaun Section

The complete logged sequence of the Tievebaun Section was digitised and numerically coded as either 1 (limestone) or 2 (calcareous shale) at 5cm intervals, with the data being entered into an excel spreadsheet. Gaps in the sequence were coded with the dummy value of 999, resulting in a dataset of 4,322 values oscillating between two states for 216.1m of rock.

Since shale and limestone are differentially susceptible to the effects of compaction, attempts were made to decompact the sequence and return it to its original thickness. The depth of burial was estimated by compiling the conodont colour alteration index (C.A.I.) values from the section. Thirty-four determinations yielded a value of 3.5-4, which is in good agreement with those (Glencar Limestone Formation = 4, Dartry Limestone Formation = 3 and the Meenymore Formation = 4) determined by Browne (1981) for rocks in the Dartry Mountains as well as the regional maturation values given in Clayton et al. (1989).

A temperature of alteration was derived from this C.A.I. value using the Arrhenius plots in Harris (1981) and Rejebian et al. (1987) based on the work of Epstein et al. (1976). For this derivation the duration of sediment burial must be constrained. Given that the youngest sediment preserved in the basins is the E_{2b} Arnsbergian aged Bencroy Shale Formation (Brandon & Hodson, 1984), a minimum duration of burial, prior to unroofing, was in the order of ~12Ma. The C.A.I. values of 3.5-4 were approximated to have resulted from a burial temperature of ~185ºC. Assuming the palaeo-geothermal gradient of 34.7ºCkm^{-1} given (Corcoran & Clayton, 2001) for the nearby Slisgarrow borehole (Co. Fermanagh) is applicable to the Tievebaun Section, then an overburden of ~5km has been removed from the section. This values correspond with vitrinite reflectance studies that suggest 3-5km of Silesian (post Viséan) cover has been removed from the youngest rocks of the Lough Allen Basin (Philcox et al., 1992). Since the majority of compaction occurs at shallower depths, early in the rocks burial history (Baldwin & Butler, 1985), the difference

between an overburden of 3km and 5km is unlikely to significantly affect the results of any compaction determinations.

The degree of compaction of limestone was calculated from the compaction curve for limestone shown in Baldwin and Butler (1985). The solidity (inverse of porosity) of limestone buried to a depth of ~5km is expected to be ~94%. Thus it is probable that the limestones have been compacted by a value of 1.6 (i.e. shortened to 0.625 of their original thickness), given an original solidity value of 59% (Baldwin & Butler, 1985). The solidity (S) value for shale was calculated using the Baldwin-Butler power-law equation given in Baldwin and Butler (1985).

$$\text{Burial depth (in km)} = 6.02\ S^{6.35}$$

A value of ~97% solidity was obtained. Taking a value of 20% solidity at the time of deposition (Baldwin & Butler, 1985), the solidity values obtained result in a degree of compaction of ~4.85 for the shale units. The digitised sequence was decompacted using these values such that where a limestone unit was encountered its range was extended by a factor of 1.6 and the range of shale units were expanded by an average factor of 4.85. A dataset of 9,677 values representing 774.16m of de-compacted sediment was created.

In an attempt to test the results of spectral analyses performed on the data sets, a second decompaction model was created. The shale in the sequence was recorded as being slightly silty and since no compaction curve for siltstone was found, the compaction values for sandstone at the respective depths were calculated and an intermediate value (with an appropriate weighting) between that for sandstone and that of shale was derived, similar to the work of Weedon and Read (1995). A solidity values of ~87% was derived for sandstone, giving a compaction value of ~1.7 taking an original solidity value of 51% (Baldwin & Butler, 1985). A weighted compaction value of 4 was decided as probably most appropriate for the silty shale portions. Since the limestone was known to be argillaceous, a weighted compaction value of 2 was used in the second model. This resulted in a dataset of 7,001 values for 700.1m of decompacted sediment.

No attempt was made to account for rate of deposition variations between the limestone and shale in order to minimise the significant assumptions involved in this preliminary investigation.

Once the digitised sections were decompacted, values relating to gaps in exposure (999) were removed, resulting in an unevenly ascending series (height up the section in cm) of data points. The models (**A** – all the rock decompacted equally = Tievebaun_Original, **B** – shale units decompacted approximately three times more than the limestone = Tievebaun_Decompact_1, **C –** shale units decompacted approximately twice as much as the limestone = Tievebaun_Decompact_2) were exported as tab delineated text files with the data in two columns, column one containing the ascending height in the stratigraphy and column two the relevant lithological classification (1 or 2). Since the data sampling (due to gaps in exposure) was unevenly spaced, the spectral analysis program REDFIT, version 3.8 (Schulz & Mudelsee, 2002) was used to analyse the data for dominant cycle periodicities. The default settings of the REDFIT program were used unless stated. The Welch window-type identifier was used in order to reduce spectral leakage (Schulz & Mudelsee, 2002). An intermediate 1500 Monte-Carlo simulations were run on each analysis. Five Welch-Overlapped-Segment-Averaging (WOSA) segments were used to smooth the data by breaking the data series into five overlapping (50%) segments each approximately one million years in duration (minimum 577ka, maximum 1.47Ma). Peaks detected as being statistically significant in the spectra of the three models analysed (as well as variations of the number of WOSA segments in Tievebaun_Decompact_1) are documented in the tables below.

Frequency (cycles/cm)	Periodicity (m)	Min. periodicity (ka)	Max. periodicity (ka)	Probable periodicity (ka)
$6.94x10^{-4}$	14.4	115.4	293.4	200
$3.75x10^{-3}$	2.7	21.3	54.3	37
$4.30x10^{-3}$	2.3	18.6	47.4	32.3
$4.86x10^{-3}$	2.1	16.5	41.9	28.6
$7.36x10^{-3}$	1.4	10.9	27.7	18.9

Dominant spectra of the Tievebaun Section (Original).

Frequency (cycles/cm)	Periodicity (m)	Min. periodicity (ka)	Max. periodicity (ka)	Probable periodicity (ka)
$1.94x10^{-4}$	51.5	115.2	293	199.8
$1.32x10^{-3}$	7.6	16.9	43.1	29.4
$2.40x10^{-3}$	4.2	9.3	23.7	16.1
$2.60x10^{-3}$	3.8	8.6	21.9	14.9

Dominant spectra of the Tievebaun Section (Decompact_1).

Frequency (cycles/cm)	Periodicity (m)	Min. periodicity (ka)	Max. periodicity (ka)	Probable periodicity (ka)
$2.14x10^{-4}$	46.7	115.5	293.7	200.2
$1.54x10^{-3}$	6.5	16	40.8	27.8
$2.57x10^{-3}$	3.9	9.6	24.5	16.7

Dominant spectra of the Tievebaun Section (Decompact_2).

Frequency (cycles/cm)	Periodicity (m)	Min. periodicity (ka)	Max. periodicity (ka)	Probable periodicity (ka)
$1.29x10^{-4}$	77.5	173.2	440.6	300.4
$2.35x10^{-3}$	4.3	9.5	24.2	16.5
$2.60x10^{-3}$	3.8	8.6	21.9	14.9

Dominant spectra of the Decompact_1_WOSA1 model section.

Frequency (cycles/cm)	Periodicity (m)	Min. periodicity (ka)	Max. periodicity (ka)	Probable periodicity (ka)
$1.94x10^{-4}$	51.5	115.2	293	199.8
$9.69x10^{-4}$	10.3	23.1	58.7	40
$1.55x10^{-3}$	6.5	14.4	36.7	25
$2.52x10^{-3}$	4.0	8.9	22.6	15.4

Dominant spectra of the Decompact_1_WOSA29 model section.

Frequency (cycles/cm)	Periodicity (m)	Min. periodicity (ka)	Max. periodicity (ka)	Probable periodicity (ka)
$1.32x10^{-3}$	7.6	16.9	43.1	29.4
$2.64x10^{-3}$	3.8	8.5	21.5	14.7

Dominant spectra of the Decompact_1_WOSA50 model section.

Frequency (cycles/cm)	Periodicity (m)	Min. periodicity (ka)	Max. periodicity (ka)	Probable periodicity (ka)
$1.38x10^{-3}$	7.2	16.2	41.2	28.1
$2.30x10^{-3}$	4.3	9.7	24.7	16.8

Table 2.3.1.3g Dominant spectra of the Decompact_1_WOSA70 model section.

APPENDIX C –

Phosphate preparation procedure for stable isotope analysis

All phosphatic micro-remains and standards that were analysed during this study were investigated in the Stable Isotope Laboratory at the Institute of Geology and Mineralogy, University of Erlangen in Germany, under the supervision of Prof. Michael Joachimski, following standard analytical procedures (outlined below).

(1) Between 0.5 and 1.5mg (the exact weight was recorded on a five figure SARTORIUS MC5 balance, see Appendix G) of clean, well preserved, phosphatic microfossil material was picked into a small plastic vial.

(2) 33µl of 2M HNO_3 (9.11ml of 65% HNO_3 was made up to 50ml with distilled H_2O) was added to the phosphatic material and the vial left for at least eight hours, or preferably overnight, to dissolve. If the material was proving particularly resistant to dissolution the vial was placed into an ultrasonic bath to aid disaggregation and thus increase reactive surface area. This step results in a clear solution with a small amount of indigestible organic material resting in the bottom of the vial.

(3) 33µl of 2M KOH (5.6g dissolved in 50ml of distilled H_2O) was added to the vials to neutralize any remaining acid.

(4) 33µl of 4% HF (5ml of 40% HF solution made up to 50ml with distilled H_2O) was then added in order to react with the Ca^{2+} ions that were in solution. The Ca ions reacted with the HF to form a dense milky white precipitate.

(5) The vials were then placed into a HERAEUS MULTIFUGE and centrifuged for 15 minutes at 2500rpm or 12 minutes at 3000rpm.

(6) The clear liquid containing the dissolved phosphate was pipetted from the original vials into new, but similarly labelled, vials leaving behind the organics and Ca-precipitate. The old vials were flushed gently with a little distilled water and this too was pipetted into the new vials.

(7) At least 500ml of silver amine solution (0.34g $AgNO_3$, 0.28g NH_4NO_3, 1ml 25% NH_3 all made up to 30ml with distilled water) was added to the phosphate-in-solution-bearing vials. As the silver amine solution was added to the vials the liquid develops a yellow cloudiness. Sufficient silver amine solution must be added such that the liquid ultimately ends up being clear.

(8) The vials were placed into an oven set at 60ºC for at least eight hours, until all the ammonia had evaporated.

(9) Distilled water was added to the vials in order to take the remaining chemical residue into solution whilst leaving green–yellow-gold Ag_3PO_4 crystals behind.

(10) The liquid was carefully pipetted out of the vial, being mindful not to disturb the Ag_3PO_4 crystals.

(11) Steps 9 and 10 were repeated several times to ensure that only Ag_3PO_4 remained in the vial. The vials were placed into an ultrasonic bath between the steps a sufficient number of times to remove the Ag_3PO_4 crystals from the walls and redeposit them loosely at the base of the vial.

(12) The last washing of water was pipetted out of the vials and they were returned to the oven at 60ºC until dry.

(13) The Ag_3PO_4 crystals were carefully tapped out of their vials into a clean and dry micro-mortar. Any foreign materials such as hairs or remaining organics were picked out under a microscope using a clean pin.

(14) The Ag_3PO_4 crystals, once clean, were then ground and homogenised using a pestle.

(15) Steps 13 and 14 were repeated at least twice until satisfied that the material was pure and homogenous. The ground material was placed into a third and final clean, labelled vial.

(16) Between 0.18 and 0.35mg of the homogenised Ag_3PO_4 powder was weighed into a small silver cup which was then folded to expel all the air and seal in the analyte. At least three analyses were taken from each sample vial and each folded silver cup was placed into a plastic gridded container. The positions of the cups were recorded on a master sheet.

(17) The folded cups were then placed into the sample carousel of the mass spectrometer from which they dropped one at a time into a High Temperature Conversion Elemental Analyser and released the phosphate-bound oxygen as CO. The $\delta^{18}O$ value of the liberated CO was analysed in the connected ThermoFinnigan Delta-plus mass spectrometer and reported vs. V-SMOW. The accuracy and reproducibility of the results was monitored through several mechanisms:

(a) Monitoring the results of the standard gases that were pumped through the system during each analysis.

(b) Comparing the results of triplicate analyses from the same horizon.

(c) Running a number of international (NBS120c) and internal (Tübingen apatite and a synthesised Ag_3PO_4) standards at the beginning of each day as well as further NBS120c samples in the middle and end of a days analysis.

(d) Running a standard of either Tübingen apatite or NBS120c (prepared in the same batch as the samples being analysed) for every four samples run.

(18) Results were adjusted for variation attributable to machine "wander", and the analytical procedure followed, by monitoring the values of isotopic standards (corrected for NBS120c = 22.6‰, Vennemann, 2002).

APPENDIX D –

Microfossil sample location in NW Ireland sections.

Tievebaun Section

S.	*Fm.*	*Sample*	*Lithology*	*Stratigraphic height within the section*
Tievebaun	Dartry Limestone	**GLTV43**	Cherty mudstone	215.15-215.4m
		GLTV42	Cherty mudstone	210.125-210.3m
		GLTV41	Cherty mudstone	203.1-203.225m
	Glencar Limestone	**GLTV40**	Wackestone	Central 20cm of 195.675-197.05m
		GLTV39	Mudstone/Wackestone	Basal 40cm of 189.15-190.65m
		GLTV18532.5NOD	Carbonate nodule	185.325m
		GLTV38	Lensoidal mudstone	181.9-182m
		GLTV37	Crinoidal wackestone	175.05-175.125m
		GLTV36	Dolomitic mudstone	169.025-169.125m
		GLTV35	Mudstone	161.85-161.9m
		GLTV34	Laterally variable wackestone	153.9-154.05m
		GLTV33	Calcilutite mudstone	146.9-146.975m
		GLTV32	Wackestone	139.5-139.6m
		GLTV31	Cherty mudstone	133.1-133.35m
		GLTV30	Argillaceous mudstone	127.25-127.4m
		GLTV29	Laterally variable mudstone	119.4-119.575m
		GLTV28	Calcilutite mudstone	111.325-111.425m
		GLTV27	Calcilutite mudstone	Centre of 102.95-103.25m
		GLTV26	Crinoidal wackestone	98.125-98.2m
		GLTV25	Wackestone/mudstone	90.8-91m
		GLTV24	Argillaceous wackestone	84.25-84.45m
		GLTV23	Wackestone	77.4-77.45m
		GLTV22	Mudstone	70.25-70.35m
		GLTV21	Wackestone	Upper 10cm of 62.75-62.9m
		GLTV20	Mudstone/wackestone	55.2-55.5m

S.	*Fm.*	*Sample*	*Lithology*	*Stratigraphic height within the section*
Tievebaun	**Benbulben Shale**	**GLTV19**	Mudstone/wackestone	Upper 17.5cm of 48.3-48.7m
		GLTV18	Wackestone	40.6-40.7m
		GLTV17	Crinoidal wackestone	35.4-35.525m
		GLTV16	Crinoidal wackestone	28.85-29m
		GLTV15	Wackestone/packstone	18.95-19.05m
		GLTV1600NOD	Carbonate nodule	16m
		GLTV14	Wackestone	13.25-13.325m
		GLTV950NOD	Carbonate nodule	9.5m
		GLTV13	Wackestone	6.15-6.2m
		GLTV12	Wackestone	0-0.25m

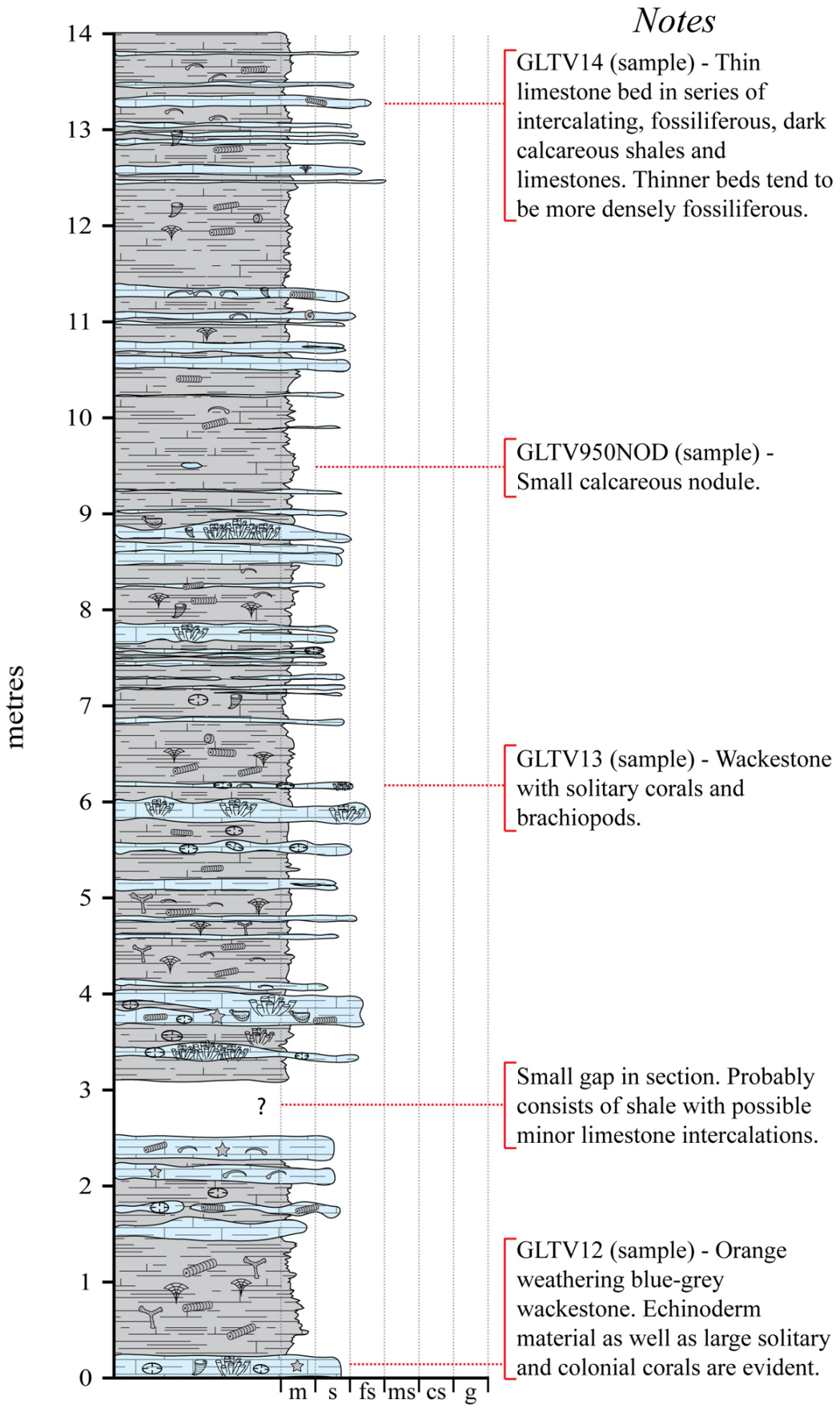
Notes
GLTV14 (sample) - Thin limestone bed in series of intercalating, fossiliferous, dark calcareous shales and limestones. Thinner beds tend to be more densely fossiliferous.
GLTV950NOD (sample) - Small calcareous nodule.
GLTV13 (sample) - Wackestone with solitary corals and brachiopods.
Small gap in section. Probably consists of shale with possible minor limestone intercalations.
GLTV12 (sample) - Orange weathering blue-grey wackestone. Echinoderm material as well as large solitary and colonial corals are evident.
metres
0
1
2
3
4
5
6
7
8
9
10
11
12
13
14
?
m
s
fs
ms
cs
g

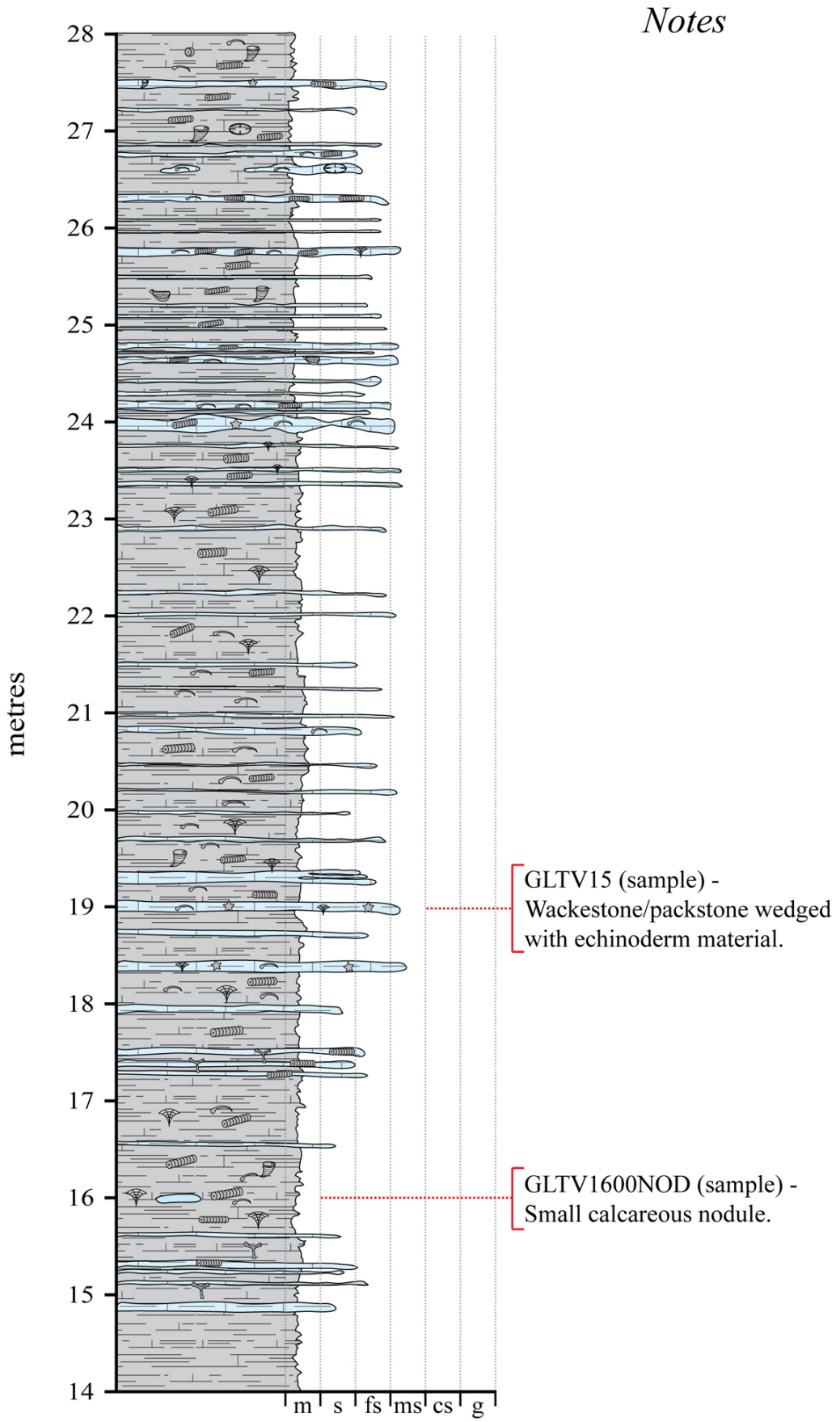
Notes
metres
28
27
26
25
24
23
22
21
20
19
18
17
16
15
14
m
s
fs
ms
cs
g
GLTV15 (sample) - Wackestone/packstone wedged with echinoderm material.
GLTV1600NOD (sample) - Small calcareous nodule.

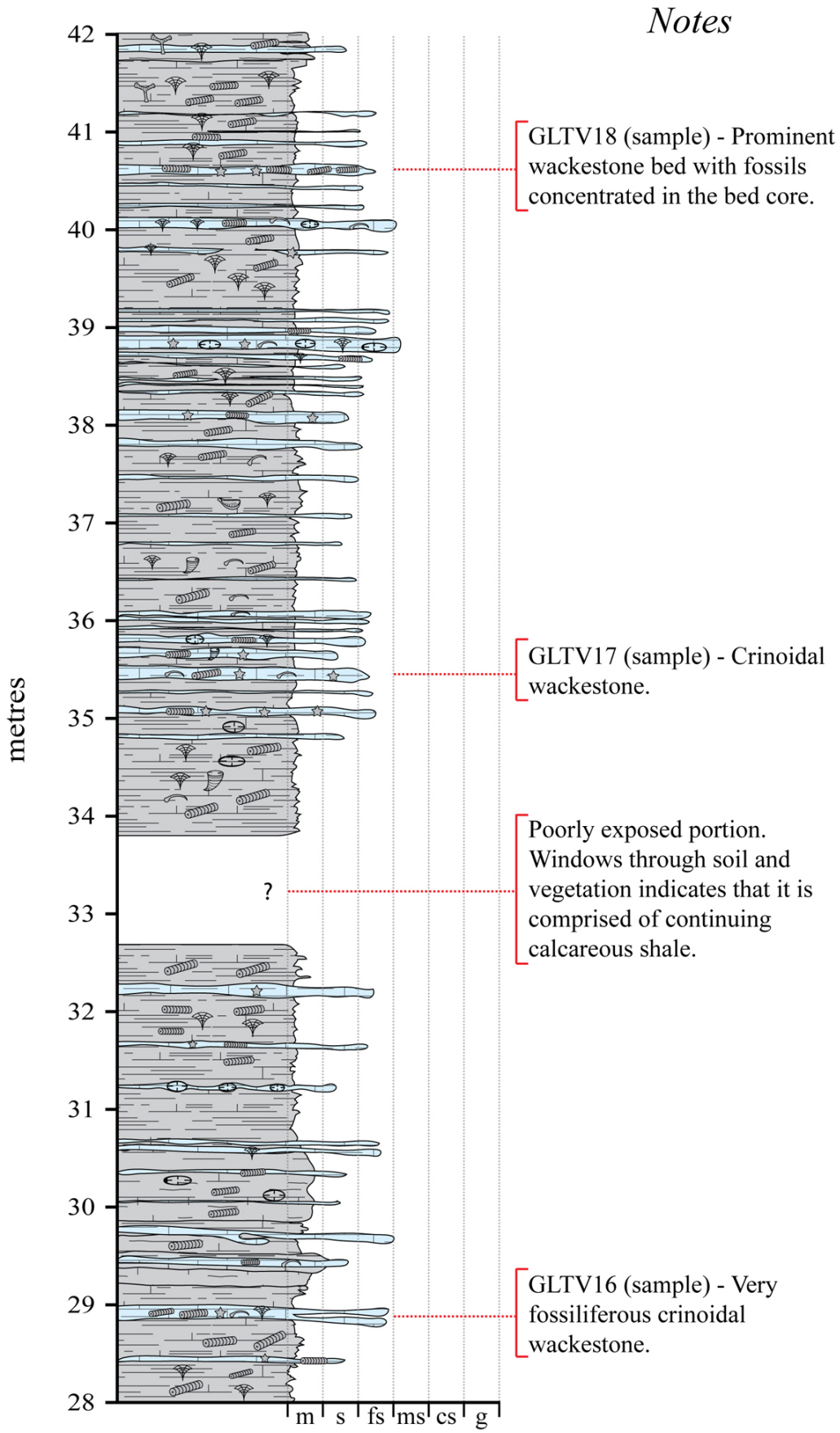
Notes
metres
42
41
40
39
38
37
36
35
34
33
32
31
30
29
28
?
m
s
fs
ms
cs
g
GLTV18 (sample) - Prominent wackestone bed with fossils concentrated in the bed core.
GLTV17 (sample) - Crinoidal wackestone.
Poorly exposed portion. Windows through soil and vegetation indicates that it is comprised of continuing calcareous shale.
GLTV16 (sample) - Very fossiliferous crinoidal wackestone.

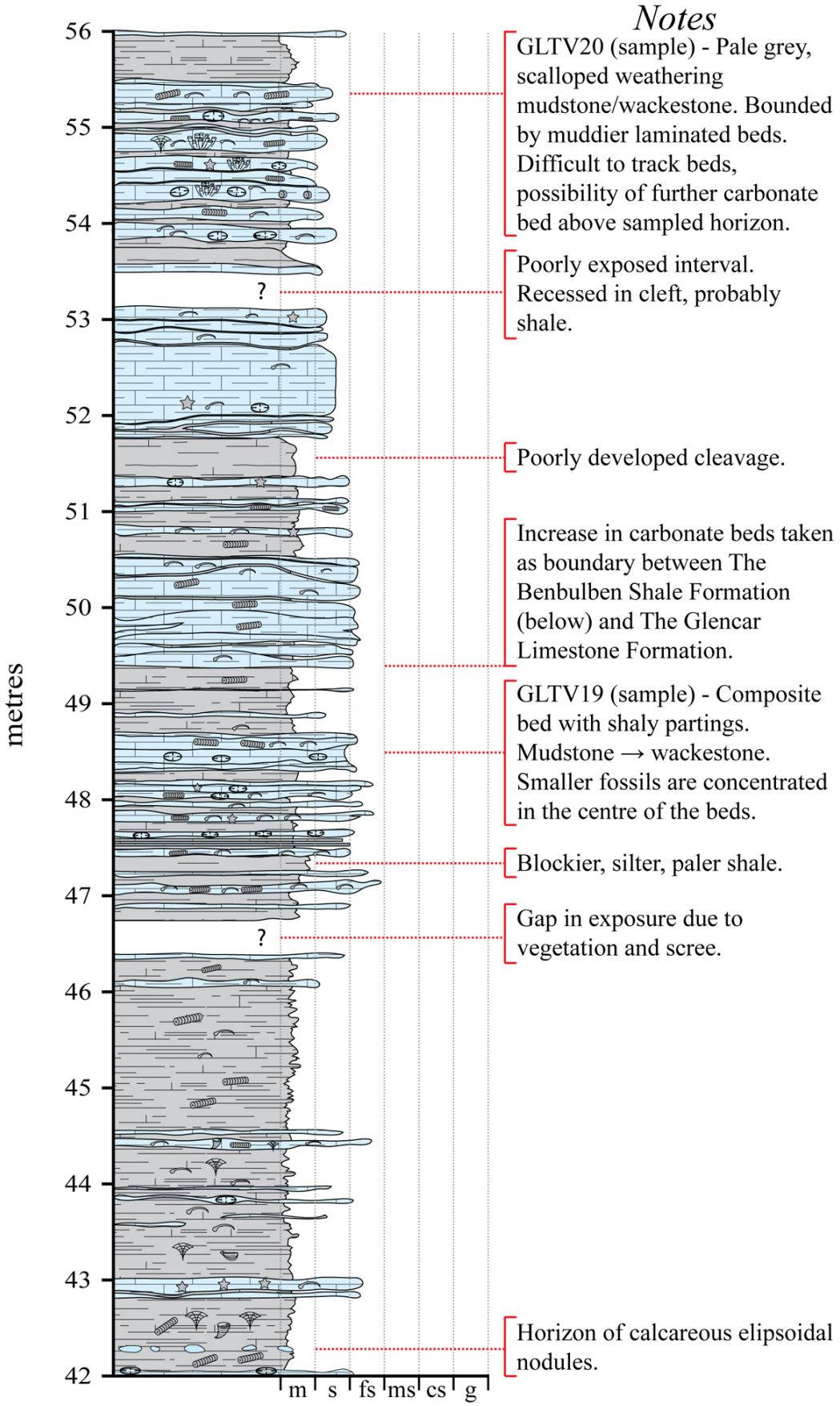
Notes
GLTV20 (sample) - Pale grey, scalloped weathering mudstone/wackestone. Bounded by muddier laminated beds. Difficult to track beds, possibility of further carbonate bed above sampled horizon.
Poorly exposed interval. Recessed in cleft, probably shale.
Poorly developed cleavage.
Increase in carbonate beds taken as boundary between The Benbulben Shale Formation (below) and The Glencar Limestone Formation.
GLTV19 (sample) - Composite bed with shaly partings. Mudstone → wackestone. Smaller fossils are concentrated in the centre of the beds.
Blockier, silter, paler shale.
Gap in exposure due to vegetation and scree.
Horizon of calcareous elipsoidal nodules.
metres
56
55
54
53
52
51
50
49
48
47
46
45
44
43
42
?
?
m
s
fs
ms
cs
g

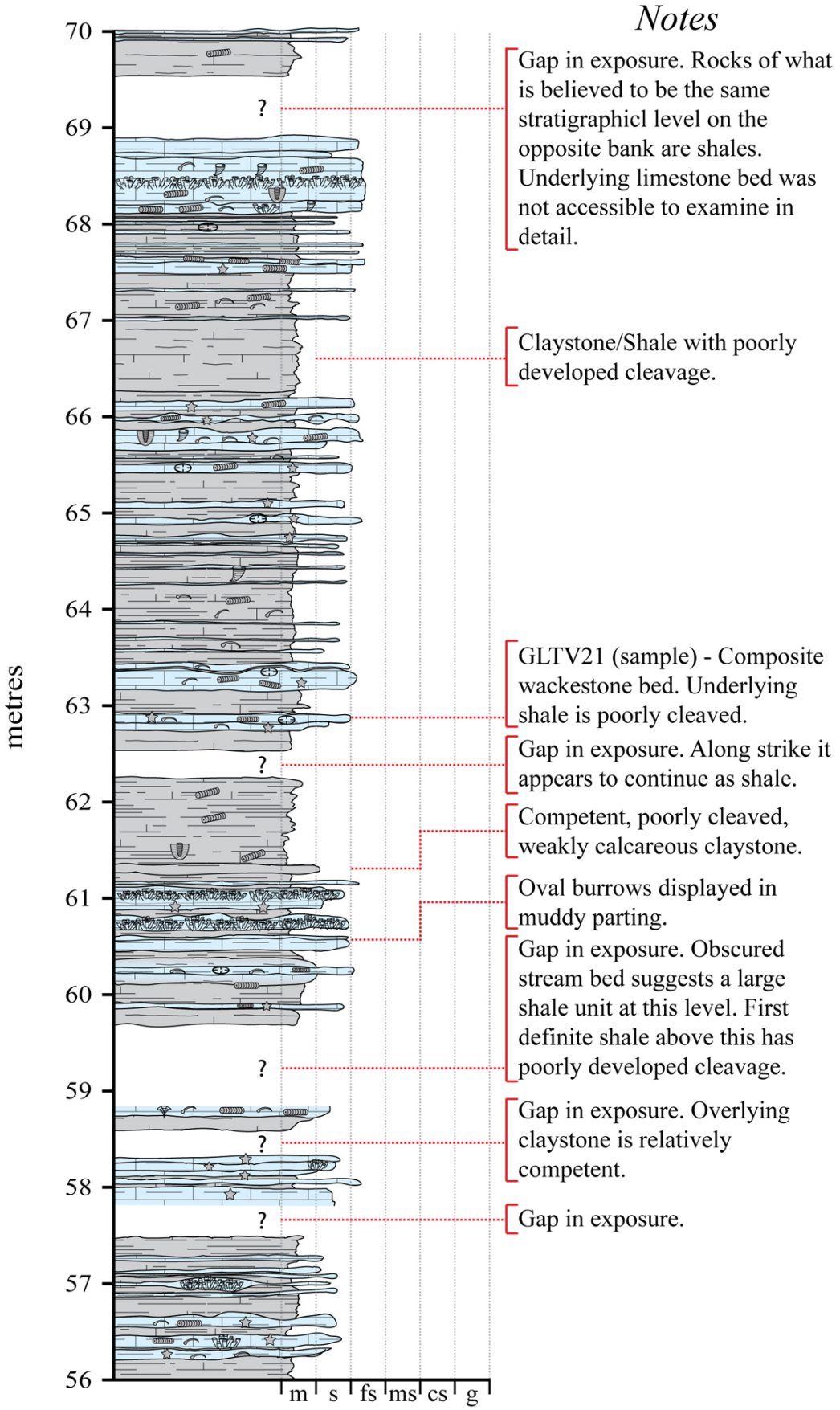
Notes
metres
70
69
68
67
66
65
64
63
62
61
60
59
58
57
56
m
s
fs
ms
cs
g
?
?
?
?
?
Gap in exposure. Rocks of what is believed to be the same stratigraphicl level on the opposite bank are shales. Underlying limestone bed was not accessible to examine in detail.
Claystone/Shale with poorly developed cleavage.
GLTV21 (sample) - Composite wackestone bed. Underlying shale is poorly cleaved.
Gap in exposure. Along strike it appears to continue as shale.
Competent, poorly cleaved, weakly calcareous claystone.
Oval burrows displayed in muddy parting.
Gap in exposure. Obscured stream bed suggests a large shale unit at this level. First definite shale above this has poorly developed cleavage.
Gap in exposure. Overlying claystone is relatively competent.
Gap in exposure.

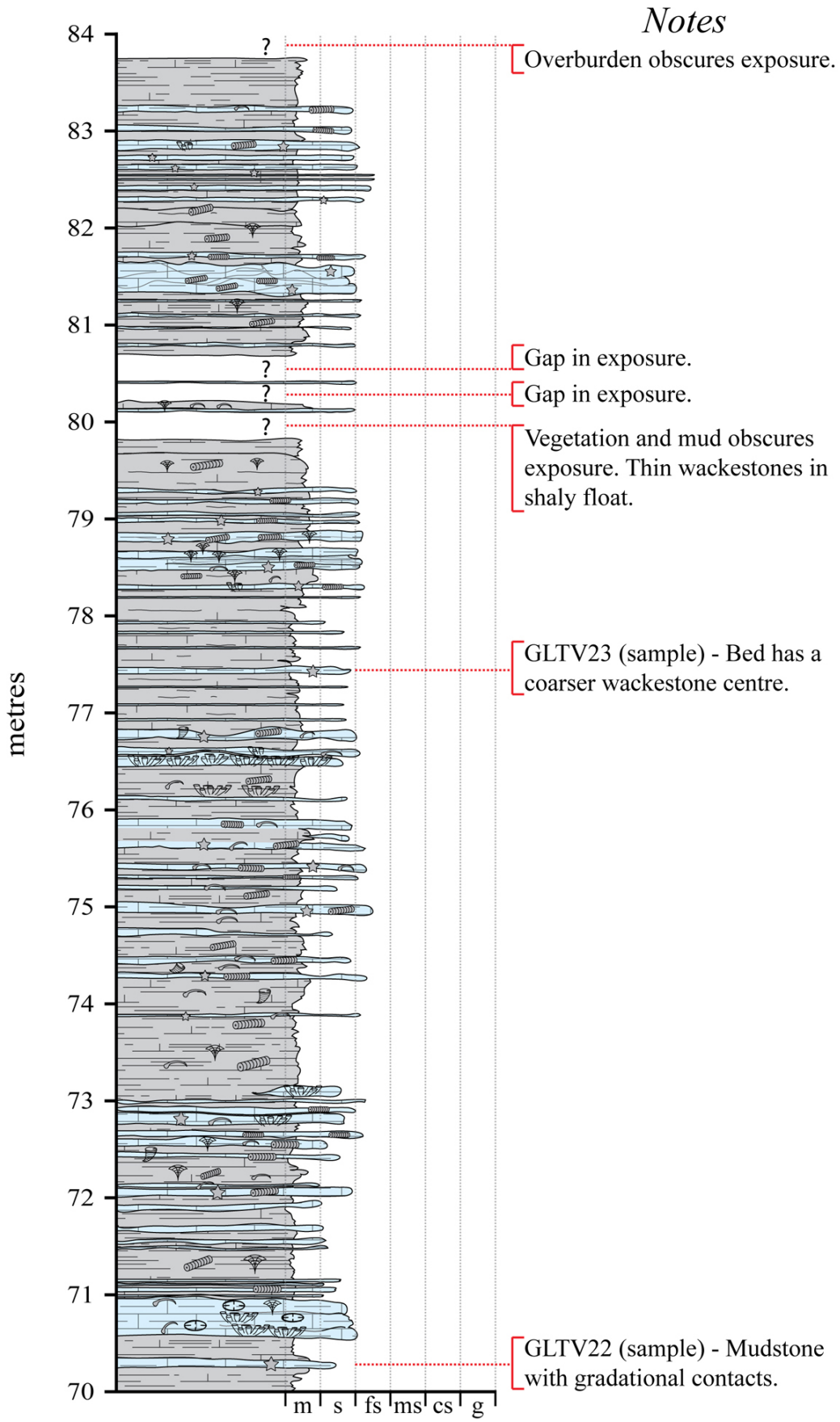
Notes
Overburden obscures exposure.
Gap in exposure.
Gap in exposure.
Vegetation and mud obscures exposure. Thin wackestones in shaly float.
GLTV23 (sample) - Bed has a coarser wackestone centre.
GLTV22 (sample) - Mudstone with gradational contacts.
metres
84
83
82
81
80
79
78
77
76
75
74
73
72
71
70
?
?
?
m
s
fs
ms
cs
g

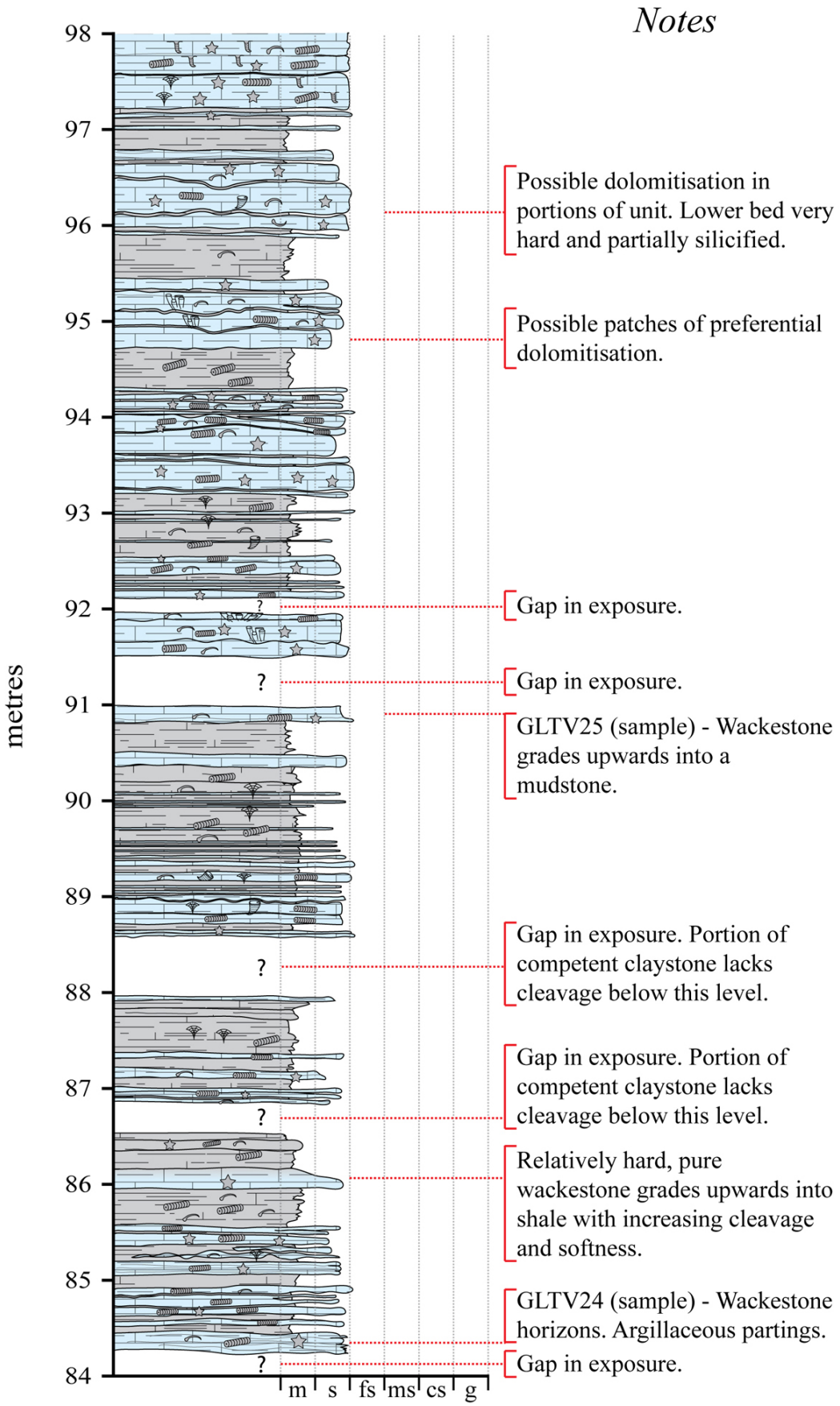
Notes
metres
98
97
96
95
94
93
92
91
90
89
88
87
86
85
84
m
s
fs
ms
cs
g
?
?
?
?
?
Possible dolomitisation in portions of unit. Lower bed very hard and partially silicified.
Possible patches of preferential dolomitisation.
Gap in exposure.
Gap in exposure.
GLTV25 (sample) - Wackestone grades upwards into a mudstone.
Gap in exposure. Portion of competent claystone lacks cleavage below this level.
Gap in exposure. Portion of competent claystone lacks cleavage below this level.
Relatively hard, pure wackestone grades upwards into shale with increasing cleavage and softness.
GLTV24 (sample) - Wackestone horizons. Argillaceous partings.
Gap in exposure.

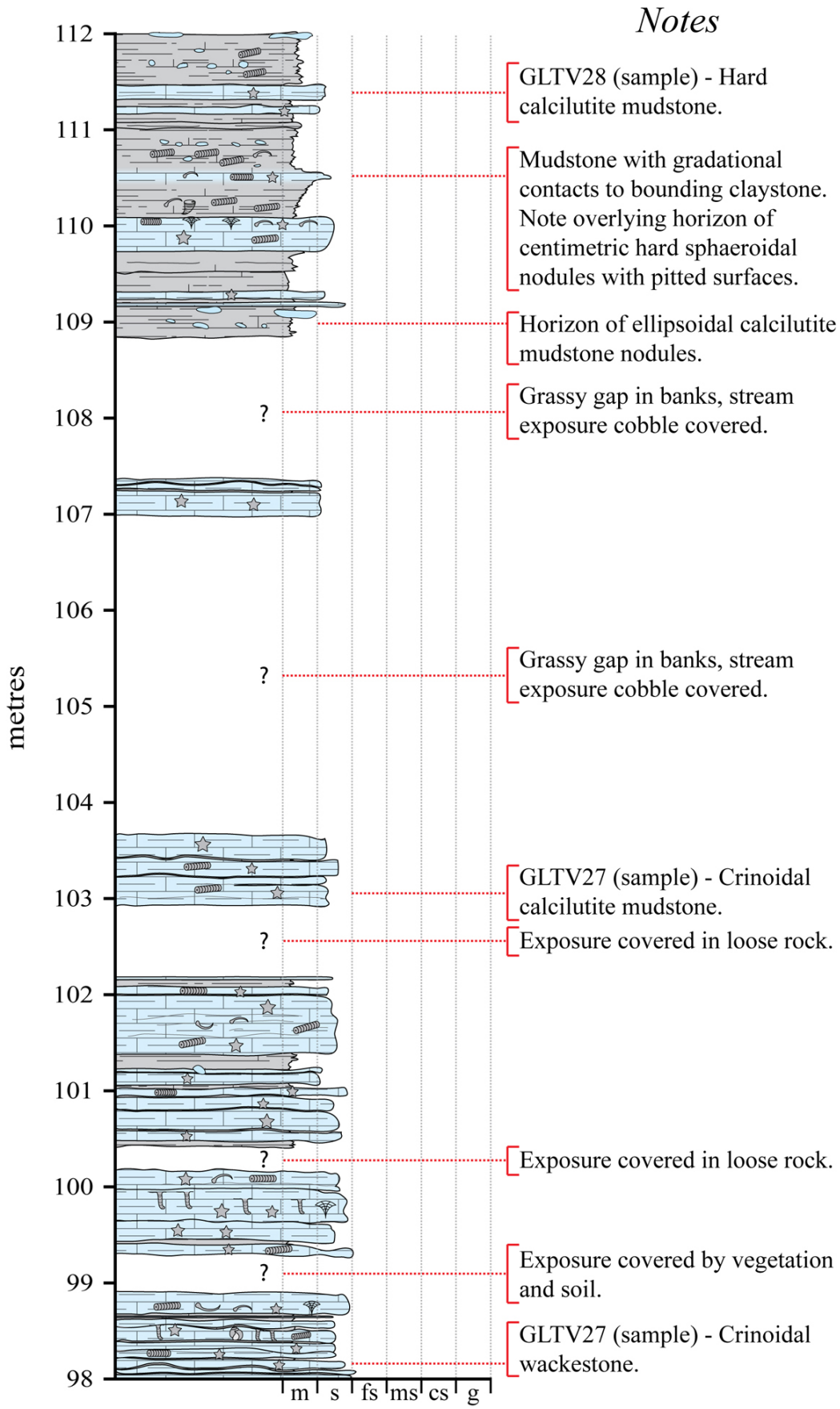
Notes
metres
112
111
110
109
108
107
106
105
104
103
102
101
100
99
98
?
?
?
?
?
m
s
fs
ms
cs
g
GLTV28 (sample) - Hard calcilutite mudstone.
Mudstone with gradational contacts to bounding claystone. Note overlying horizon of centimetric hard sphaeroidal nodules with pitted surfaces.
Horizon of ellipsoidal calcilutite mudstone nodules.
Grassy gap in banks, stream exposure cobble covered.
Grassy gap in banks, stream exposure cobble covered.
GLTV27 (sample) - Crinoidal calcilutite mudstone.
Exposure covered in loose rock.
Exposure covered in loose rock.
Exposure covered by vegetation and soil.
GLTV27 (sample) - Crinoidal wackestone.

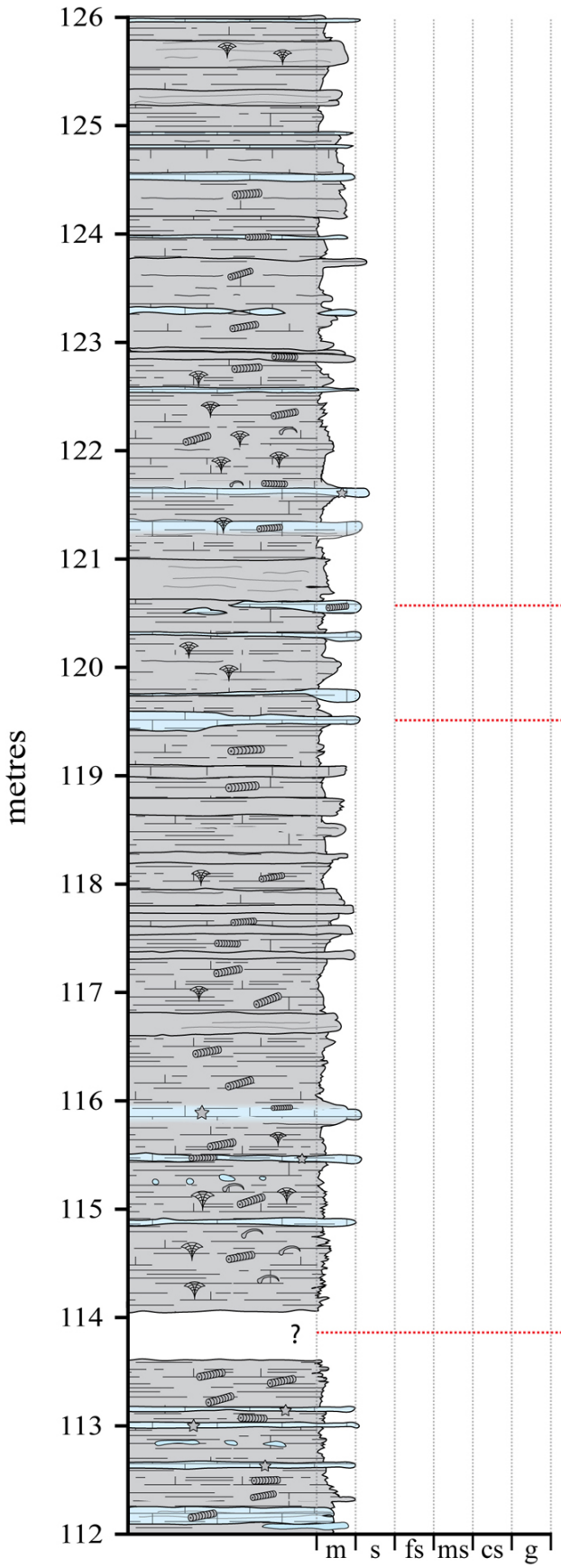

Notes

Note; large portions of this sequence of the section are comprised of poorly cleaved, more competent, calcareous, claystones and shale. Many have a coarser aspect than seen previously and are less fossiliferous. The few carbonate horizons encountered are muddier, weaker, finer and less fossiliferous than lower in the section, making it more difficult to distinguish lithologies.

Hard limestone lenses. Shale appears to run into them.

GLTV29 (sample) - Variably thick, hard mudstone with rusting dolomitised patches.

Vegetation and soil obscures exposure.

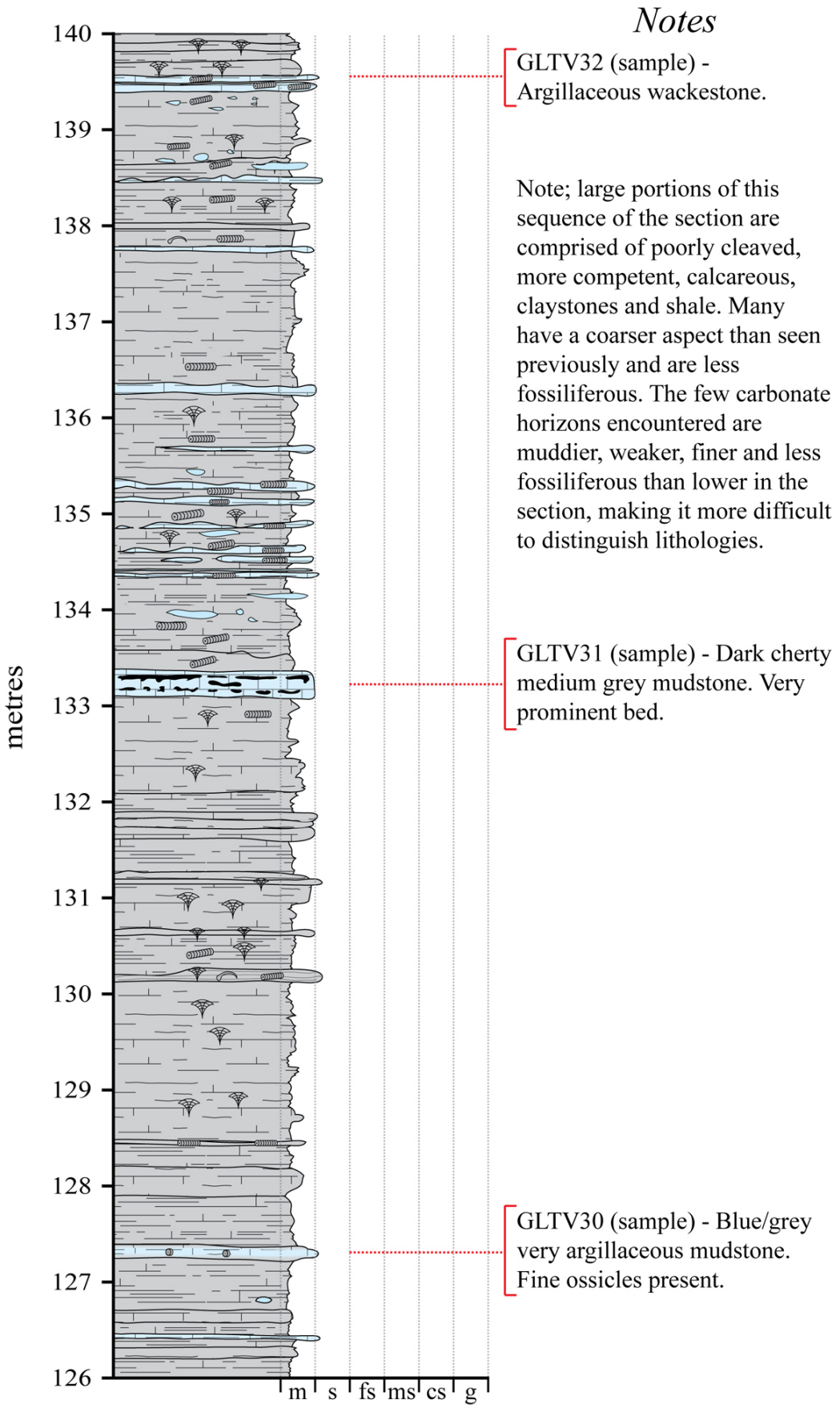
Notes
GLTV32 (sample) - Argillaceous wackestone.
Note; large portions of this sequence of the section are comprised of poorly cleaved, more competent, calcareous, claystones and shale. Many have a coarser aspect than seen previously and are less fossiliferous. The few carbonate horizons encountered are muddier, weaker, finer and less fossiliferous than lower in the section, making it more difficult to distinguish lithologies.
GLTV31 (sample) - Dark cherty medium grey mudstone. Very prominent bed.
GLTV30 (sample) - Blue/grey very argillaceous mudstone. Fine ossicles present.
metres
140
139
138
137
136
135
134
133
132
131
130
129
128
127
126
m
s
fs
ms
cs
g

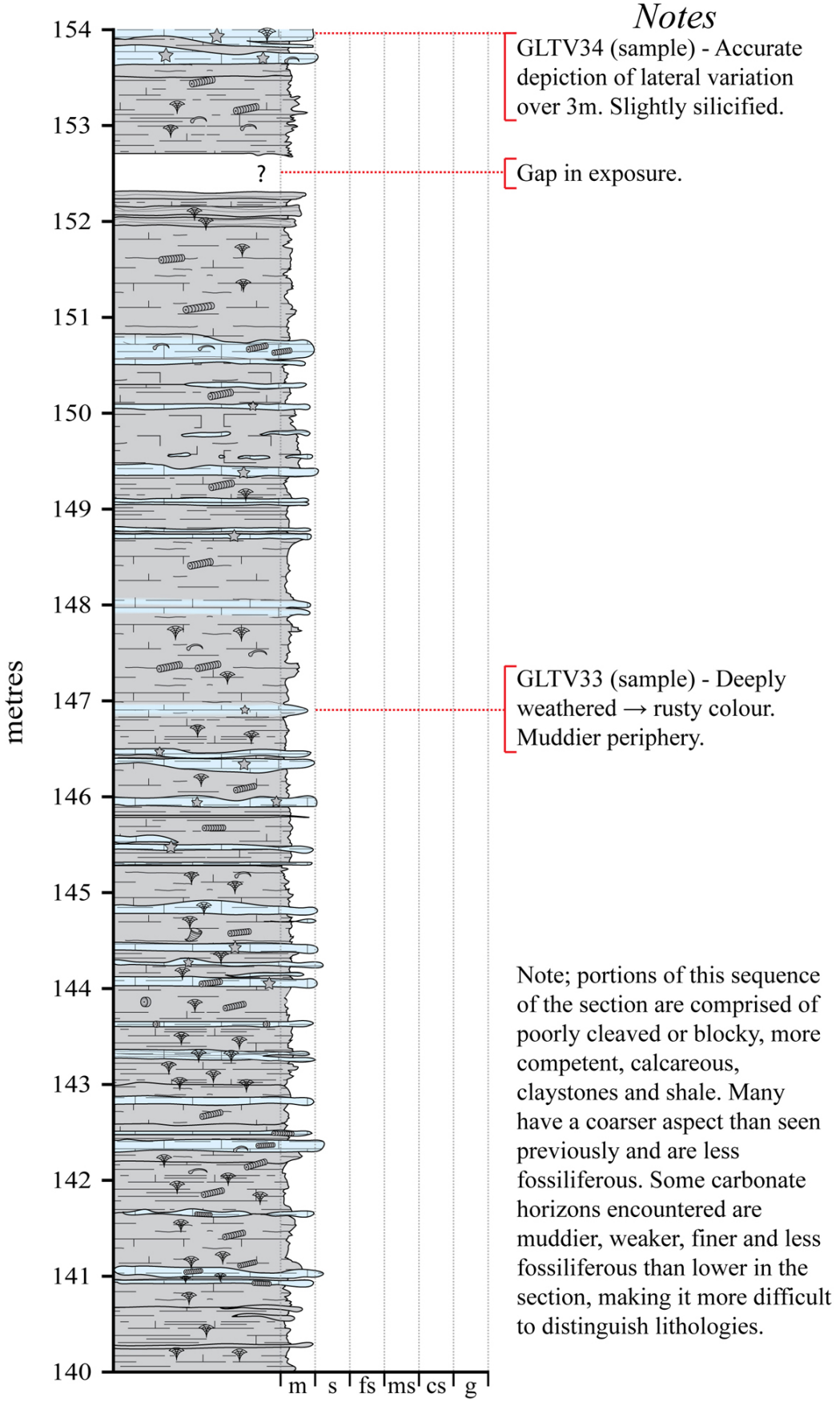

Note; portions of this sequence of the section are comprised of poorly cleaved or blocky, more competent, calcareous, claystones and shale. Many have a coarser aspect than seen previously and are less fossiliferous. Some carbonate horizons encountered are muddier, weaker, finer and less fossiliferous than lower in the section, making it more difficult to distinguish lithologies.

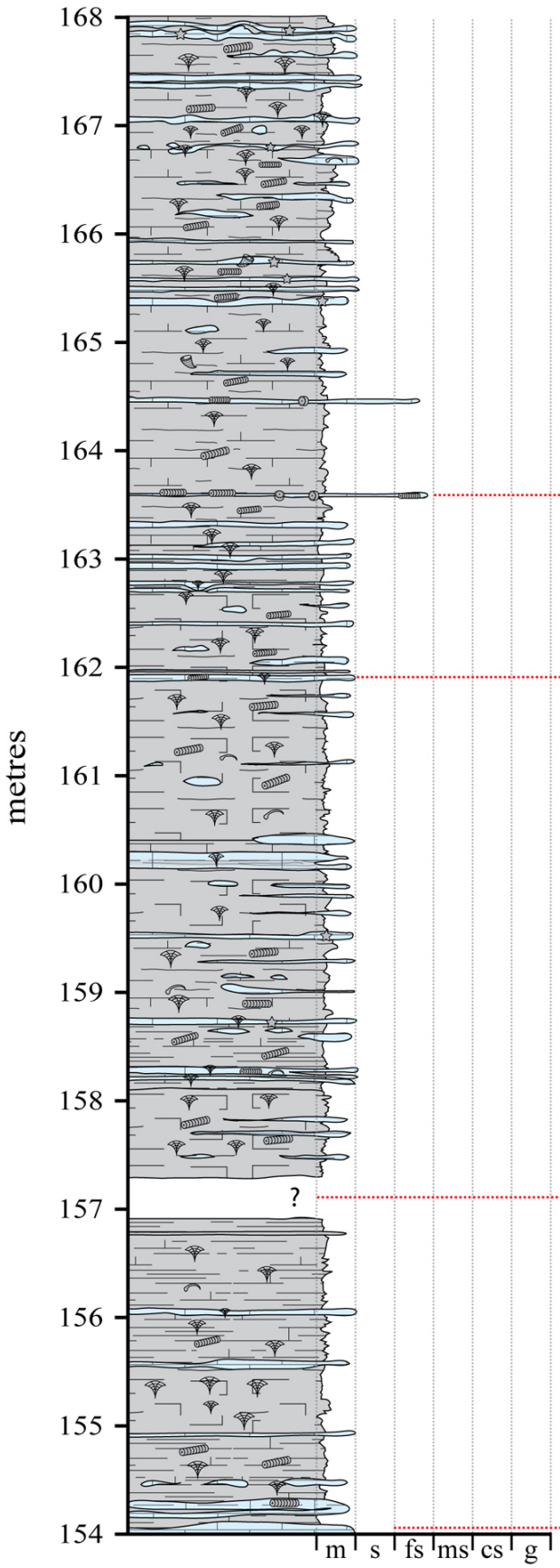

Notes

Note; limestone horizons within this portion are still very argillaceous but it does become easier to distinguish lithologies up through the sequence.

Thin densely crinoidal wackestone, relatively laterally persistent.

GLTV35 (sample) - Orange weathering mudstone. Fenestrate bryozoans common, particularly on upper surface.

Gap in exposure.

GLTV34 (sample) - Accurate depiction of lateral variation over 3m. Slightly silicified.

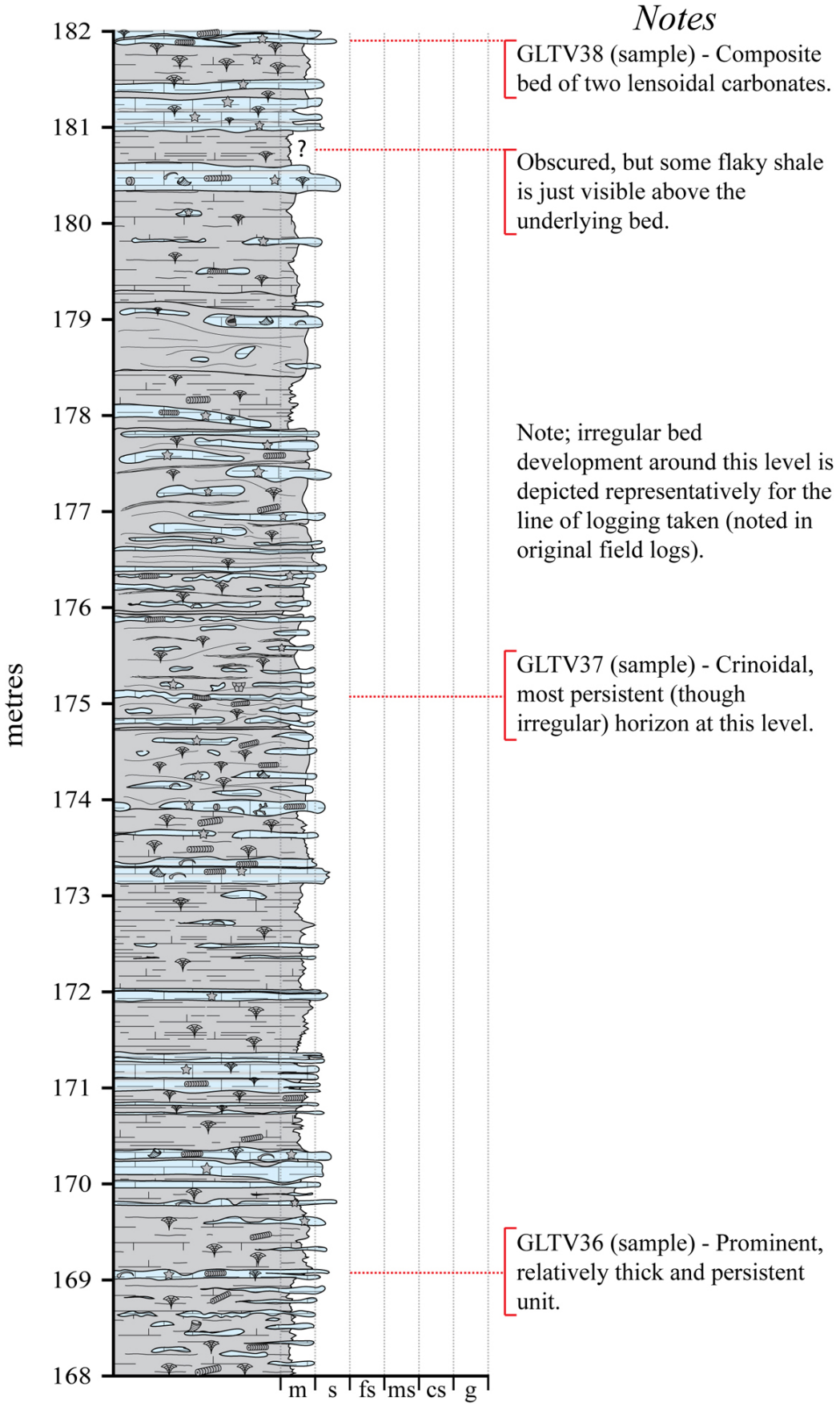
Notes
GLTV38 (sample) - Composite bed of two lensoidal carbonates.
Obscured, but some flaky shale is just visible above the underlying bed.
Note; irregular bed development around this level is depicted representatively for the line of logging taken (noted in original field logs).
GLTV37 (sample) - Crinoidal, most persistent (though irregular) horizon at this level.
GLTV36 (sample) - Prominent, relatively thick and persistent unit.
metres
182
181
180
179
178
177
176
175
174
173
172
171
170
169
168
?
m
s
fs
ms
cs
g

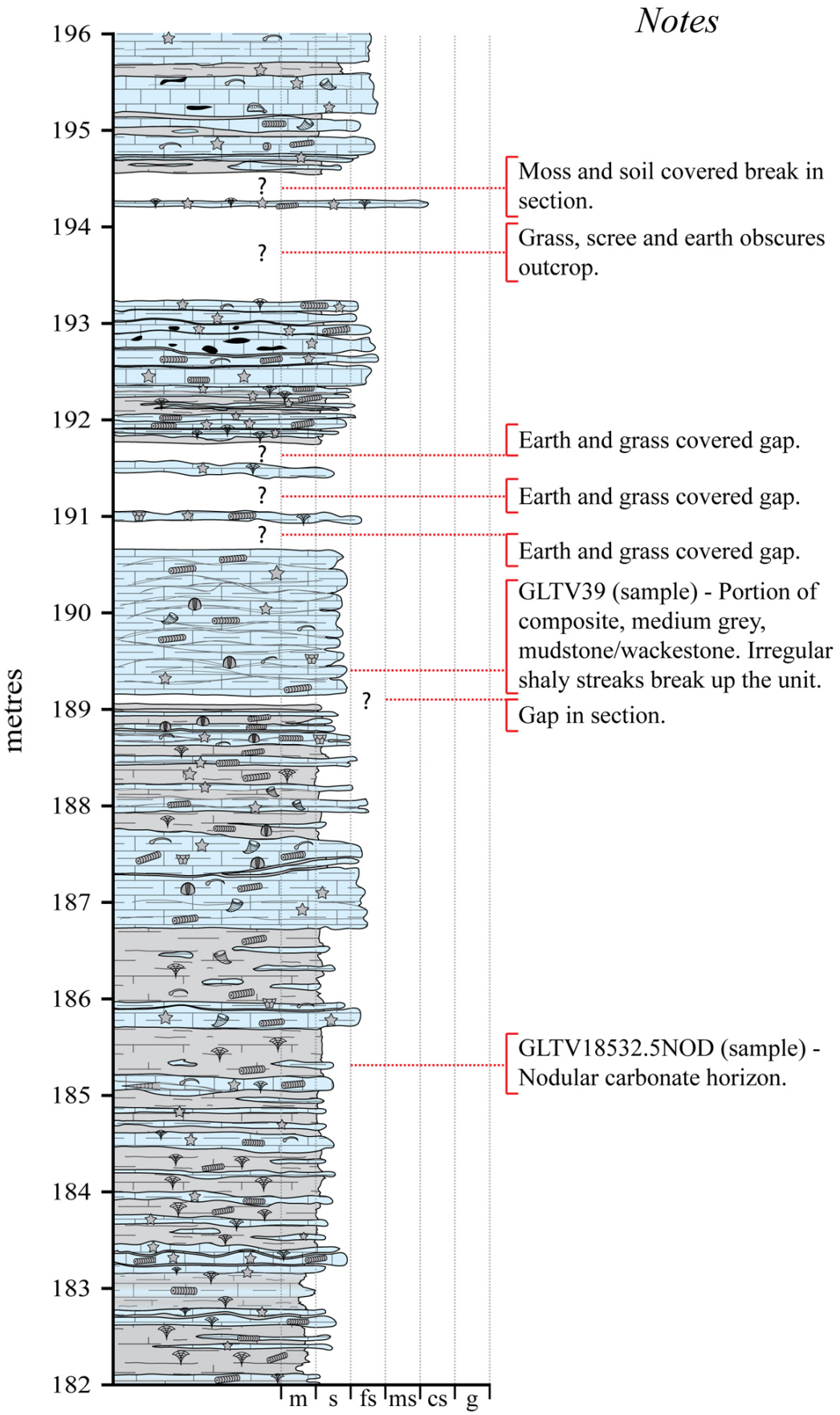
Notes
metres
196
195
194
193
192
191
190
189
188
187
186
185
184
183
182
m
s
fs
ms
cs
g
?
?
?
?
?
?
Moss and soil covered break in section.
Grass, scree and earth obscures outcrop.
Earth and grass covered gap.
Earth and grass covered gap.
Earth and grass covered gap.
GLTV39 (sample) - Portion of composite, medium grey, mudstone/wackestone. Irregular shaly streaks break up the unit.
Gap in section.
GLTV18532.5NOD (sample) - Nodular carbonate horizon.


Notes
metres
210
209
208
207
206
205
204
203
202
201
200
199
198
197
196
m
s
fs
ms
cs
g
Chert horizon is partially truncated at vertical quartz vein.
Centre of chert nodule has preferentially weathering purer carbonate.
GLTV41 (sample) - Bleached looking bed with very round purer chert nodules.
Stylolite horizon controls lower limit of chert development.
Taken as base of the Dartry Limestone Formation in this section. More pervasive silicification and reduction in fossil content. Some horizontal bioturbation evident on parting.
GLTV40 (sample) - Brachiopod rich wackestone and mudstone portions. Minor chert present.

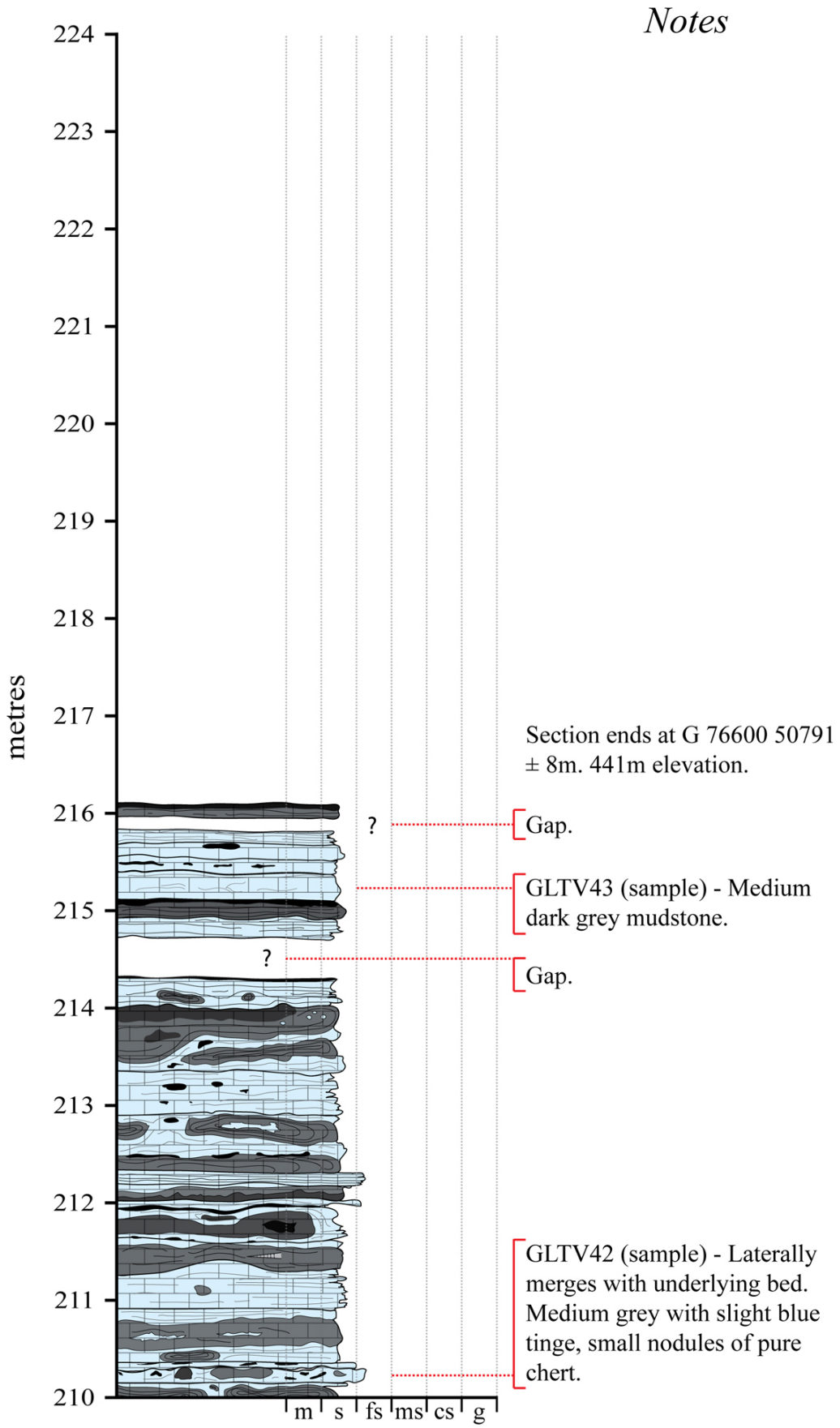
Notes
metres
224
223
222
221
220
219
218
217
216
215
214
213
212
211
210
m
s
fs
ms
cs
g
?
?
Section ends at G 76600 50791 ± 8m. 441m elevation.
Gap.
GLTV43 (sample) - Medium dark grey mudstone.
Gap.
GLTV42 (sample) - Laterally merges with underlying bed. Medium grey with slight blue tinge, small nodules of pure chert.

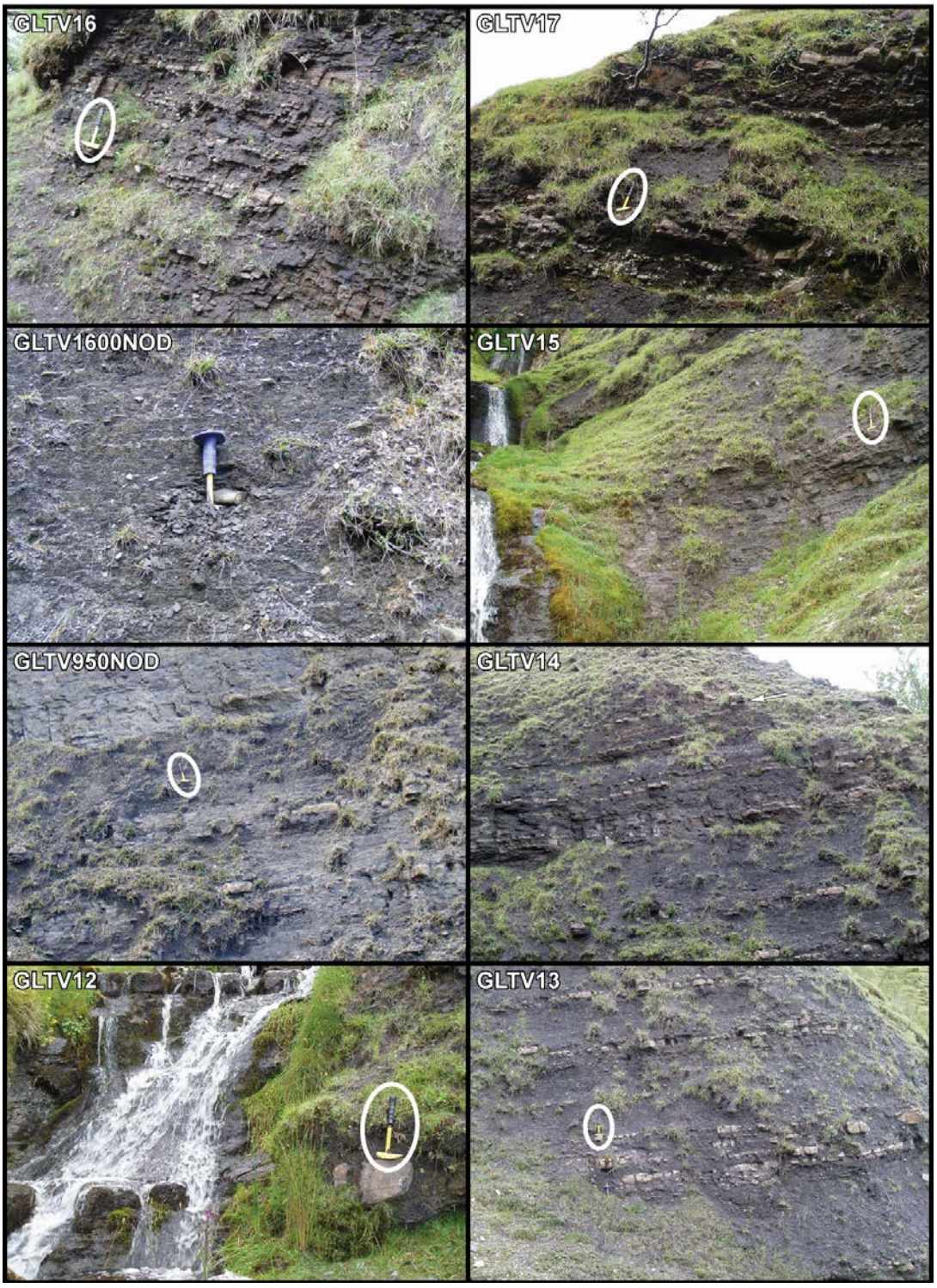

Unless stated, the hammer (circled in white) rests on top of the sampled bed. ***GLTV12*** *– West bank.* ***GLTV13*** *– West bank.* ***GLTV950NOD*** *– Hammer is slightly above and to the left of the sampled nodule horizon, west bank.* ***GLTV14*** *– Arrow indicates sampled horizon towards the top of the photograph, west bank.* ***GLTV1600NOD*** *– Chisel marks location of carbonate nodule, west bank.* ***GLTV15*** *– West bank.* ***GLTV16*** *– East bank.* ***GLTV17*** *– East bank.*

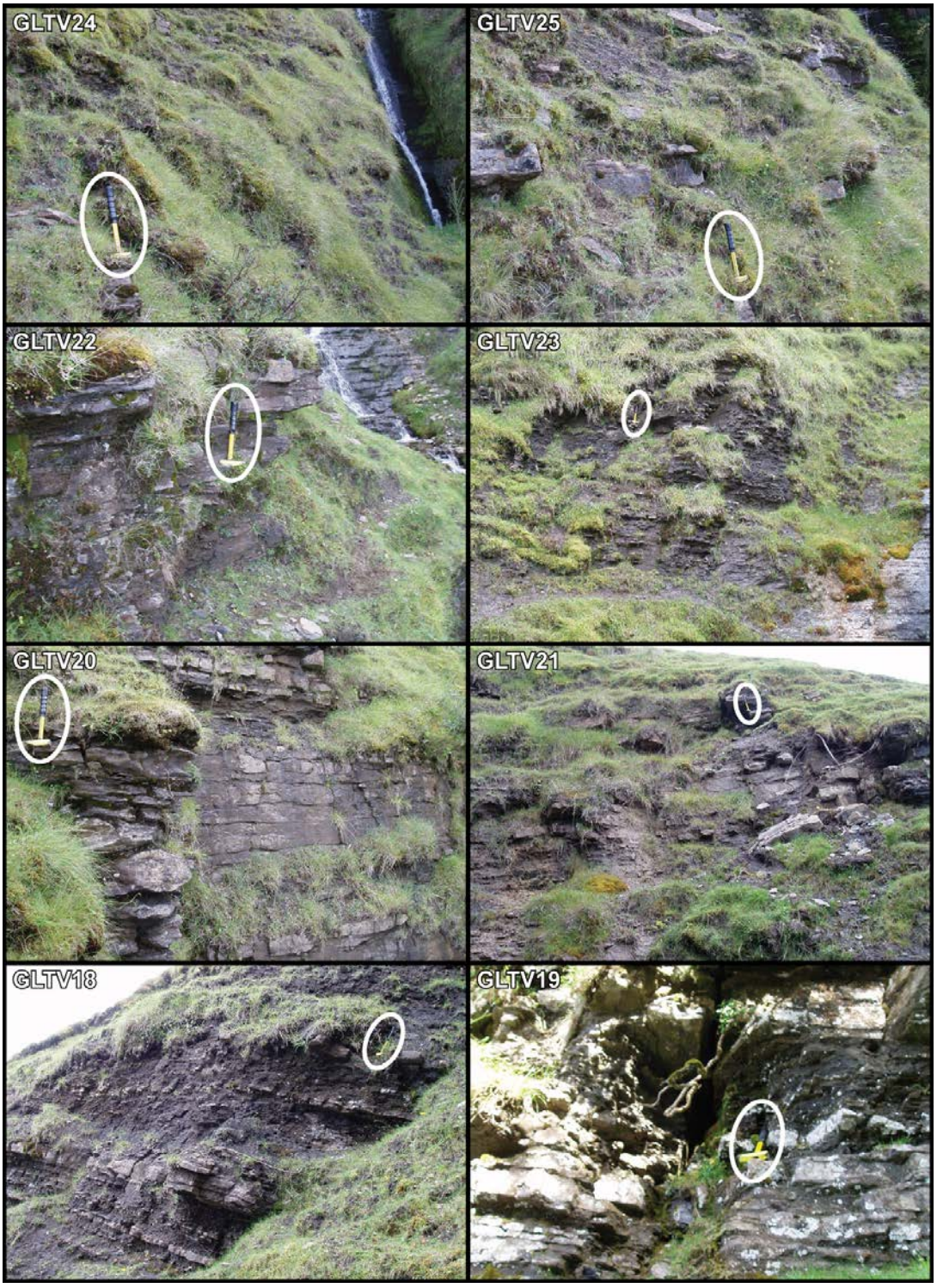

Unless stated, the hammer (circled in white) rests on top of the sampled bed. ***GLTV18*** *– East bank.* ***GLTV19*** *– East bank.* ***GLTV20*** *– East bank.* ***GLTV21*** *– West bank.* ***GLTV22*** *– Hammer head lies at the same stratigraphic height of the sampled bed, east bank.* ***GLTV23*** *– East bank.* ***GLTV24*** *– East bank.* ***GLTV25*** *– East bank.*

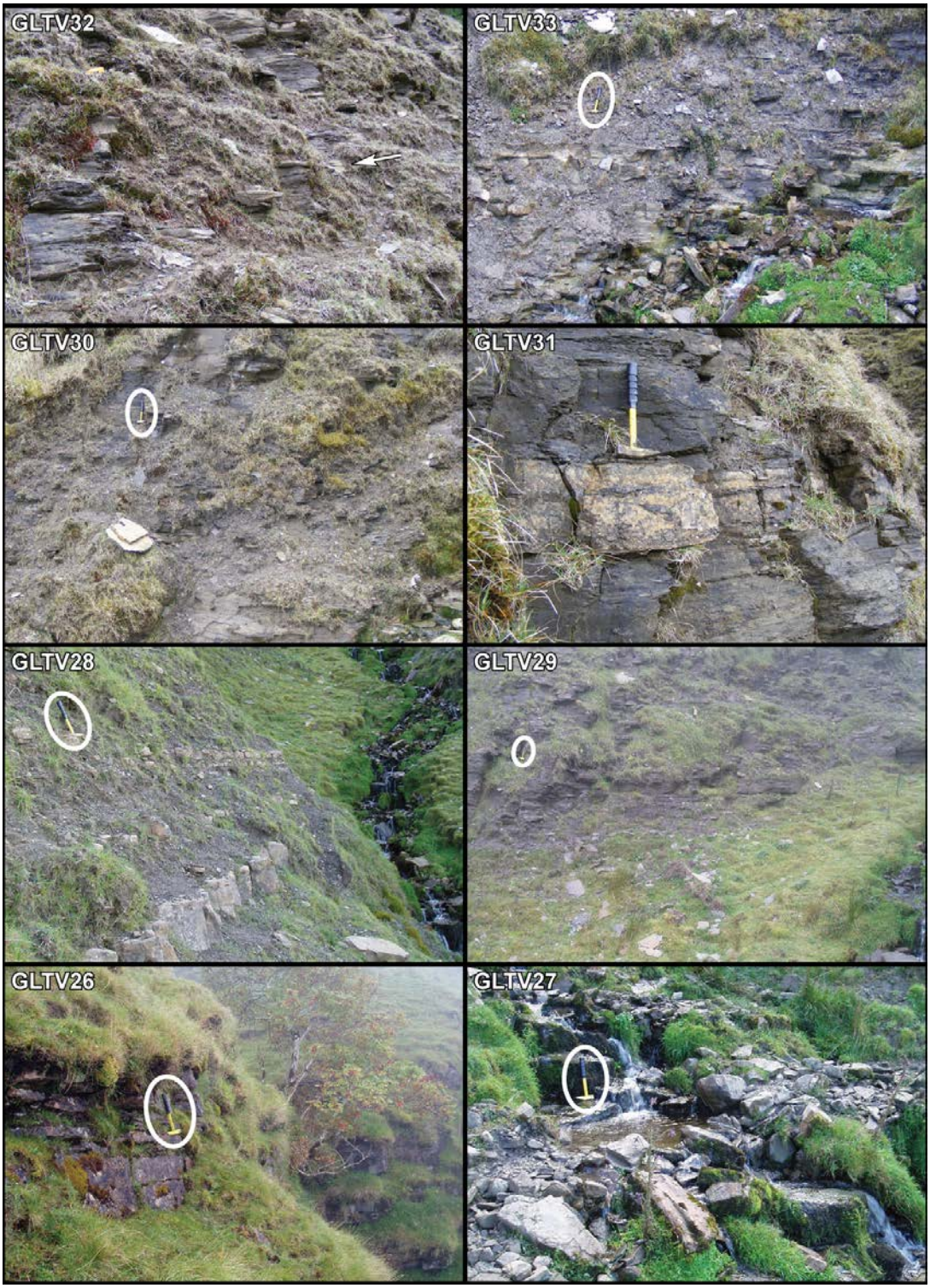

Unless stated, the hammer (typically circled in white) rests on top of the sampled bed. ***GLTV26*** *– East bank.* ***GLTV27*** *– Stream bed.* ***GLTV28*** *– East bank.* ***GLTV29*** *– East bank.* ***GLTV30*** *– East bank.* ***GLTV31*** *– East bank.* ***GLTV32*** *– The arrow (towards the right of the picture) indicates the sampled bed, east bank.* ***GLTV33*** *– East bank.*

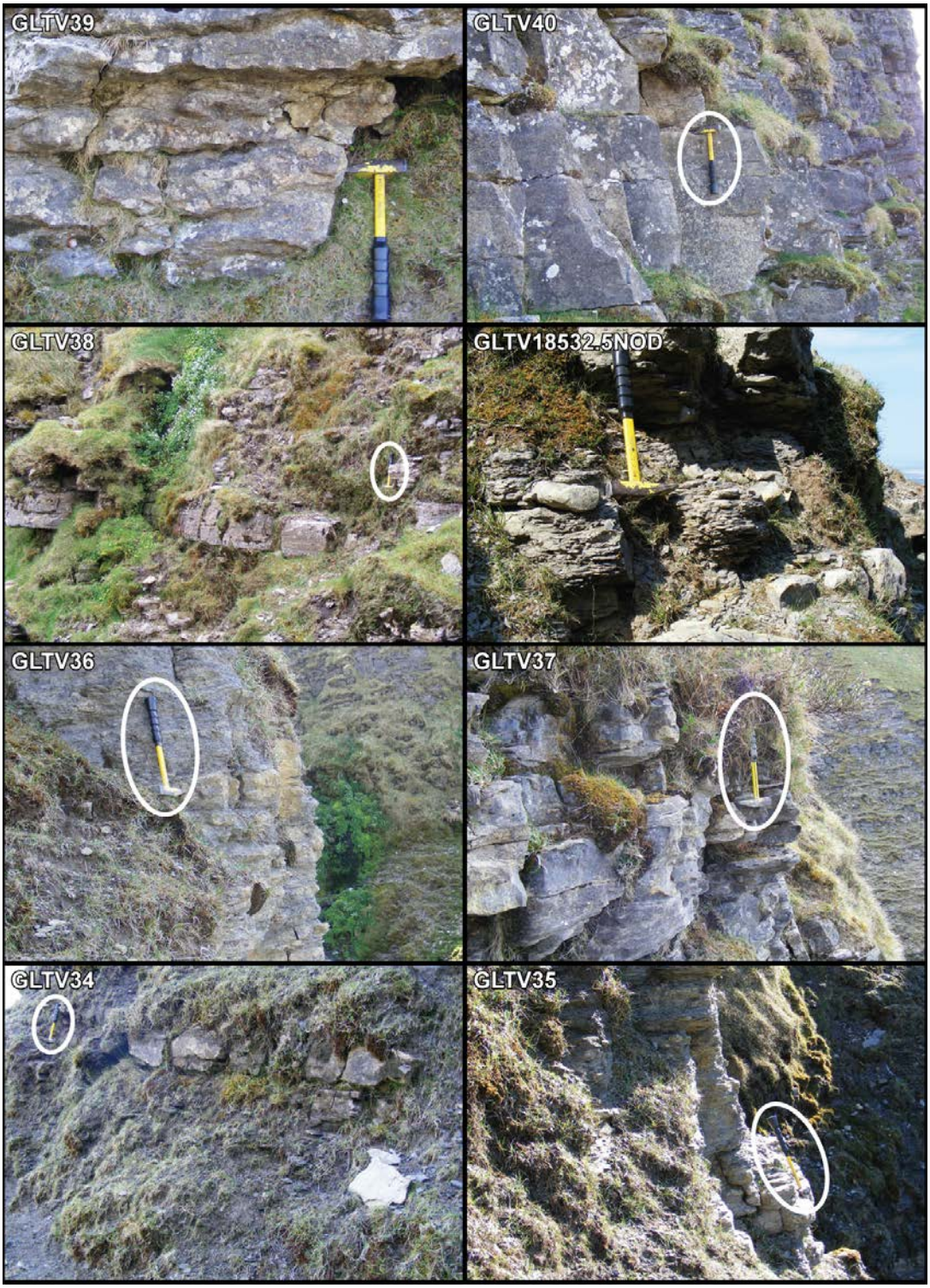

Unless stated, the hammer (typically circled in white) rests on top of the sampled bed. ***GLTV34*** *– The hammer head is positioned at the same stratigraphic height as the base of the sampled bed, east bank.* ***GLTV35*** *– East bank.* ***GLTV36*** *– The hammer head is at the same stratigraphic height as the sampled bed, east bank.* ***GLTV37*** *– East bank.* ***GLTV38*** *– The hammer head sits to the left of the sampled horizon, east bank.* ***GLTV18532.5NOD*** *– The hammer head is positioned to the right of the sampled nodule, west bank.* ***GLTV39*** *– The hammer head rests to the right of the sampled horizon, west bank.* ***GLTV40*** *– The hammer head hangs on the top of the sampled bed, west bank.*

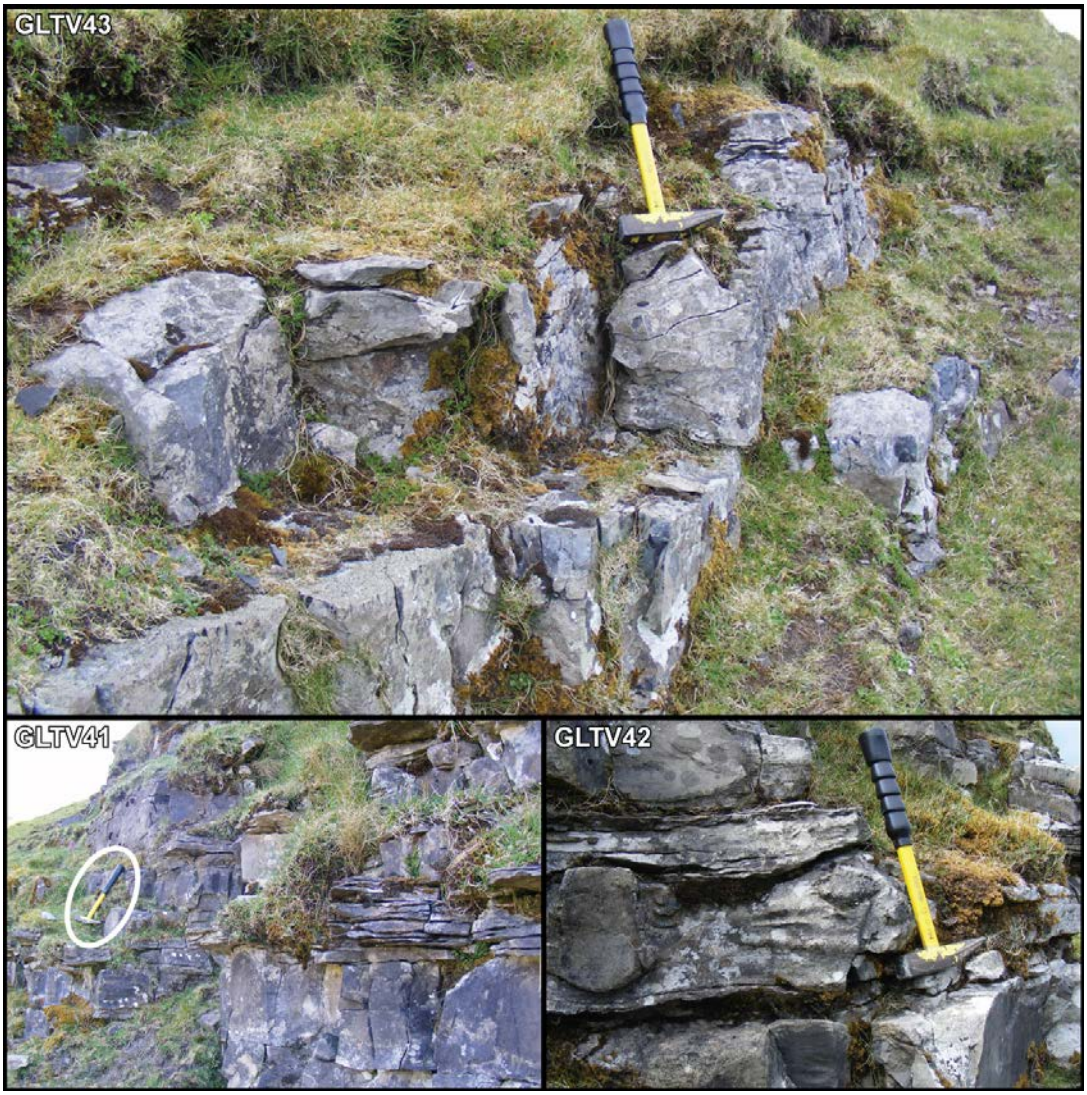

Unless stated, the hammer (typically circled in white) rests on top of the sampled bed. ***GLTV41*** *– The hammer head is positioned at the same stratigraphic height (to the left) of the sampled bed, west bank.* ***GLTV42*** *– The hammer head is located to the right of the sampled unit, west bank.* ***GLTV43*** *– West bank.*

Glencar and Glenade Sections

S.	*Fm.*	*Sample*	*Lithology*	*Stratigraphic height within the section*
Glenade	**Dartry Lmst.**	**DAGN1**	Wackestone	~10m
		DAGN2	Crinoidal wackestone	0-0.20m
Glencar	**Dartry Limestone**	**DAGL15**	Argillaceous mudstone	~113m
		DAGL14	Cherty mudstone	90.3-90.5m
		DAGL13	Cherty mudstone	83.7-83.9m
		DAGL12	Cherty wackestone	76.85-77m
		DAGL11	Cherty wackestone	70.1-70.4m
		DAGL10	Cherty mudstone	63-63.125m
		DAGL9	Cherty wackestone	56.35-56.5m
		DAGL8	Mudstone	50.25-50.4m
		DAGL7	Mudstone	42.4-42.75m
		DAGL6	Cherty wackestone	35.4-35.5m
		DAGL5	Cherty mud/wackestone	27.55-27.7m
	Glencar Limestone	**DAGL4**	Calcisiltite wackestone	21.15-21.35m
		DAGL3	Wackestone	13.975-14.25m
		DAGL2	Argillaceous mudstone	7.025-7.1m
		DAGL1	Mudstone	0-0.3m

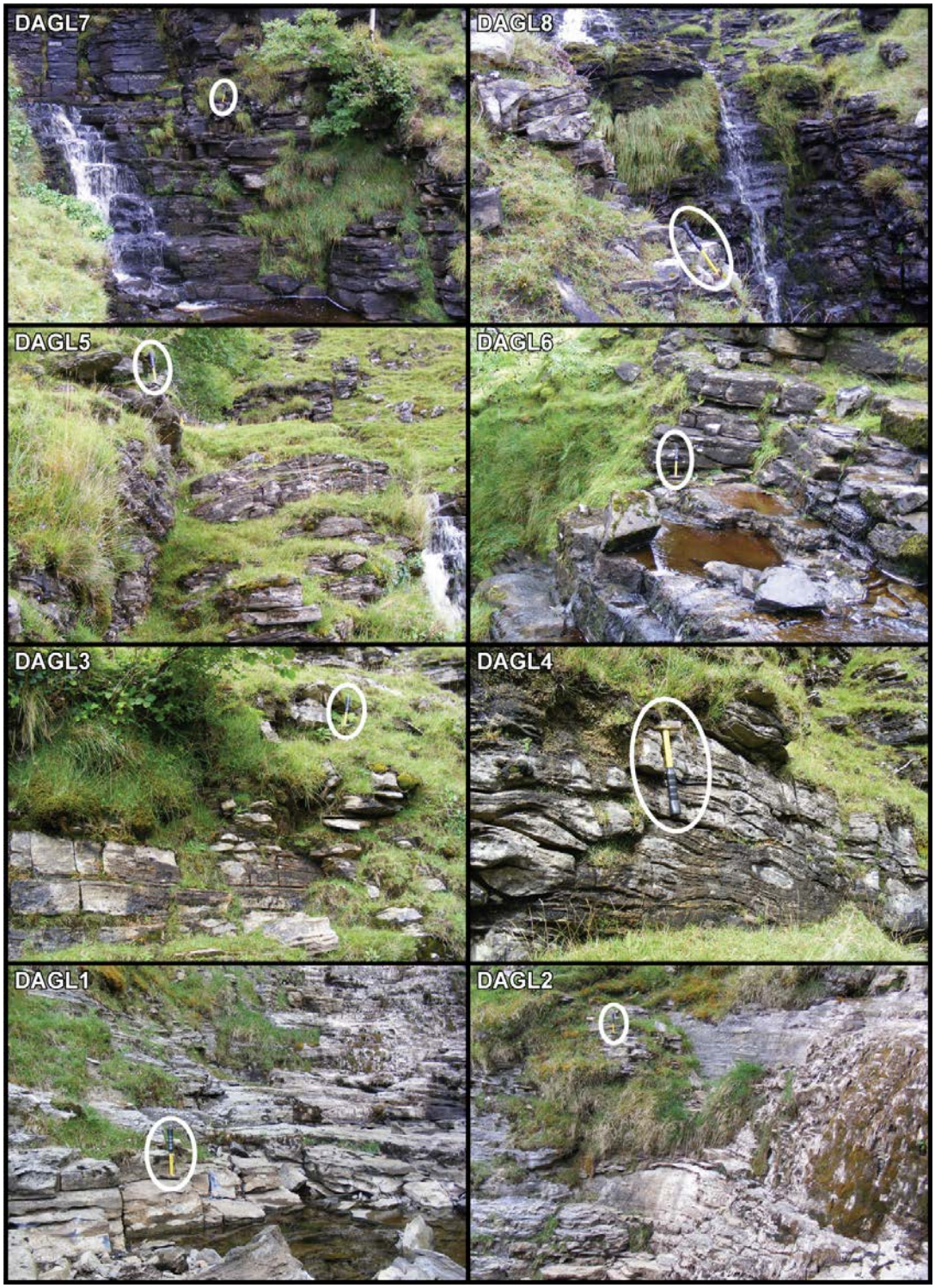

Unless stated, the hammer (typically circled in white) rests on top of the sampled bed. ***DAGL1*** *– Stream bed.* ***DAGL2*** *– West bank.* ***DAGL3*** *– The hammer head lies to the right of the sampled horizon, west bank.* ***DAGL4*** *– The hammer head hangs from the top of the sampled horizon, west bank.* ***DAGL5*** *– West bank.* ***DAGL6*** *– West bank.* ***DAGL7*** *– Stream bed.* ***DAGL8*** *– West bank.*

Unless stated, the hammer (typically circled in white) rests on top of the sampled bed. ***DAGL9*** *– East bank.* ***DAGL10*** *– Stream bed.* ***DAGL11*** *– The hammer head hangs from the top of the sampled bed, stream bed.* ***DAGL12*** *– West bank.* ***DAGL13*** *– Stream bed.* ***DAGL14*** *– Stream bed.* ***DAGL15*** *– Stream bed.*

Aghagrania Section

S.	*Fm.*	*Sample*	*Lithology*	*Stratigraphic height within the section*
Aghagrania	**C. S.**	**AGHA13**	Lime-clast wackestone	84.3m Derreens Limestone Mbr.
	Bellavally	**AGHA12**	Argillaceous mudstone	84m Corry Mbr.
		AGHA11	Calcareous mudstone	83m Corry Mbr.
		AGHA10	Cephalopodal wackestone	72.2m Sheena Shale Mbr.
		AGHA9	Cephalopodal wackestone	63.5m Lugasnaghta Shale Mbr.
		AGHA8	Mudstone	55.1m Sraduffy Mbr.
	Meenymore	**AGHA7**	Calcisiltite mudstone	44.3m Corloughlin Mbr.
		AGHA6	Calcilutite mudstone	40m Corloughlin Mbr.
		AGHA5	Laminated mudstone	32.6m Corloughlin Mbr.
		AGHA4	Argillaceous wackestone	25m Dorrusawillin Mbr.
		AGHA3.2	Bioturbated? mudstone	18.5m Drumcroman Mbr.
		AGHA3.1	Bioturbated? mudstone	18.2m Drumcroman Mbr.
		AGHA2	Chert bound mudstone	13.8m Drumcroman Mbr.
		AGHA1	Wackestone	10.1m Drumcroman Mbr.
		AGHA.A11	Calcilutite mudstone	7.7m Drumcroman Mbr.
	Dartry Lmst.	**AGHA.A2**	Crinoidal wackestone/packstone	3m
		AGHA.CAV.1	Cherty wackestone	0m

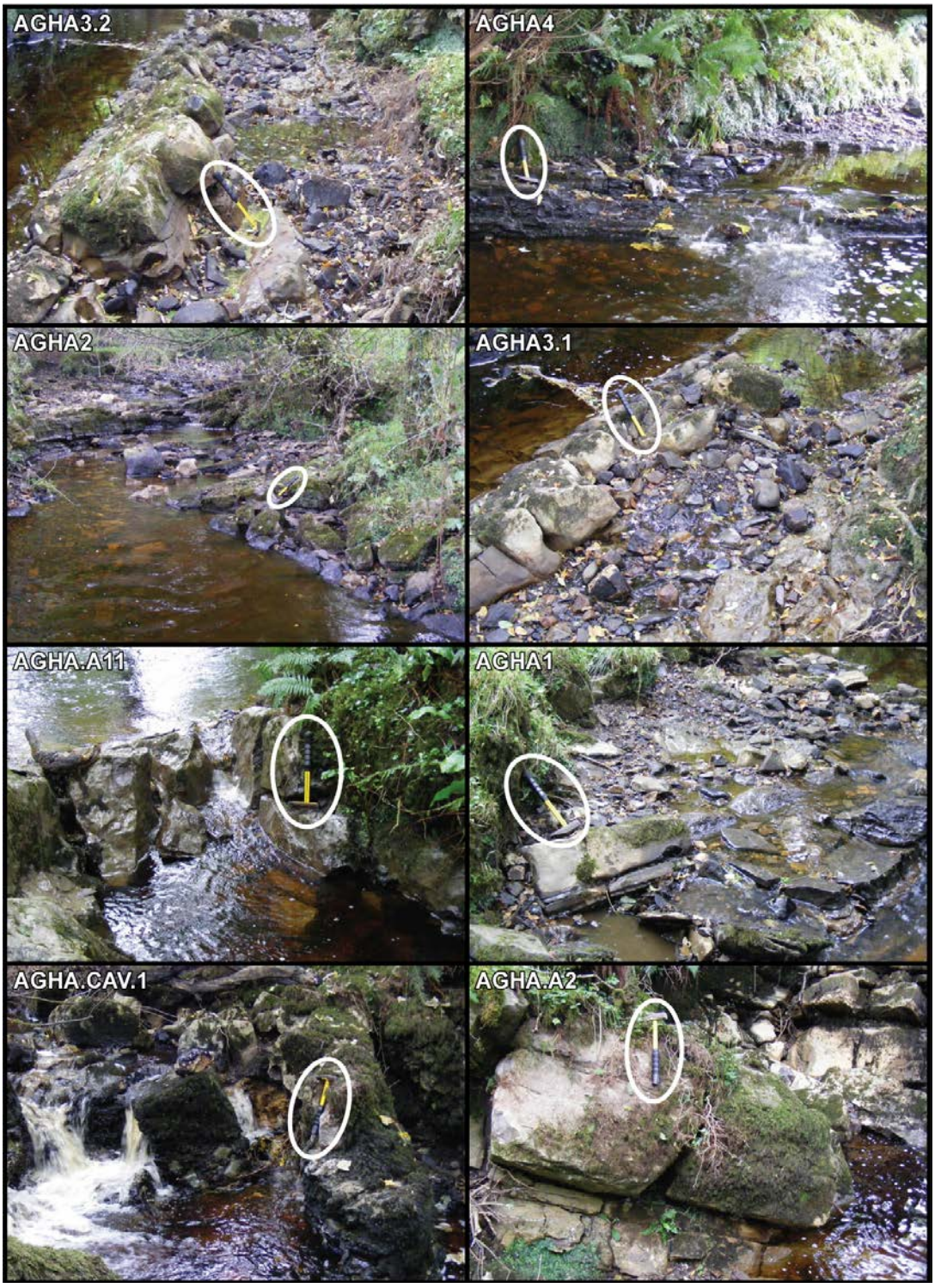

Unless stated, the hammer (circled in white) rests on top of the sampled horizon. ***AGHA.CAV.1*** *– The hammer head hangs from the top of the sampled horizon, stream outcrop.* ***AGHA.A2*** *– The hammer head hangs from the top of the sampled bed, west bank.* ***AGHA.A11*** *– The hammer head rests on the plane defining the base of the sampled horizon, east bank.* ***AGHA1*** *– West bank.* ***AGHA2*** *– East bank.* ***AGHA3.1*** *– Eastern side of stream bed.* ***AGHA3.2*** *– Eastern side of stream bed.* ***AGHA4*** *– East bank.*

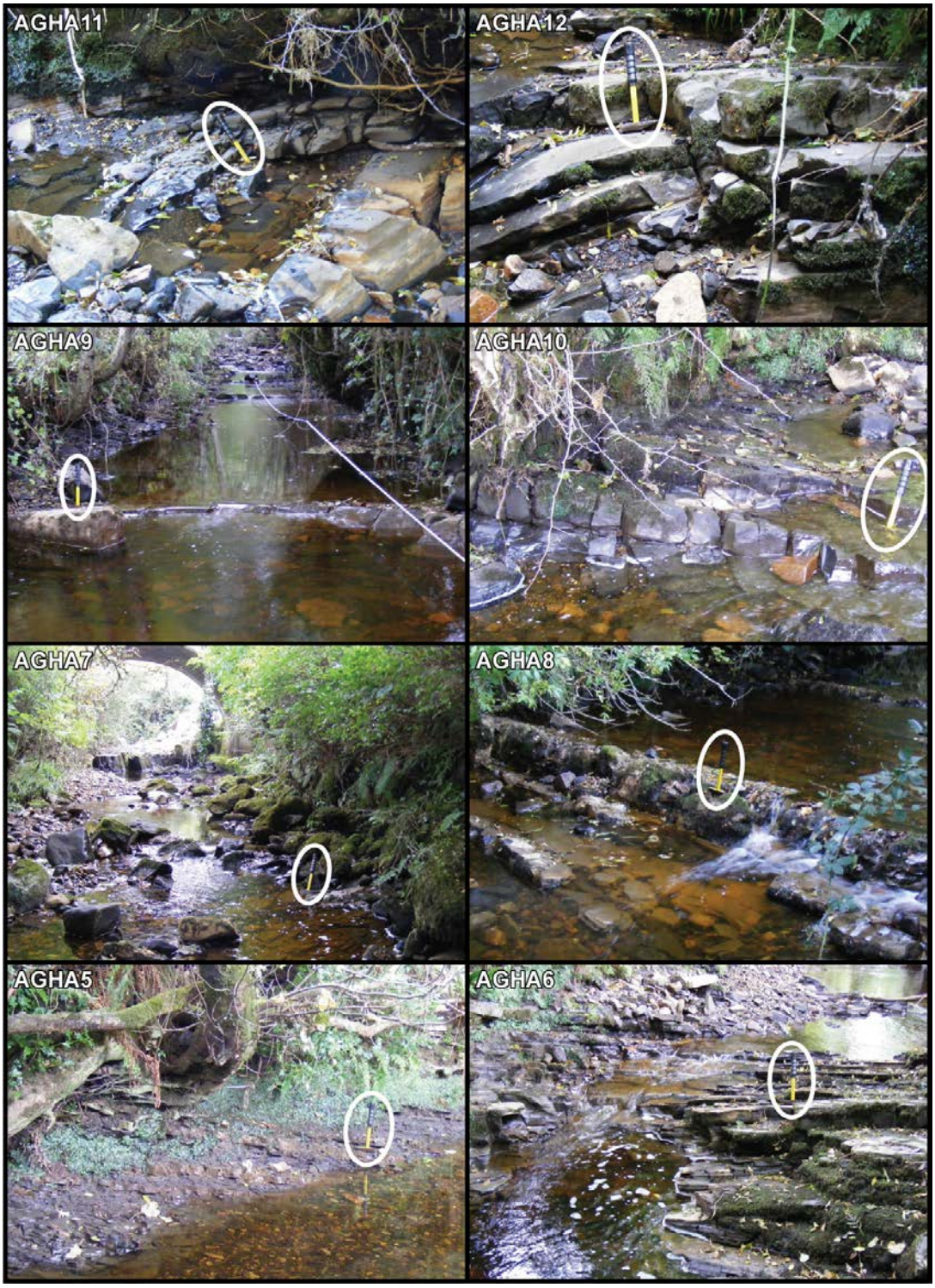

Unless stated, the hammer (circled in white) rests on top of the sampled horizon. ***AGHA5*** *– East bank.* ***AGHA6*** *– East bank.* ***AGHA7*** *– East bank.* ***AGHA8*** *– Step in stream bed.* ***AGHA9*** *– West bank.* ***AGHA10*** *– West bank.* ***AGHA11*** *– East bank.* ***AGHA12*** *– East bank.*

AGHA13 *– The hammer head rests on the top of the sampled horizon which marks the base of the Carraun Shale Formation.*

Carraun/Lugasnaghta Section

S.	Fm.	Sample	Lithology	Stratigraphic height within the section
Carraun/Lugasnaghta	Dergvone Shale	**CNLG19**	Wackestone bullion	130.1m Tonlegee Shale Mbr.
		CNLG18	Mudstone bullion	119.4m Tullyclevaun Shale Mbr.
		CNLG17	Poorly cleaved shale	72.7m Gubaveeny Shale Mbr.
	Carraun Shale	**CNLG16**	Large dolomite bullion	66.1m Camderry Mbr.
		CNLG15	Calcisiltite mudstone	61.2m Sranagross Mbr.
		CNLG14	Mudstone bullion	56.9m
		CNLG13	Calcisiltite mudstone	54.8m Ardvarney Mbr.
		CNLG12	Calcisiltite mudstone	47.6m
		CNLG11	Shell layer in a laminite	45.5m Tawnyunshinagh Mbr.
		CNLG10	Calcisiltite mudstone	44.3m
		CNLG9	Calcisiltite mudstone	39.2m
		CNLG8	Calcilutite mudstone	28.4m
		D.K. CNLG ABV. DERREENS	Fossiliferous shale	25.6m
		CNLG7	Calcilutite mudstone	23m
		CNLG6	Calcilutite wackestone	17.8m Derreens Limestone Mbr.
	Bellavally	**CNLG5**	Laminated mudstone	16m Corry Mbr.
		D.K. CNLG SHEENA	Fossiliferous shale	14.3m Sheena Shale Mbr.
		CNLG4	Laminated mudstone	7.6m Drummangarvagh Mbr.
		D.K. CNLG.A	Fossiliferous shale	2.5m Lugasnaghta Shale Mbr.
		CNLG3	Laminite and macrocell	1.4m Sraduffy Mbr.
		CNLG2	Laminite and macrocell	1.3m Sraduffy Mbr.
		CNLG1	Argillaceous wackestone	0.6m Sraduffy Mbr.

Unless stated, the hammer (typically circled in white) rests on top of the sampled bed. ***CNLG1*** *– The hammer head hangs from the top of the sampled bed, north bank.* ***CNLG2&3*** *– Note hammer for scale underlies both the sampled units (highlighted in white), stream outcrop.* ***D.K. CNLG.A*** *– The white arrow indicates the stratigraphic level sampled, north bank.* ***CNLG4*** *– The chisel (circled in white) is embedded in the sampled horizon, south bank.* ***D.K. CNLG SHEENA*** *– The white arrow indicates the stratigraphic level sampled, north bank.* ***CNLG5*** *– The sampled horizon is outlined in white, with a hammer circled in white for scale, north bank.* ***CNLG6*** *– The hammer head marks the base of the sampled bed, north bank.* ***CNLG7*** *– Stream bed.*

Unless stated, the hammer (circled in white) rests on top of the sampled horizon. ***D.K. CNLG ABV. DERREENS*** *– South bank.* ***CNLG8*** *– South bank.* ***CNLG9*** *– South bank.* ***CNLG10*** *– South bank.* ***CNLG11*** *– The hammer head is positioned stratigraphically at the base of the sampled horizon, south bank.* ***CNLG12*** *– South bank.* ***CNLG13*** *– North bank.* ***CNLG14*** *– The hammer rests on top of the sampled carbonate bullion horizon, a second bullion is visible in the centre right of the photograph, north bank.*

Unless stated, the hammer (circled in white) rests on top of the sampled horizon. ***CNLG15*** *– Step in the stream bed.* ***CNLG16*** *– South side of the stream bed.* ***CNLG17*** *– The white arrow indicates the sampled horizon, south bank.* ***CNLG18*** *– The hammer head marks the stratigraphic level of the carbonate bullion horizon sampled, south bank.* ***CNLG19*** *– Recent stream bed exposure.*

APPENDIX E –

Microfossil sample location in Co. Clare, western Ireland sections.

Kilnamona Section

S.	*Fm.*	*Sample*	*Lithology*	*Stratigraphic height within the section*
Kilnamona	**Magowna**	**KMONA11B**	Calcareous mudstone	177-180.5cm
		KMONA11A	Calcareous mudstone	167-173.5cm
		KMONA10	Calcareous mudstone	153.5-157cm
		KMONA9	Wackestone	139-148.5cm
		KMONA8	Crinoidal wackestone	130-139cm
	Slievenaglasha	**KMONA6**	Crinoidal wackestone	96-113cm
		KMONA5	Crinoidal wackestone	91-96cm
		KMONA4	Crinoidal wackestone	65-91cm
		KMONA3	Crinoidal wackestone	Top ~12cm of 21-65cm
		KMONA2	Wackestone nodules	11-21cm
		KMONA1	Crinoidal wackestone	0-11cm

All images face upstream. ***KMONA1, 2, 3 & 4*** *– White lines mark the boundaries between the labelled (on the right), sampled beds, note the hammer for scale. Note that the sample KMONA2 was extracted from the recessed shale interval marked.* ***KMONA4, 5, 6, 8 & 9*** *– White lines mark the exposed faces of the labelled (on the right), sampled beds, note the hammer for scale.* ***KMONA10, 11A & 11B*** *– White lines mark the positions of the labelled (on the right), sampled horizons, note the hammer and chisel for scale.*

St. Brendan's Well Section

S.	*Fm.*	*Sample*	*Lithology*	*Stratigraphic height within the section*
St. Brendan's Well	**Clare Shale**	**BW8**	Carbonate bullion	8.05-8.3m
		BW9	Carbonate bullion	7.25-7.35m
		BW7	Carbonate bullion	4.35-4.55m
		BW10	Carbonate bullion	3.25-3.41m
		BW6	Shale	1.1-1.25m
		BW5B	Phosphatic lag	1.01-1.05m
		BW5	Phosphatic lag	0.95-1.01m
	Magowna	**BW4**	Phosphatised limestone	0.85-0.95m
		BW3	Crinoidal wackestone	0.42-0.85m
		BW2	Argillaceous limestone	0.4-0.42m
	Slievena-glasha	**BW1**	Crinoidal wackestone	0.2-0.4m

BW1 *– The mechanical pencil points to where the bed was sampled within a joint in the bed surface, stream bed.* ***BW2*** *– The white arrow indicates the location of the sampled horizon, in the overhang between prominent limestone beds, note the hammer (circled in white) for scale.* ***BW3 & 4*** *– The hammer head marks the base of the sampled horizon BW3, whilst the solid white line defines its top. The upper portion of the bed was sampled as BW4, with the dotted white line marking the extent of probable phosphatisation.* ***BW5, 5B & 6*** *– Numbers and white arrows indicate the horizons which were sampled. Note the hammer (circled in white) for scale.* ***BW10*** *– The hammer (circled in white) sits on top of the sampled bullion horizon.* ***BW7, BW9 & BW8*** *– White arrows indicate the sampled horizons, Fields of view are ~10-15m across.*

APPENDIX F –

Catalogue of the invertebrate microfauna recovered

Although the primary focus of rock processing was to obtain conodonts and ichthyoliths (principally for stable isotope analysis and, in the case of conodonts, biostratigraphy), all microfossil structures were recorded to assemble a more complete understanding of the palaeoenvironments of the sections investigated. This appendix describes aspects of some of the most common invertebrate microfossils recovered (in order of phylum below), with plates and (finally) tables located below. Since formic acid was predominantly used to digest samples, only fossils and structures which were originally non-calcareous, or those that were secondarily replaced by a non-calcareous mineral (commonly silica or pyrite), were preserved.

Porifera

All NW Ireland sections yielded siliceous material which is attributed to sponges. The Glencar and Dartry Limestone Formations were commonly particularly rich in sponge remains. Two basic structures were identified:

- **Hexactinellid networks** comprise a series of parallel columns each of which are connected to their surrounding columns by relatively regular, simple bars with expanded attachments on both ends. The columns themselves appear to be composed of irregularly packed spicules (**Plate 1** - 4).
- **Isolated spicules** occur in a variety of forms ranging from monaxons to densely-spined polyaxons. The tips of the axons commonly bifurcate or even tetrafurcate. The arms of the spicules often appear segmented but on closer inspection are actually spiralled (**Plate 2** - 2,4 & 5).

Cnidaria

Coral remains (**Plate 3** - 1, 4 & 8) were recovered from the Dartry Mountain Sections and Kilnamona Section residues, but were richest in the Tievebaun and Glencar Section residues. Due to their (commonly) large size, the remains typically comprised unidentifiable fragments of the corallite wall. Small *Cladochonus* colony segments (**Plate 3** - 4) and immature zaphrentids were the most abundant broadly identifiable forms. In samples where silicification was especially faithful, particular zaphrentids demonstrated their initial requirement for an attachment structure (e.g. corallites partially encrusting a brachiopod valve) before they were large enough to support themselves on the seafloor (**Plate 3** - 8).

Bryozoa

A significant variety of bryozoans were identified during this study (**Plate 4** - 1-17), with the greatest diversity recovered from the Tievebaun and, to some extent, Glencar Sections. Bryozoans were broadly grouped into three categories:

- **Dome/Encrusting forms** typically have a somewhat inflated, simple outer surface with a relatively even distribution of zooecia. The bottom of the colony is characteristically irregular, conforming to the surface of whatever hard surface it was originally attached.
- **Fenestrate forms** are morphologically varied and differ in:
    1. The shape of the fenestrule.
    2. The restriction of autozooecial apertures to the fenestrule margins.
    3. The number of autozooecial apertures per fenestrule
    4. The presence of any ornament or structures such as spines.
- **Ramose forms** are the most morphologically diverse of all the bryozoan groups. Significant differences include:
    1. The cross sectional outline of the stick-like form, whether slightly flattened or perfectly round.
    2. The presence of any side branches or colony bifurcations.
    3. The restriction of autozooecial apertures to one side of the skeleton (i.e. unilaminar or bilaminar).
    4. The density of autozooecial apertures across the surface.

5. The shape of the autozooecial apertures.
6. The presence and specific location of any features or ornament such as striations, spines, nodes or fine pits.

Brachiopoda

Complete juvenile, and fragmented mature, brachiopods were commonly preserved, and at least some material was recovered from every section investigated. Both phosphatic and articulated brachiopods were recorded, the latter having been silicified, pyritised or both (some calcitic specimens were recovered from shale samples).

- Phosphatic forms (**Plate 5** - 1-2, 4-6) are characteristically delicate and concentrically growth-lined. Three basic forms were identified:
  1. Elongate ovaloid shape (**Plate 5** - 4-5).
  2. Small and sub-circular in shape (**Plate 5** - 2).
  3. Ovaloid in shape with pronounced, spaced, concentric ribs (**Plate 5** - 1 & 6).
- Calcitic forms (**Plate 6** - 1-7) come in a variety of morphologies but are generally only coarsely preserved due to the replacement process. Articulated and fragmented valves are more diverse and typically better preserved in the Tievebaun and, to some extent, Glencar Sections. Of particular note are specimens with delicate spines preserved and those that appear to exhibit evidence of durophagous predation. Although not abundant, a particular, strophic, semi-circular, concavo-convex, ribbed brachiopod commonly exhibits a relatively large hole in the ventral valve close to the most swollen portion of the shell near the umbo (**Plate 6** - 6-7). Bore holes were identifiable (in some samples) in ~30% of the ventral valves recovered, a figure which is difficult to compare with published studies (given the small population size) but appears particularly high (c.f. Mottequin & Sevastopulo, 2009).

Mollusca

Bivalves

Bivalve remains were restricted to three samples from the Dartry Limestone Formation (Glencar Section), which represent ~20m of stratigraphy. Growth-lined

valves average ~2mm in length, are invariably disarticulated and occasionally possibly bored (**Plate 5** - 3).

Gastropods

The gastropods recovered during this work were typically small and poorly mineralised (often only internal moulds remain). Details are rarely preserved (in some rare cases, fine lineations are identifiable). They occur in generally low abundances throughout all the sections investigated, but are most common in the Aghagrania and Carraun/Lugasnaghta Sections.

Cephalopods

Cephalopods were most commonly found in the younger formations of the sequences and were not found at all in the Asbian-aged Tievebaun or Glenade Sections. Only isolated examples of orthoconic nautiloids were recovered. Pyritised fragments of the siphuncle and shell of goniatites were the most commonly encountered structures (**Plate 2** - 7).

Echinodermata

Echinoderm remains were recovered (in some form) from every section investigated, but predominantly comprised crinoid ossicles, short pluricolumnals and (to a lesser extent) plates. In general, replacement mineralisation of echinoderm material tends to be much coarser than other fossils within the same sample. Rare occurrences of blastoids and archaeocidarid plates were noted in the Tievebaun and Glencar Sections. Grooved plates (which commonly bifurcate), possibly functioned to channel food or waste material and are interpreted as feeding or anal structures (**Plate 2** - 6 & 8).

Enigmatic bullet/pointed dome-shaped structures with variably developed pentaradially symmetrical ribs arranged at their base (**Plate 1** - 1-3) are thought to be echinoderms (due to their symmetry). The surfaces of the ~0.5-2mm structures are finely granular. The structures were only found in samples taken from near the Slievenaglasha-Magowna contacts in the Kilnamona and St. Brendan’s Well Sections and may be particular to this stratigraphic interval.

Arthropoda

Ostracods

Ostracods were a common component of many of the residues recovered from every section; however, due to their small size and (commonly) delicate ornamentation, valves were often incomplete due to their susceptibility to fragmentation. A large variety of morphologies (**Plate 7** - 1-7) are differentiable according to the:

- overall sphericity and shape of the valves. The shape of the hinge and the degree to which (if at all) either end of the shell is pinched into an elongate “snout” are important controls.
- size of the mature carapace.
- presence, size and position of any spines, nodes and/or protuberances.
- presence, position and character of any lineations, fringes and/or ribs.
- texture of the valve surface (typically smooth or finely granular but occasionally formed from a network of interconnecting bars).

Trilobites

A variety of (predominantly incomplete) thoracic segments, pygidia, librigenae, spines, hypostomes and cephalons were recovered from every section investigated. Surfaces range from being entirely smooth, to being lineated, granular and conspicuously spined.

Other fauna

Epibionts

A number of microfossils demonstrated a requirement for the test of another creature on which to attach and encrust. However, only those that were dependant throughout their life on the support of their biological hard-ground were considered (herein) as epibionts. In many cases it can be proven that the host was encrusted post-mortem; however, other examples appear to suggest attachment to a living organism. Successive attachments by different organisms competing for living

space were identified in one particularly detailed and productive sample (GLTV22). Three main groups were recognised:

- **Bryozoan** epibionts were relatively uncommon, small in size and comprised low mounds and domes that follow the surface of the host (**Plate 3** - 1).
- **Cornulitids** are a group of extinct, conical tube-dwelling, encrusting invertebrates which were common in the early Palaeozoic, but were present up to at least the Mississippian (Herringshaw *et al.*, 2007; Morris & Felton, 2003; Morris & Rollins, 1971; Vinn & Mutvei, 2005). Their tests were typically found isolated from their host in this study; however, where recovered attached, they are invariably associated with bryozoans (**Plate 3** - 2,5 & 7). Specimens are most commonly coiled and solitary, unlike the dense occurrences of straight forms figured by the above workers from the early Palaeozoic. The tests of the specimens recovered exhibit fine lineations running parallel with the axis of growth and pronounced ribs which ring the tube at relatively regular intervals. Several samples exhibited forms in which the shell stopped coiling and instead rose away from the encrusted surface (**Plate 3** - 7). This change in strategy is probably due to a need to move into a more favourable position within food bearing currents, possibly due to the death or re-orientation of its host, or perhaps just to satisfy the greater food requirements of the growing organism.
- **Worm casts/tubes** are represented by thin, siliceous, granular trails and tubes which snake across the surfaces of virtually all fossil materials (**Plate 3** - 6, **Plate 5** - 4). Their presence around the broken edges of fossil fragments and within living areas of the test, suggests that often the tests were encrusted post-mortem.

Tetrataxis

Tetrataxis chamber fills were commonly discovered in residues of Benbulben Shale and Glencar Limestone Formation samples from the Tievebaun Section. Specimens of the foraminifer are constructed from numerous, partially overlapping sickle shaped bodies which build up into a conical Christmas-tree structure (**Plate 2** - 1 & 3).

Plant material

Woody tissue, which has been preserved in 3d by carbon, was recovered from the Carraun/Lugasnaghta and St. Brendan's Well Sections as well as (possibly) the Tievebaun Section. Individual box-like plant cell chambers are discernable in stacked rows (**Plate 1** - 6-7).

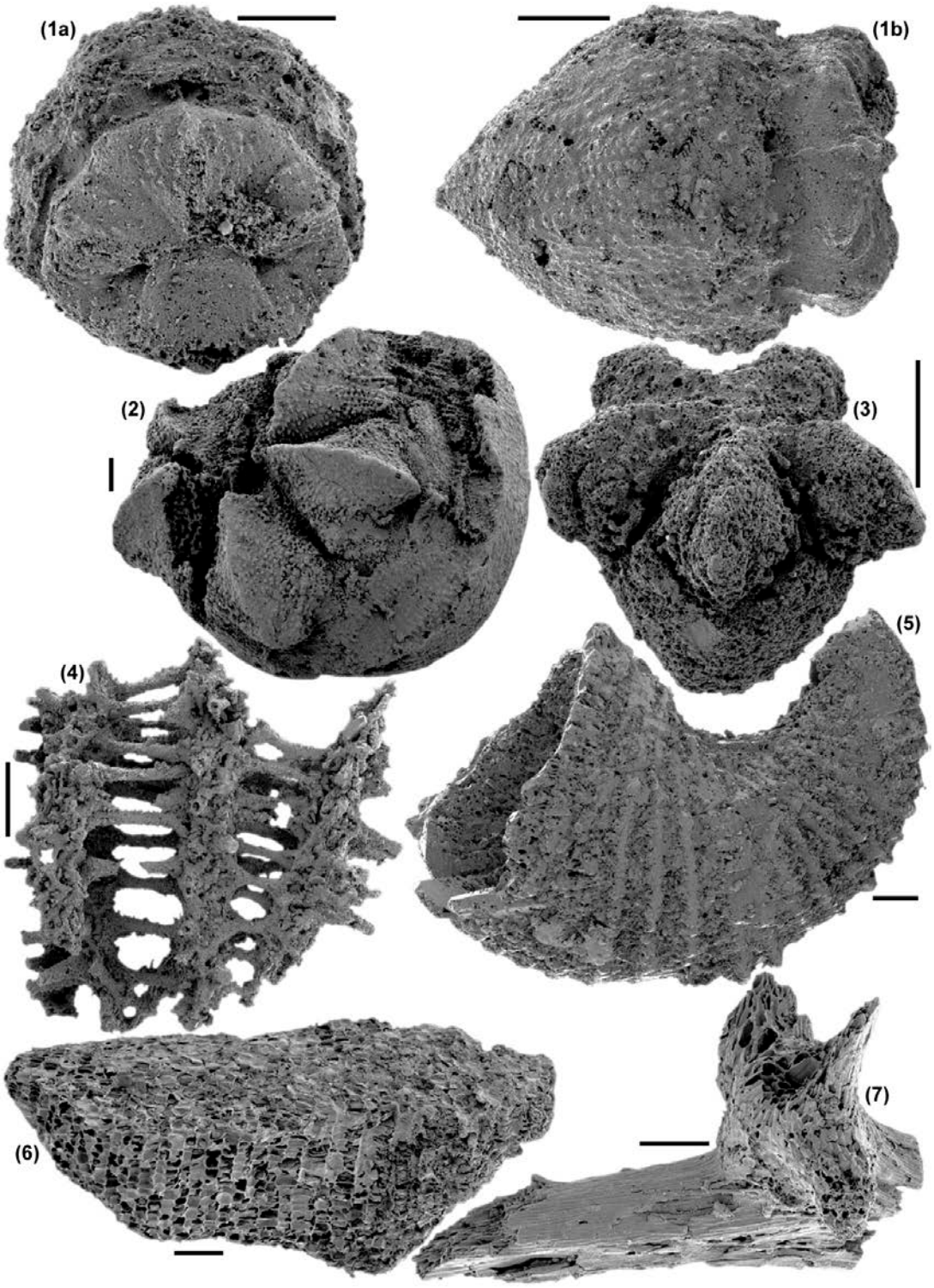

Plate 1.
All scale bars represent 200µm. ***(1a & b)*** *Basal? and lateral views of an unknown, possible echinoderm fossil – KMONA6, MB.14B.4.* ***(2 & 3)*** *Oblique-basal views of other unknown, possible echinoderm fossils – BW2, MB.14C.1 and KMONA5, MB.14A.2 respectively.* ***(4)*** *Lateral view of a probable Hexactinellid sponge latticework – DAGL11, MB.21A.5.* ***(5)*** *Lateral view of an unknown horn-like shelly fossil – DAGL11, MB.21A.7.* ***(6 & 7)*** *Oblique views of chambered woody tissue – CNLG15, MB.22B.6 and MB.22B.5 respectively.*

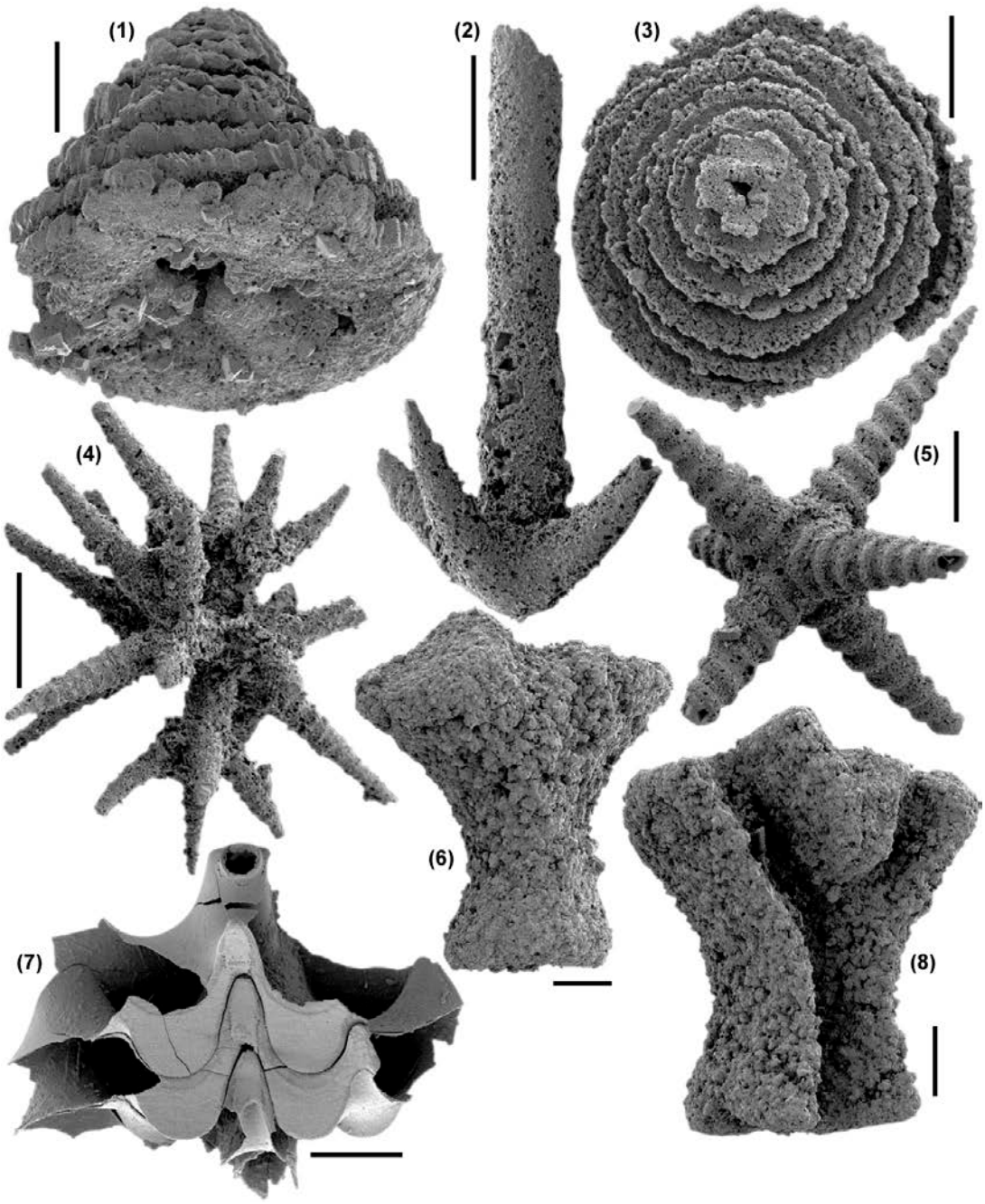

Plate 2.
All scale bars represent 200µm. ***(1 & 3)*** *Oblique-basal and dorsal views of Tetrataxis fossils – GLTV16, MB.15.2 and AGHA4, MB.22A.3 respectively.* ***(2, 4 & 5)*** *Lateral views of various sponge spicule morphologies. (2) Anchor or palm-tree – GLTV18532.5NOD, MB.20A.3. (4) Tetra-furcating sextaxon – GLTV18532.5NOD, MB.20A.4. (5) Spiralled sextaxon – GLTV18532.5NOD, MB.20A.6.* ***(6 & 8)*** *Lateral external and internal views of grooved, bifurcating echinoderm plates – both DAGL9, MB.20B.7 and MB.20B.8 respectively.* ***(7)*** *View onto the internal surface of a pyritised goniatite coil – CNLG15, MB.22B.3.*

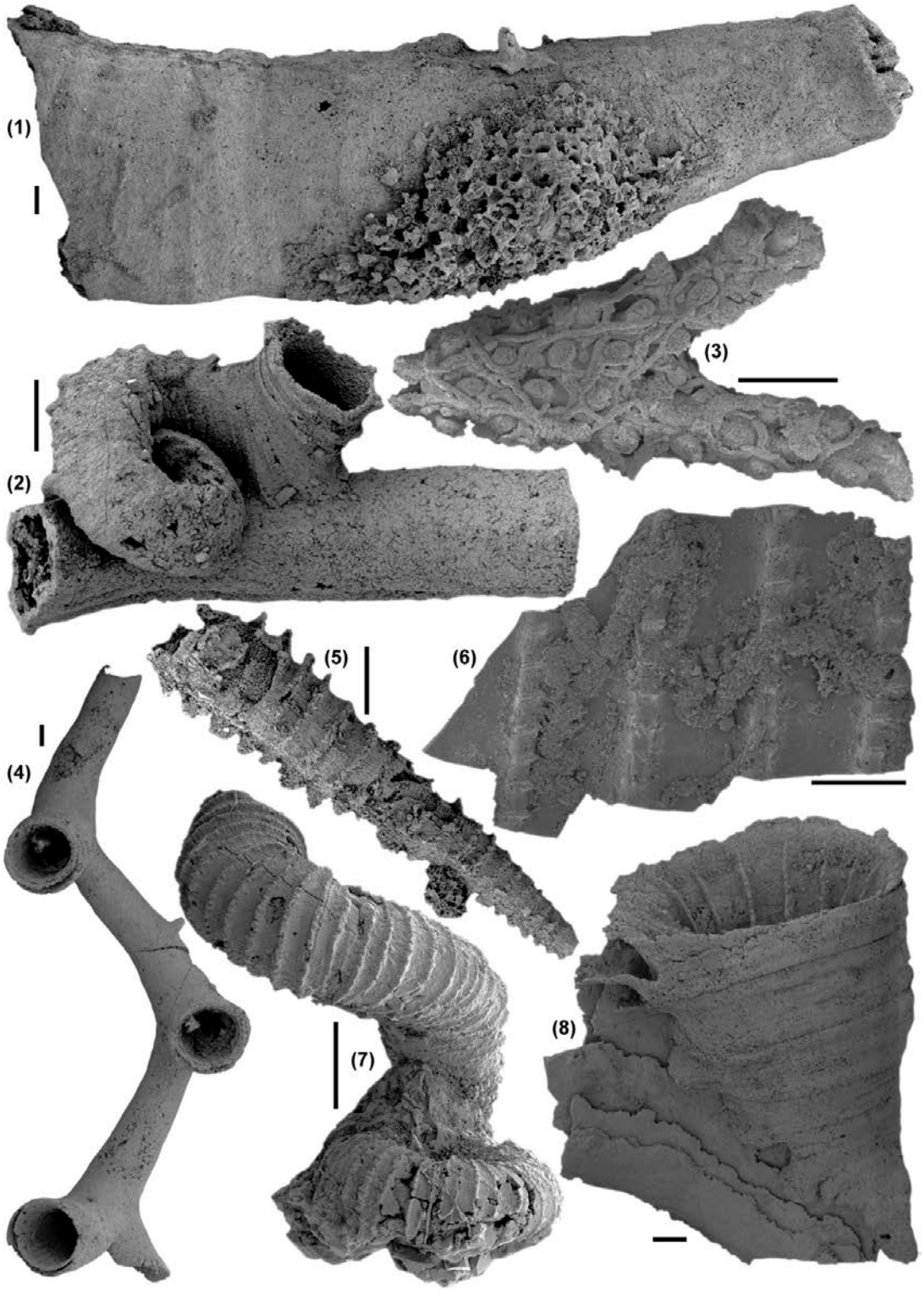

Plate 3.
All scale bars are 500µm. ***(1)*** *Lateral view of a corallite with an encrusting bryozoan - GLTV22, MB.17.9.* ***(2)*** *Lateral view of a ramose bryozoan encrusted by cornulites - GLTV22, MB.17.8.* ***(3)*** *Sediment fills of a ramose bryozoan with a fine mat of siliceous tendrils - GLTV40, MB.19C.2.* ***(4)*** *Lateral view of Cladochonus - GLTV22, MB.17.3.* ***(5)*** *Straight cornulites specimen with a distinct attachment groove - GLTV19, MB.16B.12.* ***(6)*** *Upper-surface view of a "bar-element" plate with encrusting worm trails - CNLG10, MB.6C.2.* ***(7)*** *Lateral view of a cornulites - GLTV18532.5NOD, MB.20A.5.* ***(8)*** *Lateral view of a horn coral attached to a brachiopod fragment - GLTV22, MB.17.6.*

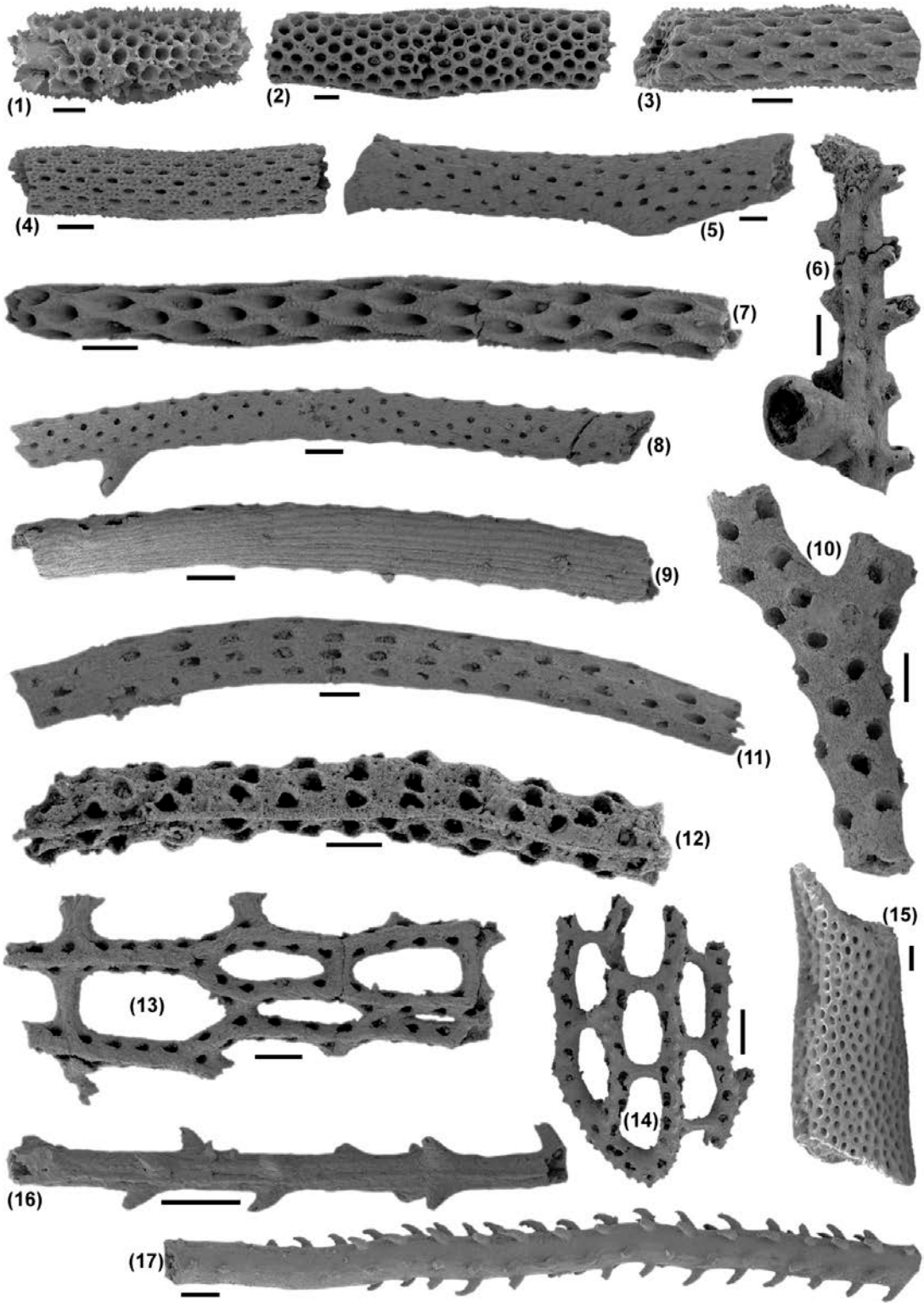

Plate 4.
All scale bars represent 500µm. ***(1-5, 7-12 & 15-17)*** *Lateral views of various ramose bryozoans – AGHA4, MB.22A.5, GLTV16, MB.15.4, GLTV35, MB.19A.1, GLTV16, MB.15.3, GLTV25, MB.18B.5, GLTV19, MB.16B.13, GLTV18, MB.16A.7, GLTV18, MB.16A.9, GLTV35, MB.19A.4, GLTV25, MB.18B.3, GLTV18532.5NOD, MB.20A.1, GLTV18, MB.16A10, GLTV18, MB.16A.3 and GLTV25, MB.18B.4 respectively.* ***(6)*** *Lateral view of a ramose bryozoan with a coiled attachment structure – GLTV18, MB.16A.5.* ***(13 & 14)*** *Lateral views of fenestrate bryozoans - GLTV18, MB.16A.6, GLTV35, MB.19A.2.*

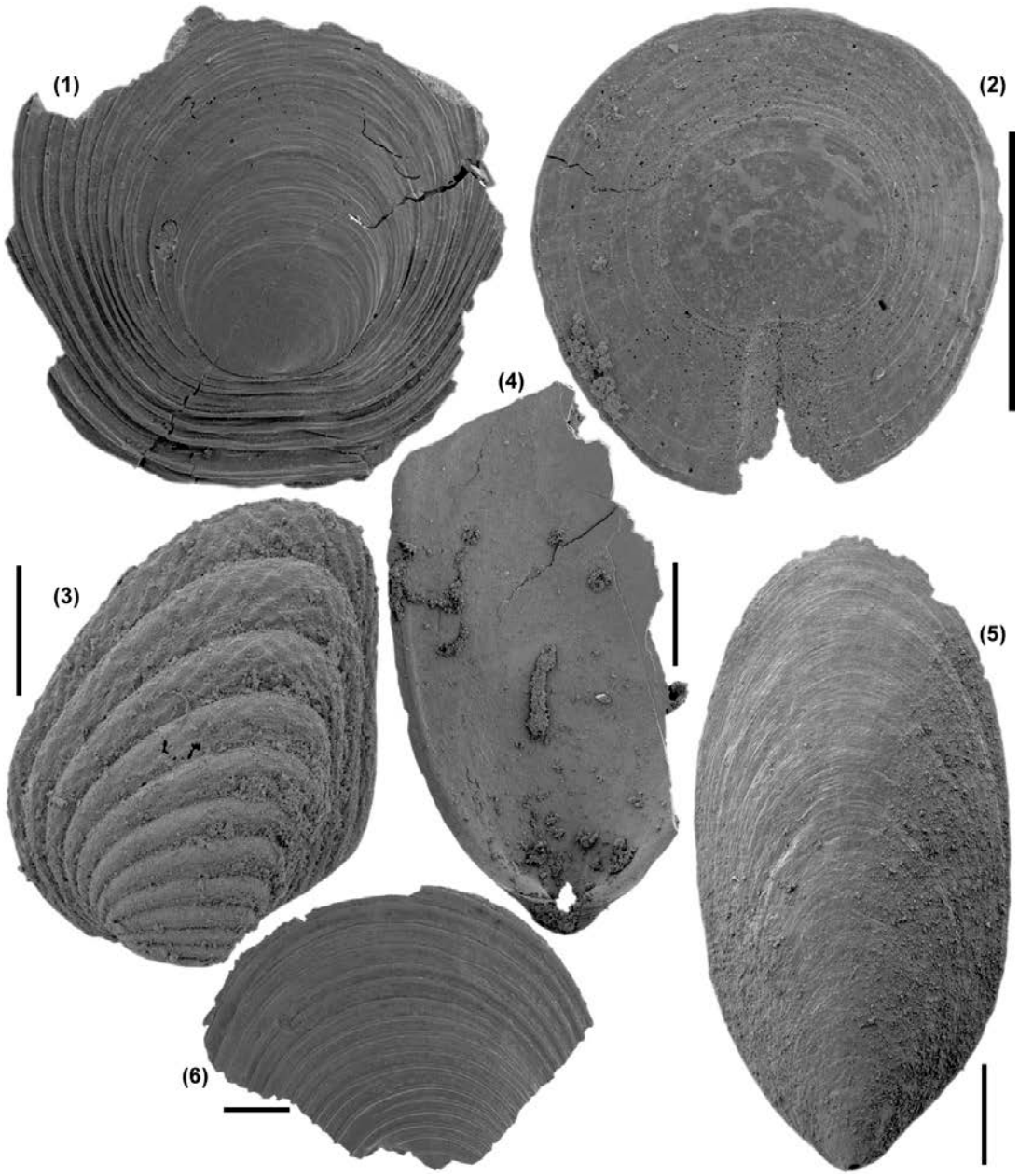

Plate 5.
All scale bars represent 500µm. ***(1 & 6)*** *External views of type 3 phosphatic brachiopod valves – KMONA3, MB.9C.13 and GLTV27, MB.4A.2 respectively.* ***(2)*** *External view of a type 2 phosphatic brachiopod valve – CNLG1, MB.24A.5.* ***(3)*** *External view of a right-hand bivalve valve – DAGL15, MB.21B.3.* ***(4 & 5)*** *Internal and external views of type 1 phosphatic brachiopod valves – CNLG1, MB.24A.4 and AGHA3.2, MB.23A.1 respectively.*

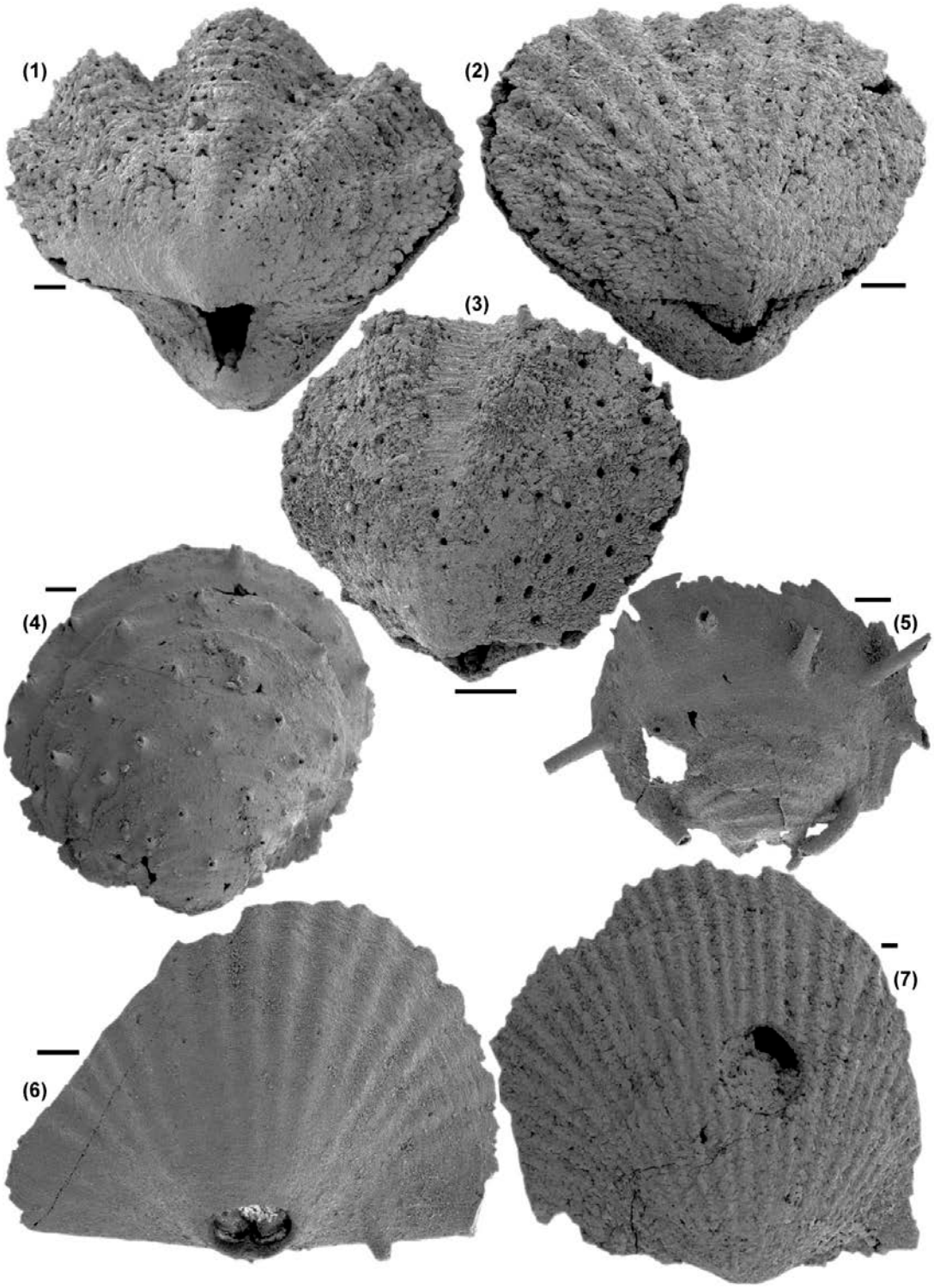

Plate 6.
All scale bars represent 200µm. ***(1-3)*** *Dorsal views of articulated silicified brachiopods – GLTV22, MB.17.1, GLTV19, MB.16B.2 and AGHA4, MB.22A.2 respectively.* ***(4 & 5)*** *Ventral views of isolated silicified spinose brachiopod valves – GLTV24, MB.18A.1 and GLTV19, MB.16B.3 respectively.* ***(6 & 7)*** *Ventral views of bored, isolated valves – GLTV35, MB.19A.5 and GLTV24, MB.18A.3 respectively.*

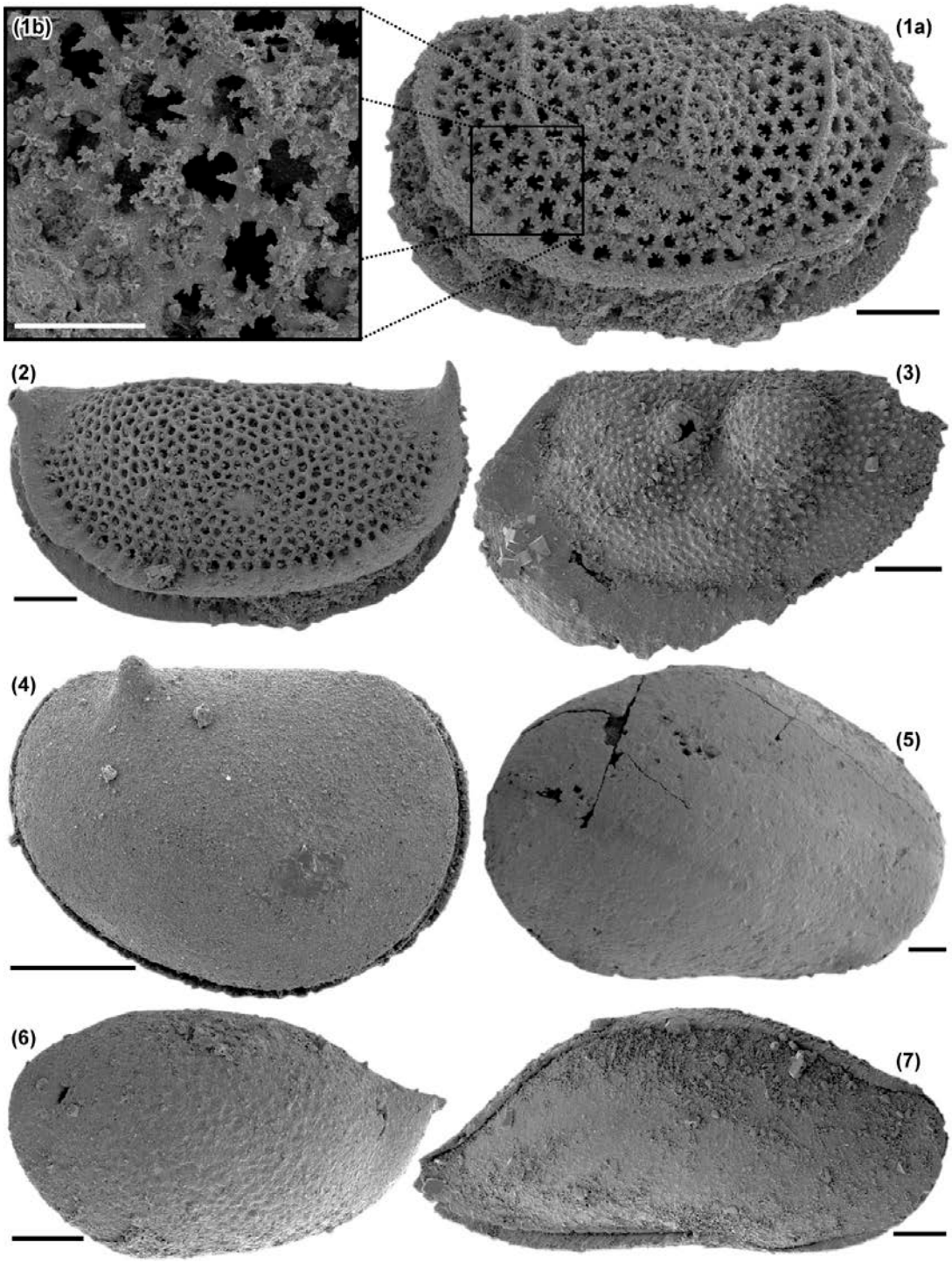

Plate 7.
The black scale bars represent 200µm whilst the white bar represents 100µm. ***(1a & b)*** *Isolated ostracod valve with fine ridges and patterning, shown in more detail in (1b) – DAGL15, MB.21B.4.* ***(2)*** *Ridged and spined, isolated ostracod valve – DAGL15, MB.21B.2.* ***(3)*** *Isolated, incomplete, noded and fringed ostracod valve – GLTV19, MB.16B.6.* ***(4)*** *Weakly spined, articulated ostracod – AGHA4, MB.22A.1.* ***(5)*** *Isolated, simple, large, swollen ostracod valve – GLTV24, MB.18A.2.* ***(6)*** *Isolated, weakly "snouted", simple ostracod valve – GLTV19, MB.16B.8.* ***(7)*** *"Snouted", articulated ostracod – GLTV19, MB.16B.4.*

Sample	**GLTV12**	**GLTV13**	**GLTV950 NOD**	**GLTV14**
Abiotic	Pyrite framboids		Pyrite framboids	Pyrite framboids
Brachiopod		Spines(?) & valve fragments	Fragments	Phosphatic & silicified valve fragments
Bryozoan	Chamber fills	Fenestrate form		Poorly preserved fenestrate
Coral		Fragments of septate form		
Echinoderm		Ossicles. Archaeocidarid plate	Pyritised & silicified small ossicles & pinnules	
Ostracod	2 dominant forms: (1) bean/kidney shaped. (2) flattened, smooth rounded form	Articulated elongate bean shaped form		Silicified egg-shaped form
Unknown	Preserved segmented ovaloid remains =(?) the septae of a planispiral organism			Silicified thin tubes

Sample	**GLTV1600 NOD**	**GLTV15**	**GLTV16**	**GLTV17**
Abiotic			Pyrite framboids	
Brachiopod		Fragments	Spines(?)	Common fragments
Bryozoan	Pyritised fenestrate colony fragments	At least 2 ramose forms & 3 fenestrate forms	Common ramose & fenestrate forms	Common ramose & fenestrate forms
coral			*Cladochonus*(?)	Fragments
Echinoderm		Ossicles		Ossicle
Epibiont		Incomplete cornulites	Coiled cornulites, some encrusting	
Ostracod	Pyritised orb-shaped form	Articulated bean shaped forms. Slightly “snouted” enlarged bean shaped form	Articulated, “snouted” bean shaped forms	Articulates “snouted” form
Other		*Tetrataxis*	Common sickle shaped internal moulds of the foraminifer *Tetrataxis*	
Trilobite		Partial genal spine	Fragments	
Unknown		Honeycomb silicified sheet =(?) bryozoan	Thin-walled tubes	

Sample	**GLTV18**	**GLTV19**	**GLTV20**	**GLTV21**	**GLTV22**
Abiotic	Pyrite framboids				Framboidal pyrite
Brachiopod	Fragmentary & articulated specimens with spine bases.	Spinose forms. Articulated heart-shaped pediculate form	Silicified valves with spine bases. Articulated pediculate, ridged sulcate forms	Spinose, sulcate, pediculate fragments. terebratulid (?). Bored specimen	Pediculate terebratulids (?) & other large sulcate forms. Spine bases preserved
Bryozoan	Stick, fenestrate & possible encrusting forms	Dominant ramose & fenestrate forms	Various ramose & fenestrate forms, some pyritised. Chamber fills	Various ramose & fenestrate forms	Various ramose & fenestrate forms. Some substantial sheets
Coral		Small horn corallites	Pyritised portions of corallite fragments. Possible *Cladochonus*	Septate coral fragments	Solitary zaphrentids. *Cladochonus* . Fragments of larger septate form
Echinoderm		Ossicles & plates		Ossicles	
Epibiont	Coiled cornulites	Coiled & conical cornulites. Encrusted brachiopods & bryozoans	Coiled & conical cornulites	Curved, conical & planispiral cornulites. Open cup-like conical encrusting structures	V. common. Encrusting worm tubes/casts & “dome” bryozoans. Attached horn corals. Coiled & curved cornulites
Gastropod			Turreted gastropod		
Ostracod	Elongate bean forms.	Various isolated & articulated: lined, fringed, tuberculate, bean-shaped & “snouted” - oval forms	Incompletely preserved articulated forms & weakly “snouted” oval pea form	Large variety of forms. Many elongate, others bear spines or swollen processes	Articulated valves are common but are low in morpholog-ical diversity
Other	*Tetrataxis*	*Tetrataxis.* Silicified “net”	*Tetrataxis*	*Tetrataxis.* Planispiral cephalopod	*Tetrataxis*
Trilobite	Thoracic segments, pygidia, hypostome, librigenae & glabella fragments	Incomplete hypostome, librigenae & pygidia remains. Some spinose	Partial librigena, genal spine & thoracic segments	Hypostome. Incomplete thoracic segments, librigenae & pygidia	Thoracic segments, hypostome & librigenae
Unknown		Silicified, slightly curved conical tube.	Silicified lattice structure.	Silicified spines	Fine lattice structure

Sample	**GLTV23**	**GLTV24**	**GLTV25**	**GLTV26**
Abiotic		Framboidal pyrite	Framboidal pyrite	Framboidal pyrite
Brachiopod	Phosphatic valve fragments. Spines, semi-circular isolated valve fragments	3 bored, weakly ribbed valves. Spinose forms	Pediculate terebratulid(?). Heart shaped, articulated forms	Phosphatic growth lined valve fragments. Silicified fragments
Bryozoan	Various ramose & fenestrate morphologies. Silicified chamber fills	Various ramose & fenestrate forms. Chamber fills. Turreted, coiled attachment structure?	Various ramose & fenestrate forms	Fenestrate & ramose forms. Chamber fills
Coral	Thin corallites	Silicified tubular corallite. Septate small horn form.	Fragments. *Cladochonus*(?)	*Cladochonus*(?)
Echinoderm		Thick semi-circular plates. Grooved anal/ feeding plates. Ossicles & pluricolumnals	Ossicles (some with cirri) & pluricolumnals. Grooved plates	Poorly preserved ossicles & pluricolumnals. Partial echinoid spine. Grooved feeding arm plate
Epibiont	Planispiral cornulites. Worm trails/casts	Conical & coiled attached cornulites. Silicified thin worm casts	Planispiral & openly coiled cornulites. Fine worm tubes/casts	Thin, irregular worm cast/tube. Coiled → open & conical cornulites
Gastropod	Possible specimen	Incomplete turreted specimen	Highly turreted, tightly coiled form	
Ostracod	Simple elliptical forms. Textured fringed form.	Large oval, “snouted”, dimpled, nodded, lineated & smaller, elongate forms	Sediment fills of unknown form. Fringed forms	Articulated elongate bean-shaped form
Other	*Tetrataxis*	*Tetrataxis*	*Tetrataxis*	*Tetrataxis*
Sponge		Siliceous, fine hexaxon.	Polyaxons	Polyaxons & branching tetra/hexaxons
Trilobite	Particularly granulose portions	Thoracic segments		
Unknown	Dark acicular bodies = carbonised wood?	Crescent pitted trilobite eye-like structure	Slightly curved spine structures. Fine branching pyrite structures	Spines. 3D siliceous latticework

Sample	**GLTV27**	**GLTV28**	**GLTV29**	**GLTV30**	**GLTV32**
Brachiopod	Ribbed phosphatic fragments. Various silicified forms, many articulated: heart-shaped, pediculate terebratulid?, fat sulcate, bored & spinose fragments	Swollen articulated form with a large delthyrium	Elongate, slightly heart-shaped form. Articulated semi-circular pediculate form.	Phosphatic forms. Bored silicified specimens	Articulation infrequent. Several specimens, 1 partially bored. Partial spine preservation on some specimens
Bryozoan	Various fenestrate forms, some rarely pyritised	Ramose forms	Various ramose & fenestrate forms	Various poor ramose & fenestrate forms	Various ramose & fenestrate forms
Coral	Horn forms some with a pronounced columella. *Cladochonus*	Horn form & other fragments		Horn form	Poorly silicified zaphrentid(?)
Echinoderm	Ossicles & pluricolumnal	Ossicles	Ossicles & pluricolumnal	Ossicles & pluricolumnal	Ossicle
Epibiont	Planispiral & slightly turreted cornulites. Worm casts/trails	Incomplete cornulites. Worm casts/tubes	Slightly conical cup-like encrusters. Granulose & planispiral cornulites	Encrusting, slightly conical cup-like form	Coiled, slightly turreted cornulites
Gastropod	Turreted striated form	Poorly silicified turreted form			
Ostracod	Articulated, elongate “snouted” form	Elongate weakly “snouted” & almost spherical articulated forms	Elongate, weakly “snouted” & articulated swollen “snouted” forms	Slightly “snouted”, “egg”-shaped & bean-shaped valves,	Spined, bean shaped, fringed + pitted & slightly “snouted” forms
Other				Striated spines	
Sponge	Branching axons, some partially spiralled				
Trilobite	Incomplete thoracic segments, cephalon & librigenae				Pygidia, librigenae & thoracic fragments
Unknown	Simple spines		Siliceous ladder-like bars		

Sample	**GLTV33**	**GLTV34**	**GLTV35**	**GLTV36**	**GLTV37**
Brachiopod	Partial phosphatic valves. Silicified ribbed & articulated heart-shaped forms. Incomplete bored(?) valve. Spines	Ridged phosphatic fragments. Silicified swollen, articulated pediculate forms & heart-shaped forms. Spines	Various phosphatic form fragments. Articulated heart-shaped & weakly ribbed bored forms	Ridged phosphatic valves. Isolated & articulated bored valves. Articulated heart-shaped form	Fragments of 2 phosphatic forms: (1) thin shelled & growth lined (2) ribbed concentric-ally. Silicified heart-shaped form
Bryozoan	Dome/ encrusting form. Various ramose & fenestrate forms. Coiling attachment structure(?)	Various ramose & fenestrate forms. Coiling gastropod-like attachment structure	Dome & various ramose & fenestrate forms. Coiled, turreted attachment structure(?)	Various ramose & fenestrate forms. Possible dome/ encrusting form	Coarsely silicified ramose & fenestrate forms
Coral	Cylindrical septate form		Columnar, septate corallite with a strong columella	Poor corallite with cubic pyrite growths	
Echinoderm		Poorly silicified ossicles, pluricolumnal & grooved feeding/anal arms	Silicified ossicles & short pluri-columnals. Basal plate of calyx	Poor pluri-columnals, ossicles & calyx plates. Archaeo-cidarid plate	Ossicles. Short cirried *Platycrinites* (?) pluricolumnal
Epibiont	Slightly conical cup-like encruster. Coiled cornulites. Thin worm cast/tubes	Gently curved & tightly coiled cornulites. Worm casts/tubes	Worm casts/trails. Slightly conical, cup-like encruster. Pyritised cornulites	Coiled cornulites. Worm tubes/casts	Conical cornulites
Ostracod	Slightly “snouted” elongate bean-shaped form	Partial valves		Small bean-shaped form	
Other				Striated spines	Simple spines
Sponge		Polyaxons	Hexaxons	Various polyaxons, mainly hexaxons some partially spiralled	Bifurcating planar tetraxon & small polyaxons
Trilobite	Partial pygidia & librigenae		Granulose & smooth thoracic segments	Short spined librigena & pygidia	

Sample	**GLTV38**	**GLTV 18532.5 NOD**	**GLTV39**
Brachiopod	Possible phosphatic fragments. Partially pyritised spinose valve fragment	Silicified spiriferid(?) form. Partially pyritised spinose valve fragment	
Bryozoan	Various ramose and fenestrate forms	Pyritised ramose & fenestrate forms	Pyritised & silicified ramose forms
Coral	Pyritised & silicified septate form. *Cladochonus*(?)	Pyritised *Cladochonus*(?)	Fragments of larger specimens wall
Echinoderm	Pyritised & silicified ossicles & pluricolumnals	Silicified grooved ossicle. Pyritised ossicle	Abundance of coarsely silicified ossicles & pluricolumnals
Epibiont	Slightly openly coiled cornulites. Slightly conical cup-like encruster	Pyritised cornulites. Siliceous worm casts/trails/tubes	
Gastropod		Partial gastropod	Coiled sediment fill. Pyritised gastropod
Ostracod	Bean-shaped form. D-shaped valve with centrally located node		Articulated slightly “snouted” form
Other		Pyritised burrows	
Sponge	Small polyaxons & spiralled tetraxon	Tetra/Bi-furcating & partly spiralled hexaxons. Anchor/ palmtree-like axon	Various spiralled/ branching/ planar axons. Snow-flake like reticulate siliceous structure
Trilobite	Fragments of librigenae, thoracic segments & pygidia. Incomplete pyritised hypostome		Protaspid(?) cephalon. Partial pyritised pygidium
Unknown	Simple spines	Pyritised simple tubes	Siliceous interweaved tendril mats line fossils

Sample	**GLTV40**	**GLTV42**	**GLTV43**
Brachiopod	Thin-shelled phosphatic fragments. Coarsely silicified valves		Phosphatic valve fragments
Bryozoan	Sediment fill & shells of fenestrate & ramose forms		
Echinoderm	Coarsely silicified pluricolumnals	Small ossicle	
Ostracod	Sediment fill		
Other			*Tetrataxis*
Sponge	Thick silicified hexaxons	Thin tetra-/hexaxons	Tetraxons
Unknown	Siliceous interweaved tendril mats line fossils	Small amount of siliceous interweaved tendril mats	

Sample	DAGL1	DAGL2	DAGL3	DAGL4	DAGL5
Brachiopod	Iridescent phosphatic valve fragments. Heart-shaped & fat delthyrium bearing articulated forms	Smooth & ridged phosphatic forms. Bored silicified valves. Silicified fragments with relatively long spines preserved	Iridescent phosphatic fragments. Bored silicified valves. Incomplete heart-shaped & spinose valves	Articulated pediculate, heart-shaped form. Possible bored valve. Terebratulid (?) form	Fragments of phosphatic valve. Heart-shaped & fat (delthyrium) articulated forms. Long-hinged growth-lined sulcate spiriferid
Bryozoan	Coarsely silicified encrusting form. Various ramose & fenestrate forms	Various ramose, fenestrate & coarsely silicified & pyritised encrusting forms	Ramose form	Various ramose forms	Ramose & fenestrate forms
Coral	Small septate horn corals with columella. *Cladochonus*		Septate, sharply expanding horn coral		
Echinoderm	Coarse ossicles, grooved plates & partially pyritised pluricolumnal	Coarsely silicified & pyritised ossicles & pluri-columnals	Poorly silicified, ossicles, plates & pluri-columnals	Coarse ossicles, plates & pluri-columnals	Partial poorly silicified ossicles
Epibiont	Coiled cornulites. Slightly conical cup-like encruster		Silicified, incomplete curved cornulites	Conical cup-like encruster. Coiled, conical & unwinding cornulites forms	Conical cornulites
Gastropod	Low-turreted form	Squat, partially pyritised turreted form	Very coarsely silicified low turreted form		
Ostracod	Simple egg & bean-shaped forms	Bean-shaped & more spherical valves	Granulose spherical & simple oval forms		Slightly “pinched” form
Other	Possible thinly ridged bivalve valve. Simple spines	Fine mesh → bryozoan related? Pelleted burrow fill(?)	Simple spines. Tubular pyrite → burrows?	Coarsely silicified involute sphericone goniatite	Poorly preserved convolute cadicone(?) goniatite
Sponge	Hexaxons & bifurcating spiralled polyaxons	Hexaxons, planar tetraxons	Poly- & hexaxons	Thick hexaxons	
Trilobite		Genal spine			

Sample	**DAGL6**	**DAGL7**	**DAGL8**	**DAGL9**	**DAGL10**
Brachiopod	Phosphatic fragments. Various SiO_2 forms include (1) heart-shaped (2) sulcate spiriferid (3) fat with a tall delthyrium (4) terebrat-ulid (5) bored	Iridescent incomplete phosphatic valve	Coarsely silicified articulated heart-shaped forms	Various coarsely silicified forms including sulcate terebratulids	Incomplete articulated forms & terebratulids
Bryozoan	Various ramose forms		Siliceous tendril scaffolding of a fenestrate	Siliceous tendril scaffolding of forms	Ramose & fenestrate forms
Coral			Coarsely silicified horn forms	Coarsely silicified corallite & *Cladochonus*	*Cladochonus*
Echinoderm	Coarsely silicified ossicles & grooved plates		Incomplete pluricolumnal	Coarsely silicified ossicles & grooved plates	Poorly silicified plate
Epibiont	Smooth planispiral & conical cornulites forms				Conical cornulites
Gastropod	Rounded & thin, tall turreted forms		Coarsely silicified mildly compressed low turreted form	Coarsely silicified mildly compressed round turreted & high turreted forms	
Other	Simple spines. Coiled involute goniatite?		Simple tubes	Spines	
Sponge	Polyaxons	Various bifurcating/ trifurcating/ simple hexaxons & spiralled polyaxons	Fine planar tetraxons & irregular/ branching polyaxons	Coarsely silicified axons & septaxon	Tetra-furcating planar tetraxon. Hexaxons
Unknown					Inter-connecting siliceous scaffolding/ mesh → sponge(?)

Sample	**DAGL11**	**DAGL12**	**DAGL13**	**DAGL14**	**DAGL15**
Brachiopod	Numerous forms, often articulated, some bored	Coarsely silicified forms including terebratulids	Articulated, poorly preserved sulcate form. Valve fragments with spines	Concentric-ally ridged phosphatic valve. Various silicified forms	Phosphatic valve fragments. Various forms, some spinose or bored
Bryozoan		Irregular ramose & dome/ encrusting form	Dome/ encrusting colony. Various ramose & fenestrate forms	Dome/ encrusting colony. Various ramose & fenestrate forms	Various ramose & fenestrate forms
Coral	*Cladochonus* & horn form	Horn forms. *Cladochonus*	*Cladochonus* & horn forms		Horn forms. *Cladochonus*
Echinoderm	Coarsely silicified ossicles & pluri-columnals	Coarsely preserved ossicles & pluri-columnals	Coarse blastoid, ossicles & grooved plate	Pluri-columnal with cirri	Coarse ossicle
Epibiont	Coiled & curved cornulites. Irregular worm casts		Planispirally coiled, curved & conical cornulites	Coiled & gently curved cornulites	Cornulites wrapping bryozoan stem
Gastropod	Rounded form		High-turreted & squat forms	Variously turreted forms	Tall turreted gastropod
Ostracod			Slightly “snouted” form. D-shaped nodded valve	Swollen/ elongate/ pinched & large oval/ bean forms	Various elongate, pinched, oval, fringed, bumped & spined forms
Other			Strongly growth lined ribbed bivalve	Growth-lined bivalves. Smooth planispiral goniatite?	Strongly growth-lined bivalves. Simple spines
Sponge	Various axons: bifurcating, spiralled, planar & irregular	Spiralled & simple polyaxons. Fine hexaxons	Fine tetraxons		Polyaxons. Bifurcating hexaxon
Trilobite					Thoracic segments. Spinose cephalon & pygidium
Unknown	Siliceous inter-connecting laddered bars → sponge (?)		Simple tubes	Simple tubes	

Sample	DAGN1	DAGN2
Brachiopod	Poorly silicified specimens. Terebratulid	
Bryozoan	Dome/encrusting colony. Silicified & pyritised fenestrate forms	Partially pyritised, poorly preserved fenestrate form
Coral	Septate corallites	
Echinoderm	Short pluricolumnals and ossicles	Coarse ossicles
Epibiont	Curved and coiled cornulites forms	
Gastropod	Coarsely silicified specimen	
Ostracod	Pyritised, finely lineated forms	
Sponge	Fine polyaxons & spiralled bifurcating hexaxons	Bifurcating hexaxons
Trilobite	Partial pygidium	
Unknown	Pinched/partially segmented dark faecal looking body	Pyritised tubes

Sample	**AGHA.CAV1**	**AGHA.A2**	**AGHA.A11**	**AGHA1**
Brachiopod	Coarse valve fragments			Incomplete silicified valves
Echinoderm	Coarse ossicles & pluricolumnals	Very coarse ossicles		Coarse ossicles & pluricolumnals
Epibiont				Thin worm trails
Ostracod				Bean-like form
Other	Simple, siliceous “sugary” tube		Thin siliceous coiled tube	Lineated spines

Sample	**AGHA3.1**	**AGHA3.2**	**AGHA4**	**AGHA8**
Brachiopod	Phosphatic valve fragments	Phosphatic valve fragments	Terebratulids, pediculate valves, some spined	
Bryozoan			Fenestrate & ramose forms	
Echinoderm		Poorly preserved ossicle fragments	Ossicles. Grooved plate	Coarsely silicified and pyritised ossicles
Epibiont		Fine worm casts	Coiled cornulites	
Gastropod		Low-coiled form		
Ostracod			Lineated, spined, snouted, D-shaped with fringe & rounded articulated forms	
Other	Small planispiral goniatite?		Thin siliceous tubes & coiled fossil. *Tetrataxis*	

Sample	**AGHA9**	**AGHA10**	**AGHA11**	**AGHA13**
Brachiopod		Phosphatic & Partial silicified valves	Pyritised articulated & spined form	Partial valves & sediment fills of articulated forms
Bryozoan				Chamber fills
Echinoderm	Pyritised ossicles	Partial ossicle	Pyritised ossicles	Ossicles
Epibiont	Thin worm trails	Silicified worm casts. Pyritised cornulites?		Masses of fine, encrusting worm trails
Gastropod	Turreted sediment fill	Pyritised turreted internal mould	Various pyritised fills	Low-turreted fill
Ostracod				Sediment fills
Other			Pyritised goniatite siphuncle	Irregular, fine interconnected siliceous masses
Trilobite		Partial hypostome, pygidium & thoracic segments		Genal spine

Sample	**CNLG1**	**CNLG2**	**D.K. CNLG.A**	**D.K. CNLG SHEENA**
Brachiopod	Phosphatic valves	Phosphatic valves	Phosphatic & semicircular pyritised valves	Partial valves 1 possibly bored?
Bryozoan		Pyritised fragment?		
Echinoderm	Pyritised grooved plate		Pinnules? Grooved plate. Partial echinoid spine?	Poorly pyritised ossicles & pinnules?
Epibiont	Thin encrusting worm trails			
Gastropod	Turreted, squat fill & tall silicified form		Turreted & squashed lineated form	Lineated, turreted sediment fill
Ostracod			Articulated valves	Snouted, simple oval & bumped, fringed valves
Other	Planispiral evolute goniatite?		Partially pyritised goniatite. Small pyritised bivalve?	Orthocone. Possible bivalve
Unknown	Coarsely pyritised, irregular columns → burrows?	Dark branching & simple textured bodies → plant?	Fine honeycomb structure	

Sample	**CNLG6**	**CNLG7**	**D.K. CNLG ABV. DERREENS**	**CNLG8**
Brachiopod	Phosphatic valves	Pyritised valve	Strophic hinged valve	
Epibiont	Siliceous worm trails			
Gastropod			Partial, pyritised turreted form	
Other	Poorly preserved pyritised goniatite	Pyritised goniatite fragment	Planispiral & orthoconic cephalopod. Pyritised goniatite sutures	Pyritised coiled fossil
Unknown				Pyritised sheets with protruding, coarse orbs

Sample	**CNLG9**	**CNLG10**	**CNLG11**	**CNLG13**
Brachiopod	Phosphatic valve	Phosphatic valve	Phosphatic valve	
Echinoderm		Incompletely dissolved ossicle		
Other		Dark textured structure → carbonised plant?		Dark textured structure → carbonised plant?
Sponge		Partial hexaxon		
Unknown				

Sample	**CNLG14**	**CNLG15**	**CNLG18**	**CNLG19**
Brachiopod		Phosphatic valve		
Other	Dark simple tubes. Dark textured structure → carbonised plant? Section of coiled fossil	Pyritised goniatite siphuncle and septae. Partially silicified goniatite? Carbonised wood?	Dark textured structure → carbonised plant? Pelleted burrow structure? Partial goniatite siphuncle	Dark textured structure → carbonised plant? Partial goniatite siphuncle

Sample	**KMONA1**	**KMONA2**	**KMONA3**	**KMONA4**
Brachiopod		Phosphatic valve fragments. Silicified valve	Phosphatic valve fragments	Phosphatic valve fragments
Coral				Poorly silicified fragment
Echinoderm	Partially dissolved calcite plates		Partially dissolved calcite plates	Partially dissolved calcite plates
Gastropod		Pyritised turreted form		
Other	Pyrite clusters	Pelleted burrow structures. Silicified coiled fossil	Pelleted burrow structures	Pelleted burrow structure
Trilobite		Pygidium fragment		

Sample	**KMONA5**	**KMONA6**	**KMONA8**	**KMONA9**
Brachiopod		Phosphatic valve fragments. Silicified articulated	Fragments	Silicified, pyrite-studded valves. Phosphatic fragments
Bryozoan		Chamber fills	Fragments	
Coral	Silicified fragments	Silicified fragments		
Echinoderm	Partially dissolved calcite plates	Partially dissolved calcite plates		Coarsely silicified ossicles
Gastropod	Poorly preserved small, turreted form	Incompletely silicified	Sediment fill	
Ostracod			Thin fragile valves	Spinose, ridged, noded & snouted forms
Other	Pyrite columns → burrows? Planispiral coiled fossil	Sediment-fill of coiled fossil. Partial siphuncle & septa attachments	Dark pelleted bodies. Partial siphuncle & septa attachments	Siphuncle and partial shell. Silicified dense “ladder”-like structure
Trilobite		Silicified pygidium fragment	Partial genal spine & thoracic segments	Silicified glabella, pygidium, thoracic segments & hypostome
Unknown	Enigmatic dark star-shaped body with bullet-like dome	Enigmatic bullet-like structures with ~pentaradial base		

Sample	BW1	BW2	BW3	BW4
Brachiopod			Phosphatic valves & incompletely pyritised valves	Phosphatic valves
Echinoderm	Coarsely silicified ossicles			Poorly silicified plates
Gastropod				Sediment fill
Ostracod				Fringed valves
Other	Pelleted burrow fills			Pelleted burrow fills
Unknown		Structures with a pentaradially symmetric finned base and a squat bullet-shaped dome top		

Sample	BW10	BW7	BW8
Brachiopod		Phosphatic valves	Phosphatic valves
Other	Partial pyritised coiled goniatite. Carbonised wood fragments?		Dark carbonised wood fragments? Partial coiled goniatite?
Trilobite			Librigenae, hypostomes & thoracic segments

APPENDIX G –

Samples for stable isotope analysis

		Sample No.	Analyte	Weight (mg)
Asbian	Glencar Limestone Fm.	GLTV39 OR1	Palaeoniscid teeth (10)	1.090
		GLTV39 AN-2	Actinopterygian scale	1.346
		GLTV36 OR1	Palaeoniscid teeth (8)	1.348
		GLTV32 OR1	Actinopterygian scales. Analyte did not react	1.048
		GLTV30 AN-2	Actinopterygian scale	1.668
		GLTV30 AN-1	Actinopterygian scales. Analyte did not react	1.367
		GLTV28	Cladodont fragment	1.218
		GLTV27 OR1	Palaeoniscid teeth (13)	1.349
		GLTV22 OR1	Actinopterygian scales (7)	1.230
		GLTV21 AN-1	Unassigned ichthyolith tooth fragments	1.445
		GLTV20 OR1	Palaeoniscid teeth (8)	0.962
?	Benbulben Shale Fm.	GLTV19 OR1	Actinopterygian scales (3)	1.174
		GLTV18 OR1	Palaeoniscid teeth (9)	0.774
		GLTV17 AN-1	Fragment of large protacrodont tooth	1.035
		GLTV16 OR2	Palaeoniscid teeth (7)	1.196
		GLTV16 OR1	“Serrated ridge” ichthyolith fragment	0.854
		GLTV15	Unassigned ichthyolith material	1.090
Holkerian		GLTV14 OR2	Palaeoniscid teeth (10)	1.043
		GLTV14 OR1	Actinopterygian scale	1.464
		GLTV13 OR1	Palaeoniscid teeth (13)	1.004
		GLTV12	Enameloid layer of large fish tooth	1.292

		Sample No.	Analyte	Weight (mg)
Asbian	Dartry Lmst. Fm.	DAGL15	Lissodus tooth fragment	1.177
	Glencar Lmst. Fm.	DAGL1 OR1	Actinopterygian scales (5)	0.841

		Sample No.	Analyte	Weight (mg)
Asbian	Dartry Lmst. Fm.	DAGN1 AN-3	Actinopterygian scale	1.070
		DAGN1 OR1	Palaeoniscid tooth. Very poor reaction	1.077

		Sample No.	Analyte	Weight (mg)
Brigantian	Carraun Sh. Fm.	AGHA13 AN-2	Outer portions of a cladodont cusp	0.960
Asbian	Bellavally Fm.	AGHA11	Cladodont cusp	~2
		AGHA10 AN2-1	Incomplete *G. bilineatus* (2) & *G. girtyi* (12) P_1-elements	1.050
		AGHA10 AN1-2	Actinopterygian scales (6)	1.243
		AGHA9 OR1	Palaeoniscid teeth (29)	1.205
		AGHA9	"Ctenacanth"-type chondrichthyan scales (9)	1.083
	Glenade Sst. Fm.			
	Meenymore Fm.	AGHA6 OR1	Palaeoniscid teeth (23)	1.005
		AGHA4 OR1	Palaeoniscid teeth (20)	1.090
		AGHA4 AN-3	Actinopterygian scales (2)	1.339
		AGHA D1	Enameloid from large orodont tooth	~1.6
		AGHA3.2	*G. bilineatus* (1), *G. girtyi* (15) P_1-elements & unknown blade (2) & platform (2) fragments	1.192
		AGHA3.1	*G. bilineatus* (4) & *G. girtyi* (16) P_1-elements	1.125
		AGHA1 OR1	Palaeoniscid teeth (10)	1.296
		AGHA1	Fragment of orodont tooth	1.051

		Sample No.	Analyte	Weight (mg)
Pendleian	Dergvone Sh. Fm.	CNLG19	*G. bilineatus* (10), *G. girtyi* (3) P_1-elements & unknown S-elements (15)	0.996
Brigantian	Carraun Sh. Fm.	CNLG15 AN-1	*G. bilineatus* (7), *G. girtyi* (9) P_1-elements & unknown platform blades (10)	1.168
		CNLG14 OR1	*G. bilineatus* (11) P_1-elements & unknown platform blades (4)	0.622
		CNLG14	Actinopterygian scales (13)	1.103
		CNLG13	Actinopterygian scales. Analyte did not react	1.232
		CNLG9 OR1	*G. bilineatus* (5), *G. girtyi* (6) P_1-elements & unknown platform blades (3)	0.860
		CNLG8 OR1	Mixed conodont assemblage, including *M. bipluti* P_1-elements	0.982
		CNLG7 AN-2	*M. bipluti* (4) P_1-elements	1.027
		CNLG6 OR1	*G. bilineatus* (2), *G. girtyi* (4) P_1-elements & unknown blade fragments (6)	0.683
Asbian	Bellavally Fm.	CNLG A2	Acanthodian scales (15)	~1
		CNLG A1	*G. girtyi* (9) P_1-elements & unknown platform blades (7)	~1
		CNLG1 AN2-1	*G. bilineatus* (4), *G. girtyi* (14) P_1-elements & unknown platform blades (4)	1.036
		CNLG1 AN1	Actinopterygian scales (2). Analyte did not react	1.223

		Sample No.	Analyte	Weight (mg)
Pendleian	Magowna Fm.	**KMONA10 OR1**	*G. bilineatus* (9), *G. girtyi* (4) & P_1-elements	**0.602**
		KMONA9 AN-1	*G. bilineatus* (20) P_1-elements	**1.108**
		KMONA8 AN-3	*G. bilineatus* (13) P_1-elements	**1.172**
Brigantian	Slievenaglasha Fm.	**KMONA6 AN5-2**	*L. commutata* (10), *L. monocostata* (4), *L. mononodosa* (8), *L. nodosa* (2), *L. ziegleri* (2) & unassigned *Lochriea* (9) P_1-elements	**0.953**
		KMONA6 AN4-1	*G. bilineatus* (26) P_1-elements	**1.147**
		KMONA6 AN3-3	Palaeoniscid teeth (24)	**1.135**
		KMONA6 AN2-3	Large cladodont cusps (2)	**1.237**
		KMONA6 AN1-1	Actinopterygian scales (2)	**1.161**
		KMONA5 AN7-2	Large cladodont tooth	**1.255**
		KMONA5 AN6-2	*L. commutata* (18), *L. mononodosa* (6), *L. nodosa* (5), *L. ziegleri* (1) & unassigned *Lochriea* (5) P_1-elements	**1.100**
		KMONA5 AN5-3	*G. girtyi* (25) P_1-elements	**1.129**
		KMONA5 AN4-1	*G. bilineatus* (21) P_1-elements	**0.992**
		KMONA5 AN3-3	Palaeoniscid teeth (25)	**1.169**
		KMONA5 AN2	*Thrinacodus* (6) teeth	**1.098**
		KMONA5 AN1-3	Actinopterygian scales (2)	**1.141**
		KMONA4 AN4-2	*L. commutata* (9), *L. costata* (1), *L. monocostata* (3), *L. mononodosa* (3), *L. nodosa* (1), *L. ziegleri* (4) & unassigned *Lochriea* (11) P_1-elements	**1.137**
		KMONA4 AN3-3	*G. bilineatus* (12), *G. homopunctatus* (3) & *G. girtyi* (12) P_1-elements	**0.987**
		KMONA4 AN2-2	Incomplete cladodont tooth	**1.067**
		KMONA4 AN1-3	Actinopterygian scales (2)	**0.967**
		KMONA3 OR1	Actinopterygian scales (7)	**1.297**
		KMONA3 AN-1	*G. bilineatus* (13), *G. homopunctatus* (3), *G. girtyi* (2) P_1-elements & *Lochriea* P_1-elements (4)	**1.050**
		KMONA2 OR1	*G. girtyi* (13) P_1-elements & unknown platform blades (5)	**0.907**
		KMONA1 OR1	Cladodont cusp	**1.261**
		KMONA1 AN-2	*G. bilineatus* (8), *G. homopunctatus* (4), *G. girtyi* (10) P_1-elements & *Lochriea* P_1-elements (5)	**1.064**

			Sample No.	Analyte	Weight (mg)
Bashkirian	**Clare Sh. Fm.**		**BW10 AN2-1**	30 Incomplete *Idiognathoides* & *Declinognathodus* P_1-elements	**0.930**
			BW10 AN1-3	Acanthodian scales (12)	**0.966**
			BW8 AN-1	25 Incomplete *Idiognathoides* & *Declinognathodus* P_1-elements	**1.047**
Serpu-khovian		**PO_4 lag**			
Viséan	**Magowna Fm.**		**BW4 AN3-3**	Assorted conodont elements	**1.227**
			BW4 AN2-1	Juvenile *G. bilineatus* (44) P_1-elements	**0.934**
			BW4 AN1	Mature *G. bilineatus* (4) P_1-elements	**1.042**
			BW3 AN2	*G. homopunctatus* (55) P_1-elements	**1.011**
			BW3 AN1-2	*G. bilineatus* (14) P_1-elements	**1.149**
			BW2 OR1	Actinopterygian scales (2). Analyte did not react	**0.895**
			BW2 AN-2	Cladodont tooth. Analyte did not react	**0.757**
	Slievena-glasha Fm.		**BW1 AN2**	*G. homopunctatus* (41) P_1-elements	**0.820**
			BW1 AN1-3	*G. bilineatus* (22) P_1-elements	**1.045**

APPENDIX H –

SEM stub maps and museum numbers

All specimens figured in this work have been lodged into the James Mitchell Museum in the National University of Ireland, Galway. The following plates map out the distribution of the figured specimens on their respective SEM stubs. The museum numbers are the same as those given but with the prefix “JMM.”

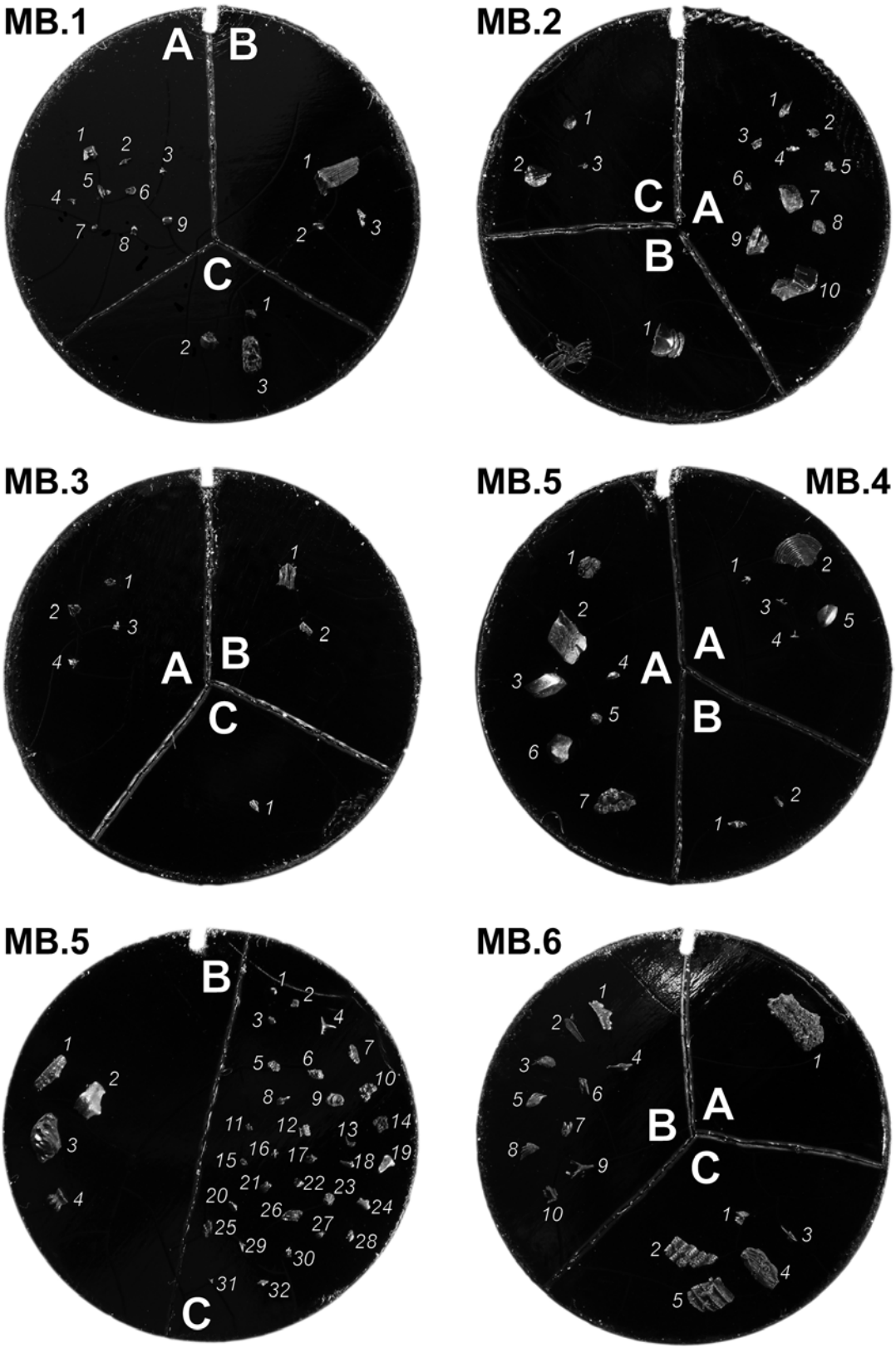
MB.1
A
B
C
MB.2
C
A
B
MB.3
A
B
C
MB.5
MB.4
A
A
B
MB.5
B
C
MB.6
A
B
C

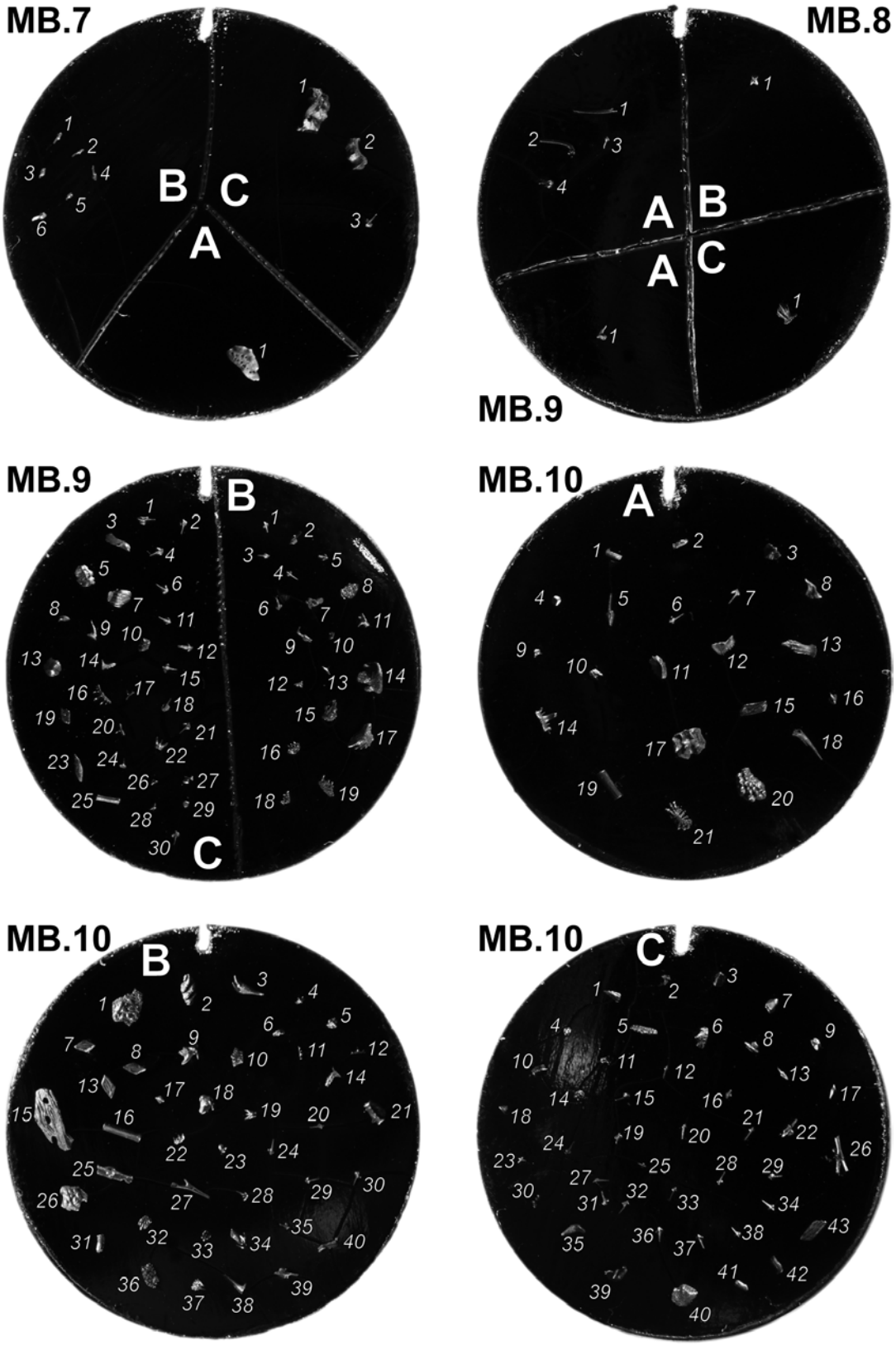
MB.7
B
C
A
MB.8
A
B
A
C
MB.9
MB.9
B
C
MB.10
A
MB.10
B
MB.10
C

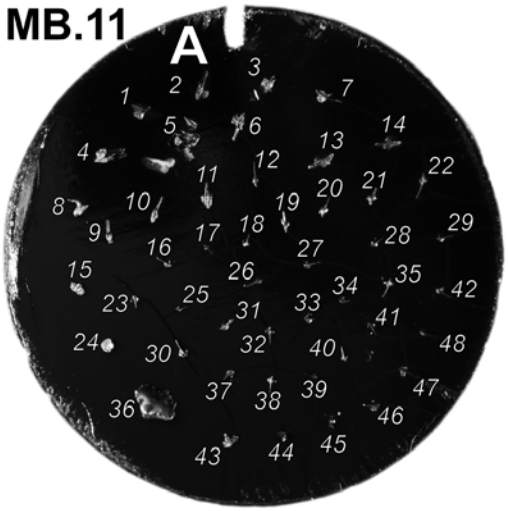
MB.11
A

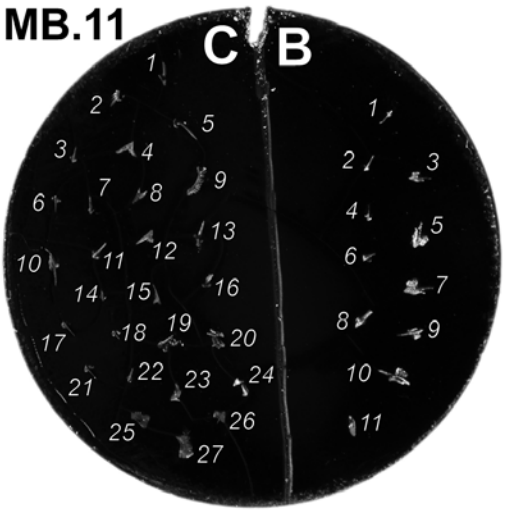
MB.11
C
B

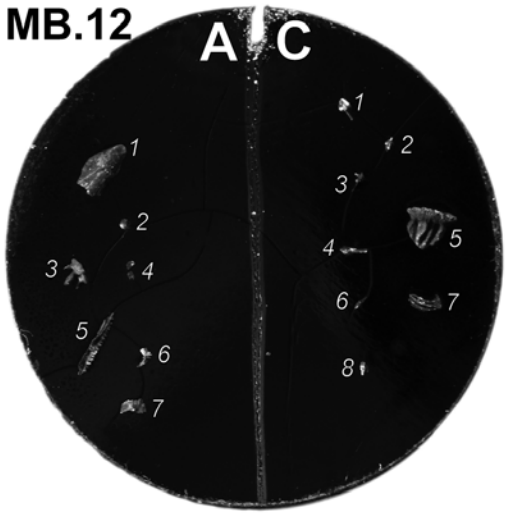
MB.12
A
C

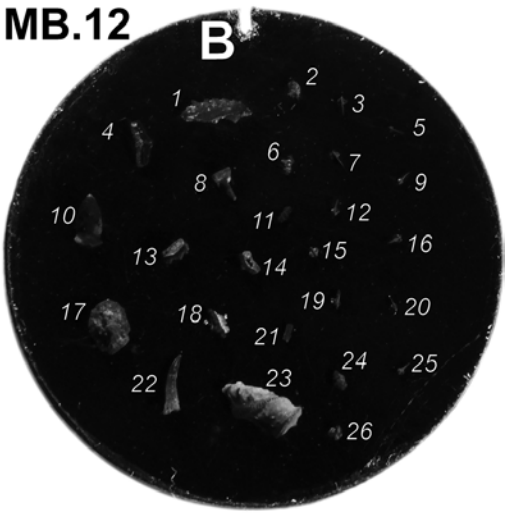
MB.12
B

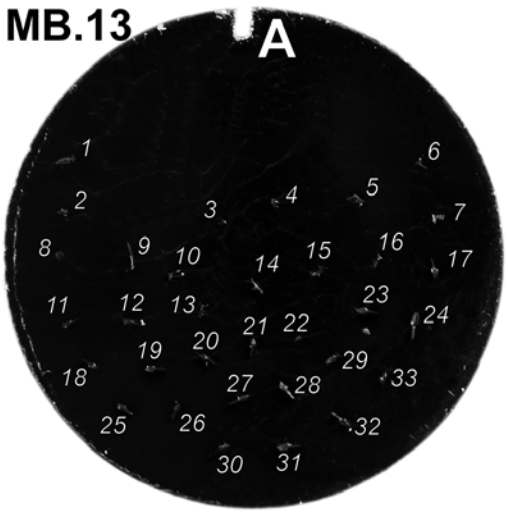
MB.13
A

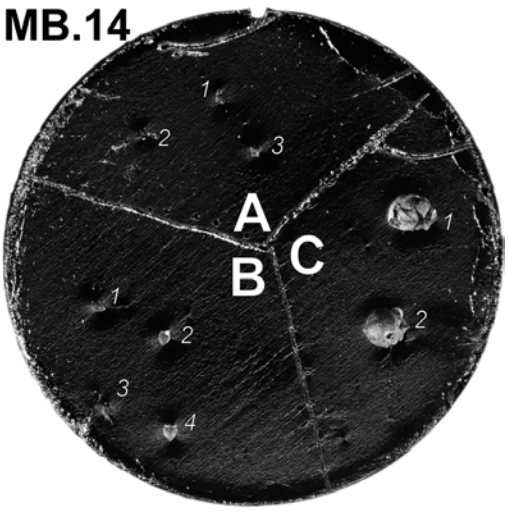
MB.14
A
B
C


MB.15
1
2
3
4
5
6
7
8
9

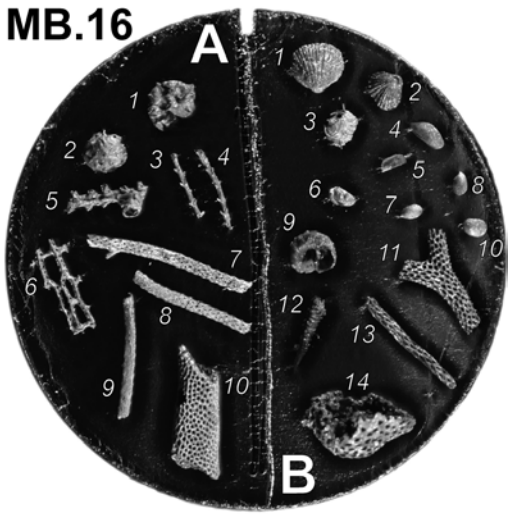
MB.16
A
B
1
2
3
4
5
6
7
8
9
10
11
12
13
14


MB.17
1
2
3
4
5
6
7
8
9
10

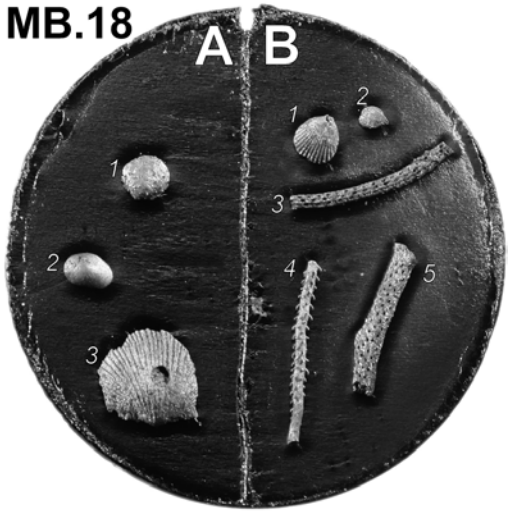
MB.18
A
B
1
2
3
4
5

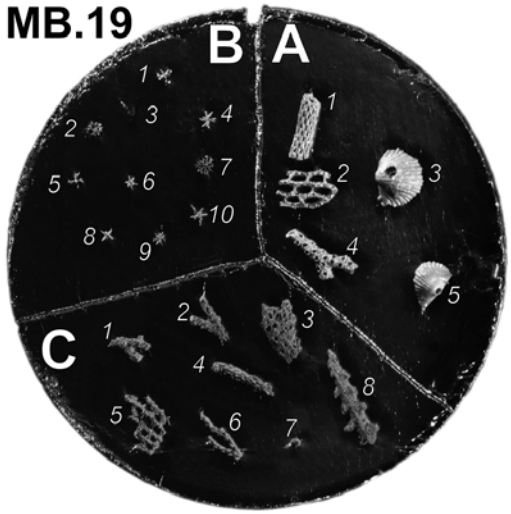
MB.19
B
A
C
1
2
3
4
5
6
7
8
9
10

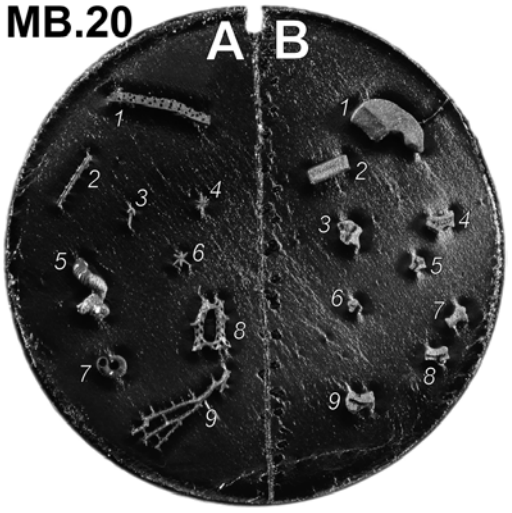
MB.20
A
B
1
2
3
4
5
6
7
8
9

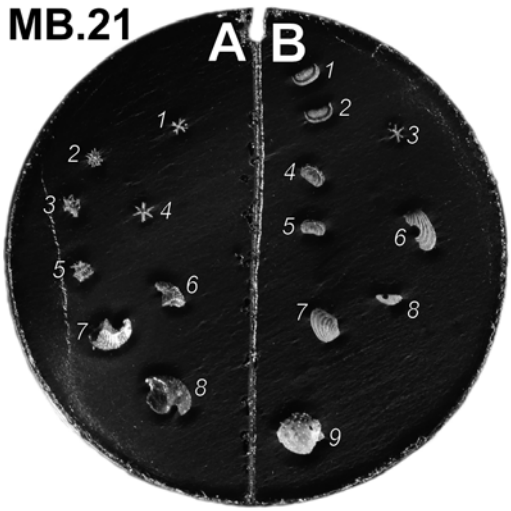
MB.21
A
B

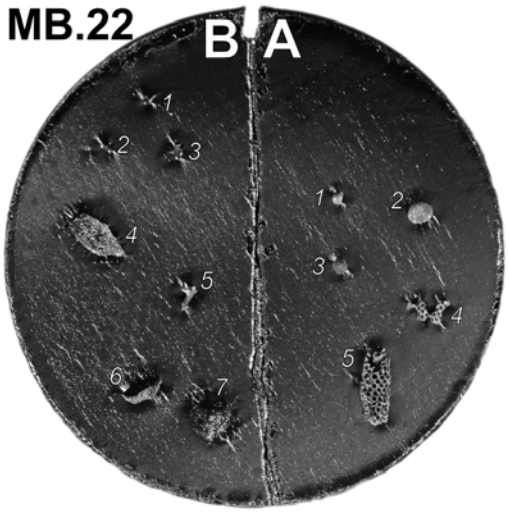
MB.22
B
A

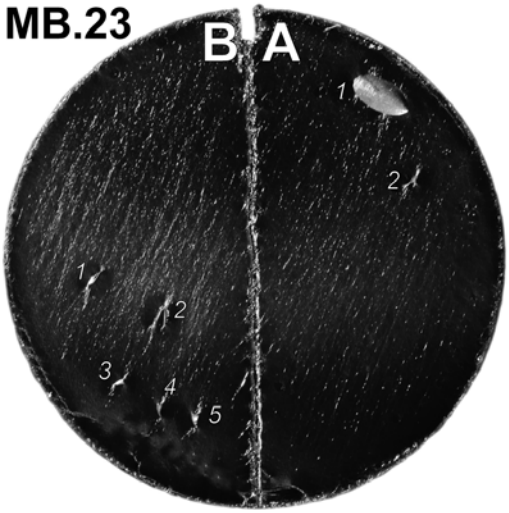
MB.23
B
A

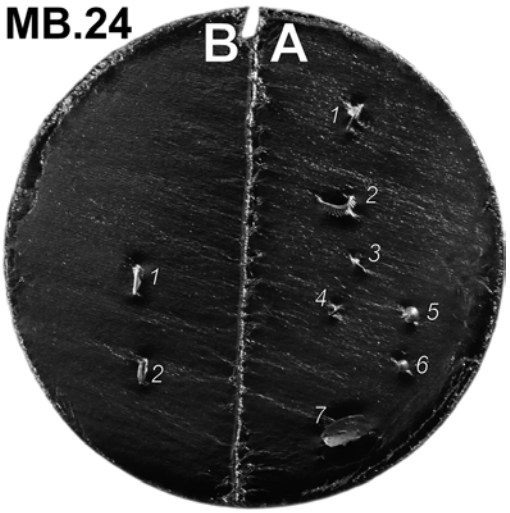
MB.24
B
A

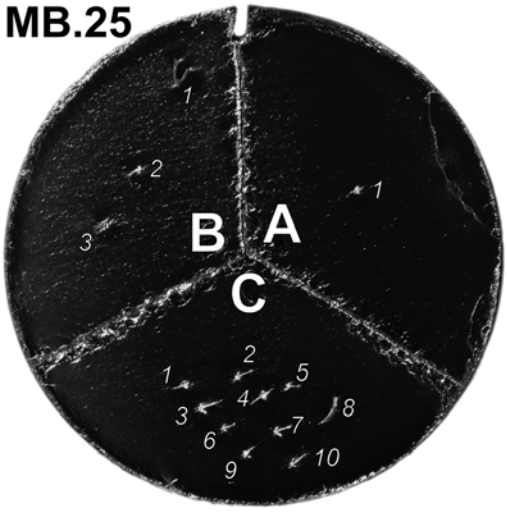
MB.25
B
A
C


MB.26

MB.27

MB.BW4

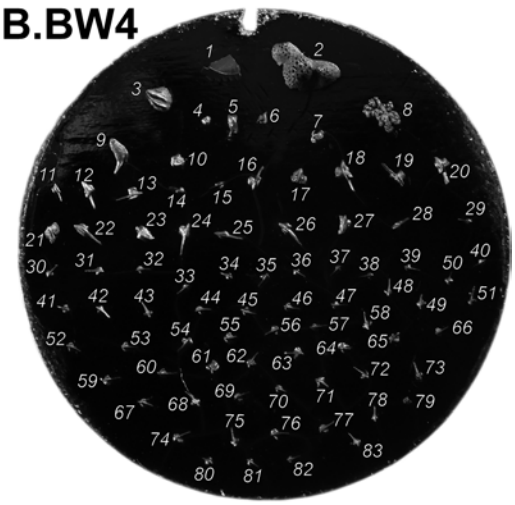

MB.CNLG3 _1

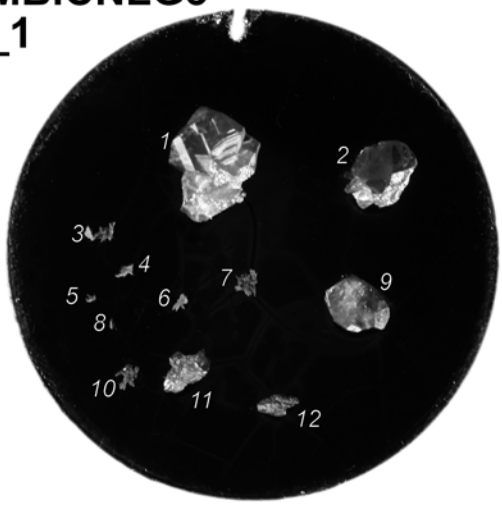

MB.CNLG3 _2

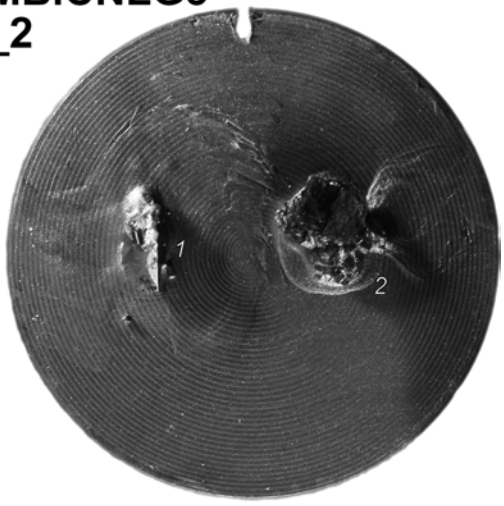

MB.CNLG3 _3

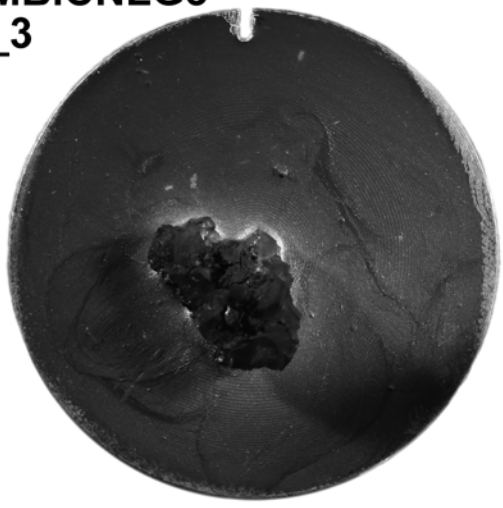

MB.CNLG3 _4

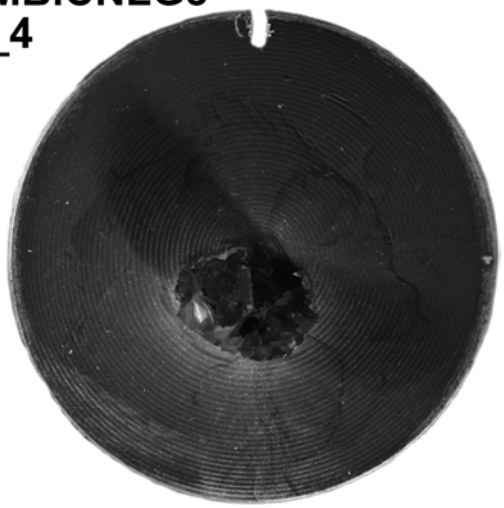

MB.KMONA5


1
2
3
4
5
6
7
8
9
10
11
12
13
14
15
16
17
18
19
20
21
22
23
24
25
26
27
28
29
30
31
32
33
34
35
36
37
38
39
40
41
42
43
44